# Dry eye disease and neuropathic corneal pain : translational exploration of novel therapeutic and diagnostic strategies

Adrián Guerrero Moreno

**PhD thesis**
**Sorbonne Université**
École doctorale 394 Physiologie, Physiopathologie et Thérapeutique

**Adrián GUERRERO MORENO**

# Dry eye disease and neuropathic corneal pain:
*translational exploration of novel therapeutic and diagnostic strategies*

*Thesis defence: 9th September 2022*

Jury members:

| | |
|---|---|
| Pr Philipp STEVEN | Rapporteur |
| Dr Frederic SIMONIN | Rapporteur |
| Pr Juana GALLAR | Examiner |
| Dr William ROSTÈNE | Examiner |
| Dr Annabelle RÉAUX LE GOAZIGO | Supervisor |

# Acknowledgements

I would like to thank all the people from of the European network Integrated Training in Dry Eye Disease Drug Development including my colleagues, supervisors, external advisory board and specially to the project managers Paz Yáñez and Maya Berg. It has been very gratifying to see how we were all moving forward in a common project.

Many thanks also to the members of my annual PhD thesis committee Luc Maroteaux and specially Juan Gallar who have been following and supporting my advance during these years.

Thanks to the other members of the jury Philipp Steven, Frederic Simonin and William Rostène, who agreed to examine this work.

I would like to thank also Stéphane Mélik Parsadaniantz and specially Christophe Baudouin and Hong Liang for their feedback and support, for make me confident in presenting my results.

A big thank to my thesis supervisor, Annabelle Réaux-Le Goazigo, for her patience and kindness, and for the enormous time and effort she has dedicated to me. It has been a pleasure to work under your supervision. You have made me grow and learn a lot of things.

I would also like to thank Eduardo Reig but especially Nathan Moreau for his strong support in the writing of this thesis.

I would like to thank Alfredo Dominguez. Ha sido un placer trabajar codo con codo y aprender tanto juntos.

To all my colleagues in the lab for making me feel like family. Thanks to Noémie Bonneau, Tiffany Migueon, Elodie Reboussin, Murat Akkurt, Tristan Hourcade, Jian Huang and Karima Kessal.

Thank you very much to Laura Frutos and Almudena Iñigo. He disfrutado y aprendido mucho colaborando con vosotras.

Un grand merci à toutes les personnes de l'animalerie, en particulier Manu, Quenol et Julie. Vous m'avez beaucoup aidé.

To all the people from Institut de la Vision. It has been wonderful to work in this environment. Special thanks to Irene Elices, Francesco Trapani, Catherine Botto, Rémi Karadayi, Stephane Fouquet, Jothini John, Lauriane Delay, Christina Zeitz, Christophe Roubeix, Guillaume Blot, Caroline Nous, Marcela Garita, Morgane Belle, Juan Antonio Moreno and all my colleagues from the PhD retreat.

The greatest thanks to those who, even if they had no choice, gave their all. Many thanks to my mice.

To my former mentors who dedicated their time to train me so that I could get here. Diego Echevarría, Eduardo de Puelles, Ramón Reig, Elisa Checa y Cristina Soto.

A la gente que me ha acompañado y apoyado en esta etapa, especialmente a Natalia, Miguel, Sara y Alicia.

A mis amigos por estar ahí cuando los necesitaba: Javi, Alberto, Tere, Alex, Fran, Jota, Raquel, Carla, Paula, Amanda, Quique y tantos más que no caben aquí.

Y finalmente las gracias más especiales a toda mi familia. No hay palabras para explicar lo afortunado que soy de teneros. Gracias mamá y papá por haberme apoyado siempre y habérmelo dado todo. A mi abuela, allá donde esté, ya soy científico.

# Abstract

Dry eye disease (DED) is a multifactorial disease of the ocular surface, often leading to chronic ocular pain, with limited efficient treatment options. In numerous cases, it can be associated with neuropathic corneal pain (NCP), even more difficult to manage. Treating NCP is highly challenging, and there is still a current lack of available topical nerve-targeted treatment to alleviate ocular pain. This is very relevant as it represents a debilitating condition that can dramatically affect the quality of life of the patient.

The present translational research project aims to improve the management of DED-related neuropathic pain by increasing our understanding of DED pathophysiology, by investigating new treatment options for DED-related pain and by trying to improve the diagnosis of DED-related neuropathic pain.

The corneal epithelium is the most densely innervated tissue by nociceptors in the human body, with 600 terminals/mm$^2$. It is an excellent tissue to study the morphological and functional properties of peripheral nociceptors as well as neuro-immune interactions, not only because of its huge nerve density, but also because of its easy accessibility.

In this line, preclinical studies from our team have focused on the elucidation of cellular and molecular mechanisms of analgesia following the targeting of the ocular opioid system for the management of corneal pain. The first part of the PhD project explored the therapeutic potential of targeting the corneal opioid system using topical treatments in two animal models of acute inflammatory pain and of chronic pain associated with DED. We provided the first demonstration that mu opioid receptor (MOR) is expressed in mouse corneal nerves. We also detected the expression of MOR mRNA in most polymodal neurons and revealed it was overexpressed in the V1 branch of the TG in both models of ocular pain. Furthermore, we showed that topical ocular administration of DAMGO, a MOR agonist, significantly reduced both mechanical and chemical corneal hypersensitivity in both models of corneal pain. Overall, these data provide evidence that activation of corneal opioid receptors could constitute a therapeutic approach for the treatment of corneal pain.

The second part of the project assessed potential biomarkers of DED-related NCP in human patients and novel phenotyping strategies to improve the diagnosis and thus management of NCP in DED in clinical practice. We conducted a retrospective case-control clinical study evaluating patient clinical and *in vivo* confocal microscopy (IVCM) imaging data from a cohort of patients with corneal neuropathic pain in two etiological subsets of DED: auto-immune-related DED (AIDE) and primary meibomian gland dysfunction (MGD)-related DED. IVCM images analysis revealed that AIDE-related NCP patients displayed increased nerve tortuosity and number of microneuromas whereas MGD-related NCP patients had reduced nerve density and increased number, perimeter, and area of microneuromas compared with healthy controls. Furthermore, a higher number of microneuromas was found in MGD-related NCP compared to AIDE-related NCP or painless MGD. Additional IVCM-based parameters described microneuromas, such as area and perimeter could actually be useful to discriminate between etiological subsets of DED, an initial step towards better patient phenotyping and thus better personalized pain management.

In conclusion, this research project explored new avenues for the management of DED with the hope of eventually helping to improve the quality of life of patients suffering from this highly burdensome ocular disease.

# Résumé

La sécheresse oculaire (SO) est une maladie multifactorielle de la surface oculaire, qui entraîne souvent des douleurs oculaires chroniques, avec des options thérapeutiques efficaces limitées. Dans de nombreux cas, cette SO peut être associée à une douleur neuropathique cornéenne (DNC), encore plus difficile à gérer. Le traitement de la DNC est très difficile et il n'existe toujours pas de traitement topique ciblé pour la soulager.
Le projet translationnel de cette thèse vise à améliorer la compréhension de la physiopathologie de la DNC associée à la sécheresse oculaire, en étudiant de nouvelles options thérapeutiques et en essayant d'améliorer le diagnostic de cette douleur neuropathique.
La cornée est le tissu le plus densément innervé de l'organisme comprenant 600 terminaisons/$mm^2$ et constitue un excellent tissu pour étudier les propriétés morphologiques et fonctionnelles des nocicepteurs périphériques, non seulement en raison de son innervation mais également de son accessibilité.
La première partie du projet de thèse a exploré le potentiel thérapeutique du ciblage du système opioïdergique cornéen à l'aide de traitements topiques (instillations) dans deux modèles murins de douleur cornéenne inflammatoire aiguë et de DNC chronique associée à la SO. Nos données anatomiques ont mis en évidence l'expression du récepteur mu opioïdergique (MOR) sur les terminaisons cornéennes, dans les neurones polymodaux du ganglion trigéminal et que son expression (mRNA) est augmentée dans les deux modèles de douleur cornéenne. Enfin, un traitement chronique (instillations) avec du DAMGO, un agoniste sélectif du récepteur MOR, réduit significativement l'hypersensibilité mécanique et chimique cornéenne dans les deux modèles animaux. En conclusion, ces données montrent que les récepteurs opioïdergiques cornéens seraient une cible thérapeutique potentielle dans le traitement de la douleur cornéenne.
En parallèle de ces études précliniques, la seconde partie du projet de thèse a porté sur l'étude des changements cellulaires de la surface oculaire de patients souffrant de DNC liée à la SO afin d'améliorer le diagnostic et donc la gestion de cette douleur. L'étude clinique rétrospective a analysé les données cliniques et les images de microscopie confocale in vivo (IVCM) obtenues chez des patients présentant des étiologies différentes de la SO (SO liée à un dysfonctionnement auto-immun (AIDE) ou liée à un dysfonctionnement primaire des glandes de Meibomius (MGD)). L'analyse d'image a révélé que les patients AIDE atteints de DNC présentaient une tortuosité des nerfs cornéens et un nombre de névromes plus importants, tandis que les patients MGD douloureux présentaient une densité des nerfs cornéens réduite ainsi qu'un nombre de névromes (périmètre et surface plus grands) par rapport aux sujets sains. En outre, un nombre plus élevé de névromes a été observé dans les DNC liées à la MGD par rapport aux patients AIDE douloureux. Ainsi, les paramètres morphologiques pris en compte dans cette étude pour décrire les névromes, tels que leur surface et leur périmètre, pourraient être utiles pour un meilleur phénotypage des patients et donc une meilleure gestion personnalisée de la douleur cornéenne.
En conclusion, cette thèse a exploré de nouvelles voies pour la prise en charge de la DNC avec l'espoir de contribuer à terme à l'amélioration de la qualité de vie des patients souffrant de cette pathologie oculaire très invalidante.

# Scientific meetings and communications

- **FENS Forum 2022.** Federation of European Neuroscience Societies. 9th – 13th July 2022. Paris, France.
  - **Targeting mu opioid receptor to alleviate dry eye disease-associated chronic corneal allodynia in mice.** Guerrero-Moreno A, Reboussin E, Baudouin C, Melik Parsadaniantz S, Réaux-Le Goazigo A. (poster)
- **IT-DED$^3$ Outreach Symposium**. European Network on dry eye disease drug development. 2nd December 2021. Quinze-Vingts National Ophthalmology Hospital, Paris, France.
  - **Pain in dry eye disease: from the lab bench to the clinic.** (available online, oral communication)
- **IASP congress**. International Association for the Study of Pain. 9th-11th June and 16th-18th June 2021 (online)
- **European Dry eye society congress**.

  First edition: 18th and 19th June de 2021. (online, based in Paris, France):
  - **Biomarkers for diagnosis of Dry eye disease.** Section *IT-DED3: A European consortium for innovation*. Guerrero-Moreno A, Akkurt M, Brignole-Baudouin F, Réaux-Le Goazigo A, Baudouin, C (oral communication)
  - **Analysis of corneal nerve abnormalities in painful dry eye disease patients.** Guerrero-Moreno A, Liang H, Moreau N, Luzu J, Rabut G, Melik Parsadaniantz S, Labbé A, Baudouin C, Réaux–Le Goazigo A (poster)

  Second edition: 10th and 11th June 2022. Paris, France.

- **Doctoral School Days.** Physiology, physiopathology and therapeutics doctoral school, Sorbonne Université

  21th edition: May, 2021. Online, based in Paris, France:
  - **Corneal pain and dry eye disease: a clinical retrospective study.** Guerrero-Moreno A, Liang H, Moreau N, Luzu J, Rabut G, Melik Parsadaniantz S, Labbé A, Baudouin C, Réaux–Le Goazigo A (poster)

  20th edition: May 2019. Paris, France:

- **Distribution of the mu-opioid receptor in the corneal nociceptive pathway during inflammatory ocular pain.** Guerrero-Moreno A, Joubert F, Fakih D, Baudouin C, Mélik Parsadaniantz S, Reaux-Le Goazigo A. (poster)

- **10 years celebration event of the Institut de la Vision.** 27th November 2019. Paris, France:
  - **Mu-opioid receptor, a therapeutic target for corneal inflammatory pain relief?.** Guerrero-Moreno A, Joubert F, Fakih D, Baudouin C, Rostene W, Mélik Parsadaniantz S, Réaux-Le Goazigo A. (poster).
- **22nd EVER Congress.** European Association for Vision and Eye Research. 17th-19th October 2019. Nice, France:
  - **Upregulation of the mu-opioid receptor in the cornea and trigeminal ganglion following corneal inflammatory pain.** Guerrero-Moreno A, Joubert F, Fakih D, Baudouin C, Mélik Parsadaniantz S, Reaux-Le Goazigo A. (poster)
  - **Exploring the role of opioids and chemokines in dry eye.** Talk representing WP1 from IT-DED$^3$ in the Joint meeting Ocuther-IT-DED$^3$, satellite to EVER congress. (oral communication)
- **15th symposium of the French Pain Research Network.** Brain and Spine Institute, Pitié-Salpêtrière Hospital. 22th & 23th March, 2019. Paris, France.

## Publications

- **Corneal nerve abnormalities in painful dry eye disease patients.** Guerrero-Moreno A, Liang H, Moreau N, Luzu J, Rabut G, Melik Parsadaniantz S, Labbé A, Baudouin C, Réaux–Le Goazigo A. **Biomedicines** 2021, 9(10), 1424.
- **Morphological and functional changes of corneal nerves and their contribution to peripheral and central sensory abnormalities.** Guerrero-Moreno A**,** Baudouin C, Mélik-Parsadaniantz S, Réaux-Le Goazigo A. **Front. Cell. Neurosci**. doi: 10.3389/fncel.2020.610342. PMID: 33362474 **Review**
- **How does chronic dry eye shape peripheral and central nociceptive systems?** Guerrero-Moreno A**,** Fakih D, Melik Parsadaniantz S, Réaux-Le Goazigo A. **Neural Regen Res**. 2021 Feb;16(2):306-307. doi: 10.4103/1673-5374.290895. PMID: 32859787. **Review**

- ✓ **Topical treatment with a mu opioid receptor agonist alleviates corneal allodynia and corneal nerve sensitization in mice.** Joubert F, Guerrero-Moreno A, Fakih D, Reboussin E, Gaveriaux-Ruff C, Acosta MC, Gallar J, Sahel JA, Bodineau L, Baudouin C, Rostène W, Mélik-Parsadaniantz S, Réaux-Le Goazigo A. **Biomed Pharmacother**. 2020 Dec;132:110794. doi: 10.1016/j.biopha.2020.110794. Epub 2020 Oct 6. PMID: 33035833.
- ✓ **Capsazepine decreases corneal pain syndrome in severe dry eye disease.** Fakih D, Guerrero-Moreno A, Baudouin C, Reaux-Le Goazigo A., Melik Parsadaniantz S. **J Neuroinflammation**. 2021 May 11;18(1):111. doi: 10.1186/s12974-021-02162-7. PMID: 33975636.

## Courses, webinars and other achievements

- ✓ Co-organizer of **1st PhD Student Retreat of the Vision Institute**. From 23rd to 27th March 2022. Peisey, Vanoise national parc, France.
- ✓ **IT-DED³ Fellow Board representative** 2020-2021.
- ✓ **16th National Course of Neurosciences.** Organizers: José M. Delgado García, Pablo de Olavide University, Sevilla and Alberto Ferrús, Cajal Institute, CSIC, Madrid. 20th-24th September 2021. Carmona, Sevilla, Spain.
- ✓ **Summer school in Needs of the DED Patient & Clinical Studies in DED** (included in IT-DED³ program). Sorbonne University. 15th-19th June 2021. online.
- ✓ **IT-DED³ training program** 2020-2021 (webinars, online):
  - 'Trends in publishing' by Prof. Arto Urtti (University of Eastern Finland). November 2020.
  - 'Societal impact' by Dr. Stefan de Jong (University of Chicago). December 2020.
  - 'How to pitch your project' by Prof. Dr. Robin De Cock (University of Antwerp). February 2021
  - 'Analytical tools' by Prof. Dr. Rosario Bronze (iBET - Food & Health Division, ITQB NOVA, Lisbon). March 2021.
  - 'EU R&I programmes' by Aurélie Pachkoff-Singh (Institut de la Vision, Paris). May 2021.
- ✓ Webinar **'Presentation of the European Dry Eye Society'** (EUDES). February 2021.
- ✓ **IT-DED³ Virtual Annual Meeting 2021.** 28th January 2021.
- ✓ Webinar **'Building your linkedin profile'**. Sorbonne University. November 2020.

- ✓ **Global Dry eye and ocular surface webinar**. Joint meeting KKESH, TFOS and PanCornea. June 2020. Online.
- ✓ **IT-DED³ Virtual Annual Meeting 2020.** 19th March 2020. Online.
- ✓ **Workshop 'Presenting with impact'** (included in IT-DED³ training program). The Floor is Yours. Hans Van de Water. 8th May, 2020. Online.
- ✓ Online course: **Understanding Clinical Research: Behind the Statistics** (April 2020, 30h). Online platform Coursera. Juan H Klopper, University of Cape Town.
- ✓ **Winter school in Good Research Practices** (included in IT-DED³ training program). 14th-18th January, 2019. Univerisidad de Valladolid, Valladolid, Spain.
- ✓ **Quintessence Assessment.** IT-DED³ and Quintessence Consulting. From December 2018 to June 2021. Online.
- ✓ **Recruitment Event of IT-DED³.** Integrated training network in dry eye disease drug development consortium. 24th May 2018. University of Antwerp, Belgium.

## Involvement in teaching, supervision or mentoring

- 2021-2022: Teaching to 1st year PhD students in the laboratory. Animal experimentation techniques (ocular pain model implementation: surgical DED mice model and BAK instillation model; behavioral and sensitivity tests, tear measurement, topical treatment, euthanasia and perfusion), sample extraction, histological techniques (immunostaining and *in situ* hybridization), microscopy imagining, image analysis and interpretation.
- 2019-2020: Participation in the supervision and teaching of a PhD student coming from Institute of Neurosciences (Spain) developing her doctoral international stay in our laboratory. Teaching in behavioral tests, clinical examination of ocular surface, histological techniques and RNA extraction.
- 2018-2019: Participation in the supervision of an international Master 2 student in Vision Science (National Autonomous University of Mexico and Sorbonne University) developing their master thesis in our laboratory. Teaching in histological techniques.

# Foreword

Ocular pain, *i.e.* pain of the ocular surface, is a frequent concern in ophthalmological practice and a leading cause for consultation, with an often important impact on the patient's quality of life, especially in cases of chronic ocular pain. Briefly speaking, ocular pain results either from ocular surface damage or changes to peripheral or central nerves in the corneal nociceptive pathway, sometimes both. From a clinical standpoint, such ocular pain can be of complex diagnosis (and thus management) especially in cases with minimal to no discernible ocular surface alterations, as can be found in the context of corneal neuropathic pain for instance.

Among the numerous etiologies of ocular pain, dry eye disease is a prototypical example of such clinical and scientific issues, as it is a frequent but still underdiagnosed condition with insufficient management, especially of the associated nociceptive and/or neuropathic pain.

The research project developed in this thesis thus aimed to better understand, from both a scientific and clinical perspective, the corneal nociceptive system in various ocular surface diseases and more specifically in the context of dry eye disease-related corneal neuropathic pain. Such increased understanding has brought new insights and novel treatment options for the management of ocular pain, as will be developed herein.

# Table of contents

# Chapter 1: Understanding ocular pain in physiology and disease: *the example of dry eye disease-related corneal pain*

## I. Pain, nociception and dry eye disease: basic concepts

### I.1 Defining pain: *beyond sensation*

The International Association for the Study of Pain (IASP) defines pain as ***"****an unpleasant sensory and emotional experience associated with, or resembling that associated with, actual or potential tissue damage"* (Raja et al., 2020).

Acute pain is usually short-lived, most often resolving within 3–6 months. In some cases, however, acute pain may transition to chronic pain, as the result of aberrant activity in peripheral and/or central nociceptive pathway. It is well documented that neuronal plasticity, microglial and astrocyte activation, and immune-cell infiltration contribute to the pathophysiological changes associated with the development of chronic pain (Hiraga et al., 2022). Chronic pain leads to psychological and physical deterioration resulting in a major public health concern owing to the high cost of medical treatment and the loss of productivity in the workplace.

Pain is a very subjective experience, leading to a great variability between individual response to the same input (Fillingim, 2017). There is no objective, quantitative, absolute and direct measure of the experience of pain; thus, self-report pain assessment tools are used and are essential to make an accurate diagnosis and establish the most beneficial treatment.

Variability in pain reporting depends on a large and heterogeneous variety of factors, including possible genetic factors. It has been found that genetic defects affecting sensory system development and its physiological function can determine pain states, but they will result from complex interactions between genetic variants and environmental factors (Denk and McMahon, 2017). Other investigated factors that could affect pain experience and reporting include demographic factors such as gender, age, ethnicity, cultural background and socioeconomic status (Rahim-Williams et al., 2012), but also emotional and cognitive factors such as current mood, the attention state, the emotional and affective values given to the pain, and several psychiatric comorbidities (Loeser and Melzack, 1999). It is important to note that most of these data rely on epidemiological studies and their application in individual elucidation of cause-effect is difficult. In that aim, numerous neuroimaging studies have been

carried out in recent years to correlate these external factors with functional neurocircuitry (Anderson and Losin, 2016).

## I.2 Nociception and classification of pain

**Nociception** is the neural process of encoding noxious stimuli, in contrast with **pain** which defines the conscious experience associated with nociception.

Due to the heterogeneity of pain in its duration, anatomical presentation, etiology, intensity and pathophysiology, there are many ways in which pain can be classified.

From a physiological and pathophysiological standpoint, pain can be classified as:

- **Nociceptive pain,** defined by IASP as "*pain that arises from actual or threatened damage to non-neural tissue and is due to the activation of nociceptors*". It represents a physiological protective warning signal against imminent or ongoing tissue damage, leading the individual to escape from the pain-inducing stimulus. As indicated in IASP's definition, it emerges from the activation of receptors expressed by primary sensory neurons in the peripheral nervous system, known as nociceptors, as consequence of noxious mechanical, thermal or chemical stimuli that persists only as long as the stimulus is maintained.
- **Inflammatory pain,** a type of nociceptive pain that results from the activation and sensitization of nociceptors by inflammatory mediators (cytokines, prostaglandins, leukotrienes, protons and ATP). It is an adaptive response protecting the organism during the healing phase post-injury.
- **Neuropathic pain,** defined by the IASP as "*pain caused by a lesion or disease of the somatosensory nervous system*". Neuropathic pain can be described as peripheral or central, depending on whether the lesion affects the peripheral or central nervous system. Neuropathic pain often lacks a protective function and thus represents a pathological pain state.

**Peripheral and central sensitization**

If a painful noxious stimulus is able to damage the tissue, immune cells will infiltrate the injury site and produce inflammatory mediators as part of the physiological healing process, that can activate nociceptors thus resulting in inflammatory pain. When the noxious stimulus or the levels of inflammatory mediators exceed a determined intensity and/or duration, they

can trigger molecular changes that eventually will increase the responsiveness of sensory neurons in a process known as **sensitization**. Such sensitization process can occur in peripheral sensory neurons (**peripheral sensitization**) or central sensory neurons (**central sensitization**) (Melik Parsadaniantz et al., 2015), (Guerrero-Moreno et al., 2020).

The sensitization process can translate as **hyperalgesia**, *i.e.* an exacerbated painful response to a noxious stimulus, and when severe can lead to **allodynia**, *i.e.* a painful response to a normally innocuous stimulus.

Conversely, release of peptides as Substance P (SP) and calcitonin gene-related peptide (CGRP) by primary neurons can activate immune cells through the process of **neurogenic inflammation**. Both processes can occur concurrently in the context of persistent and/or pathological pain, highlighting the importance of peripheral and central neuro-immune interactions in the development of pain. Such homeostatic processes protect the body from exogenous and endogenous harmful agents and/or events, providing an evolutionary advantage in a hostile environment, helping the species to survive and adapt.

Nociceptive and neuropathic pain as well peripheral and central sensitization have been well studied and described at the level of the dorsal root ganglion (DRG) and spinal cord (Melik Parsadaniantz et al., 2015). Of note, all these conditions may also occur in the cornea and more specifically in dry eye disease, although the underlying cellular and molecular mechanisms are still not fully understood.

### I.3 Dry eye disease and ocular pain

Dry eye disease (DED) is defined as a ‘‘*multi-factorial disease of the ocular surface characterized by a loss of homeostasis of the tear film, and accompanied by ocular symptoms, in which tear film instability and hyper-osmolarity, ocular surface inflammation and damage, and neuro-sensory abnormalities play etiological roles*" (Craig et al., 2017). DED affects, at least in a symptomatic way, 5 to 50% of the adult population in developed countries (North America, Europe and Asia). The prevalence increases with age, especially after 50 years and is more prevalent in women than in men. The magnitude of this increased risk in women varies significantly from study to study, usually ranging from 20 to 80% (Stapleton et al., 2017). The most consistent risk factors are age, gender, ethnicity, meibomian gland dysfunction,

connective tissue disease, Sjögren's syndrome, androgen deficiency, computer use, contact lens wear, estrogen replacement therapy, hematopoietic stem cell transplantation but also certain environmental conditions and medications (Stapleton et al., 2017). DED has gained recognition as a significant public health issue given its prevalence, morbidity and associated financial burden.

Symptoms of dry eye encompass visual disturbances, such as fluctuating or blurry vision, and dysesthesias (*i.e.* unpleasant abnormal sensations, often described as itch, dryness, foreign-body sensation and irritation) but also painful sensations, at the level of the ocular surface (Craig et al., 2017). Such painful sensations are reported by patients as being evoked by exposure to wind, light (photophobia), low humidity and extreme temperatures.

There is a growing interest in the study of pain in DED for two main reasons. First, there is a clear –currently unmet– need to better manage this disease (and related pain) as it represents a debilitating condition that can affect dramatically the patient's quality of life (Saldanha et al., 2018). Second, investigating pain in DED can help gain a better understanding on the underlying neuro-sensory abnormalities that have been implicated in the disease's pathophysiology as indicated in the aforementioned definition (Craig et al., 2017, Guerrero-Moreno et al., 2020, Tsubota et al., 2020).

## II. The homeostatic ocular surface

### II.1 The concept of ocular surface

The ocular surface is the anterior part of the eyeball in direct contact with the external environment, comprised of the superficial epithelium of both the cornea and conjunctiva. From a functional point of view, the ocular surface is also composed of lacrimal and lipid glands, the tear drainage system, the tear film and the eyelids (**Figs. 1 and 2**) (Cher, 2014).

Its main role is to protect and isolate the structures inside the eye from the external environment, including potentially harmful and pathogenic agents. Additionally, the cornea and its overlying tear film are in charge of approximately 70% of light refraction onto the lens which further focuses it onto the retina. Tears, produced by ocular adnexa, are important in the maintenance of corneal homeostasis; especially considering that the cornea is an avascular tissue, depending on the tear film for absorption of nutrients and oxygen. Tears also

clear the ocular surface of cellular debris and lubricate the tarsal-cornea/conjunctiva interface to avoid damage during blinking (Sridhar, 2018).

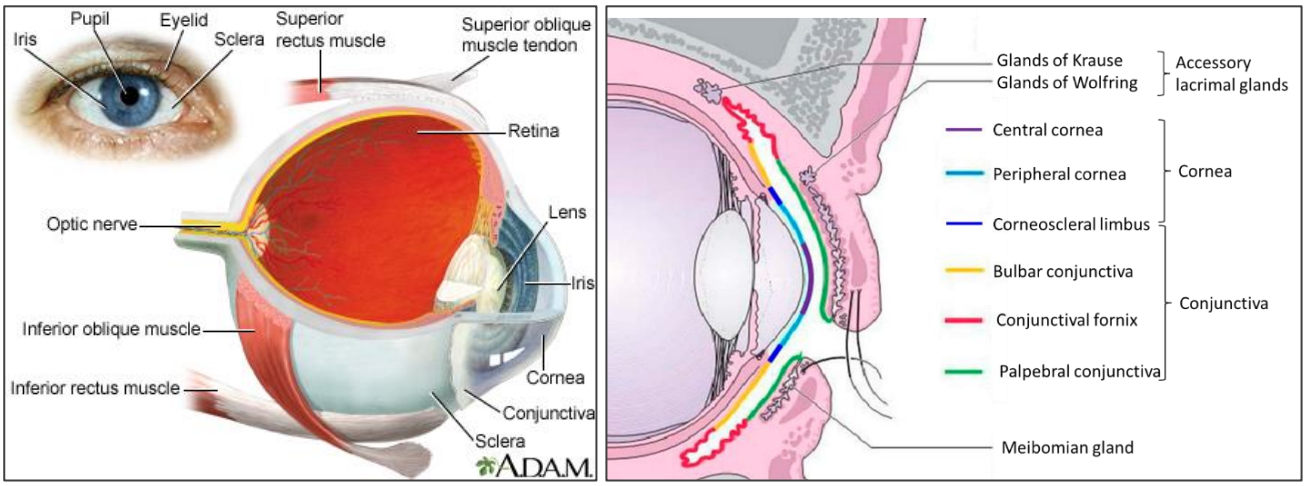


**Figure 1: Eye anatomy and the ocular surface**

***Left panel.*** Anatomical view of the human eye. *From Olson, 2008.*
***Right panel.*** Cornea and conjunctiva are continuous epithelia that can be further subdivided anatomically in different segments. Glands of Krause are located in the fornix while glands of Wolfring lie on the edge of the tarsus. Meibomian glands are perpendicular to the eyelid where they open their secretory duct. *From Therithal info (Chennai), 2018.*

### II.2 Lacrimal glands

The liquid part of tears as well as electrolytes and proteins are produced by the main and accessory exocrine lacrimal glands, the main lacrimal gland providing the major part of the tear liquid. The basic unit of the lacrimal gland is the acinus, an alveolar-shaped structure composed by secretory cells connected by ducts (Schechter et al., 2010). Acini are grouped in lobules, tree-shaped structures which are in turn organized in lobes. Each gland is composed by several lobes. In these structures, the lacrimal fluid is produced via a merocrine secretion of proteins and mucins, and the transepithelial secretion of electrolytes and water that are then excreted by the main secretory duct (Obata, 2006) **(Fig. 2)**.

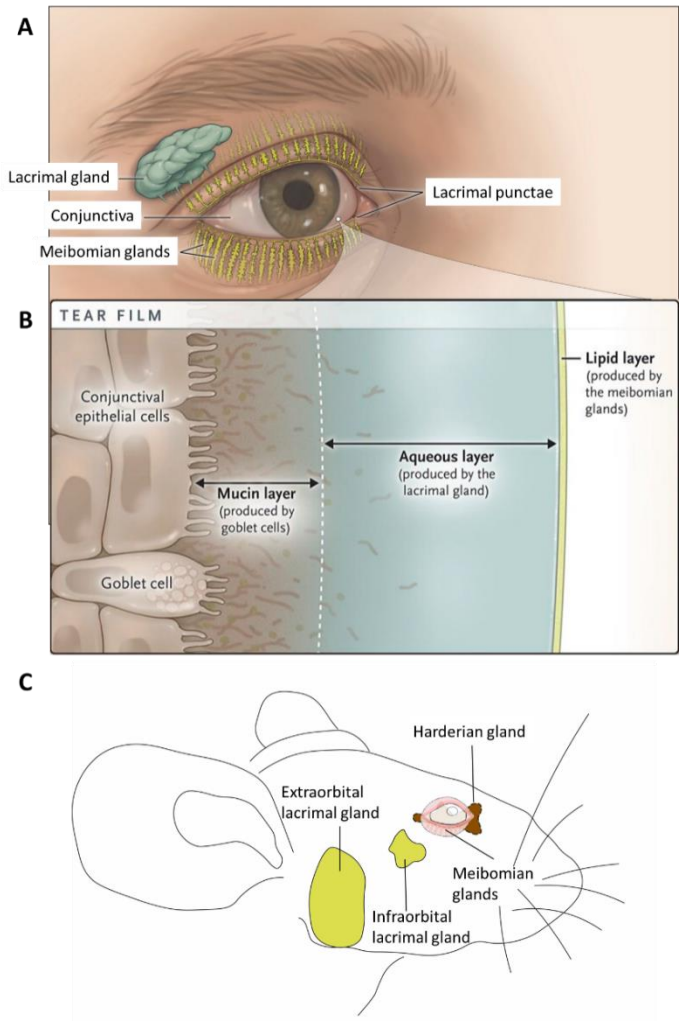


**Figure 2: Components of the tear system in the ocular surface**

**A.** Human ocular surface. The main lacrimal gland is located in the supero-lateral aspect of the orbit, within the lacrimal fossa. Meibomian glands are placed parallel to each other, inside of the eyelid and perpendicular to its edge.

**B.** Principal layers of the tear film.

**C.** Mouse ocular surface. Aqueous tears in mouse are produced by the extra-orbital lacrimal gland and the infra-orbital lacrimal gland. The lipid layer is produced mainly by the Harderian gland, just behind the eye and the meibomian glands, placed along the eyelid.

*Images A and B from Elevation vision.*

In humans, the main lacrimal gland is placed around the lateral edge of the levator palpabrae superioris muscle and is divided in the orbital and palpebral lobes, although both are continuous with each other. The orbital lobe is located in the lacrimal fossa, while the palpebral lobe is located at the edge of the levator palpebrae, in contact with the superior and lateral fornix of the conjunctiva. Both palpebral and orbital lobes extend secretory ducts opened through the superior conjunctival fornix (Obata, 2006).

The accessory lacrimal glands are located in the lamina propria of conjunctiva and could be classified anatomically as glands of Krause when located in the fornix and glands of Wolfring when they lie within the edge of the tarsus, between the ends of the meibomian glands (Obata, 2006) (**Figs. 1 and 2**).

In mice, the main lacrimal gland is split in two different anatomical subdivisions with a common secretory duct. The biggest is the extra-orbital lacrimal gland, located

subcutaneously anterior to the ear and the smallest, the intra-orbital lacrimal gland, attached to the bulbar conjunctiva (**Fig. 2C**) (Gossman, 2004).

Lacrimal glands, both main and accessory, are innervated in both species by sympathetic fibers from the superior cervical ganglia and, more abundantly, by parasympathetic fibers from the pterygopalatine or ciliary ganglia. Both sympathetic and parasympathetic fibers control protein and electrolyte secretion by acting directly on the glands, while sympathetic fibers also control blood vessel contraction and dilation as an indirect mechanism of lacrimal flow control. Sensory fibers originated from the trigeminal ganglion have also been found (Gossman, 2004).

### II.3 Meibomian Glands

Meibomian glands secrete the lipid phase of the tear film, which prevents excessive evaporation of the tear fluid. Each individual gland is composed of a long central duct completely surrounded by acini, which produce meibum, a lipidic secretion, through an holocrine secretory mechanism. Holocrine secretion consists of the rupture of the cell's plasma membrane to release its intracellular contents along with membrane lipids. Each acinus is connected to the central duct by a ductule. In the interior of the central duct, endogenous microorganisms modify the lipidic content of meibum, before its secretion via a keratinized secretory duct placed in the eyelid (**Fig. 2**) (Butovich, 2017, Obata, 2002).

In humans, there are around 31 independent meibomian glands in the upper lid and around 26 in the lower lid, parallel to each other and perpendicular to the lid margin (Knop et al., 2011). They are elongated through all the tarsal plates in a way that during blinking, compression from the orbicularis muscle promotes "peristaltic" meibum flow. The other force driving meibum secretion is the continuous replacement of meibocytes, the cells that compose the acinus (Knop et al., 2011).

Innervation and blood supply of meibomian glands are similar to that of lacrimal glands, presenting as a dense meshwork of parasympathetic and sympathetic fibers originating in the pterygopalatine ganglion and cervical ganglion respectively. Also, they receive some sensory fibers from the trigeminal ganglion (Satoh et al., 1996); (Knop et al., 2011).

As sebaceous glands, they are highly influenced by lipophilic hormones. Androgens and, more specifically testosterone, are the most important, originating from both the blood supply and

*de novo* local synthesis. Androgens modulate numerous genes in meibomian glands leading to an increase in lipid production via the binding of their respective intracellular receptors. Estrogens, on the other hand, have the opposite effect, directly inhibiting androgen activity and therefore inhibiting lipid production. Hence, the imbalance of these hormones is an important factor in the onset and development of DED secondary to meibomian gland dysfunction (Knop et al., 2011).

From an anatomical and functional standpoint, mouse meibomian glands are very similar to humans (Gossman, 2004).

### II.4 Harderian gland

The Harderian gland (HG) contributes to the lipid phase of the tear film (**Fig. 2**). HG is a gland associated with the nictitating membrane (also known as the third eyelid), and thus is found only in species that possess this structure, such as rodents (including mice) but not primates or humans. It is attached to the posterior region of the orbit and its duct opens through the nictitating membrane. As the other glands, it is comprised of an acinar epithelium connected by ducts. Sympathetic and parasympathetic fibers surround this gland. In most animal species this gland has numerous functions in immunity, pheromones secretion, thermoregulation and osmo-regulation, but their role in rodents apart from lacrimal secretion is unclear (Payne, 1994, Satoh et al., 1996).

### II.5 Conjunctiva

The conjunctiva is a highly vascularized tissue surrounding the cornea (**Fig. 1**). It acts as a barrier against environmental dangers, secretes water and electrolytes for the tear film and keeps the eye moist to facilitate ocular movements and blinking. It extends from the lid margin covering the inner surface of the palpebrae to the dorsal and ventral fornix (palpebral conjunctiva), where it folds through the sclera up to the corneoscleral limit (bulbar conjunctiva). It is comprised of a vascularized collagenous connective tissue (stroma) covered by an epithelium composed by epithelial and goblet cells. Those **goblet cells** are apocrine cells scattered among the epithelial cells and are responsible of the secretion of gel-forming mucins contributing to the muco-aqueous nature of the tear film lubricating the eye (Bron et al., 2017).

## II.6 Cornea

The cornea is an avascular (depleted of lymphatic and blood vessels) transparent tissue which protects, similarly to the conjunctiva, the internal part of the eye from external dangers. In humans, it constitutes a convex aspheric optical system with a refractive index of 1.3375, 40-44 diopters, accounting for 70% of total light refraction in the eye, which is thus very important for correct vision. Such refractive power is under the influence of the air-tear film-cornea interface (Winkler et al., 2015), that is altered in cases of DED thus accounting for the blurry vision that frequently accompanies such disease (Montes-Mico, 2007).

The cornea's diameter is around 11.5 mm in the horizontal axis and 10.5 mm in the vertical axis with a curvature radius of 7.8 mm. Corneal thickness increases from center (551-565 µm) to periphery (612-640 µm) in humans. In C57BL/6 mice, corneal diameter is 2.6 ± 0.2 mm and thickness is 137.02 ± 14.0 µm in the central cornea and 90.55 ± 1.9 µm in the peripheral cornea (Henriksson et al., 2009).

As the cornea is an avascular tissue, its cells receive necessary blood components through the tear film and aqueous humor. The cornea is composed of different layers: epithelium, Bowman's layer, stroma, Descemet's membrane, and endothelium. (Henriksson et al., 2009; DelMonte and Kim, 2011; Eghrari et al., 2015; Masterton and Ahearne, 2018; Sridhar, 2018; Downie et al., 2021).

### A. Corneal epithelium

The corneal epithelium is the most innervated structure in the human body. It is composed of approximately 600 terminals/mm$^2$ ; the cornea is thus 300 to 600 times more sensitive than skin and 20-40 times than the dental pulp (Muller et al. , 2003; Marfurt et al., 2010). The corneal epithelium is a stratified non-keratinizing squamous epithelium of cells laterally attached via intercellular tight junctions. This provides an epithelial barrier that avoids the entry of tears, toxins and pathogenic organism in the intercellular spaces (Sridhar, 2018). The corneal epithelium is 40-50 µm thick in humans (DelMonte and Kim, 2011) and 40.59 ± 5.8 µm thick in C57BL/6 mice (Henriksson et al., 2009). It is composed by three different sub-layers and a basal membrane (**Fig. 3**):

- **Superficial epithelium:** composed by 2-3 layers of flat polygonal cells. Its surface is composed of microvilli covered by a charged glycocalyx, increasing the area in contact with the tear film and its stability.
- **Wing cells or supra-basal epithelium:** composed also by 2-3 layers of flat cells, although less flat than the superficial epithelium.
- **Basal cells:** They are a single layer of columnar epithelium, characterized by their abundant intercellular junctions including gap junctions and *zonulae adherens*, attached to the underlying basement membrane by hemi-desmosomes.
- **Basement membrane:** an acellular layer secreted by basal cells and composed of type IV collagen and laminin that serve as physical barrier between the epithelium and the stroma. (DelMonte and Kim, 2011; Eghrari et al., 2015; Downie et al., 2021)

In mice, the layout is similar to humans; however, they have about 12 cell layers in total (Henriksson et al., 2009).

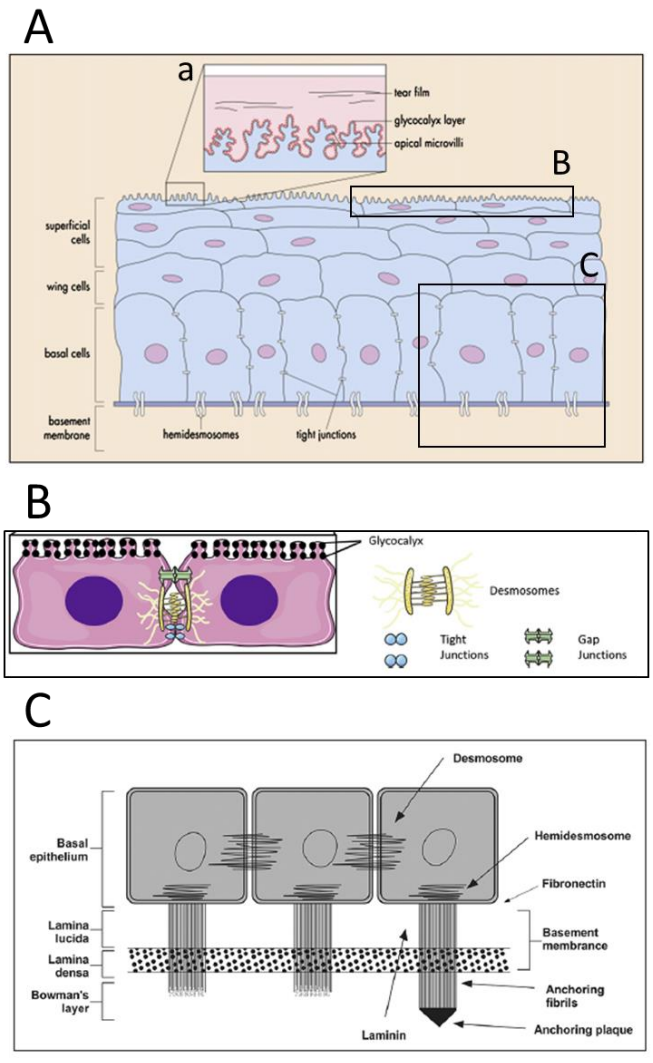


**Figure 3: Histological structure of the corneal epithelium**

**A.** Cross-sectional view of the corneal epithelium and its layers. It should be noted that the number of cell layers and junctions has been simplified. **"a"** square shows the superficial microvilli covered by a glycocalyx layer in contact with the tear film. *Adapted from DelMonte and Kim, 2011.*
**B.** Superficial epithelial cells intercellular junctions. *Adapted from Masterton and Ahearne, 2018.*
**C.** Basal epithelium-basement membrane scaffold comprised of hemi-desmosomes. *Adapted from Sridhar, 2018.*

Epithelial stem cells with great mitotic capacity are located at the corneoscleral limbus. From there, they differentiate into transient amplifying cells and migrate to peripheral and central cornea in a radial manner. Once there, they can differentiate again into basal cells and become part of this cell layer. Basal cells may divide to give rise to wing cells, which will then continue to ascend towards the superficial cornea. With each differentiation, these cells lose some mitotic activity until they lose it completely giving rise to wing cells (DelMonte and Kim, 2011, Eghrari et al., 2015).

### B. Stroma

The human stroma is approximately 470 µm thick, representing 90% of the corneal thickness, being thicker in the periphery than in the center. The principal characteristics of this structure are its transparency and mechanical strength which rely on the highly organized network of type I and V collagen fibers and extracellular matrix comprised of proteoglycans and glycoproteins. This network is produced and maintained by **keratocytes**, able to synthesize collagen and extracellular matrix components but also matrix metalloproteinases. The stroma of the cornea plays essential roles in corneal functions, mainly light transmission.

The **Bowman layer** (also known as Bowman's membrane) is an acellular, membrane-like zone located immediately posterior to the basement membrane of the epithelium. It is an acellular condensate of collagen and proteoglycans with no regenerative ability, with a thickness of 8-12 µm, exclusive to primates. It protects the sub-epithelial nerve plexus which arises from the anterior stroma.

The anterior stroma, due to its superior packing density is more rigid than the posterior stroma, maintaining corneal shape even after extreme swelling for example (DelMonte and Kim, 2011; Eghrari et al., 2015; Sridhar, 2018; Downie et al., 2021) .

Just in the deepest limit of the stroma, an additional layer has been described: the pre-Descemet or **Dua's layer**, 10.15 ± 3.6 µm thick and very resistant to mechanical forces, although its existence remains controversial (Dua et al. , 2013).

### C. Endothelium

**Descemet's membrane** is the basement membrane of the corneal endothelium. It measures approximately 3 µm in thickness in children, gradually thickening to 10 µm in adults.

The corneal endothelium is a 4 µm thick monolayer of hexagonal flat cells without mitotic activity constituting a honeycomb-like appearance. Their main function is to maintain the deturgesced state of the corneal stroma, *i.e.* its relative dehydration (78% water content) as compared to the hypertonic aqueous humor, necessary for stromal transparency. To this aim, adjacent cells share extensive lateral inter-digitations and both gap and tight junctions. In their lateral membranes, they contain a high density of $Na^+/K^+$-ATPase pumps which force the water to remain outside the cornea. Additionally, they are closely connected to the Descemet's membrane by hemi-desmosomes, in a similar fashion as that of epithelial basal cells and their basement membrane (DelMonte and Kim, 2011; Eghrari et al., 2015; Sridhar, 2018; Downie et al., 2021).

## II.7 The immune system of the ocular surface

To completely understand the structure and function of the ocular surface immune system, cornea, limbus and conjunctiva have to be studied as a whole as they compose a continuous epithelium. Epithelial cells form tight junctions and proliferate constitutively constituting together with Bowman's membrane a physical barrier to exogenous agents. Additionally, those epithelial cells segregate antimicrobial peptides to the tear film (Foulsham et al., 2018; Liu and Li, 2021). The cornea, unlike the conjunctiva, must remain transparent to allow light to enter the eye for proper vision. This specific requirement largely shapes the functioning of the immune system as an exacerbated immune response in this tissue would result in corneal opacification and thus vision loss. In this sense, the cornea is an "**immuno-privileged tissue**". It is an avascular structure, lacking blood and lymphatic vessels, limiting the migration of circulatory immune cells from blood and antigen-presenting cells and sensitized lymphocytes to and from lymphatic vessels (Foulsham et al., 2018). The corneal epithelium maintains the "immature" state of immune cells and inhibits vessel growth by cellular signals such as the membrane expression of programmed death ligand-1 (PD-L1) which, upon binding to its receptor on effector T cells, triggers their apoptosis (Stern et al., 2010). The corneal epithelium also expresses Fas ligand, which inhibits neovascularisation and induces apoptosis of immune

cells (Stern et al., 2010). Another molecule constitutively expressed by corneal epithelium is thrombospondin-1 (TSP-1), an extracellular matrix protein whose immunoregulatory function is principally performed by transforming the latent form of transforming growth factor-β (TGF-β) produced by goblet cells, to its functional activated form, which serves as a critical anti-inflammatory cytokine (Stern et al., 2010). Corneal epithelial cells also maintain the avascular state by producing soluble vascular endothelium growth factor receptor-1 and membrane-expressed vascular endothelium growth factor R-3, which sequester the angiogenic factors vascular endothelium growth factor-A and vascular endothelium growth factor-C, respectively, thus reducing unwanted angiogenesis (Stern et al., 2010).

The most relevant immune cells at the level of the ocular surface are dendritic cells, Langerhans cells, macrophages and lymphocytes (**Fig. 4**).

### A. Dendritic cells

Dendritic cells (DCs) are antigen-presenting cells (APCs), morphologically characterized by their membranous or spiny projections. Other terms used to identify DCs, especially in clinical imaging studies, are "APCs", "dendritiform cells" or just "immune cells" (Chinnery et al., 2021).

DCs are hematopoietic cells ($CD45^+$) and have phagocytic capacity ($Iba1^+$) (Chinnery et al., 2021). In the absence of inflammation, DCs density is concentrated in the conjunctiva and decreases from the limbus to the center of the cornea.

Many of them are called "tolerogenic DCs", as they possess diminished antigen presentation, production of regulatory cytokines, and generation and expansion of regulatory T ($T_{reg}$) cells. At the corneal level this "immature" state of the DCs is characterized by low expression levels of major histocompatibility complex MHC class II (MHC-II) antigens (Stern et al., 2010).

According to their origin and membrane markers, DCs can be classified at the ocular surface into different subtypes:

- **Conventional DCs (cDCs)**: They originate from a specific myeloid precursor of cDC which, after reaching the ocular surface via blood vessels, establishes and differentiates into $CD11b^+$ $CD11c^+$ cells. cDCs constitute for the majority of DCs on the ocular surface and, after activation, are primarily responsible for the lymphocyte sensitization that leads to the adaptive immune response (Chen et al., 2022).

- **Plasmacytoid DCs (pDCs)**: They are a special type of DCs of lymphoid or myeloid origin. In contrast to cDCs, these cells express low levels of CD11c and do not express CD11b. They account for 15-25% of all haematopoietic cells ($CD45^+$) at the corneal level and appear to be a key cell type capable of inducing tolerance by promoting generation of $T_{reg}$ cells and preventing their dysfunction. Similarly to epithelial cells, pDCs express TSP-1 and PD-L1, inhibiting T-cell action (Stern et al., 2010; Chen et al., 2022).

The protrusions of DCs are continuously stretched between epithelial cells, contributing to their antigen-trapping function (Liu and Li, 2021). Once they have captured and processed an antigen, they migrate to the lymph nodes in the drainage region and trigger the tolerance or amplification of naive T-cells depending on the immunological context (Liu and Li, 2021), playing an essential role in triggering adaptive immune responses. The imbalance in this process is thought to participate to the development of DED (Foulsham et al., 2018; Chen et al., 2022).

### B. Langerhans Cells

At the corneal level, the term Langerhans cells (LCs) has sometimes been used interchangeably to refer to DCs. However, they are a slightly different cell type, expressing Langerin and containing Birbeck granules. In contrast to DCs, LCs are found exclusively in the epithelium and express low levels of CD11b while being positive for CD11c. Ontogenetically, LCs originate from fetal liver monocytes that colonize the outer epithelia and are maintained by local proliferation. While this cell type is the most abundant APCs at the skin level, in the cornea they seem to constitute a minority of APCs. Like DCs, LCs are professional APCs capable of triggering the T-lymphocyte-mediated immune response (Hamrah et al. , 2002; Frutos-Rincon et al. , 2022).

### C. Macrophages

Macrophages are ubiquitously present innate immune cells in humans and both invertebrate and vertebrate animals. They are specialized cells involved in the detection, phagocytosis ($Iba1^+$) and destruction of bacteria and other harmful organisms and particles. Macrophages also promote the homeostasis of different tissues *via* local trophic, regulatory and repair functions. Typically, the term "macrophage" is given to monocytes (circulating blood cells)

when they settle in a given tissue such as the cornea. However, there are also primitive macrophages that have remained in the cornea since embryonic stages (Liu and Li, 2021). Macrophages represent most of the stromal $CD45^+$ cells in central cornea (Brissette-Storkus et al., 2002). Following inflammation or injury, additional monocytes from the peripheral blood arrive to the cornea. Once in the cornea, monocytes differentiate into inflammatory macrophages contributing to phagocytosis and play a role in initiating the pro-inflammatory immune response.

### D. T-cells

T-cells are a type of lymphocyte originating from the thymus with different functions depending on their subtype:

- **Regulatory T ($T_{reg}$) cells** ($CD4^+$ $CD25^+$)**,** also known as suppressor T cells: They modulate the immune system maintaining tolerance to self-antigens and contributing to anti-microbial defense. They are the principal immunoregulatory actors that restrict and suppress pro-inflammatory effector T-cell response by secreting TGF-β and IL-10, contributing to the "immune privilege" of the ocular surface (Chen et al., 2022).
- **T helper ($T_H$) cells** ($CD4^+$ $CD3^+$): They are important in the initiation and development of the immune response due to their ability to produce interleukins. This cell type is further divided into three subtypes:
    - **$T_H1$**: Produces IL-2 and interferon gamma contributing to the cellular immune response.
    - **$T_H2$**: Produces IL-4, IL-5 and IL-6 mediating the humoral immune response.
    - **$T_H17$**: Produces IL-17 inhibiting the action of $T_{reg}$ cells.
- **Cytotoxic T cells** ($CD3^+$ $CD8^+$): Once activated, they are the main effectors of the cytotoxic activity of the cellular immune response.

At the level of the ocular surface, these cell types have been found mostly in the conjunctiva and corneal limbus in non-inflammatory conditions. These T-cells play a vital role in maintaining ocular surface homeostasis (Liu and Li, 2021). Conversely, pathological imbalance of the function of these cells can trigger numerous ocular surface diseases. In the case of DED, an increase in the activity of $T_H1$ and $T_H17$ cells has been reported. In a mouse model of DED, accumulation of infiltrating $CD4^+$ T cells is associated

with increased cytokine production, epithelial cell apoptosis and decreased goblet cell density (Stern et al., 2010).

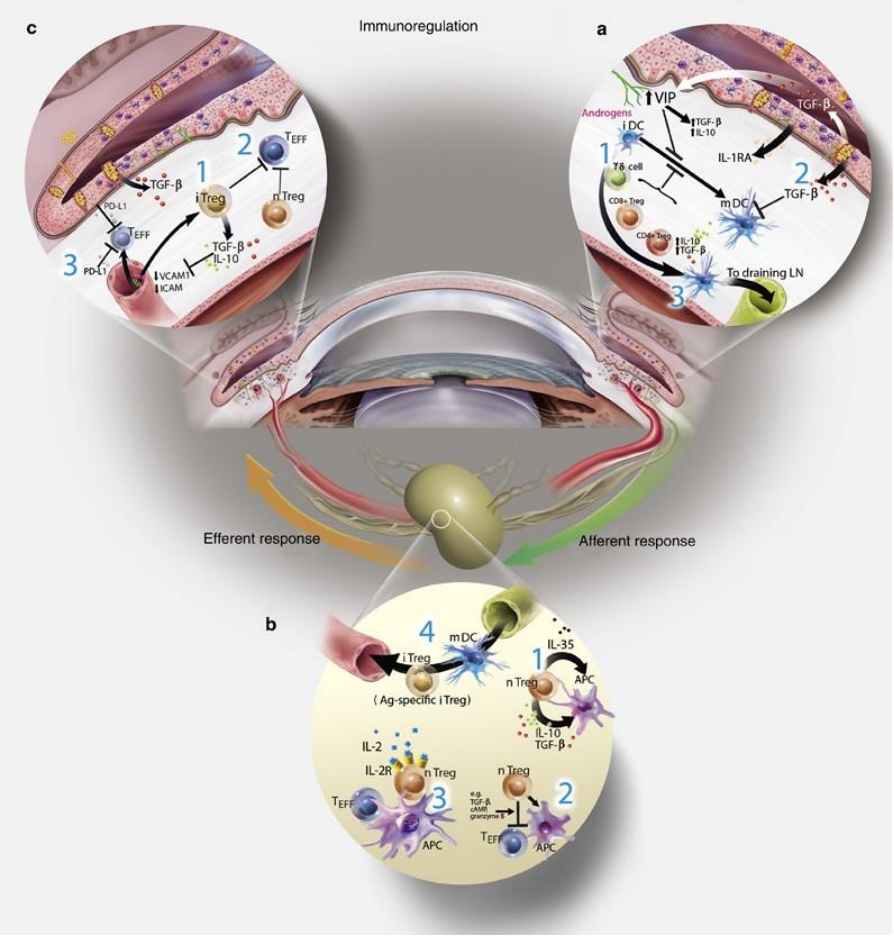


**Figure 4: Immunoregulation of the ocular surface**

**(a)** The ocular surface tissues contain a variety of soluble and cellular factors to reduce inflammation-induced pathology. Those implicated in immunoregulation within the ocular surface tissues include: (1) natural $T_{reg}$ ($nT_{reg}$) cells, which represent many of the conjunctival intraepithelial lymphocytes, and are thought to dampen or inhibit the inflammatory/autoimmune response on the ocular surface; (2) the anti-inflammatory cytokine TGF-β present on the ocular surface, that has profound suppressive effect on resident dendritic cell maturation in the cornea, autoreactive T-cell proliferation, differentiation, and survival, and $T_{reg}$ differentiation and maintenance. The activity of the potent acute response proinflammatory cytokine interleukin (IL)-1 is modulated by the IL-1 receptor antagonist (IL-1RA), expressed and secreted by corneal and conjunctival epithelial cells. Vasoactive intestinal peptide (VIP) also seems to be protective; VIP secreted by sensory nerve endings in the cornea increases production of TGF-β and IL-10 and inhibits expression of proinflammatory cytokines/chemokines, IL-1β, tumor necrosis factor (TNF)-α, interferon (IFN)-γ, and CXCL2. Hormones are also implicated in curbing inflammation and maintaining corneal homeostasis. In addition, the corneal epithelium also expresses vascular endothelium growth factor (VEGF) receptor-1 to sequester VEGF and reduce neovascularization. APCs bearing self-antigen derived at the ocular surface may migrate to the regional lymph nodes to promote antigen-specific inducible $T_{reg}$ (iTregs).

**(b)** Immunoregulation in the lymphoid organs: nTregs may exert their immunosuppressive function by (1) releasing soluble factors (e.g., TGF-β, IL-10), (2) cell–cell contact, which disables

pathogenic effector T cells and/or APCs, and/or competing for soluble factors (e.g., IL-2). (4) $iT_{regs}$ may use similar mechanisms to inhibit cells bearing or responding to autoantigens. It is possible that these $T_{reg}$-dependent mechanisms may also function within the ocular surface tissues.
**(c)** Other peripheral immunoregulatory mechanisms: additional mechanisms also limit access and effector function of autoreactive T cells within the ocular surface tissues: (1) TGF-β and (2) $nT_{regs}$ and $iT_{regs}$ are suggested to suppress infiltrating autoreactive lymphocytes and low-level expression of integrins in the healthy ocular surface endothelial cells, coupled with expression of the programmed death ligand-1 (PD-L1), negatively regulates activated T cells within the ocular surface tissues. *From Stern et al., 2010.*

# III. The corneal nociceptive pathway

## III.1 The cornea: *a nociceptive hub*

As previously stated, the corneal epithelium is the most densely innervated tissue by nociceptors in the human body, with 600 terminals/$mm^2$ (Muller et al., 2003; Marfurt et al., 2010). It is an excellent tissue to study the morphological and functional properties of peripheral nociceptors as well as neuro-immune interactions, not only because of its huge nerve density, but also because of its easy accessibility.

The most superficial corneal nerve endings are the **intra-epithelial terminals**. They distribute between epithelial cells and some of them even emerge beyond the exterior border of the superficial epithelial layer, in direct contact with the tear film. Three different morphologies have been described for these fibers (**Fig. 5**): complex, ramified and simple. As previously explained, the corneal epithelium is a dynamic structure, with an average epithelial cell lifespan of 7-10 days. It would therefore be expected that the intraepithelial terminals, intimately linked to these cells, would also be dynamic structures, although there are no extensive studies on the subject to this day.

The intraepithelial terminals emerge after a 90° angle turn from the sub-basal nerve fibers located at the interface between Bowman's layer and the basal epithelial cells. Such sub-basal nerve fibers are organized parallel to the ocular surface in a dense meshwork with abundant anastomoses in the so-called **sub-basal plexus** (**Fig. 5C**)**.** They arise from nerves originating from the corneal stroma that are defasciculated into multiple fibers just as they cross Bowman's membrane. This penetration of Bowman's membrane is perpendicular and therefore the fibers rotate again to remain parallel to the ocular surface. The sub-basal plexus can be studied in humans using *in vivo* confocal microscopy (IVCM, detailed in section ahead), including pathological states as DED. Based on IVCM and associated histological studies, it is

known that sub-basal nerve density increases from the peripheral to central cornea, with the frequent formation of whorl-like or “vortex” patterns near the center. Furthermore, pathological states affect sub-basal nerve density (Muller et al., 2003). Mice do not have a Bowman’s membrane but their corneal nerves still penetrate the epithelial basement membrane when they emerge from the stroma to form the sub-basal plexus. It has been demonstrated that this phenomenon is supported by dendritic cells (Gao et al., 2016).

Just below the Bowman’s membrane, corneal fibers are organized in a **sub-epithelial plexus** (**Fig. 5C**), less developed in mice than in humans. Those fibers emerge from groups of axons, the so-called **main stromal nerve bundles** or **stromal nerve trunks** (**Fig. 5C**) who branch successively before penetrating the Bowman’s layer. Altogether, these nerves are concentrated in the anterior one-third of the corneal stroma in a radial manner, parallel to the ocular surface. They penetrate the stroma from the corneoscleral limbus losing their myelin sheath in the case of myelinated fibers. In humans, stromal nerves penetrate from the corneoscleral limbus at regular intervals. However, in mice, the nerves penetrate from four quadrants and defasciculate irregularly until they cover the cornea (Frutos-Rincon et al., 2022).

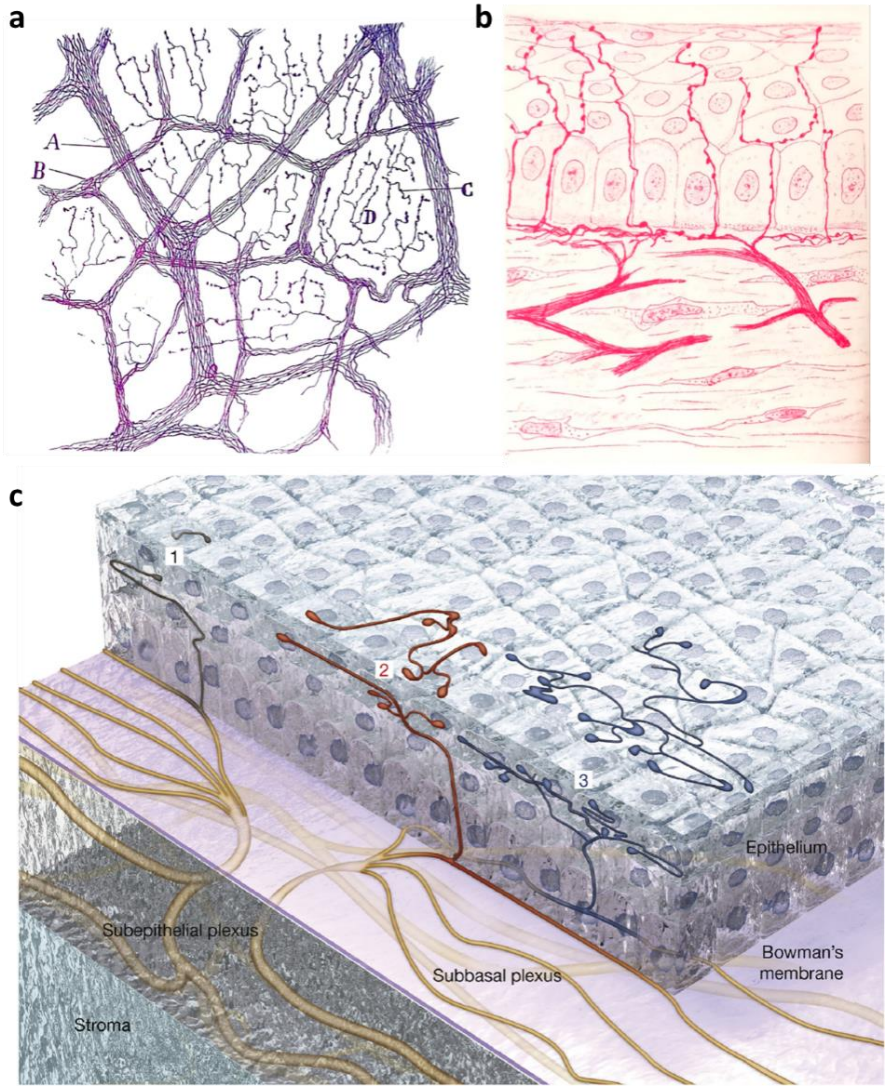


**Figure 5: The corneal innervation**
**a,b.** Early drawings from Ramon y Cajal depicting corneal innervation. **a:** Rabbit corneal plexus stained by methylene blue. **A:** fundamental plexus (stromal plexus); **B:** sub-basal plexus; **C:** inter-epithelial terminal branches (intraepithelial terminations) **D:** sub-epithelial terminal branches. **b.** Nerve endings in adult rabbit corneal epithelium. Staining by gold chloride. Note how the finest nerve fibrils run between the epithelial elements, ending in varicosities near the corneal surface. *From Ramón y Cajal, 1909*.
**c.** Modern representation of corneal innervation showing the different layers and nerve morphologies: complex (1, black), ramified (2, red) and simple (3, blue).
*From Belmonte et al. , 2017.*

### III.2 Classification of corneal fibers

Corneal nerve fibers can be classified based on different criteria. First, corneal nerve fibers can be separated depending on their hodology and function between **sensitive fibers**, when they belong to the somato-sensory system, and **sympathetic** or **parasympathetic fibers** when they are part of the autonomic nervous system**.**

Corneal fibers can also be classified based on their conduction velocity. Two subtypes of sensory neurons have been described in the cornea:

- **Unmyelinated C fibers**: Their conduction velocity in the cornea is 0.96 ± 0.22 m/s (mean ± SD) (MacIver and Tanelian, 1993), so their diameter should range between 0.2 and 1.5 µm but it has never been experimentally corroborated.
- **Aδ fibers:** Their conduction velocity in the cornea was 2.82 ± 0.54 m/s (MacIver and Tanelian, 1993). This is an abnormally low value for this type of myelinated fiber (that should be higher than 5 m/s), which is explained by the fact that they lose their myelin as they enter the cornea. Their diameter will therefore be smaller than typical Aδ fibers (1-5 µm).

Unlike somatic nerve innervation, the cornea lacks Aβ fibers.

Electrophysiological studies have allowed a classification of the corneal nerves based on their sensory modalities in mechano-nociceptors, cold receptors and poly-modal nociceptors. Finally, histological studies can characterize corneal nerves on the basis of different markers:

- **Peptidergic:** They express SP or CGRP.
- **Non-peptidergic:** They do not express either SP or CGRP but have affinity for isolectin B4.
- **Expression of specific channels:** Differential expression of TRPV1 (transient receptor potential cation channel subfamily V member 1), TRPM8 (transient receptor potential cation channel subfamily member 8) and Piezo2 allows histological classification of corneal fibers depending on their primary sensory modality (warm, cold and touch respectively).

The different classes of corneal nerve fibers and their functional classification has been the subject of a review we published as part of this project (Guerrero-Moreno et al., 2020).

### III.3 Corneal nerves: *from the eye to the trigeminal ganglion*

Corneal sensory fibers circle the orbit through the **uveal nerves** (May, 2004). Once they reach the posterior part of the orbit, they navigate around the optic nerve in the **long ciliary nerves** to converge into the **nasociliary nerve** then enter the **trigeminal ganglion** (**Fig. 6**).

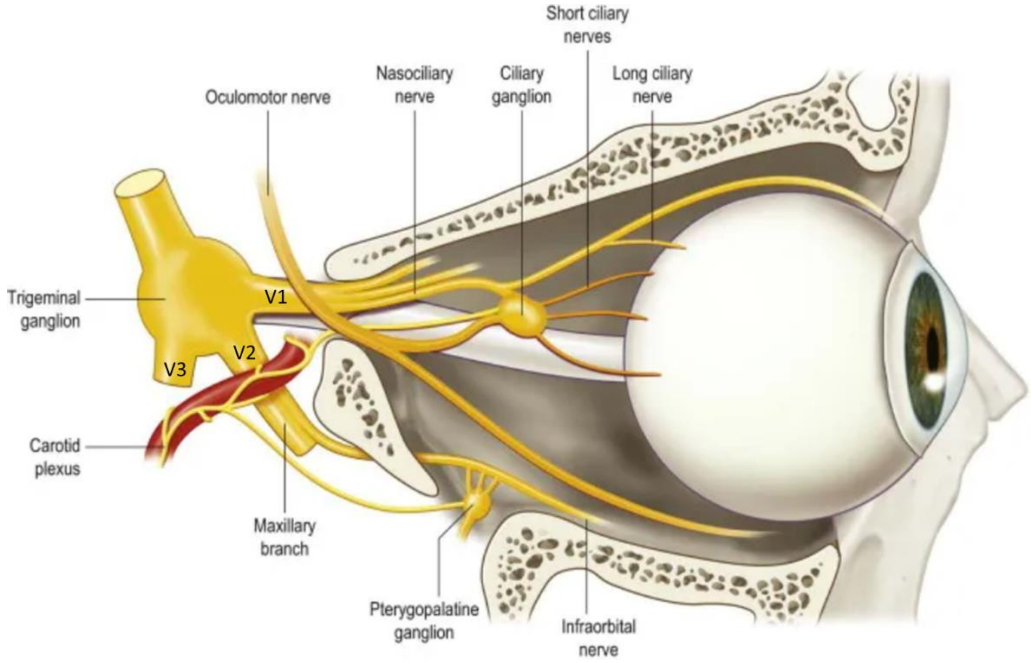


**Figure 6: Innervation of the eye**
Medial view of the orbit showing the sensory and autonomic nerves directed to the eye. The ophthalmic ($V_1$) branch of the trigeminal ganglion gives the nasociliary nerve that sends long and short ciliary nerves to the eyeball, the last through the ciliary ganglion. Frontal and lacrimal nerves are not shown in this picture. The maxillary ($V_2$) branch gives the infraorbital nerve that innervates, among other regions, the lower eyelid. Sympathetic fibers from the superior cervical ganglion, travelling within the carotid plexus and parasympathetic branches of the ciliary and the pterygopalatine ganglia join short ciliary nerves. *Adapted from Rubin, 2007*.

The **trigeminal ganglion** (TG), historically known as the Gasserian ganglion, the semi-lunar ganglion or Gasser's ganglion, is a canoe-shaped structure located parallel to the base of the skull, in Meckel's cave. There are two parallel trigeminal ganglia per individual, one on the right and the other on the left, each innervating their corresponding ipsilateral structures. The human TG contains around 27,400 somas of pseudo-unipolar neurons, which extend one end of their axons to the structures they innervate, including the face, the ocular surface and the cerebrovascular system, and the other to the brain stem trigeminal nuclear complex. Those somas are segregated in the ganglion depending on their respective trigeminal branch:

- **Ophthalmic branch ($V_1$)**: It innervates the superior part of the face, including the eye. Several nerves bring sensory information to the somas of this branch, including the nasociliary nerve (branching into the long ciliary nerve which contains sensory afferents from the cornea and conjunctiva), the lacrimal nerve (which innervates the lacrimal gland and upper eyelid) and the frontal nerve.
- **Maxillary branch ($V_2$)**: It innervates the mid-face from the lower eyelid to the upper lip.

- **Mandibular branch ($V_3$):** It receives afferents from the inferior part of the face including the mandible, lower lip and the tongue. Differently to the other two branches, it also contains motoneurons responsible for motor control of masticatory muscles.

As previously indicated, primary sensory neurons innervating the cornea originate from the $V_1$ trigeminal branch. Corneal neurons represent only 1-5% of total trigeminal neurons (Marfurt and Del Toro, 1987; Launay et al., 2015), but a single sensory neuron can give rise to a very large number of corneal endings. Corneal neuron somas in TG are small or medium size of 20-33 µm diameter in rodents and 31-33 µm in bigger mammals (Al-Aqaba et al., 2019).

### III.4 The trigeminal brainstem sensory complex: *a gate to the brain*

The trigeminal brainstem sensory complex also known as trigeminal brainstem nuclear complex, is a columnar structure in the brainstem receiving afferents from different cephalic regions. It is subdivided rostrally in the nucleus principalis or main sensory trigeminal nucleus and caudally in the three spinal trigeminal nuclei (Sp5): subnucleus oralis (Vo), interpolaris (Vi) and caudalis (Vc) (**Fig. 7**).

Corneal first-order neurons send fibers to discrete regions in CNS at the level of Sp5 where the first synapse of the pathway takes place (Marfurt and Del Toro, 1987). Neurons receiving corneal afferents are located in the transition region between caudal Vi and rostral Vc (Vi/Vc) subnuclei and between Vc and upper cervical cord junction (Vc/C1) region (Marfurt and Del Toro, 1987) (**Fig. 7B**). Although both regions encode intensity of mechanical, thermal and chemical stimuli, they respond differently to each. Most neurons in Vi/Vc junction have their receptive field covering the entire ocular surface, while Vc/C1 neurons receive inputs from smaller receptive fields (Meng and Bereiter, 1996; Belmonte et al., 2017). Vi/Vc neurons project to the superior salivatory nucleus that control lacrimation and the facial motor nucleus in charge of blinking (Pellegrini et al., 1995) conferring this neuronal population a role in ocular homeostasis (Belmonte et al., 2017). Vc/C1 neurons, however, project to the facial motor nucleus, pontine parabrachial nucleus, sensory thalamus and hypothalamus (Stapleton et al., 2013) suggesting a sensory-discriminative role in ocular pain (Belmonte et al., 2017).

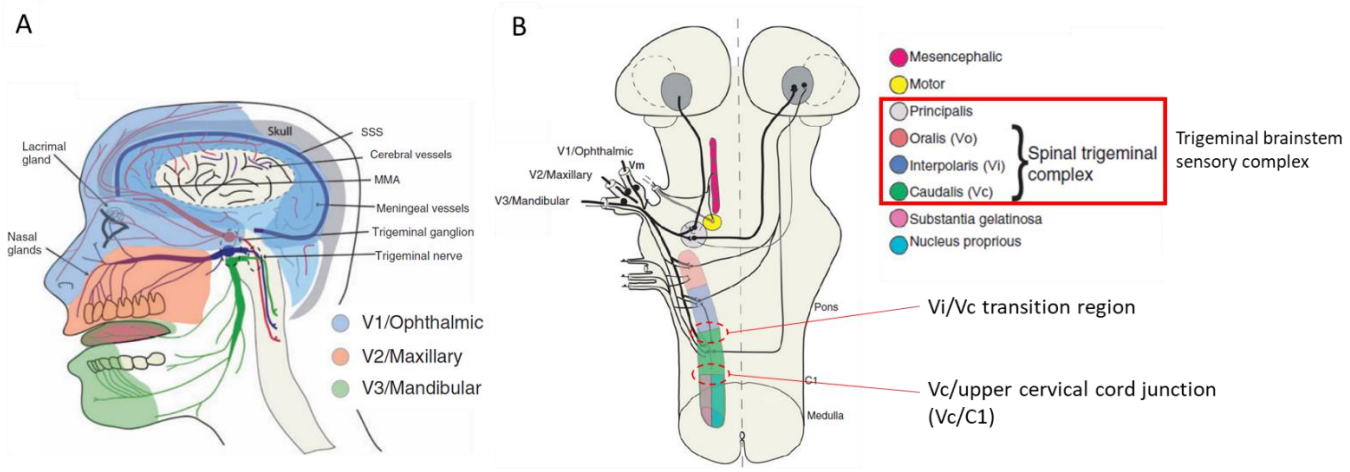


**Figure 7: Craniofacial sensory innervation from the trigeminal ganglion and trigeminal brainstem sensory complex.**
**A.** The trigeminal ganglion is split into three branches: the ophthalmic or first division ($V_1$), the maxillary or second division ($V_2$), and the mandibular or third division ($V_3$). Each branch innervates a specific region of the head. *MMA = Middle meningeal artery; SSS = superior sagittal sinus.* **B** Afferents from the trigeminal nerve branches including corneal sensory neurons connect with second order neurons in the trigeminal brainstem sensory complex. Corneal sensory neurons synapse specifically at the level of Vi/Vc and Vc/C1 (red circles). *Modified from Vila-Pueyo et al. , 2019.*

### III.5 Supraspinal integration of corneal pain

Apart from the aforementioned primary corneal neurons that synapse in the brainstem, little is known about the functional supraspinal circuits, implicated in the perception and modulation of corneal pain, that constitute the "**corneal pain matrix"**. Indeed, very limited neuro-imaging studies have examined the corneal trigeminal system in humans ( DaSilva et al. , 2002; Borsook et al. , 2003,) and only one study has reported the representation of corneal pain in the primary somatosensory cortex (Moulton et al. , 2012). These clinical studies focused on the somatosensory perception of physiological acute pain while functional information about chronic or pathological corneal pain are still lacking. Other preclinical studies related to corneal pain have used pERK and c-Fos immunoreactivity as markers of neural activation. These studies have shown cell activation in the insular cortex, anterior cingulate cortex, rostral ventromedial medulla and medial prefrontal cortex (Xiang et al. , 2017; Lin and Yen, 2018). Structures related to emotional and autonomic aspects of pain, such as the amygdala or hypothalamic nuclei, remain unexplored in the context of corneal pain. This was explored in our team, in a chronic dry eye disease model, showing neuronal activation in the amygdala in this pathological context (Fakih et al., 2021) (see page 159 for details).

## IV. Functional importance of corneal innervation in physiology and disease

Corneal afferents are responsible for several physiological events involving the ocular surface. They control the blink reflex, contribute to the spontaneous blinking rhythm (also under the control of other superior structures), tearing and corneal sensation.

### IV.1 Role of corneal innervation in blinking

The pathways that generate the trigeminal **blink reflex** involve corneal neurons at the level of their brainstem projections. As stated before, the central projections of corneal neurons synapse at the level of Vi/Vc transition region to second order neurons which project directly to the facial motor nucleus. This nucleus contains motoneurons innervating the superior palpebrae muscle, responsible for eye blinking. Vi/C1 neurons also play a role in the blink reflex through its connection with parabrachial regions as evidenced through unspecific electrical stimulation of the ocular surface (Berardelli et al., 1985; Pellegrini et al., 1995; Henriquez and Evinger, 2005, 2007,).

**Eye-blink conditioning** studies in rabbit and rodents have uncovered the central structures related to this phenomenon, such as the motor and prefrontal cortices, the hippocampus, the amygdala, the red nucleus or the claustrum (Lopez-Ramos and Delgado-Garcia, 2021).

**Spontaneous blinking,** which plays a physiological role in corneal lubrication, is modulated by corneal sensory input and by central states. In humans, it was shown that the spontaneous blink rate could be modulated by concentrating on a specific task (Wu et al. , 2014) or could be altered in pathological states such as Parkinson's disease (Kimura et al., 2017). Furthermore, reduced ocular surface sensitivity decreases spontaneous blinking rate (Doughty et al., 2009), a process mediated by TRPM8-expressing neurons (Quallo et al., 2015).

### IV.2 Role of corneal innervation in tearing

**Reflex tearing** can be evoked by mechanical, thermal or cold stimulation of the central cornea when its exceeds a certain intensity (Acosta et al., 2004; Situ and Simpson, 2010). However, **spontaneous tearing** contributing to normal tear film homeostasis is mediated only by the detection of changes in ocular surface osmolarity and soft drops in temperature (<1°C) detected by TRPM8-expressing corneal neurons (Hirata and Meng, 2010; Parra et al., 2010; Hirata and Oshinsky, 2012).

### IV.3 Role of corneal innervation in peripheral and central sensory abnormalities in dry eye disease *(Review 1 - Guerrero-Moreno et al. Front Cell Neurosci. 2020)*

In the following publication, additional information pertaining to the corneal nociceptive pathway under homeostatic conditions, as well as its involvement in ocular surface diseases, especially DED, is provided. This review focused on the latest findings in animal models as well as the corneal nerve changes found in painful DED patients, with a specific focus on neuro-immune interactions.

frontiers in Cellular Neuroscience

REVIEW
published: 10 December 2020
doi: 10.3389/fncel.2020.610342

# Morphological and Functional Changes of Corneal Nerves and Their Contribution to Peripheral and Central Sensory Abnormalities

*Adrian Guerrero-Moreno*[1], *Christophe Baudouin*[1,2,3], *Stéphane Melik Parsadaniantz*[1] *and Annabelle Réaux-Le Goazigo*[1]*

[1] Sorbonne Université, INSERM, CNRS, Institut de la Vision, IHU FOReSIGHT, Paris, France, [2] CHNO des Quinze-Vingts, IHU FOReSIGHT, INSERM-DGOS CIC 1423, Paris, France, [3] Department of Ophthalmology, Ambroise Paré Hospital, AP-HP, University of Versailles Saint-Quentin-en-Yvelines, Boulogne-Billancourt, France

The cornea is the most densely innervated and sensitive tissue in the body. The cornea is exclusively innervated by C- and A-delta fibers, including mechano-nociceptors that are triggered by noxious mechanical stimulation, polymodal nociceptors that are excited by mechanical, chemical, and thermal stimuli, and cold thermoreceptors that are activated by cooling. Noxious stimulations activate corneal nociceptors whose cell bodies are located in the trigeminal ganglion (TG) and project central axons to the trigeminal brainstem sensory complex. Ocular pain, in particular, that driven by corneal nerves, is considered to be a core symptom of inflammatory and traumatic disorders of the ocular surface. Ocular surface injury affecting corneal nerves and leading to inflammatory responses can occur under multiple pathological conditions, such as chemical burn, persistent dry eye, and corneal neuropathic pain as well as after some ophthalmological surgical interventions such as photorefractive surgery. This review depicts the morphological and functional changes of corneal nerve terminals following corneal damage and dry eye disease (DED), both ocular surface conditions leading to sensory abnormalities. In addition, the recent fundamental and clinical findings of the importance of peripheral and central neuroimmune interactions in the development of corneal hypersensitivity are discussed. Next, the cellular and molecular changes of corneal neurons in the TG and central structures that are driven by corneal nerve abnormalities are presented. A better understanding of the corneal nerve abnormalities as well as neuroimmune interactions may contribute to the identification of a novel therapeutic targets for alleviating corneal pain.

**Keywords: cornea, trigeminal ganglion, pain, inflammation, peripheral and central sensitization**

OPEN ACCESS

***Edited by:***
*Takayoshi Masuoka,*
*Kanazawa Medical University, Japan*

***Reviewed by:***
*Ignacio Alcalde,*
*Instituto Universitario Fernández-Vega, Spain*
*Ian Meng,*
*University of New England, United States*
*Yuichi Hori,*
*Toho University, Japan*

***Correspondence:**
*Annabelle Réaux-Le Goazigo*
*annabelle.reaux@inserm.fr*

***Specialty section:***
*This article was submitted to Cellular Neurophysiology, a section of the journal Frontiers in Cellular Neuroscience*

***Received:*** *25 September 2020*
***Accepted:*** *18 November 2020*
***Published:*** *10 December 2020*

***Citation:***
*Guerrero-Moreno A, Baudouin C, Melik Parsadaniantz S and Réaux-Le Goazigo A (2020) Morphological and Functional Changes of Corneal Nerves and Their Contribution to Peripheral and Central Sensory Abnormalities. Front. Cell. Neurosci. 14:610342. doi: 10.3389/fncel.2020.610342*

## INTRODUCTION

The cornea is the most densely innervated tissue in the human body. Corneal innervation is estimated as 300–600 times and 20–40 more innervated than skin and tooth pulp (Muller et al., 2003; Marfurt et al., 2010). The human corneal innervation is organized into four layers: mid stromal nerves, subepithelial plexus, subbasal nerve plexus, and intraepithelial nerve terminals

(Muller et al., 2003; Marfurt et al., 2019). The sensory innervation comes from corneal primary afferent neurons whose cell bodies are located in the ophthalmic (V1) branch of the trigeminal ganglion (TG). Corneal neurons represent only 1–5% of total trigeminal neurons (Marfurt and Del Toro, 1987; Launay et al., 2015). The central axons of corneal sensory neurons terminate in two regions of the spinal trigeminal complex (V or Sp5): the sensory trigeminal subnucleus interpolaris/caudalis (Vi/Vc) transition and the subnucleus caudalis/upper cervical cord (Vc/C1) junction regions (Marfurt and Del Toro, 1987; Strassman and Vos, 1993; Meng and Bereiter, 1996). The second order neurons project to the thalamus and synapse with third order neurons projecting to cortical regions (primary somatosensory cortex) (**Figure 1**). Therefore, any corneal injury or corneal nerve abnormalities may trigger molecular, cellular, and functional changes within the TG and the central nervous system, which may contribute to acute and chronic pain.

## FUNCTIONAL CLASSIFICATION OF CORNEAL FIBERS

The cornea receives sensitive and autonomous innervation. Corneal nerve fibers have been classified according to different criteria—morphology (intraepithelial nerves), conduction velocity (diameter, myelinated or not), and function/modality (stimulus sensitivity and specificity, electrophysiological properties)—and according to the expression of very specific biochemical markers. Unlike somatic nerve innervation, the cornea lacks A-beta fibers. Cornea is composed of two types of fibers:

- the high speed myelinated Aδ fibers with a larger diameter represent about 20% of the total population of corneal afferent fibers (MacIver and Tanelian, 1993a; Bron et al., 2014).
- slower-conducting unmyelinated C fibers with a small diameter are the most frequent (around 80%) (Gallar et al., 1993; MacIver and Tanelian, 1993a; Hirata and Meng, 2010).

Two sub-populations of C fibers have been identified: peptidergic and non-peptidergic fibers. In rodents, peptidergic fibers contain substance P (SP, 10–20%) or calcitonin gene-related peptide (CGRP, 40–60%). All $SP^+$ terminals are $CGRP^+$ in mice (Ivanusic et al., 2013). Other mediators are also found, such as neurokinin A, serotonin, somatostatin, as well as cholecystokinin or gastrin (Gonzalez-Coto et al., 2014). In humans, to date, only substance P and CGRP have been clearly identified in corneal fibers. A second population of C fibers, the non- peptidergic C fibers, does not express these peptides but has a strong affinity for isolectin B4. In mice, about 20% of corneal neurons are non-peptidergic (Ivanusic et al., 2013).

The majority of corneal nerve fibers are nociceptive and cold thermoreceptors fibers and the remaining fibers are sympathetic or parasympathetic post-ganglion fibers of the autonomic nervous system.

Autonomic nervous fibers of sympathetic (upper cervical ganglion) and parasympathetic system (ciliary ganglion) participate in the regulation of corneal wound healing and re-epithelialization (Jones and Marfurt, 1996; Xue et al., 2018; Xiao et al., 2019). Theses biological processes involve a number of concerted events including cell migration, proliferation, inflammation, and differentiation and extracellular matrix remodeling (Ljubimov and Saghizadeh, 2015). Interestingly, it was recently reported that the mouse autonomous system modulates inflammation and epithelial renewal after corneal abrasion through the activation of distinct local macrophages (Xue et al., 2018; Xiao et al., 2019).

In rodents and cats, these fibers represent about 10% of corneal fibers. Parasympathetic fibers, originating from the ciliary ganglion, contain intestinal vasoactive peptide (VIP), neuropeptide Y, galanin, and Met-enkephalin (Jones and Marfurt, 1998; Muller et al., 2003).

Electrophysiological studies showed that the cornea is innervated by three distinct classes of peripheral sensory nerve fibers:

**Mechano-nociceptors** (Aδ fibers) are activated only by soft mechanic forces in the order of magnitude closed to that required to damage corneal epithelial cells. In general, mechano-nociceptors only fire when a mechanical stimulus is applied or removed in a phasic way (Belmonte et al., 1991; MacIver and Tanelian, 1993b). Piezo2, a long transmembrane protein and non-selective cation channel mechanically activated (Coste et al., 2010; Shin et al., 2019), has emerged as a marker of mechano-nociceptors in primary sensory neurons.

**Cold receptors** (Aδ and C fibers) are activated by thermal changes (Gallar et al., 1993; Carr et al., 2003). These are classified into two subgroups (Alcalde et al., 2018).

- *High background-low threshold (HB-LT) cold receptors* are the principal generators of spontaneous activity (high background) at ocular surface constant temperature. These fibers change their firing frequency according to slight temperature changes (1–2°C, low threshold). Additionally, they detect changes in ocular surface osmolarity (Hirata and Meng, 2010; Parra et al., 2014; Gonzalez-Gonzalez et al., 2017). A hyperosmolar tear film with values close to those found in dry eye patients increases the sensitivity of cold-sensitive neurons.
- *Low background-high threshold (LB-HT) cold receptors* do not contribute as HB-LT to basal ongoing activity (low background), but instead fire under sharp drops in temperature (>4°C) (Gonzalez-Gonzalez et al., 2017).

TRPM8 (transient receptor potential cation channel subfamily M member 8) is considered as a marker of cold receptors. TRPM8 is activated by menthol and by cold (<23°C) (McKemy et al., 2002; Peier et al., 2002). Due to these characteristics, it is the putative principal sensor of cold.

Indeed, TRPM8 receptors appear to be first activated on the ocular surface after evaporation of the tear film (Belmonte et al., 2017) and mild cooling of the ocular surface has been reported to increase lacrimation via TRPM8 activation of corneal cool primary afferent neurons (Robbins et al., 2012). In the same line,

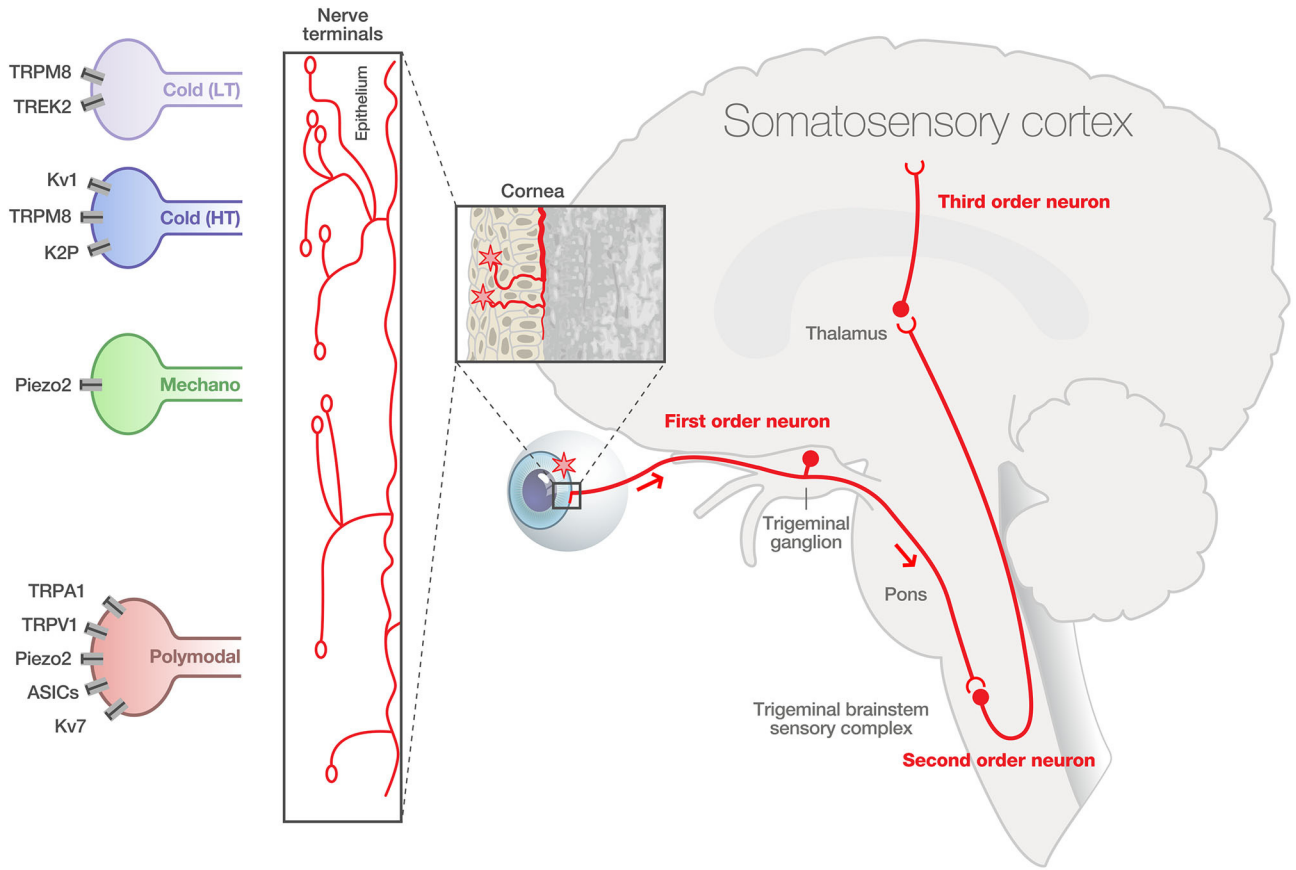


**FIGURE 1 |** Physiological corneal pain processing. The cornea contained a high density and heterogeneity of A delta and C fibers expressing specialized transient receptor channels, able to respond to diverse environmental stimuli of varying intensities (cold, mechanical, and polymodal). The intraepithelial nerve fibers exhibit distinct morphologies: complex, ramified, and simple. First order sensory neurons innervating the cornea have their cell body in the ophthalmic branch (V1) of the trigeminal ganglion (TG). The central terminals of these pseudo unipolar neurons synapse in the trigeminal brainstem sensory complex with second order nociceptive projection neurons. These neurons project to the thalamus and synapse with third-order neurons projecting to cortical regions (primary somatosensory cortex). LT, low-threshold cold thermoreceptors; HT, high-threshold cold thermoreceptors. Modified from Belmonte et al. (2015) and Rosenthal and Borsook (2016).

it was found that TRPM8 knockout mice have a lower level of basal tear flow (Parra et al., 2010).

**Polymodal nociceptors** (Aδ and C fibers) are the most abundant population in the cornea (Gonzalez-Gonzalez et al., 2017). These fibers are activated by different types of stimuli:

- *Mechanical:* In contrast to pure mechano-nociceptors, polymodal nociceptors have a lower threshold and fire continuously (tonic) while the stimulus is present (Gallar et al., 1993).
- *Thermal*: They are activated by temperatures above 37°C (Gallar et al., 1993).
- *Chemical*: There is a broad variety of molecules activating these nociceptors, including protons (pH drops) and inflammatory mediators (prostaglandins, bradykinin, and capsaicin) (Chen et al., 1997).

TRPV1 (transient receptor potential cation channel subfamily V member 1), a non-selective cation channel, is considered as a marker of polymodal sensory fibers (Belmonte et al., 1991). Thus, it represents the principal sensor of hot painful stimulus.

Retrograde tracing anatomical experiments were used to identify the whole population of corneal neurons in the TG and to determine the proportion of the corneal neurons expressing the molecular marker of polymodal, mechanoreceptors and cold cells. This studies have demonstrated by *in situ* hybridization that Piezo2 represents 28–30% of corneal afferent neurons in guinea pig TGs and do not co-express TRPV1 (Alamri et al., 2015) or TRPM8 (Bron et al., 2014). The co-expression of TRPM8 and TRPV1 occurs in 6% of $TRPV1^+$ cells corresponding to 31% of $TRPM8^+$ cells (Alamri et al., 2015). Interestingly, all SP-reactive neurons were also $TRPV1^+$ in rats (Murata and Masuko, 2006). Therefore, they constitute separate populations of corneal sensory neurons. The proportion of corneal neurons expressing TRPV1 varies depending on the animal species and the tracer used: in rats, 37% when traced with cholera toxin (Murata and Masuko, 2006) and 23% when traced

with Fluoro-Gold (Nakamura et al., 2007); in guinea pigs, it reaches 45% of corneal neurons when traced with Fast blue (Alamri et al., 2015). TRPM8 is expressed in 8–15% of corneal neurons in guinea pigs (Bron et al., 2014; Alamri et al., 2015) and 18–22% in mice (Ivanusic et al., 2013; Alcalde et al., 2018).

Anatomical studies focusing on corneal nerve terminals found that corneal polymodal ($TRPV1^+$) and cold ($TRPM8^+$) neurons have distinct nerve terminal morphologies. It was demonstrated that, compared to TRPV1 neurons, TRPM8-IR corneal nerve endings in both guinea pig and mouse corneal epithelia had complex (longer and more branched) morphology (Ivanusic et al., 2013; Alamri et al., 2015, 2018; He et al., 2019) (**Figure 1**). The presence of $Piezo2^+$ channels has been recently found in corneal nerve fibers in mice (Fernandez-Trillo et al., 2020).

Accumulating fundamental and clinical studies have reported morphological, structural, and/or functional corneal nerve abnormalities, which may contribute to pain-related sensory abnormalities.

## NOCICEPTION, PAIN, AND NEUROSENSORY ABNORMALITIES

Nociception is the neural process of encoding noxious stimuli, whereas pain is defined as *an unpleasant sensory and emotional experience associated with, or resembling that associated with, actual or potential tissue damage* [the International Association for the Study of Pain (IASP)] (Raja et al., 2020).

Nociceptive pain is a physiological protective warning signal against imminent or ongoing tissue damage. Nociceptive pain starts at the periphery by the activation of nociceptors by physical tissue destruction or by chemical exposure, or thermal processes. Inflammatory pain occurs in the presence of tissue injury and active inflammation. It is the consequence of the activation and alteration of nociceptor function both by immune signals and signals arising from damaged cells (Woolf, 2020).

In this context, proinflammatory mediators participate in the sensitization of the nerves, meaning the reduction of the pain threshold (allodynia) and exacerbated response to a painful stimulus (hyperalgesia). Therefore, sensitization can occur both in the periphery (peripheral sensitization) and in the central nervous system (central sensitization).

Pain can extend beyond its protective usefulness, lasting in the absence of nociceptive stimuli. Neuropathic pain, a chronic pain condition, is defined by the IASP as "*pain caused by a lesion or disease of the somatosensory nervous system*." By definition, the origin of the neuropathic pain can be peripheral or central. There is important interest in the field, as the current treatments for alleviating neuropathic pain are often inefficacious and/or produce severe side effects.

In the ocular surface, and more specifically in the cornea, all of these physiological and pathophysiological conditions can occur. Pain can manifest as a result of a noxious stimulus or damage in the ocular surface anatomy (nociceptive pain), or it can result from abnormalities in the ocular surface neurosensory apparatus itself (neuropathic pain).

Neurosensory abnormalities within the corneal nociceptive pathway could lead to pathological conditions such as pain and ocular discomfort that are hallmark of dry eye disease (DED) and the emerging ocular neuropathic pain. Corneal neuropathic pain may have various etiological origins, which include DED, persistent corneal nerve injury, and photorefractive surgeries (Dieckmann et al., 2017; McMonnies, 2017; Aggarwal et al., 2019). Dry eye is defined as a *"multifactorial disease of the ocular surface characterized by a loss of homeostasis of the tear film, and accompanied by ocular symptoms, in which tear film instability and hyperosmolarity, ocular surface inflammation and damage, and neurosensory abnormalities play etiological roles"* (Craig et al., 2017). The prevalence of DED, which ranges from 5 to 50% of the adult population, increases with age, especially after 50 years, and affects more women than men (Stapleton et al., 2017). DED has gained recognition as a public health problem given its prevalence, morbidity, and cost implications.

Importantly, the cellular and molecular mechanisms underlying the neurosensory abnormalities observed after corneal damage and in DED are currently an open and very active research field.

This increasing understanding of the corneal nerve morphological and functional aspects will bring new insights into their contribution to the physiology and pathophysiology of corneal pain perception and will provide novel opportunities for more efficient therapeutic treatments for this ocular surface diseases.

In the context of other ocular surface diseases, excellent reviews have already provided detailed information about the morphological and functional abnormalities of corneal nerves in herpetic keratitis, neuropathic keratitis, or keratoconus (Cruzat et al., 2017) and diabetes (Markoulli et al., 2018).

The purpose of this review is first to provide an overview of the morphological, molecular, and cellular changes of corneal nerves in rodents after corneal damage and persistent DED. The cellular and molecular changes of corneal neurons in the TG driven by corneal nerve abnormalities are discussed next. Moreover, we depict how peripheral neuroimmune interactions shape the peripheral and the central nervous system. Clinical evidence for corneal nerve abnormalities associated with DED and corneal neuropathic pain is also presented as well as several important questions that remain to be addressed.

## FUNDAMENTAL STUDIES ON MORPHOLOGIC ABNORMALITIES OF CORNEAL NERVE TERMINALS

The cornea is a valuable tissue for studying peripheral sensory nerve morphology and function due to its transparency, dense innervation, and accessibility. Corneal nerve structure and function are adversely affected by many ophthalmic and systemic disorders. Experimental descriptive studies exploring the changes of corneal nerve morphology have improved our understanding of how corneal nerve density is altered under DED and corneal injury conditions. Thus, transgenic thy1-yellow fluorescent protein (thy1-YFP) mice, in which corneal nerves express the

YFP protein driven by thy1 promoter, represent a useful model for *in vivo* investigation of peripheral nerve structure (Yu and Rosenblatt, 2007; Namavari et al., 2011; Chaudhary et al., 2012; Sarkar et al., 2012, 2019; Bouheraoua et al., 2019). A decrease in stromal nerve fiber density as well as inflammation were observed in corneas from thy1-YFP mice submitted to experimental DED induced by chronic topical instillation with benzalkonium chloride, a quaternary ammonium used as preservative (Sarkar et al., 2012).

In addition, immunohistochemistry detecting all corneal nerve fibers in tissue samples and *in vivo* confocal microscopy (IVCM, a non-invasive high-resolution real-time imaging device allowing layer-by-layer analysis of the corneal ultrastructure) have covered aspects of the morphological basis of corneal nerve changes in rodents both in physiological and pathophysiological conditions. A decrease in corneal nerve density was reported in preclinical models of experimental DED induced by prolonged (28 days) (Simsek et al., 2019) or acute (up to 10 days) (Stepp et al., 2018a) scopolamine administration. Similar observations were made in cd25 null mice, which constitute a model of Sjögren Syndrome dry eye (Stepp et al., 2018b).

Tear hyperosmolarity plays a critical role in the initiation and/or perpetuation of DED, which could have consequences with respect to corneal nerve abnormality. Indeed, a reduction in the density of corneal intraepithelial nerves and terminals, in addition to a sensitized ocular surface to hypertonicity, was also recently reported in a murine model of tear hyperosmolarity (Guzman et al., 2020).

Furthermore, surgically induced chronic dry eye models obtained after the unilateral removal of extra-orbital lacrimal gland in mice (Yamazaki et al., 2017) or after the excision of the extraorbital lachrymal gland and Harderian gland had similar findings (Fakih et al., 2019): a reduction in corneal nerve density accompanied with corneal allodynia. Finally, structural abnormalities including a profound loss of nerve density in the sub-basal nerves and increasing of beading and tortuosity of stromal nerve trunks also occurred in a model of corneal injury-induced neuropathic pain (Cho et al., 2019; Pham and Bazan, 2020).

Altogether, these morphological changes in corneal density innervation reported from the fundamental studies above resemble those observed in patients with corneal injury, patients who underwent refractive surgery, and patients with DED and ocular neuropathic pain (see paragraph dedicated to clinical data). One key initiative is to determine the precise underlying molecular mechanisms responsible for these morphological changes.

Recent advances in tissue clearing methods and light-sheet fluorescence microscopy have provided unprecedented access to structural and molecular information from intact tissues. A 3D high resolution imaging of an intact eyeball using a tissue clearing system derived from CLARITY and advanced light sheet microscopy in wild type fluorescently labeled transgenic mice of Prox-1-GFP or Thy1-YFP (Yang et al., 2020) was recently reported. The technology, applicable to various mouse strains (wild type or fluorescently labeled), and a spectrum of ocular components and cell types (i.e., corneal nerves, blood vessels, immune cells...) represent multiple opportunities for further architectural/morphological studies in basal and pathological ocular conditions.

## EVIDENCE FOR FUNCTIONAL ABNORMALITIES OF CORNEAL NERVE TERMINALS IN EXPERIMENTAL MODELS OF CORNEAL INJURY AND DED

Corneal nerve dysfunction has been reported in multiple ocular surface conditions including DED, herpetic keratitis, and after surgery (see review McKay et al., 2019). Peripheral sensitization is defined as increased responsiveness and a reduced threshold of nociceptive neurons in the periphery of the stimulation. Such phenomenon can occur in the cornea (see reviews Belmonte et al., 2004, 2017). Indeed, chronic peripheral nerve injury and local inflammation are known to participate in the development of peripheral sensitization. Immune cells locally release cytokines, chemokines, lipids, and growth factors that act on peripheral nociceptors. In turn, nociceptors actively release neuropeptides from their peripheral nerve terminals that modulate the activity of innate and adaptive immune cells (Chiu et al., 2012; Baral et al., 2019).

The development of ocular pain after corneal damage or persistent DED is believed to be due to the abnormal hyperexcitability (sensitization) of corneal nerve terminals. Single corneal nerve terminals and ciliary nerve fiber activity recordings are the two main experimental approaches currently reported to evaluate the functional changes of ongoing or evoked nerve activity in fundamental studies. Single unit extracellular recordings to evaluate polymodal and cold-sensitive corneal nerve terminals have been described using *ex vivo* isolated corneas in mice and in guinea pigs (Acosta et al., 2013, 2014; Kovacs et al., 2016b; Gonzalez-Gonzalez et al., 2017; Hirata et al., 2017; Alamri et al., 2018; Pina et al., 2019).

Extracellular recordings of ciliary nerve fiber activity have been described in whole eye preparations *in vivo* in cats (Gallar et al., 1993; Acosta et al., 2001, 2007) and *ex vivo* in isolated guinea pigs (McLaughlin et al., 2010; Acosta et al., 2013, 2014), rabbits (Beuerman et al., 1992), and mice (Fakih et al., 2019; Joubert et al., 2019). *Ex vivo* extracellular recordings of ciliary nerve activity being performed in double compartment chambers offer the possibility of applying chemical, mechanical, and thermal stimulations directly to the cornea to specifically study the responses of polymodal nociceptors, mechano-nociceptors, and cold thermoreceptors. By using this approach, a recent study showed a correlation between corneal hypersensitivity (decreased mechanical threshold), higher spontaneous ciliary nerve fiber activity, and the higher responsiveness of corneal polymodal nerve fibers from mice submitted to an acute corneal nerve injury associated with local inflammation (Joubert et al., 2019). The abnormal responses of the polymodal nociceptors (lower activation and decreased latency of the impulse discharge) observed may be a consequence of inflammation, known to play a major role in corneal nerve sensitization (McMahon and Wood, 2006; Gallar et al., 2007; Parra et al., 2014).

Another category of corneal nerve fiber changes their modalities after corneal injury and DED: cold TRPM8 corneal fibers. The contribution of TRPM8 channels to cold transduction in peripheral nerve terminals was confirmed in TRPM8-KO mice. KO animals do not show a response to noxious cold stimulus (Madrid et al., 2006). In lacrimo-deficient guinea pigs, cold nerve terminals exhibited enhanced spontaneous activity (hyperexcitability) and cold response in addition to a reduced cold threshold to cooling ramps compared to nerve terminals recorded from control animals (Kovacs et al., 2016a,b) (**Figure 2**).

The changes in corneal cold thermoreceptor firing were also observed experimentally after a peripheral corneal axotomy (Pina et al., 2019). Corneal injury evoked electrophysiological alterations in TRPM8 corneal neurons, which manifest by an enhanced sensitivity of the corneal TG neurons to cold (Pina et al., 2019). The application of menthol (10 μM), a TRPM8 agonist, induced a more pronounced increase in the firing rate in corneas of injured mice than in those of sham animals (Pina et al., 2019) (**Figure 2**).

Furthermore, a study reported that tear fluid hyperosmolarity (325–1,005 mOsm·kg-1), recognized as an important pathogenic factor in dry eye syndrome, increases nerve impulse activity of cold thermoreceptor endings of the cornea (Parra et al., 2014).

Thus, abnormal activity and the responsiveness of peripheral corneal cold thermoreceptors underlie the unpleasant sensations experienced by patients with DED.

In line with these observations, a severe DED induced by the excision of extraorbital lachrymal and Harderian glands in mice provoked corneal mechanical allodynia and corneal inflammation associated with an increase in the ongoing ciliary nerve fiber electrical activity compared to control mice (Fakih et al., 2019) (**Figure 2**). In addition, during photorefractive keratectomy, another corneal injury condition, functional and morphologic alterations in mechanical, polymodal, and cold sensory nerve fibers of the cornea have been noted, which can lead to postoperative pain (Bech et al., 2018).

In preclinical models of other corneal and conjunctival disorders characterized by an important inflammatory component, such as allergic keratoconjunctivitis (Acosta et al., 2013) or UV Keratitis (Acosta et al., 2014), an inhibition of cold receptors and sensitization of polymodal nociceptors were reported. These results contrast with the preclinical and clinical data from DED condition, in which both populations of corneal fibers (polymodal and thermoreceptors) showed sensitization (abnormal responsiveness and spontaneous firing). These aspects have been recently reviewed (Belmonte, 2019).

Nociceptive nerve terminals contain specific elements for detecting, transmitting, and modulating noxious signals (Waxman, 1999). Among them, the spike initiation zone located in the axon initial segment (AIS) corresponds to the site where action potentials are initiated and represents a critical element in neuronal excitability (Yamada and Kuba, 2016). Structural properties, such as the location relative to the soma and the length of the AIS, can change in an activity-dependent manner that can fine-tune the neuronal output properties (Jones and Svitkina, 2016; Yamazaki et al., 2017). A recent study has not only identified the precise location of the NaV-dependent spike initiation zone in nociceptive corneal nerve terminals *in vivo*, but has also demonstrated a plasticity in the spike initiation zone (Goldstein et al., 2019). Corneal inflammation shifts the Nav-spike initiation zone toward the terminal end, rendering it hyperexcitable in a model of inflammation-induced peripheral hyperalgesia (Goldstein et al., 2019).

Taken together, corneal nerve damage and inflammation trigger corneal sensory nerve dysfunctions (mostly sensitization); these peripheral nerve abnormalities may account for ocular pain syndromes. The above studies also reinforce the importance of neuroimmune interactions that participate in corneal hypersensitivity, inflammation, and spontaneous and evoked corneal nerve fiber hyperactivity.

Nociceptors and immune cells interact bidirectionally, a communication made possible by the wide spectrum of cells involved and by the receptors and ligands they express (Jain et al., 2020). From these multiple interactions has emerged the notion of neuroimmune interactome, a comprehensive map of the bidirectional ligand-receptor "interactome" between sensory neurons and immune cells (Jain et al., 2020). In the future, peripheral neuroimmune interactome could be constructed during pathological conditions such as corneal inflammation and corneal pain conditions. Enhancing our knowledge of the nociceptor and immune cell communication as well as the plasticity of both actors may contribute to the identification of novel therapeutic targets.

## MOLECULAR AND FUNCTIONAL CHANGES IN TRIGEMINAL CORNEAL NEURONS AFTER CORNEAL INJURY/UNDER PATHOLOGICAL CONDITIONS

After peripheral nerve injury, primary sensory neurons show molecular and functional changes, resulting in hyperactivity and hyperexcitability (Berta et al., 2017). These maladaptive changes have been well-documented in dorsal root ganglion neurons in various inflammatory and pain models, but less is known about the possible alterations in the corneal nociceptive trigeminal pathways following ocular surface damage.

Anatomical studies using retrograde-labeled corneal neuron experiments have found a higher expression of TRPV1 in TRPM8$^+$ cold-sensing corneal neurons in the TG in a model of DED, suggesting an enhanced responsiveness of TRPM8$^+$ cells and leading to a cold allodynia (Hatta et al., 2019; Li et al., 2019). Moreover, single cell RT-PCR indicated that all TRPM8$^+$/TRPV1+neurons express substance P (Tac1), while fewer TRPM8$^+$/TRPV1- neurons express Tac1. It was proposed that TRPV1-dependent neuronal sensitization facilitates the release of the neuropeptide substance P from TRPM8$^+$ cold-sensing neurons to signal nociception in response to cold (Li et al., 2019). However, such results are in contradiction with a retrograde tracing study which found that SP and TRPM8 were expressed in different TG neurons, suggesting that TRPM8$^+$ corneal cells are non-peptidergic (He et al., 2019).

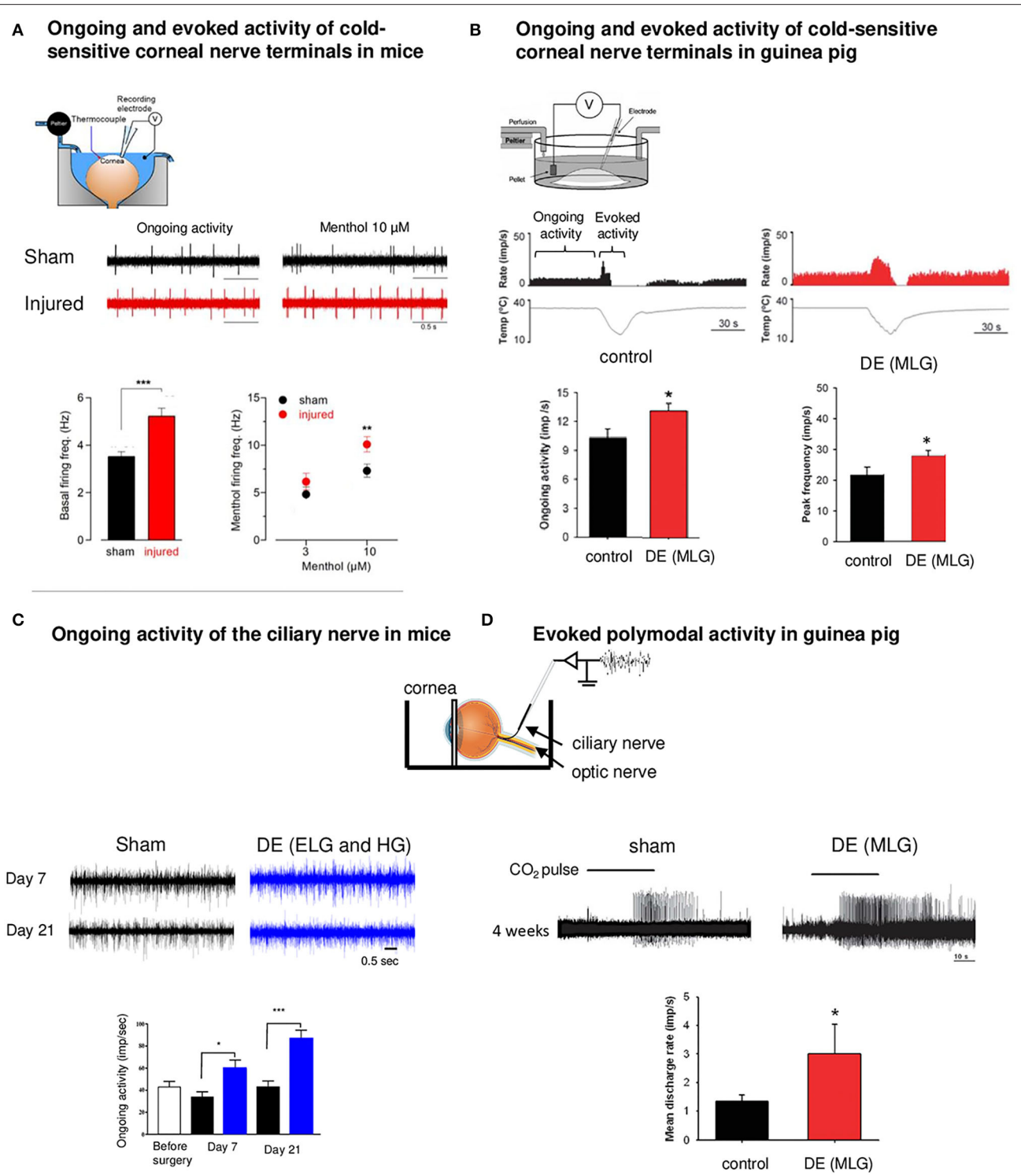


**FIGURE 2 |** Functional abnormalities of corneal nerves following corneal damage and DE condition. *Ex vivo* electrophysiological recordings of corneal nerves in models of corneal nerve damage and DE conditions. **(A)** Electrophysiological set-up. Spontaneous (ongoing) and evoked (menthol 10 µM) activity of cold sensitive corneal nerve terminals in a mouse model of corneal nerve injury (red traces) relative to control (sham animals, black traces). Note the increase in corneal nerve activity for both conditions in the injured cornea. Data plotted as mean ± SEM. $^{*}P < 0.05$, $^{**}P < 0.01$, $^{***}P < 0.001$. **(B)** Electrophysiological set-up of ongoing and evoked activity of cold nerve terminals in a guinea pig model of DE obtained after the main lachrymal gland (MLG) excision. Ongoing activity and peak frequency evoked by cooling-ramp were increased 4 weeks after MLG excision. **(C)** Electrophysiological set-up for extracellular recording of the ciliary nerve. Ongoing ciliary nerve activity 7 days and 21 days after the excision of extraorbital (ELG) and Harderian gland (HG) in mice (blue traces) relative to sham animals (black traces). In both conditions, we noted higher ongoing (spontaneous) firing frequency in DE animals. **(D)** Activity of polymodal nerve fibers activated by 30 s $CO_2$ pulse in control (sham) and

*(Continued)*

**FIGURE 2 |** MLG guinea pigs 4 weeks after surgery. The mean discharge rate during the $CO_2$ pulse was higher after the surgery compared to sham. Note the higher responsiveness of polymodal nerve fibers (decreased latency) in DE animals. Modified from Acosta et al. (2013), Kovacs et al. (2016b), Fakih et al. (2019), and Pina et al. (2019).

Several studies have reported changes in mRNA expression in TG following corneal damage. For example, abnormal SP and TRPM8 gene expression was found associated with corneal hypersensitivity in a model of corneal surgery (epithelium removal and one-third of the anterior stroma with a 2 mm trephine). These molecular and cellular changes occurring in the TG may contribute to the pathogenesis of corneal surgery-induced chronic pain (He et al., 2019). In a model of corneal alkali-burn injury, the increased gene expression of pro-inflammatory cytokines, tumor necrosis factor (TNF alpha), interleukin (IL)-6, SP, and its receptor NK1 (NK1) were reported in the ipsilateral TG (Ferrari et al., 2014). Changes in mRNA expression were also found in TG from an experimental model of DED obtained after 7 days of topical benzalkonium chloride (BAK). This model developed corneal inflammation and corneal hypersensitivity, and an increase in the gene expression of pro-inflammatory cytokines (IL-6 and TNF-alpha) was reported (Launay et al., 2016). Additionally, neuronal activation (FOS), neuronal injury (ATF3), astrocyte (GFAP), and oxidative (INOS2 and NOX4) markers were found to be increased in the ipsilateral TG from animals submitted to a chronic DED characterized by corneal nerve damage, inflammation, and corneal hypersensitivity (Fakih et al., 2019).

Growing evidence indicates that both CGRP and SP play a key role in the development of peripheral sensitization and are implicated in the development of neurogenic inflammation (Chiu et al., 2012), giving a rational to all changes previously described. In this line, SP has a robust effect on monocytes and macrophages and triggers their release of pro-inflammatory cytokines, including IL-1, TNF, and IL-6, via ERK/p38 MAPK-mediated NF-κB activation. Interestingly, both neuropeptides have been found to be abundant in corneal neurons, and a transcriptome signature in the TG using unbiased RNA sequencing revealed an upregulation of tachykinin precursor 1 (*Tac1*) that encodes SP and Calcb, which encodes CGRP after corneal injury (Pham et al., 2020).

Monitoring c-Fos, ATF3, and c Jun immunopositive cells is a commonly used approach to studying the activation and damage of primary sensory neurons from dorsal root and trigeminal ganglia. cFos, c-Jun, and ATF3 protein expressions were shown to be increased in the ipsilateral TG from animals with corneal damage (De Felipe and Belmonte, 1999; Launay et al., 2016; Fakih et al., 2019; Reaux-Le Goazigo et al., 2019). Both CGRP and ATF3 protein expressions in TG cell bodies increased after injury and returned to a normal level by 1 week, paralleling the time course of changes in nociceptive responses (Hegarty et al., 2018). These increased expressions of FOS, CGRP, and ATF3 in primary sensory neurons may contribute to the activation of central pain pathways in response to sustained ocular stimulation, leading to the centralization of pain (Levine et al., 1993).

Under local inflammation or after tissue damage, cytokines, prostaglandins, nerve growth factor, and bradykinin signals increase TRPV1 expression and/or TRPV1 activity in sensory neurons (Pinho-Ribeiro et al., 2017). In the context of DED, TRPV1 protein levels have been found to increase in the ipsilateral TG, and this TRPV1 upregulation was associated with enhanced eye wipe behavior after hypertonic saline and capsaicin instillation in a rat model for aqueous tear-deficient DE (Bereiter et al., 2018).

In the same way, it has been observed that capsazepine, a TRPV-1 antagonist, prevented dry eye sensitization of cool cells to capsaicin (Hatta et al., 2019) and reduced polymodal responsiveness to acidic stimulation in an allergic eye model (Acosta et al., 2013). Moreover, TRPV-1 pharmacological blockade decreases SP release in cold allodynia (Li et al., 2019).

Neurons in sensory dorsal and trigeminal ganglia are surrounded by satellite glial cells (SGCs) (Hanani, 2005). Activation of SGCs is characterized by GFAP upregulation in the injured trigeminal nerve branch associated with the development of hyperalgesia (Vit et al., 2006; Katagiri et al., 2012), but this has not been observed under non-pathological conditions (Shinoda et al., 2019). Interestingly, increased spontaneous pain behavior and corneal allodynia have been associated with morphological changes (hypertrophy) and upregulation of GFAP protein expression in the SGCs at the level of the ipsilateral trigeminal nerve V1 branch in preclinical models of corneal injury (Launay et al., 2016; Fakih et al., 2019; Reaux-Le Goazigo et al., 2019).

In addition, accumulative evidence reports that immune cells as monocytes/macrophages infiltrate into the TG and become activated, following orofacial pathologies, including peripheral trigeminal nerve trauma and orofacial inflammation (Iwata and Shinoda, 2019). Fundamental studies performed in mice reported that corneal injury induced an increase and activated resident and proliferated macrophages in mouse TGs (Ferrari et al., 2014; Launay et al., 2016; Fakih et al., 2019; Reaux-Le Goazigo et al., 2019). The infiltrated monocytes/macrophages show larger soma and thicker ramifications; such morphological structural changes indicate their activation (Shinoda et al., 2019). The above observations suggest that immune cells and resident glia in the TG could play a significant role in the modulation of ocular pain. The specific role of both the population of cells should be better investigated in the future in the context of ocular pain.

Though RTqPCR and immunohistochemistry have provided some important information about neuronal, glial activations and cellular morphological abnormalities following corneal pain conditions, the major limitation of these techniques is that they lack the ability to monitor the dynamic of these neuronal changes. Functional studies have been performed in trigeminal neurons to better understand their activation and how various corneal nerve injuries may alter their modalities. *In vivo* electrophysiology works have assessed action potentials from single neurons and/or clusters of neurons in rodent TGs (Lopez de Armentia et al., 2000; Veiga Moreira et al., 2007; Hirata and Meng, 2010; Kurose and

Meng, 2013; Hirata et al., 2015; Quallo et al., 2015) under normal and pathological conditions. The literature is not as rich as the one from DRG neurons, but it provides important information about changes in the neuronal properties of corneal neurons under physiological and DE conditions.

Understanding the effect of ocular surface damage on corneal nociceptive neurons is crucial for developing a potential antalgic treatment against corneal pain. To this aim, several studies based on single unit recordings of corneal nociceptive neurons located in the TG have been assessed in preclinical models of DED and corneal injury to provide valuable insight into the normal and pathologic response of the corneal neurons. These studies highlighted the relationship between the electrophysiological signature (both fiber conduction velocity and electrical properties) and the altered responsiveness to various sensory modalities (chemical, thermal, and mechanical) of afferents innervating the cornea.

Thus, *in vivo* extracellular electrophysiological recordings performed in rat TG single neurons that innervated the cornea, before, and up to 3 h after, the ocular application of continuous hyperosmolar tears demonstrated that dry responses of corneal dry-sensitive neurons were depressed or even completely abolished by the hyperosmolarity of tears (Hirata et al., 2015).

In a moderate dry eye experimental model obtained after unilateral extraorbital lacrimal gland excision, Kurose et al. demonstrated by a single unit extracellular recording of trigeminal neurons (8–10 weeks after the surgery) that dry eye sensitized corneal cool cells to the TRPM8 agonist menthol and to cool stimulation (Kurose and Meng, 2013). In the same experimental model, Hatta et al. showed that dry eye increased responsiveness to noxious heat and activation by capsaicin through TRPV1 (Hatta et al., 2019) (**Figure 3**). Pina et al. further demonstrated, in a mouse model of corneal injury, changes in cold sensitivity of corneal neurons in the TG through an enhanced functional expression of TRPM8 channels, suggesting that the increase in ocular dryness sensation and basal tearing rate observed after refractive surgery could be related to a disturbance in the TRPM8 responsiveness of cold sensory neurons (Kovacs et al., 2016b; Pina et al., 2019) (**Figure 3**).

## EVIDENCE THAT CORNEAL NERVE ABNORMALITIES SHAPE THE CENTRAL NERVOUS SYSTEM IN RODENTS

Corneal nociceptors, like other primary somatosensory neurons, are pseudo unipolar. They send a peripheral axon to innervate the corneal and a central axon to synapse on second-order neurons at two different locations of the brain stem nuclear complex: the Vi/Vc (trigeminal subnucleus interpolaris/caudalis transition region) and Vc/C1 (caudalis/upper cervical cord junction) areas of the trigeminal subnucleus caudalis region (**Figure 1**). Persistent ongoing activity in primary nociceptors may generate extensive changes in central pain processing-related structures, leading to maladaptive neuroplasticity. In addition, proinflammatory mediators participate not only in the sensitization of peripheral nerve terminals but also in the transfer of nociceptive information from the periphery to the central nervous system (Grace et al., 2014; Melik Parsadaniantz et al., 2015). More specifically, activated glial cells, which produce various proinflammatory cytokines (TNF alpha, IL-6, IL1 beta), neurotrophic factors, and chemokines, contribute to neuronal excitability and a central sensitization mechanism under trigeminal pain states (Iwata et al., 2011, 2017; Melik Parsadaniantz et al., 2015; Goto et al., 2016).

Recent studies have shown that acute (Launay et al., 2016) and persistent (Fakih et al., 2019) ocular pain conditions induce a higher density of Iba1-immunopositive microglial cells and higher levels of CD68 and ITGAM genes in the ipsilateral trigeminal brainstem sensory complex. Aside from immune cell activation, increased levels of the GFAP protein and gene expression, astrocyte marker in the brain, were reported in this central structure. Moreover, the upregulation of pro-inflammatory markers IL-6 and IL-1β, INOS2 genes, and ATF3 and FOS markers in the trigeminal brainstem sensory complex (TBSC) was associated with the development of corneal hypersensitivity (Fakih et al., 2019) (**Figure 4**). These findings strongly suggest that neuronal–glial and neuroinflammatory interactions occur after corneal nerve injury in the central nervous system, which may account for the development and persistence of the ocular pain reported in DED patients.

Persistent ongoing activity in primary nociceptors may also lead to central sensitization, which is defined as "*an amplification of neural signaling within the central nervous system that elicits pain hypersensitivity*," (Woolf, 2011) and a functional remodeling of presynaptic sites. Piccolo, one of the components of the presynaptic zone, plays a key role in synaptic plasticity by facilitating/managing the secretion of synaptic vesicles, and increased expression was reported in an orofacial pain model (Thibault et al., 2016). The upregulated expression of Piccolo in the brainstem in mice with persistent ocular pain associated with DED indicated that persistent ongoing corneal nociceptor activity induced profound synaptic reorganization, which may contribute to the chronicity of ocular pain. These central cellular rearrangements (neuroinflammation, astrocytes and microglial activation, and enhancements of excitatory synaptic transmission protein) are in line with the reported sensitization of ocular-responsive neurons of the caudal trigeminal brainstem in persistent tear deficiency in rats (Rahman et al., 2015) (**Figure 4**). These neuroplastic changes observed in the TG and TBSC under corneal pain are likely to play a role in the establishment and maintenance of central sensitization that is seen in many centralized pain disorders like fibromyalgia and migraine.

There is also a wealth of evidence to show that contralateral structural and molecular changes can occur both in the periphery and the central nervous system in response to a unilateral insult (Koltzenburg et al., 1999; Shenker et al., 2003; Ferrari et al., 2014; Lee et al., 2019).

For example, unilateral corneal damage induces inflammatory responses in contralateral mouse eyes (Yamaguchi et al., 2016; Lee et al., 2019), the TG (Ferrari et al., 2014), and the central nervous system (Launay et al., 2016). Indeed, FOS-like positive neurons were seen in the contralateral trigeminal brainstem after corneal nerve damage (Launay et al., 2016). Contralateral responses

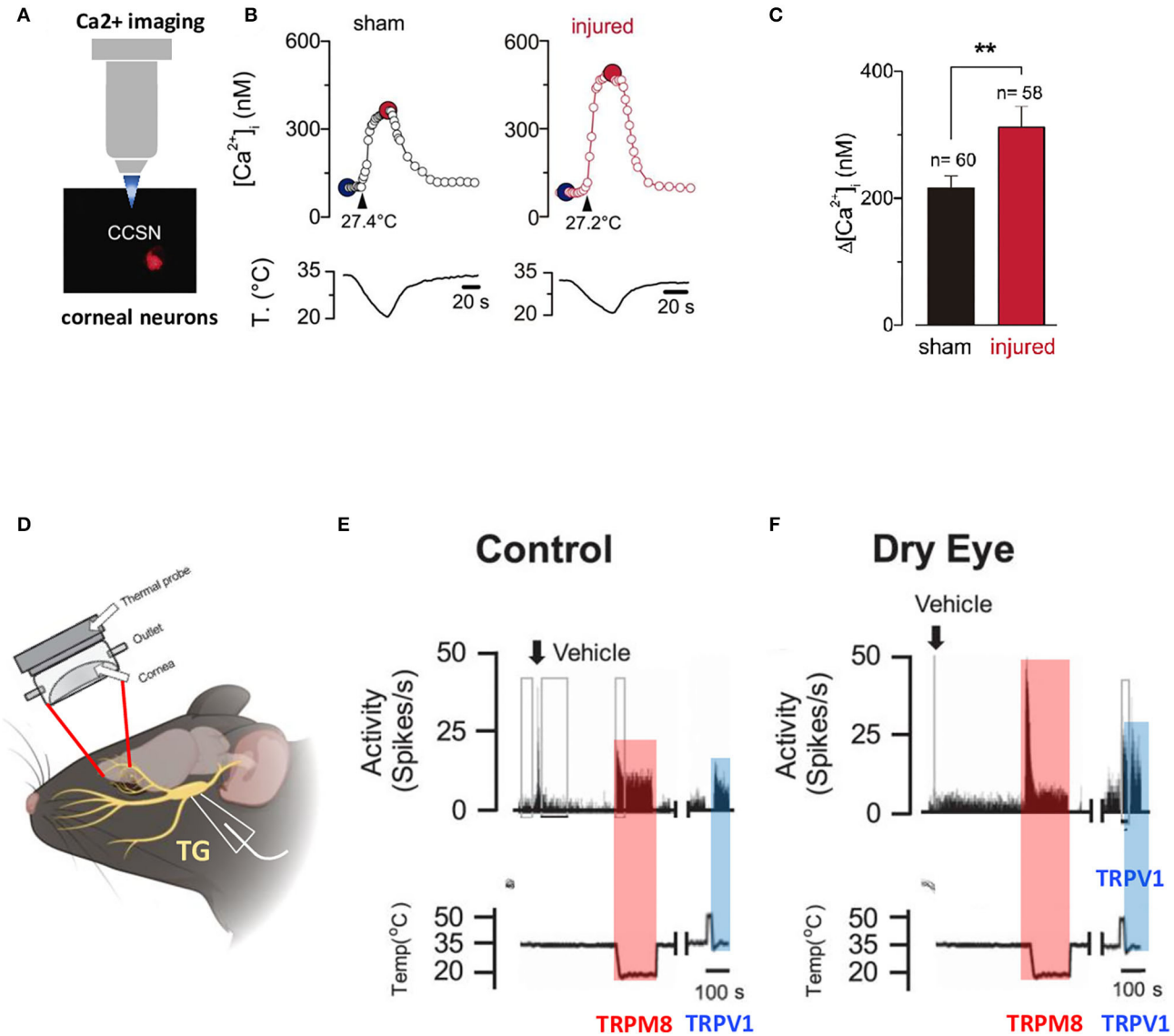


**FIGURE 3 |** Altered responsiveness of corneal neurons following peripheral nerve damage and after lacrimal gland excision. **(A)** Altered cold sensitivity of corneal neurons induced by peripheral nerve damage. Calcium imaging on FM 1–43 labeled corneal neurons in culture. **(B)** Cold-evoked $[Ca^{2+}]$i response to a temperature ramp of two representative corneal neurons from sham (black trace) and injured (red trace) mice. Large dots indicate the basal (blue) and maximal (red) $[Ca^{2+}]$i during the cold stimulus. **(C)** Bar graphs of the mean amplitude of $[Ca^{2+}]$i rises evoked by cold stimulation in the corneal neurons from sham and injured mice. Modified from Pina et al. (2019). Data plotted as mean ± SEM. $^{**}p = 0.0014$. **(D)** Illustration of the custom-made chamber designed with inflow and outflow portals for maintaining a constant environment on the surface of the cornea while recording from neuronal cell bodies located in the TG. **(E,F)** Effects of vehicle and cool and heat-evoked activity in control **(E)** and lacrimal gland excision (LGE) animals **(F)**. Neuronal activity recorded from control animals and animals 2 weeks after LGE, following vehicle, cold stimulation (TRPM8 activation), and 3 μM capsaicin (TRPV1 activation) applications to the cornea. Copyright © 2019 the American Physiological Society (Hatta et al., 2019).

were demonstrable not only in rodents, but also in the human eye (Hamrah et al., 2010, 2013; Postole et al., 2016; Yamaguchi et al., 2016), and there are several reasons supporting that these contralateral responses are mediated through neural mechanisms rather than reflecting a systemic effect (Shenker et al., 2003; Gong et al., 2020).

Increased corneal peripheral nociceptive input may result in neuronal activity within the higher-order neurons within the brain, particularly in regions associated with the pain matrix (the thalamus, insula, anterior cingulate cortex, prefrontal cortex, and somatosensory cortex). Only one study has been reported to date in this area of investigation. It showed in a mouse model of corneal alkali burn that corneal spontaneous pain activated the neuropathic central pain matrix (Xiang et al., 2017). Increased phospho-ERK positive neurons were detected in the subnucleus caudalis/upper cervical cord (Vc/V1), the insular cortex, the

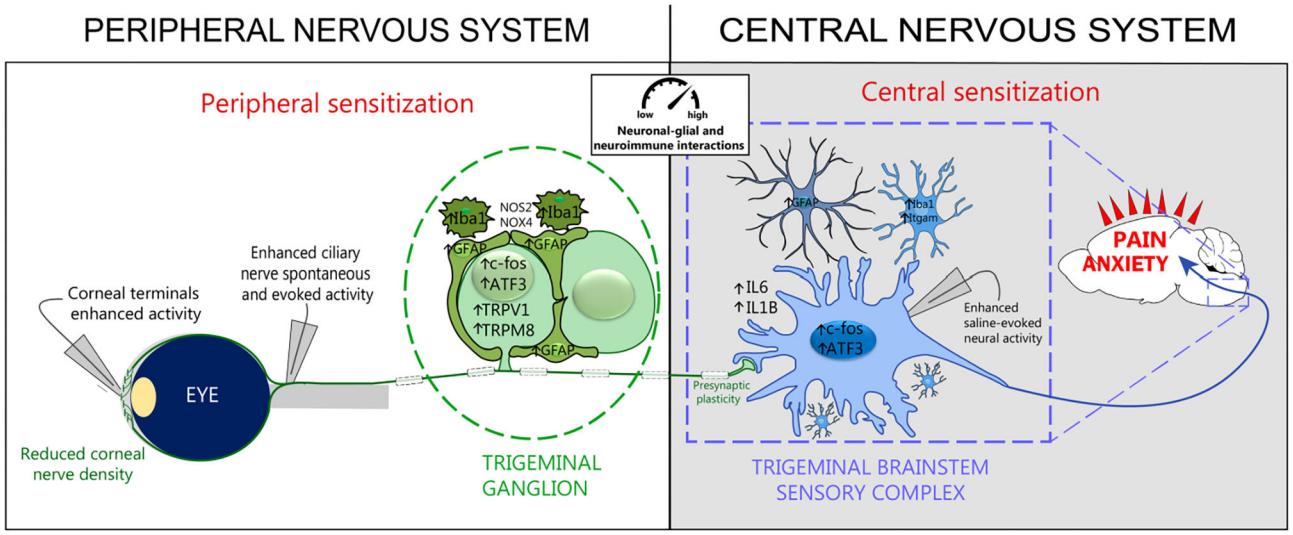


**FIGURE 4 |** Peripheral and central sensitization associated with persistent dry eye pain. Experimental persistent dry eye triggers corneal nerve abnormalities, neuroimmune interactions, and peripheral and central sensitization. Electrophysiological recordings reveal increased activity in corneal terminals, ciliary nerves, and trigeminal brainstem sensory complex neurons. Histological and molecular studies show neuronal activation (c-Fos) and injury (ATF3), *de novo* channel production (TRPV1, TRPM8), glial activation (Iba1, GFAP, Itgam), oxidative stress (NOS2, NOX4), proinflammatory responses (IL6, IL1B), and synaptic-enhancer plasticity at the level of TG and TBSC. These cellular and molecular changes lead to pain and promote anxiety-like behaviors. Modified from Guerrero-Moreno et al. (2021).

anterior cingulated cortex, and the rostroventral medulla. Many experiments are still needed to precisely determine the nature of central structures that are recruited during acute and persistent ocular pain.

## CLINICAL EVIDENCE OF CORNEAL NERVE ABNORMALITIES AND DYSFUNCTIONS

As previously stated, the new definition of DED includes somatosensory abnormalities as a core mechanism (Craig et al., 2017). The measurement of corneal sensitivity in patients could provide the first evidence for somatosensory abnormalities, but practical tools are still lacking to assess hypersensitivity and hyperexcitability, as well as explore other stimuli than simple mechanical responses. The persistence of ocular pain in a subset of patients with dry eye syndromes is a major challenge in the management of ocular pain (Rosenthal and Borsook, 2016; Mehra et al., 2020). It is therefore crucial to identify diagnostic modalities that can accurately predict or identify neuropathic pain.

Corneal sensitivity can be assessed by the Belmonte non-contact gas and the Cochet-Bonnet esthesiometers. The Belmonte non-contact gas esthesiometer allows one to measure corneal sensory abnormalities following mechanical, thermal, and chemical corneal stimulations, i.e., the detection of polymodal function for both A delta and C fibers.

Patients with dry eye exhibit corneal hypoesthesia after mechanical, thermal, and chemical stimulation, and this condition seems to be related to damage to the corneal sensory innervation (Bourcier et al., 2005). Some studies in patients with dry eye or neuropathic pain symptoms have found reduced corneal sensitivity to mechanical, thermal, and chemical stimuli compared to controls (Bourcier et al., 2005), while others have found increased mechanical sensitivity (Spierer et al., 2016). Unfortunately, complex sensing esthesiometers are only scarcely available and are not routine devices, despite their high potential for exploring DED and corneal sensitivity.

The Cochet-Bonnet contact esthesiometer is another device that has been widely used to characterize somatosensory disturbances within the human eye and more specifically for evaluations of mechanical nociceptor (A delta fibers) responses. Some studies have reported a reduced sensitivity to mechanical stimuli in DE patients (Adatia et al., 2004; Labbe et al., 2012) exhibiting a decreased corneal nerve density.

The maladaptive processes responsible for corneal pain can take place in either the peripheral or the central nervous system. Functional somatosensory testing, also known as the proparacaine challenge test, is useful for assessing the peripheral or central location of pain generators in patients. This functional test consists of a topical instillation of 0.5% proparacaine (an anesthetic commonly used in ophthalmology) and determines whether pain is abolished or not. The persistence of ocular pain suggests a central location, whereas a peripheral origin is confirmed by pain relief (Goyal and Hamrah, 2016; Crane et al., 2017). Patients with peripheral neuropathic pain would be the principal beneficiaries of topical painkillers, while systemic approaches would be preferred for patients with central neuropathic pain.

A functional assessment of corneal sensitivity is generally combined with a morphological analysis of the corneal nerve.

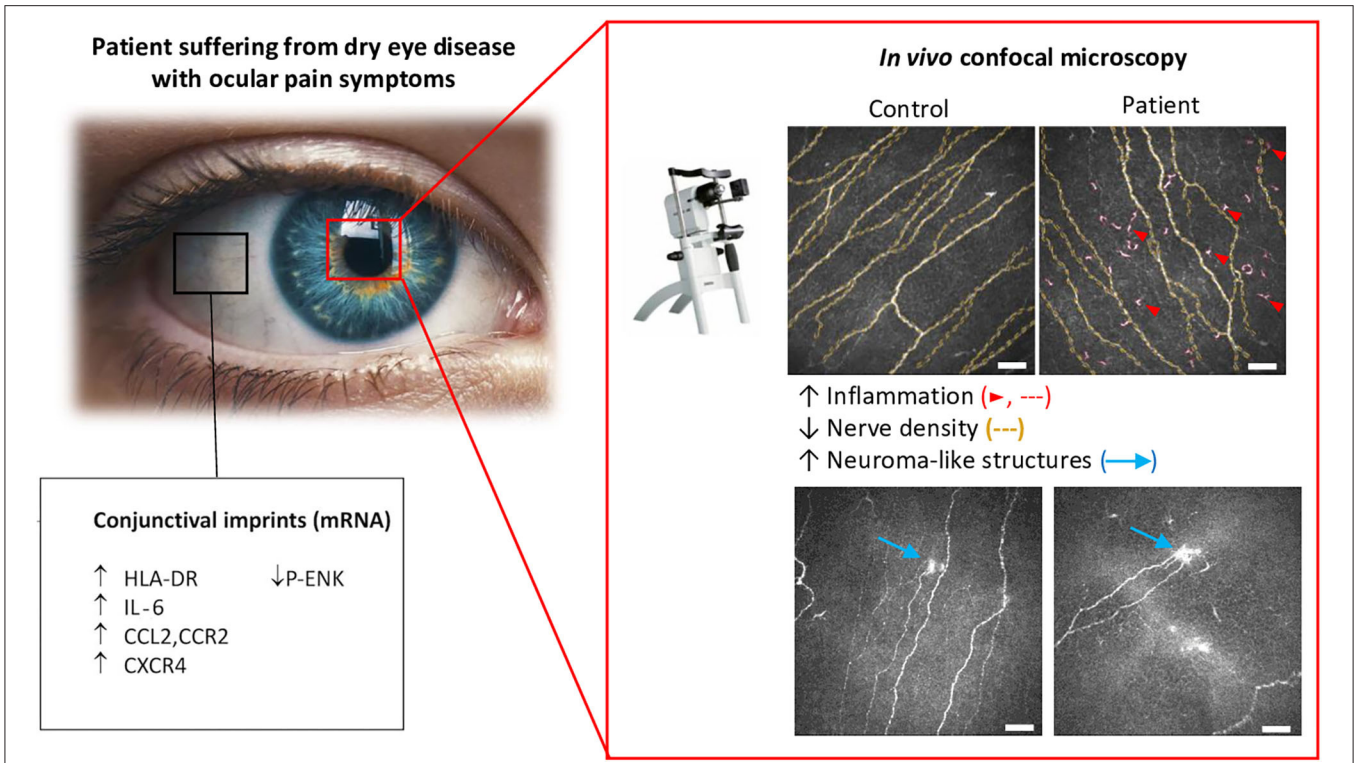


**FIGURE 5 |** Morphological and molecular changes in the ocular surface from dry eye patients with persistent ocular pain. Conjunctival imprints show higher levels of the proinflammatory markers, HLA-DR, IL-6, and CCL2, and of the chemokine receptors, CCR2 and CXCR4. In contrast, a decrease in the enkephalin precursor P-ENK was found in DE patients. Corneal IVCM imaging showed a decrease in nerve density, which was accompanied by a higher density of hyperreflective (putative inflammatory) cells and the presence of microneuroma-like structures in DED patients with pain syndromes. Modified from Nicolle et al. (2018).

IVCM is a non-invasive technique providing real-time, high-resolution corneal imaging in both humans and laboratory animals. IVCM studies allow for the longitudinal imaging and quantification of cellular changes in, e.g., dendritic and keratocyte cells, and of sub-basal nerve plexus morphology in corneas over time. Excellent reviews have described the broad changes in the sub-basal nerve layer by using IVCM imaging in healthy controls and patients (Cruzat et al., 2017; Al-Aqaba et al., 2019; Labetoulle et al., 2019). Quantification of IVCM images have evidenced that sub-basal nerves undergo a significant decrease in the number and density in patients with dry eye symptoms compared to healthy subjects (Bourcier et al., 2005; Benitez-Del-Castillo et al., 2007; Labbe et al., 2012, 2013; Levy et al., 2017; Nicolle et al., 2018) (**Figure 5**). Other morphological corneal nerve abnormalities have been observed in DE patients, such as nerve sprouting, increased thickness, tortuosity, and beading (for review Galor et al., 2018). Recent studies in patients with neuropathic corneal pain have also demonstrated decreased corneal nerve density associated with allodynia (Hamrah et al., 2017), photoallodynia (Aggarwal et al., 2015), and post-LASIK neuralgia (Theophanous et al., 2015). Those corneal nerve changes can be quantified automatically by emerging specialized software, representing a very promising tool for clinical assessments (Annunziata et al., 2016; Giannaccare et al., 2019).

Chronic pain induced after nerve injury is generally associated with prominent morphological and epigenetic changes within the afferent fibers. After nerve damage, destroyed peripheral nerves start to regenerate and form neuromas that exhibit abnormal responsiveness and spontaneous discharges (ectopic firing) (Fawcett and Keynes, 1990). These functional changes are the consequence of altered expressions of ion channel proteins in the soma and in regenerating nerve terminals. Neuroma structures have emerged as other important morphological changes in corneal nerves and have been suggested as clinical imagining biomarkers (hallmark) of corneal neuropathic pain (Aggarwal et al., 2019; Bayraktutar et al., 2020; Moein et al., 2020). Taken together, these studies suggest that a corneal neuroma may represent an important pathological feature of peripheral nerve abnormalities in patients with ocular pain. Interestingly, topical treatment with autologous serum tears reduced corneal nerve abnormalities, improved corneal nerve regeneration, and alleviated corneal pain (Aggarwal et al., 2019). Future directions are needed to determine when and how the morphological changes occur on the ocular surface and which subpopulations of corneal neurons are hit.

In recent years, clinical research regarding neuroimmune crosstalk has focused increasingly on the neuroimmune interactions in the cornea. Among the resident immune cells, epithelial dendritic cells predominantly reside in the basal

epithelium of the human cornea. These resident corneal dendritic cells play a key role in maintaining the homeostasis of corneal nerves (Gao et al., 2016). However, corneal damage or corneal nerve abnormalities can disrupt the balance between immune cells and peripheral nerves. Accumulative evidence has revealed, in the cornea from patients with DED and corneal neuropathic pain, increased activated dendritic cells and a close anatomical proximity between peripheral nerves and immune cells (Shetty et al., 2016; Tepelus et al., 2017; Aggarwal et al., 2020).

As stated before, fundamental and clinical studies have well-demonstrated that repeated damage to the ocular surface and corneal nerves *per se* can cause peripheral and central sensitization mechanisms, explaining the centralized pain in some patients with corneal neuropathic pain. However, the neuronal circuits participating in corneal pain are not fully understood. Over the past decade, brain imaging investigations have shed light on neural correlations with pain perception and modulation. New developments in structural, functional, and neurochemical imaging, such as resting-state connectivity, functional magnetic resonance imaging (fMRI), and γ-aminobutyric acid spectroscopy, have shed light on persistent non-ocular pain (Grachev et al., 2000; Harris and Clauw, 2012; Legarreta et al., 2020).

To date, only one case study from Moulton et al. (2012) has reported by means of fMRI the nature of hemodynamic responses evoked by corneal pain in the human brain. fMRI imaging revealed an activation of the contralateral somatosensory cortex, ventral posteromedial thalamus, and the anterior cingulated cortex during the painful state.

## CONCLUDING REMARKS AND FUTURE PERSPECTIVES

The cornea, the most densely innervated tissue in the human body, offers multiple advantages in fundamental and clinical research, as it is an excellent model to study the function and morphology of nociceptive nerve fibers, peripheral nerve damage, nerve regeneration, and sensory abnormalities. Accumulative clinical and animal model studies have identified morphological and functional abnormalities of corneal nerve terminals associated with ocular surface diseases. The last decade has also seen a rapid expansion in our knowledge regarding the nature of the cellular and molecular mechanisms, as well as the neuroimmune interactions that take place in the cornea, the TG, which contains the primary sensory neurons, and higher central structures. However, many questions remain unanswered. Among them, unraveling neuroimmune crosstalk mechanisms leading to inflammation and pain would bring a more comprehensive picture of the entire neuroinflammatory process and represents an exciting and expanding research domain. In the future, there is also an urgent need to elucidate the time window for restoring corneal nerve morphological and functional abnormalities and to identify a more specific target and their signaling pathways in corneal nociceptors, which may offer alternative treatments.

Finally, recent advances in *in vivo* functional imaging technology, together with automatic frameworks for clinical assessment, bi- and three-photo microscopy imaging, viral-mediated optogenetic control of peripheral nerve expressing light sensitive opsins, chemogenetics, and the development of simple or dual knockout mice, may help in solving the puzzle of these maladaptive changes in the corneal nociceptive pathways.

## AUTHOR CONTRIBUTIONS

AG-M and AR-L equally contributed to drafting the manuscript and the figures. AR-L conceptualized the review. AG-M and AR-L wrote the manuscript. AG-M, AR-L, CB, and SMP contributed to the article and approved the manuscript.

## FUNDING

This work was supported by Sorbonne Université and the Institut National de la Santé et de la Recherche Médicale, ANR, LabEx LIFESENSES (ANR-10-LABX-65), and IHU FOReSIGHT (ANR-18-IAHU-01). AG-M was funded by a H2020-MSCA-ETN program (IT-DED$^3$) (Grant Agreement 765608).

## REFERENCES

Acosta, M. C., Belmonte, C., and Gallar, J. (2001). Sensory experiences in humans and single-unit activity in cats evoked by polymodal stimulation of the cornea. *J. Physiol.* 534, 511–525. doi: 10.1111/j.1469-7793.2001.t01-1-00511.x

Acosta, M. C., Luna, C., Graff, G., Meseguer, V. M., Viana, F., Gallar, J., et al. (2007). Comparative effects of the nonsteroidal anti-inflammatory drug nepafenac on corneal sensory nerve fibers responding to chemical irritation. *Invest. Ophthalmol. Vis. Sci.* 48, 182–188. doi: 10.1167/iovs.06-0710

Acosta, M. C., Luna, C., Quirce, S., Belmonte, C., and Gallar, J. (2013). Changes in sensory activity of ocular surface sensory nerves during allergic keratoconjunctivitis. *Pain* 154, 2353–2362. doi: 10.1016/j.pain.2013.07.012

Acosta, M. C., Luna, C., Quirce, S., Belmonte, C., and Gallar, J. (2014). Corneal sensory nerve activity in an experimental model of UV keratitis. *Invest. Ophthalmol. Vis. Sci.* 55, 3403–3412. doi: 10.1167/iovs.13-13774

Adatia, F. A., Michaeli-Cohen, A., Naor, J., Caffery, B., Bookman, A., and Slomovic, A. (2004). Correlation between corneal sensitivity, subjective dry eye symptoms and corneal staining in Sjogren's syndrome. *Can. J. Ophthalmol.* 39, 767–771. doi: 10.1016/S0008-4182(04)80071-1

Aggarwal, S., Colon, C., Kheirkhah, A., and Hamrah, P. (2019). Efficacy of autologous serum tears for treatment of neuropathic corneal pain. *Ocul. Surf.* 17, 532–539. doi: 10.1016/j.jtos.2019.01.009

Aggarwal, S., Kheirkhah, A., Cavalcanti, B. M., Cruzat, A., Colon, C., Brown, E., et al. (2015). Autologous serum tears for treatment of photoallodynia in patients with corneal neuropathy: efficacy and evaluation with *in vivo* confocal microscopy. *Ocul. Surf.* 13, 250–262. doi: 10.1016/j.jtos.2015.01.005

Aggarwal, S., Kheirkhah, A., Cavalcanti, B. M., Cruzat, A., Jamali, A., and Hamrah, P. (2020). Correlation of corneal immune cell changes with clinical severity in dry eye disease: An *in vivo* confocal microscopy study. *Ocul. Surf.* doi: 10.1016/j.jtos.2020.05.012. [Epub ahead of print].

Alamri, A., Bron, R., Brock, J. A., and Ivanusic, J. J. (2015). Transient receptor potential cation channel subfamily V member 1 expressing corneal sensory neurons can be subdivided into at least three subpopulations. *Front. Neuroanat.* 9:71. doi: 10.3389/fnana.2015.00071

Alamri, A. S., Wood, R. J., Ivanusic, J. J., and Brock, J. A. (2018). The neurochemistry and morphology of functionally identified corneal polymodal nociceptors and cold thermoreceptors. *PLoS ONE* 13:e0195108. doi: 10.1371/journal.pone.0195108

Al-Aqaba, M. A., Dhillon, V. K., Mohammed, I., Said, D. G., and Dua, H. S. (2019). Corneal nerves in health and disease. *Prog. Retin. Eye Res.* 73:100762. doi: 10.1016/j.preteyeres.2019.05.003

Alcalde, I., Inigo-Portugues, A., Gonzalez-Gonzalez, O., Almaraz, L., Artime, E., Morenilla-Palao, C., et al. (2018). Morphological and functional changes in TRPM8-expressing corneal cold thermoreceptor neurons during aging and their impact on tearing in mice. *J. Comp. Neurol.* 526, 1859–1874. doi: 10.1002/cne.24454

Annunziata, R., Kheirkhah, A., Aggarwal, S., Hamrah, P., and Trucco, E. (2016). A fully automated tortuosity quantification system with application to corneal nerve fibres in confocal microscopy images. *Med. Image Anal.* 32, 216–232. doi: 10.1016/j.media.2016.04.006

Baral, P., Udit, S., and Chiu, I. M. (2019). Pain and immunity: implications for host defence. *Nat. Rev. Immunol.* 19, 433–447. doi: 10.1038/s41577-019-0147-2

Bayraktutar, B. N., Ozmen, M. C., Muzaaya, N., Dieckmann, G., Koseoglu, N. D., Muller, R. T., et al. (2020). Comparison of clinical characteristics of post-refractive surgery-related and post-herpetic neuropathic corneal pain. *Ocul. Surf.* 18, 641–650. doi: 10.1016/j.jtos.2020.07.006

Bech, F., Gonzalez-Gonzalez, O., Artime, E., Serrano, J., Alcalde, I., Gallar, J., et al. (2018). Functional and morphologic alterations in mechanical, polymodal, and cold sensory nerve fibers of the cornea following photorefractive keratectomy. *Invest. Ophthalmol. Vis. Sci.* 59, 2281–2292. doi: 10.1167/iovs.18-24007

Belmonte, C. (2019). Pain, dryness, and itch sensations in eye surface disorders are defined by a balance between inflammation and sensory nerve injury. *Cornea 38(Suppl* 1), S11–S24. doi: 10.1097/ICO.0000000000002116

Belmonte, C., Acosta, M. C., and Gallar, J. (2004). Neural basis of sensation in intact and injured corneas. *Exp. Eye Res.* 78, 513–525. doi: 10.1016/j.exer.2003.09.023

Belmonte, C., Acosta, M. C., Merayo-Lloves, J., and Gallar, J. (2015). What causes eye pain? *Curr. Ophthalmol. Rep.* 3, 111–121. doi: 10.1007/s40135-015-0073-9

Belmonte, C., Gallar, J., Pozo, M. A., and Rebollo, I. (1991). Excitation by irritant chemical substances of sensory afferent units in the cat's cornea. *J. Physiol.* 437, 709–725. doi: 10.1113/jphysiol.1991.sp018621

Belmonte, C., Nichols, J. J., Cox, S. M., Brock, J. A., Begley, C. G., Bereiter, D. A., et al. (2017). TFOS DEWS II pain and sensation report. *Ocul. Surf.* 15, 404–437. doi: 10.1016/j.jtos.2017.05.002

Benitez-Del-Castillo, J. M., Acosta, M. C., Wassfi, M. A., Diaz-Valle, D., Gegundez, J. A., Fernandez, C., et al. (2007). Relation between corneal innervation with confocal microscopy and corneal sensitivity with noncontact esthesiometry in patients with dry eye. *Invest. Ophthalmol. Vis. Sci.* 48, 173–181. doi: 10.1167/iovs.06-0127

Bereiter, D. A., Rahman, M., Thompson, R., Stephenson, P., and Saito, H. (2018). TRPV1 and TRPM8 channels and nocifensive behavior in a rat model for dry eye. *Invest. Ophthalmol. Vis. Sci.* 59, 3739–3746. doi: 10.1167/iovs.18-24304

Berta, T., Qadri, Y., Tan, P. H., and Ji, R. R. (2017). Targeting dorsal root ganglia and primary sensory neurons for the treatment of chronic pain. *Expert Opin. Ther. Targets* 21, 695–703. doi: 10.1080/14728222.2017.1328057

Beuerman, R. W., Snow, A., Thompson, H., and Stern, M. (1992). Action potential response of the corneal nerves to irritants. *Lens Eye Toxic. Res.* 9, 193–210.

Bouheraoua, N., Fouquet, S., Marcos-Almaraz, M. T., Karagogeos, D., Laroche, L., and Chedotal, A. (2019). Genetic analysis of the organization, development, and plasticity of corneal innervation in mice. *J. Neurosci.* 39, 1150–1168. doi: 10.1523/JNEUROSCI.1401-18.2018

Bourcier, T., Acosta, M. C., Borderie, V., Borras, F., Gallar, J., Bury, T., et al. (2005). Decreased corneal sensitivity in patients with dry eye. *Invest. Ophthalmol. Vis. Sci.* 46, 2341–2345. doi: 10.1167/iovs.04-1426

Bron, R., Wood, R. J., Brock, J. A., and Ivanusic, J. J. (2014). Piezo2 expression in corneal afferent neurons. *J. Comp. Neurol.* 522, 2967–2979. doi: 10.1002/cne.23560

Carr, R. W., Pianova, S., Fernandez, J., Fallon, J. B., Belmonte, C., and Brock, J. A. (2003). Effects of heating and cooling on nerve terminal impulses recorded from cold-sensitive receptors in the guinea-pig cornea. *J. Gen. Physiol.* 121, 427–439. doi: 10.1085/jgp.20038814

Chaudhary, S., Namavari, A., Yco, L., Chang, J. H., Sonawane, S., Khanolkar, V., et al. (2012). Neurotrophins and nerve regeneration-associated genes are expressed in the cornea after lamellar flap surgery. *Cornea* 31, 1460–1467. doi: 10.1097/ICO.0b013e318247b60e

Chen, X., Gallar, J., and Belmonte, C. (1997). Reduction by antiinflammatory drugs of the response of corneal sensory nerve fibers to chemical irritation. *Invest. Ophthalmol. Vis. Sci.* 38, 1944–1953.

Chiu, I. M., von Hehn, C. A., and Woolf, C. J. (2012). Neurogenic inflammation and the peripheral nervous system in host defense and immunopathology. *Nat. Neurosci.* 15, 1063–1067. doi: 10.1038/nn.3144

Cho, J., Bell, N., Botzet, G., Vora, P., Fowler, B. J., Donahue, R., et al. (2019). Latent sensitization in a mouse model of ocular neuropathic pain. *Transl. Vis. Sci. Technol.* 8:6. doi: 10.1167/tvst.8.2.6

Coste, B., Mathur, J., Schmidt, M., Earley, T. J., Ranade, S., Petrus, M. J., et al. (2010). Piezo1 and Piezo2 are essential components of distinct mechanically activated cation channels. *Science* 330, 55–60. doi: 10.1126/science.1193270

Craig, J. P., Nichols, K. K., Akpek, E. K., Caffery, B., Dua, H. S., Joo, C. K., et al. (2017). TFOS DEWS II definition and classification report. *Ocul. Surf.* 15, 276–283. doi: 10.1016/j.jtos.2017.05.008

Crane, A. M., Feuer, W., Felix, E. R., Levitt, R. C., McClellan, A. L., Sarantopoulos, K. D., et al. (2017). Evidence of central sensitisation in those with dry eye symptoms and neuropathic-like ocular pain complaints: incomplete response to topical anaesthesia and generalised heightened sensitivity to evoked pain. *Br. J. Ophthalmol.* 101, 1238–1243. doi: 10.1136/bjophthalmol-2016-309658

Cruzat, A., Qazi, Y., and Hamrah, P. (2017). *In vivo* confocal microscopy of corneal nerves in health and disease. *Ocul. Surf.* 15, 15–47. doi: 10.1016/j.jtos.2016.09.004

De Felipe, C., and Belmonte, C. (1999). c-Jun expression after axotomy of corneal trigeminal ganglion neurons is dependent on the site of injury. *Eur. J. Neurosci.* 11, 899–906. doi: 10.1046/j.1460-9568.1999.00498.x

Dieckmann, G., Goyal, S., and Hamrah, P. (2017). Neuropathic corneal pain: approaches for management. *Ophthalmology* 124, S34–S47. doi: 10.1016/j.ophtha.2017.08.004

Fakih, D., Zhao, Z., Nicolle, P., Reboussin, E., Joubert, F., Luzu, J., et al. (2019). Chronic dry eye induced corneal hypersensitivity, neuroinflammatory responses, and synaptic plasticity in the mouse trigeminal brainstem. *J. Neuroinflamm.* 16:268. doi: 10.1186/s12974-019-1656-4

Fawcett, J. W., and Keynes, R. J. (1990). Peripheral nerve regeneration. *Annu. Rev. Neurosci.* 13, 43–60. doi: 10.1146/annurev.ne.13.030190.000355

Fernandez-Trillo, J., Florez-Paz, D., Inigo-Portugues, A., Gonzalez-Gonzalez, O., Del Campo, A. G., Gonzalez, A., et al. (2020). Piezo2 mediates low-threshold mechanically-evoked pain in the cornea. *J. Neurosci.* 40, 8976–8993. doi: 10.1523/JNEUROSCI.0247-20.2020

Ferrari, G., Bignami, F., Giacomini, C., Capitolo, E., Comi, G., Chaabane, L., et al. (2014). Ocular surface injury induces inflammation in the brain: *in vivo* and *ex vivo* evidence of a corneal-trigeminal axis. *Invest. Ophthalmol. Vis. Sci.* 55, 6289–6300. doi: 10.1167/iovs.14-13984

Gallar, J., Acosta, M. C., Gutierrez, A. R., and Belmonte, C. (2007). Impulse activity in corneal sensory nerve fibers after photorefractive keratectomy. *Invest. Ophthalmol. Vis. Sci.* 48, 4033–4037. doi: 10.1167/iovs.07-0012

Gallar, J., Pozo, M. A., Tuckett, R. P., and Belmonte, C. (1993). Response of sensory units with unmyelinated fibres to mechanical, thermal and chemical stimulation of the cat's cornea. *J. Physiol.* 468, 609–622. doi: 10.1113/jphysiol.1993.sp019791

Galor, A., Moein, H. R., Lee, C., Rodriguez, A., Felix, E. R., Sarantopoulos, K. D., et al. (2018). Neuropathic pain and dry eye. *Ocul. Surf.* 16, 31–44. doi: 10.1016/j.jtos.2017.10.001

Gao, N., Lee, P., and Yu, F. S. (2016). Intraepithelial dendritic cells and sensory nerves are structurally associated and functional interdependent in the cornea. *Sci. Rep.* 6:36414. doi: 10.1038/srep36414

Giannaccare, G., Pellegrini, M., Sebastiani, S., Moscardelli, F., Versura, P., and Campos, E. C. (2019). *In vivo* confocal microscopy morphometric analysis of corneal subbasal nerve plexus in dry eye disease using newly developed fully automated system. *Graefes Arch. Clin. Exp. Ophthalmol.* 257, 583–589. doi: 10.1007/s00417-018-04225-7

Goldstein, R. H., Barkai, O., Inigo-Portugues, A., Katz, B., Lev, S., and Binshtok, A. M. (2019). Location and plasticity of the sodium spike initiation zone in nociceptive terminals *in vivo*. *Neuron* 102, 80–812.e805. doi: 10.1016/j.neuron.2019.03.005

Gong, X., Ren, Y., Fang, X., Cai, J., and Song, E. (2020). Substance P induces sympathetic immune response in the contralateral eye after the first eye cataract surgery in type 2 diabetic patients. *BMC Ophthalmol.* 20:339. doi: 10.1186/s12886-020-01598-4

Gonzalez-Coto, A. F., Alonso-Ron, C., Alcalde, I., Gallar, J., Meana, A., Merayo-Lloves, J., et al. (2014). Expression of cholecystokinin, gastrin, and their receptors in the mouse cornea. *Invest. Ophthalmol. Vis. Sci.* 55, 1965–1975. doi: 10.1167/iovs.13-12068

Gonzalez-Gonzalez, O., Bech, F., Gallar, J., Merayo-Lloves, J., and Belmonte, C. (2017). Functional properties of sensory nerve terminals of the mouse cornea. *Invest. Ophthalmol. Vis. Sci.* 58, 404–415. doi: 10.1167/iovs.16-20033

Goto, T., Oh, S. B., Takeda, M., Shinoda, M., Sato, T., Gunjikake, K. K., et al. (2016). Recent advances in basic research on the trigeminal ganglion. *J. Physiol. Sci.* 66, 381–386. doi: 10.1007/s12576-016-0448-1

Goyal, S., and Hamrah, P. (2016). Understanding neuropathic corneal pain–gaps and current therapeutic approaches. *Semin. Ophthalmol.* 31, 59–70. doi: 10.3109/08820538.2015.1114853

Grace, P. M., Hutchinson, M. R., Maier, S. F., and Watkins, L. R. (2014). Pathological pain and the neuroimmune interface. *Nat. Rev. Immunol.* 14, 217–231. doi: 10.1038/nri3621

Grachev, I. D., Fredrickson, B. E., and Apkarian, A. V. (2000). Abnormal brain chemistry in chronic back pain: an *in vivo* proton magnetic resonance spectroscopy study. *Pain* 89, 7–18. doi: 10.1016/S0304-3959(00)00340-7

Guerrero-Moreno, A., Fakih, D., Parsadaniantz, S. M., and Reaux-Le Goazigo, A. (2021). How does chronic dry eye shape peripheral and central nociceptive systems? *Neural Regen. Res.* 16, 306–307. doi: 10.4103/1673-5374.290895

Guzman, M., Miglio, M., Keitelman, I., Shiromizu, C. M., Sabbione, F., Fuentes, F., et al. (2020). Transient tear hyperosmolarity disrupts the neuroimmune homeostasis of the ocular surface and facilitates dry eye onset. *Immunology* 161, 148–161. doi: 10.1111/imm.13243

Hamrah, P., Cruzat, A., Dastjerdi, M. H., Pruss, H., Zheng, L., Shahatit, B. M., et al. (2013). Unilateral herpes zoster ophthalmicus results in bilateral corneal nerve alteration: an *in vivo* confocal microscopy study. *Ophthalmology* 120, 40–47. doi: 10.1016/j.ophtha.2012.07.036

Hamrah, P., Cruzat, A., Dastjerdi, M. H., Zheng, L., Shahatit, B. M., Bayhan, H. A., et al. (2010). Corneal sensation and subbasal nerve alterations in patients with herpes simplex keratitis: an *in vivo* confocal microscopy study. *Ophthalmology* 117, 1930–1936. doi: 10.1016/j.ophtha.2010.07.010

Hamrah, P., Qazi, Y., Shahatit, B., Dastjerdi, M. H., Pavan-Langston, D., Jacobs, D. S., et al. (2017). Corneal nerve and epithelial cell alterations in corneal allodynia: an *in vivo* confocal microscopy case series. *Ocul. Surf.* 15, 139–151. doi: 10.1016/j.jtos.2016.10.002

Hanani, M. (2005). Satellite glial cells in sensory ganglia: from form to function. *Brain Res. Brain Res. Rev.* 48, 457–476. doi: 10.1016/j.brainresrev.2004.09.001

Harris, R. E., and Clauw, D. J. (2012). Imaging central neurochemical alterations in chronic pain with proton magnetic resonance spectroscopy. *Neurosci. Lett.* 520, 192–196. doi: 10.1016/j.neulet.2012.03.042

Hatta, A., Kurose, M., Sullivan, C., Okamoto, K., Fujii, N., Yamamura, K., et al. (2019). Dry eye sensitizes cool cells to capsaicin-induced changes in activity via TRPV1. *J. Neurophysiol.* 121, 2191–2201. doi: 10.1152/jn.00126.2018

He, J., Pham, T. L., Kakazu, A. H., and Bazan, H. E. P. (2019). Remodeling of substance p sensory nerves and transient receptor potential melastatin 8 (TRPM8) cold receptors after corneal experimental surgery. *Invest. Ophthalmol. Vis. Sci.* 60, 2449–2460. doi: 10.1167/iovs.18-26384

Hegarty, D. M., Hermes, S. M., Morgan, M. M., and Aicher, S. A. (2018). Acute hyperalgesia and delayed dry eye after corneal abrasion injury. *Pain Rep.* 3:e664. doi: 10.1097/PR9.0000000000000664

Hirata, H., and Meng, I. D. (2010). Cold-sensitive corneal afferents respond to a variety of ocular stimuli central to tear production: implications for dry eye disease. *Invest. Ophthalmol. Vis. Sci.* 51, 3969–3976. doi: 10.1167/iovs.09-4744

Hirata, H., Mizerska, K., Dallacasagrande, V., Guaiquil, V. H., and Rosenblatt, M. I. (2017). Acute corneal epithelial debridement unmasks the corneal stromal nerve responses to ocular stimulation in rats: implications for abnormal sensations of the eye. *J. Neurophysiol.* 117, 1935–1947. doi: 10.1152/jn.00925.2016

Hirata, H., Mizerska, K., Marfurt, C. F., and Rosenblatt, M. I. (2015). Hyperosmolar tears induce functional and structural alterations of corneal nerves: electrophysiological and anatomical evidence toward neurotoxicity. *Invest. Ophthalmol. Vis. Sci.* 56, 8125–8140. doi: 10.1167/iovs.15-18383

Ivanusic, J. J., Wood, R. J., and Brock, J. A. (2013). Sensory and sympathetic innervation of the mouse and guinea pig corneal epithelium. *J. Comp. Neurol.* 521, 877–893. doi: 10.1002/cne.23207

Iwata, K., Imamura, Y., Honda, K., and Shinoda, M. (2011). Physiological mechanisms of neuropathic pain: the orofacial region. *Int. Rev. Neurobiol.* 97, 227–250. doi: 10.1016/B978-0-12-385198-7.00009-6

Iwata, K., Katagiri, A., and Shinoda, M. (2017). Neuron-glia interaction is a key mechanism underlying persistent orofacial pain. *J. Oral Sci.* 59, 173–175. doi: 10.2334/josnusd.16-0858

Iwata, K., and Shinoda, M. (2019). Role of neuron and non-neuronal cell communication in persistent orofacial pain. *J. Dent. Anesth. Pain. Med.* 19, 77–82. doi: 10.17245/jdapm.2019.19.2.77

Jain, A., Hakim, S., and Woolf, C. J. (2020). Unraveling the plastic peripheral neuroimmune interactome. *J. Immunol.* 204, 257–263. doi: 10.4049/jimmunol.1900818

Jones, M. A., and Marfurt, C. F. (1996). Sympathetic stimulation of corneal epithelial proliferation in wounded and nonwounded rat eyes. *Invest. Ophthalmol. Vis. Sci.* 37, 2535–2547.

Jones, M. A., and Marfurt, C. F. (1998). Peptidergic innervation of the rat cornea. *Exp. Eye Res.* 66, 421–435. doi: 10.1006/exer.1997.0446

Jones, S. L., and Svitkina, T. M. (2016). Axon initial segment cytoskeleton: architecture, development, and role in neuron polarity. *Neural Plast.* 2016:6808293. doi: 10.1155/2016/6808293

Joubert, F., Acosta, M. D. C., Gallar, J., Fakih, D., Sahel, J. A., Baudouin, C., et al. (2019). Effects of corneal injury on ciliary nerve fibre activity and corneal nociception in mice: a behavioural and electrophysiological study. *Eur. J. Pain* 23, 589–602. doi: 10.1002/ejp.1332

Katagiri, A., Shinoda, M., Honda, K., Toyofuku, A., Sessle, B. J., and Iwata, K. (2012). Satellite glial cell P2Y12 receptor in the trigeminal ganglion is involved in lingual neuropathic pain mechanisms in rats. *Mol. Pain* 8:23. doi: 10.1186/1744-8069-8-23

Koltzenburg, M., Wall, P. D., and McMahon, S. B. (1999). Does the right side know what the left is doing? *Trends Neurosci.* 22, 122–127. doi: 10.1016/S0166-2236(98)01302-2

Kovacs, I., Dienes, L., Perenyi, K., Quirce, S., Luna, C., Mizerska, K., et al. (2016a). Lacosamide diminishes dryness-induced hyperexcitability of corneal cold sensitive nerve terminals. *Eur. J. Pharmacol.* 787, 2–8. doi: 10.1016/j.ejphar.2016.05.044

Kovacs, I., Luna, C., Quirce, S., Mizerska, K., Callejo, G., Riestra, A., et al. (2016b). Abnormal activity of corneal cold thermoreceptors underlies the unpleasant sensations in dry eye disease. *Pain* 157, 399–417. doi: 10.1097/j.pain.0000000000000455

Kurose, M., and Meng, I. D. (2013). Dry eye modifies the thermal and menthol responses in rat corneal primary afferent cool cells. *J. Neurophysiol.* 110, 495–504. doi: 10.1152/jn.00222.2013

Labbe, A., Alalwani, H., Van Went, C., Brasnu, E., Georgescu, D., and Baudouin, C. (2012). The relationship between subbasal nerve morphology and corneal sensation in ocular surface disease. *Invest. Ophthalmol. Vis. Sci.* 53, 4926–4931. doi: 10.1167/iovs.11-8708

Labbe, A., Liang, Q., Wang, Z., Zhang, Y., Xu, L., Baudouin, C., et al. (2013). Corneal nerve structure and function in patients with non-sjogren dry eye: clinical correlations. *Invest. Ophthalmol. Vis. Sci.* 54, 5144–5150. doi: 10.1167/iovs.13-12370

Labetoulle, M., Baudouin, C., Calonge, M., Merayo-Lloves, J., Boboridis, K. G., Akova, Y. A., et al. (2019). Role of corneal nerves in ocular surface homeostasis and disease. *Acta Ophthalmol.* 97, 137–145. doi: 10.1111/aos.13844

Launay, P. S., Godefroy, D., Khabou, H., Rostene, W., Sahel, J. A., Baudouin, C., et al. (2015). Combined 3DISCO clearing method, retrograde tracer and ultramicroscopy to map corneal neurons in a whole adult mouse trigeminal ganglion. *Exp. Eye Res.* 139, 136–143. doi: 10.1016/j.exer.2015.06.008

Launay, P. S., Reboussin, E., Liang, H., Kessal, K., Godefroy, D., Rostene, W., et al. (2016). Ocular inflammation induces trigeminal pain, peripheral and central neuroinflammatory mechanisms. *Neurobiol. Dis.* 88, 16–28. doi: 10.1016/j.nbd.2015.12.017

Lee, H. K., Kim, K. W., Ryu, J. S., Jeong, H. J., Lee, S. M., and Kim, M. K. (2019). Bilateral effect of the unilateral corneal nerve cut on both ocular surface and lacrimal gland. *Invest. Ophthalmol. Vis. Sci.* 60, 430–441. doi: 10.1167/iovs.18-26051

Legarreta, M. D., Sheth, C., Prescot, A. P., Renshaw, P. F., McGlade, E. C., and Yurgelun-Todd, D. A. (2020). An exploratory proton MRS examination of gamma-aminobutyric acid, glutamate, and glutamine and their relationship to affective aspects of chronic pain. *Neurosci. Res.* doi: 10.1016/j.neures.2020.03.002. [Epub ahead of print].

Levine, J. D., Fields, H. L., and Basbaum, A. I. (1993). Peptides and the primary afferent nociceptor. *J. Neurosci.* 13, 2273–2286. doi: 10.1523/JNEUROSCI.13-06-02273.1993

Levy, O., Labbe, A., Borderie, V., Hamiche, T., Dupas, B., Laroche, L., et al. (2017). Increased corneal sub-basal nerve density in patients with Sjogren syndrome treated with topical cyclosporine A. *Clin. Exp. Ophthalmol.* 45, 455–463. doi: 10.1111/ceo.12898

Li, F., Yang, W., Jiang, H., Guo, C., Huang, A. J. W., Hu, H., et al. (2019). TRPV1 activity and substance P release are required for corneal cold nociception. *Nat. Commun.* 10:5678. doi: 10.1038/s41467-019-13536-0

Ljubimov, A. V., and Saghizadeh, M. (2015). Progress in corneal wound healing. *Prog. Retin. Eye Res.* 49, 17–45. doi: 10.1016/j.preteyeres.2015.07.002

Lopez de Armentia, M., Cabanes, C., and Belmonte, C. (2000). Electrophysiological properties of identified trigeminal ganglion neurons innervating the cornea of the mouse. *Neuroscience* 101, 1109–1115. doi: 10.1016/S0306-4522(00)00440-1

MacIver, M. B., and Tanelian, D. L. (1993a). Free nerve ending terminal morphology is fiber type specific for A delta and C fibers innervating rabbit corneal epithelium. *J. Neurophysiol.* 69, 1779–1783. doi: 10.1152/jn.1993.69.5.1779

MacIver, M. B., and Tanelian, D. L. (1993b). Structural and functional specialization of A delta and C fiber free nerve endings innervating rabbit corneal epithelium. *J. Neurosci.* 13, 4511–4524. doi: 10.1523/JNEUROSCI.13-10-04511.1993

Madrid, R., Donovan-Rodriguez, T., Meseguer, V., Acosta, M. C., Belmonte, C., and Viana, F. (2006). Contribution of TRPM8 channels to cold transduction in primary sensory neurons and peripheral nerve terminals. *J. Neurosci.* 26, 12512–12525. doi: 10.1523/JNEUROSCI.3752-06.2006

Marfurt, C., Anokwute, M. C., Fetcko, K., Mahony-Perez, E., Farooq, H., Ross, E., et al. (2019). Comparative anatomy of the mammalian corneal subbasal nerve plexus. *Invest. Ophthalmol. Vis. Sci.* 60, 4972–4984. doi: 10.1167/iovs.19-28519

Marfurt, C. F., Cox, J., Deek, S., and Dvorscak, L. (2010). Anatomy of the human corneal innervation. *Exp. Eye Res.* 90, 478–492. doi: 10.1016/j.exer.2009.12.010

Marfurt, C. F., and Del Toro, D. R. (1987). Corneal sensory pathway in the rat: a horseradish peroxidase tracing study. *J. Comp. Neurol.* 261, 450–459. doi: 10.1002/cne.902610309

Markoulli, M., Flanagan, J., Tummanapalli, S. S., Wu, J., and Willcox, M. (2018). The impact of diabetes on corneal nerve morphology and ocular surface integrity. *Ocul. Surf.* 16, 45–57. doi: 10.1016/j.jtos.2017.10.006

McKay, T. B., Seyed-Razavi, Y., Ghezzi, C. E., Dieckmann, G., Nieland, T. J. F., Cairns, D. M., et al. (2019). Corneal pain and experimental model development. *Prog. Retin. Eye Res.* 71, 88–113. doi: 10.1016/j.preteyeres.2018.11.005

McKemy, D. D., Neuhausser, W. M., and Julius, D. (2002). Identification of a cold receptor reveals a general role for TRP channels in thermosensation. *Nature* 416, 52–58. doi: 10.1038/nature719

McLaughlin, C. R., Acosta, M. C., Luna, C., Liu, W., Belmonte, C., Griffith, M., et al. (2010). Regeneration of functional nerves within full thickness collagen-phosphorylcholine corneal substitute implants in guinea pigs. *Biomaterials* 31, 2770–2778. doi: 10.1016/j.biomaterials.2009.12.031

McMahon, S. B., and Wood, J. N. (2006). Increasingly irritable and close to tears: TRPA1 in inflammatory pain. *Cell* 124, 1123–1125. doi: 10.1016/j.cell.2006.03.006

McMonnies, C. W. (2017). The potential role of neuropathic mechanisms in dry eye syndromes. *J. Optom.* 10, 5–13. doi: 10.1016/j.optom.2016.06.002

Mehra, D., Cohen, N. K., and Galor, A. (2020). Ocular surface pain: a narrative review. *Ophthalmol. Ther.* 9, 1–21. doi: 10.1007/s40123-020-00263-9

Melik Parsadaniantz, S., Rivat, C., Rostene, W., and Reaux-Le Goazigo, A. (2015). Opioid and chemokine receptor crosstalk: a promising target for pain therapy? *Nat. Rev. Neurosci.* 16, 69–78. doi: 10.1038/nrn3858

Meng, I. D., and Bereiter, D. A. (1996). Differential distribution of Fos-like immunoreactivity in the spinal trigeminal nucleus after noxious and innocuous thermal and chemical stimulation of rat cornea. *Neuroscience* 72, 243–254. doi: 10.1016/0306-4522(95)00541-2

Moein, H. R., Akhlaq, A., Dieckmann, G., Abbouda, A., Pondelis, N., Salem, Z., et al. (2020). Visualization of micro-neuromas by using *in vivo* confocal microscopy: an objective biomarker for the diagnosis of neuropathic corneal pain? *Ocul. Surf.* 18, 651–656. doi: 10.1016/j.jtos.2020.07.004

Moulton, E. A., Becerra, L., Rosenthal, P., and Borsook, D. (2012). An approach to localizing corneal pain representation in human primary somatosensory cortex. *PLoS ONE* 7:e44643. doi: 10.1371/journal.pone.0044643

Muller, L. J., Marfurt, C. F., Kruse, F., and Tervo, T. M. (2003). Corneal nerves: structure, contents and function. *Exp. Eye Res.* 76, 521–542. doi: 10.1016/S0014-4835(03)00050-2

Murata, Y., and Masuko, S. (2006). Peripheral and central distribution of TRPV1, substance P and CGRP of rat corneal neurons. *Brain Res.* 1085, 87–94. doi: 10.1016/j.brainres.2006.02.035

Nakamura, A., Hayakawa, T., Kuwahara, S., Maeda, S., Tanaka, K., Seki, M., et al. (2007). Morphological and immunohistochemical characterization of the trigeminal ganglion neurons innervating the cornea and upper eyelid of the rat. *J. Chem. Neuroanat.* 34, 95–101. doi: 10.1016/j.jchemneu.2007.05.005

Namavari, A., Chaudhary, S., Sarkar, J., Yco, L., Patel, K., Han, K. Y., et al. (2011). *In vivo* serial imaging of regenerating corneal nerves after surgical transection in transgenic thy1-YFP mice. *Invest. Ophthalmol. Vis. Sci.* 52, 8025–8032. doi: 10.1167/iovs.11-8332

Nicolle, P., Liang, H., Reboussin, E., Rabut, G., Warcoin, E., Brignole-Baudouin, F., et al. (2018). Proinflammatory markers, chemokines, and enkephalin in patients suffering from dry eye disease. *Int. J. Mol. Sci.* 19:1221. doi: 10.3390/ijms19041221

Parra, A., Gonzalez-Gonzalez, O., Gallar, J., and Belmonte, C. (2014). Tear fluid hyperosmolality increases nerve impulse activity of cold thermoreceptor endings of the cornea. *Pain* 155, 1481–1491. doi: 10.1016/j.pain.2014.04.025

Parra, A., Madrid, R., Echevarria, D., del Olmo, S., Morenilla-Palao, C., Acosta, M. C., et al. (2010). Ocular surface wetness is regulated by TRPM8-dependent cold thermoreceptors of the cornea. *Nat. Med.* 16, 1396–1399. doi: 10.1038/nm.2264

Peier, A. M., Moqrich, A., Hergarden, A. C., Reeve, A. J., Andersson, D. A., Story, G. M., et al. (2002). A TRP channel that senses cold stimuli and menthol. *Cell* 108, 705–715. doi: 10.1016/S0092-8674(02)00652-9

Pham, T. L., and Bazan, H. E. P. (2020). Docosanoid signaling modulates corneal nerve regeneration: effect on tear secretion, wound healing, and neuropathic pain. *J. Lipid Res.* doi: 10.1194/jlr.TR120000954. [Epub ahead of print].

Pham, T. L., Kakazu, A. H., He, J., Jun, B., Bazan, N. G., and Bazan, H. E. P. (2020). Novel RvD6 stereoisomer induces corneal nerve regeneration and wound healing post-injury by modulating trigeminal transcriptomic signature. *Sci. Rep.* 10:4582. doi: 10.1038/s41598-020-61390-8

Pina, R., Ugarte, G., Campos, M., Inigo-Portugues, A., Olivares, E., Orio, P., et al. (2019). Role of TRPM8 channels in altered cold sensitivity of corneal primary sensory neurons induced by axonal damage. *J. Neurosci.* 39, 8177–8192. doi: 10.1523/JNEUROSCI.0654-19.2019

Pinho-Ribeiro, F. A., Verri, W. A. Jr., and Chiu, I. M. (2017). Nociceptor sensory neuron-immune interactions in pain and inflammation. *Trends Immunol.* 38, 5–19. doi: 10.1016/j.it.2016.10.001

Postole, A. S., Knoll, A. B., Auffarth, G. U., and Mackensen, F. (2016). *In vivo* confocal microscopy of inflammatory cells in the corneal subbasal nerve plexus in patients with different subtypes of anterior uveitis. *Br. J. Ophthalmol.* 100, 1551–1556. doi: 10.1136/bjophthalmol-2015-307429

Quallo, T., Vastani, N., Horridge, E., Gentry, C., Parra, A., Moss, S., et al. (2015). TRPM8 is a neuronal osmosensor that regulates eye blinking in mice. *Nat. Commun.* 6:7150. doi: 10.1038/ncomms8150

Rahman, M., Okamoto, K., Thompson, R., Katagiri, A., and Bereiter, D. A. (2015). Sensitization of trigeminal brainstem pathways in a model for tear deficient dry eye. *Pain* 156, 942–950. doi: 10.1097/j.pain.0000000000000135

Raja, S. N., Carr, D. B., Cohen, M., Finnerup, N. B., Flor, H., Gibson, S., et al. (2020). The revised international association for the study of pain

definition of pain: concepts, challenges, and compromises. *Pain*. 161, 1976–1982. doi: 10.1097/j.pain.0000000000001939

Reaux-Le Goazigo, A., Poras, H., Ben-Dhaou, C., Ouimet, T., Baudouin, C., Wurm, M., et al. (2019). Dual enkephalinase inhibitor PL265: a novel topical treatment to alleviate corneal pain and inflammation. *Pain* 160, 307–321. doi: 10.1097/j.pain.0000000000001419

Robbins, A., Kurose, M., Winterson, B. J., and Meng, I. D. (2012). Menthol activation of corneal cool cells induces TRPM8-mediated lacrimation but not nociceptive responses in rodents. *Invest. Ophthalmol. Vis. Sci.* 53, 7034–7042. doi: 10.1167/iovs.12-10025

Rosenthal, P., and Borsook, D. (2016). Ocular neuropathic pain. *Br. J. Ophthalmol.* 100, 128–134. doi: 10.1136/bjophthalmol-2014-306280

Sarkar, J., Chaudhary, S., Namavari, A., Ozturk, O., Chang, J. H., Yco, L., et al. (2012). Corneal neurotoxicity due to topical benzalkonium chloride. *Invest. Ophthalmol. Vis. Sci.* 53, 1792–1802. doi: 10.1167/iovs.11-8775

Sarkar, J., Milani, B., Kim, E., An, S., Kwon, J., and Jain, S. (2019). Corneal nerve healing after in situ laser nerve transection. *PLoS ONE* 14:e0218879. doi: 10.1371/journal.pone.0218879

Shenker, N., Haigh, R., Roberts, E., Mapp, P., Harris, N., and Blake, D. (2003). A review of contralateral responses to a unilateral inflammatory lesion. *Rheumatology* 42, 1279–1286. doi: 10.1093/rheumatology/keg397

Shetty, R., Sethu, S., Deshmukh, R., Deshpande, K., Ghosh, A., Agrawal, A., et al. (2016). Corneal dendritic cell density is associated with subbasal nerve plexus features, ocular surface disease index, and serum vitamin d in evaporative dry eye disease. *Biomed Res. Int.* 2016:4369750. doi: 10.1155/2016/4369750

Shin, K. C., Park, H. J., Kim, J. G., Lee, I. H., Cho, H., Park, C., et al. (2019). The Piezo2 ion channel is mechanically activated by low-threshold positive pressure. *Sci. Rep.* 9:6446. doi: 10.1038/s41598-019-42492-4

Shinoda, M., Kubo, A., Hayashi, Y., and Iwata, K. (2019). Peripheral and central mechanisms of persistent orofacial pain. *Front. Neurosci.* 13:1227. doi: 10.3389/fnins.2019.01227

Simsek, C., Kojima, T., Nagata, T., Dogru, M., and Tsubota, K. (2019). Changes in murine subbasal corneal nerves after scopolamine-induced dry eye stress exposure. *Invest. Ophthalmol. Vis. Sci.* 60, 615–623. doi: 10.1167/iovs.18-26318

Spierer, O., Felix, E. R., McClellan, A. L., Parel, J. M., Gonzalez, A., Feuer, W. J., et al. (2016). Corneal mechanical thresholds negatively associate with dry eye and ocular pain symptoms. *Invest. Ophthalmol. Vis. Sci.* 57, 617–625. doi: 10.1167/iovs.15-18133

Stapleton, F., Alves, M., Bunya, V. Y., Jalbert, I., Lekhanont, K., Malet, F., et al. (2017). TFOS DEWS II epidemiology report. *Ocul. Surf.* 15, 334–365. doi: 10.1016/j.jtos.2017.05.003

Stepp, M. A., Pal-Ghosh, S., Tadvalkar, G., Williams, A., Pflugfelder, S. C., and de Paiva, C. S. (2018a). Reduced intraepithelial corneal nerve density and sensitivity accompany desiccating stress and aging in C57BL/6 mice. *Exp. Eye Res.* 169, 91–98. doi: 10.1016/j.exer.2018.01.024

Stepp, M. A., Pal-Ghosh, S., Tadvalkar, G., Williams, A. R., Pflugfelder, S. C., and de Paiva, C. S. (2018b). Reduced corneal innervation in the CD25 null model of sjogren syndrome. *Int. J. Mol. Sci.* 19:3821. doi: 10.3390/ijms19123821

Strassman, A. M., and Vos, B. P. (1993). Somatotopic and laminar organization of fos-like immunoreactivity in the medullary and upper cervical dorsal horn induced by noxious facial stimulation in the rat. *J. Comp. Neurol.* 331, 495–516. doi: 10.1002/cne.903310406

Tepelus, T. C., Chiu, G. B., Huang, J., Huang, P., Sadda, S. R., Irvine, J., et al. (2017). Correlation between corneal innervation and inflammation evaluated with confocal microscopy and symptomatology in patients with dry eye syndromes: a preliminary study. *Graefes Arch. Clin. Exp. Ophthalmol.* 255, 1771–1778. doi: 10.1007/s00417-017-3680-3

Theophanous, C., Jacobs, D. S., and Hamrah, P. (2015). Corneal neuralgia after LASIK. *Optom. Vis. Sci.* 92, e233–240. doi: 10.1097/OPX.0000000000000652

Thibault, K., Riviere, S., Lenkei, Z., Ferezou, I., and Pezet, S. (2016). Orofacial neuropathic pain leads to a hyporesponsive barrel cortex with enhanced structural synaptic plasticity. *PLoS ONE* 11:e0160786. doi: 10.1371/journal.pone.0160786

Veiga Moreira, T. H., Gover, T. D., and Weinreich, D. (2007). Electrophysiological properties and chemosensitivity of acutely dissociated trigeminal somata innervating the cornea. *Neuroscience* 148, 766–774. doi: 10.1016/j.neuroscience.2007.03.056

Vit, J. P., Jasmin, L., Bhargava, A., and Ohara, P. T. (2006). Satellite glial cells in the trigeminal ganglion as a determinant of orofacial neuropathic pain. *Neuron Glia Biol.* 2, 247–257. doi: 10.1017/S1740925X07000427

Waxman, S. G. (1999). The molecular pathophysiology of pain: abnormal expression of sodium channel genes and its contributions to hyperexcitability of primary sensory neurons. *Pain Suppl.* 6, S133–140. doi: 10.1016/S0304-3959(99)00147-5

Woolf, C. J. (2011). Central sensitization: implications for the diagnosis and treatment of pain. *Pain* 152, S2–15. doi: 10.1016/j.pain.2010.09.030

Woolf, C. J. (2020). Capturing novel non-opioid pain targets. *Biol. Psychiatry* 87, 74–81. doi: 10.1016/j.biopsych.2019.06.017

Xiang, Y., Zhou, W., Wang, P., Yang, H., Gao, F., Xiang, H., et al. (2017). Alkali burn induced corneal spontaneous pain and activated neuropathic pain matrix in the central nervous system in mice. *Cornea* 36, 1408–1414. doi: 10.1097/ICO.0000000000001336

Xiao, C., Wu, M., Liu, J., Gu, J., Jiao, X., Lu, D., et al. (2019). Acute tobacco smoke exposure exacerbates the inflammatory response to corneal wounds in mice via the sympathetic nervous system. *Commun. Biol.* 2:33. doi: 10.1038/s42003-018-0270-9

Xue, Y., He, J., Xiao, C., Guo, Y., Fu, T., Liu, J., et al. (2018). The mouse autonomic nervous system modulates inflammation and epithelial renewal after corneal abrasion through the activation of distinct local macrophages. *Mucosal. Immunol.* 11, 1496–1511. doi: 10.1038/s41385-018-0031-6

Yamada, R., and Kuba, H. (2016). Structural and functional plasticity at the axon initial segment. *Front. Cell. Neurosci.* 10:250. doi: 10.3389/fncel.2016.00250

Yamaguchi, T., Hamrah, P., and Shimazaki, J. (2016). Bilateral alterations in corneal nerves, dendritic cells, and tear cytokine levels in ocular surface disease. *Cornea* 35(Suppl. 1), S65–S70. doi: 10.1097/ICO.0000000000000989

Yamazaki, R., Yamazoe, K., Yoshida, S., Hatou, S., Inagaki, E., Okano, H., et al. (2017). The Semaphorin 3A inhibitor SM-345431 preserves corneal nerve and epithelial integrity in a murine dry eye model. *Sci. Rep.* 7:15584. doi: 10.1038/s41598-017-15682-1

Yang, Y., Li, G., and Chen, L. (2020). High resolution three-dimensional imaging of the ocular surface and intact eyeball using tissue clearing and light sheet microscopy. *Ocul. Surf.* 18, 526–532. doi: 10.1016/j.jtos.2020.04.009

Yu, C. Q., and Rosenblatt, M. I. (2007). Transgenic corneal neurofluorescence in mice: a new model for *in vivo* investigation of nerve structure and regeneration. *Invest. Ophthalmol. Vis. Sci*. 48, 1535–1542. doi: 10.1167/iovs.06-1192

**Conflict of Interest:** The authors declare that the research was conducted in the absence of any commercial or financial relationships that could be construed as a potential conflict of interest.

# V. Dry eye disease: *a prototypical example of chronic ocular pain*

## V.1 The evolution of the concept of dry eye disease

The concept of dry eye, or at least an understanding of the need for tears, has been recognized by healers for over 3,500 years, as the first mention of our tears was recorded in 1550 BC as “the water within” in ancient Egyptian documents known as the Ebers Papyrus (Hirschberg, 1982).

One of the first terms used in modern literature to refer to this clinical entity was **kerato-conjunctivitis sicca**. It reflects its inflammatory component, literally meaning corneal (kerato-) and conjunctival (conjunctiv-) inflammation (-itis) with the associated descriptor “dry” (sicca). Nowadays this nomenclature is not so commonly used in the literature to refer to “primary” DED, especially following the emergence of modern definitions of DED.

A preliminary attempt to develop a consensus definition for DED was made in **1995** by the American National Eye Institute/Industry Dry Eye Workshop (Lemp, 1995):

“*Dry eye is a disorder of the tear film due to tear deficiency or excessive evaporation, which causes damage to the interpalpebral ocular surface and is associated with symptoms of ocular discomfort*.”

It highlights some elements that will be important in the current view of DED:

- The definition establishes that it is a disease that affects the tear film (this will change in the future).
- It specifies the suspected etiology: tear deficiency (which will be known later on as aqueous deficient dry eye) or excessive evaporation (later on referred to as evaporative dry eye).
- The term "ocular surface" makes its apparition, which will be important in the future.
- The first sign of DED is established: damage.
- The symptomatology is established: ocular discomfort.

In **1998**, Stern et al. proposed the physiological concept of the **Lacrimal Functional Unit** (LFU) referring to the neural arc and innervated surfaces and glands in charge of the control, modulation and production of tears (Stern et al., 1998), that will be important to understand the underlying pathophysiology of DED. The LFU is composed of:

- The ocular surface: lacrimal glands (main and accessory), meibomian glands, cornea, conjunctiva and eyelids.
- Afferent sensory fibers from the ocular surface. The somas of those neurons are in the $V_1$ branch of the trigeminal ganglion. They send axons to the central nervous system at the level of brainstem.
- Integration of the sensory afferents and modulation of the autonomic efferents in the central nervous system.
- Efferent parasympathetic and sympathetic fibers emerging from the pterygo-palatine or ciliary ganglia and superior cervical ganglia, respectively, up to the main and accessory lacrimal glands.

A major advance in the conceptualization of this ocular surface disease occurred in 2007, when the Report of the International **Dry Eye Workshop** (DEWS), product of deliberation of world experts in the field and organized by the **Tear Film & Ocular Surface Society** (TFOS), was published. The aim of one of the subcommittees was to reach a consensus on a new definition of DED, which was as follows :

> *"Dry eye is a multi-factorial disease of the tears and ocular surface that results in symptoms of discomfort, visual disturbance, and tear film instability with potential damage to the ocular surface. It is accompanied by increased osmolarity of the tear film and inflammation of the ocular surface."*(Nichols et al., 2013)

In this definition, several changes and innovations in the conceptualization of DED appear:

- It is no longer a disease affecting solely the **tears**, but the whole **ocular surface**.
- The etiology is **multi-factorial**, meaning that the disease can arise from a variety of sources.
- It establishes an essential **sign**: **tear film instability**, which can lead to **damage** and other signs: **increased osmolarity** of the tear film and **inflammation** of the ocular surface.
- In addition to the **symptom** of eye discomfort, visual disturbance is added.

Another important model to understand the current concept of DED is the "**vicious cycle**"(Baudouin, 2007; Baudouin et al. , 2013; Baudouin et al. , 2016). This image helps to better understand the etiology and pathophysiology of DED and therefore to propose new therapeutic approaches. The idea is that DED has several triggers or entry points that once initiated feed a vicious circle that is maintained even after the disappearance of the initial

trigger. The initial triggers of DED can therefore be very diverse but give rise to the same disease (**Fig. 8**). For the sake of simplicity, we will start with the instability of the tear film, which has historically been considered the origin of DED. This instability can lead to changes in tear film composition and notably an increase in its osmolarity. If this hyper-osmolarity is sustained over time, it can damage cells in contact with the tear film including corneal and conjunctival epithelial cells. This hyper-osmolarity can also sensitize corneal nerve terminals, specifically the cold thermo-receptors, leading on the one hand to the symptoms of DED and on the other hand to an overstimulation of the lacrimal glands in an attempt to reverse this hyper-osmolarity. This corneal damage can lead to sustained inflammation of the ocular surface, becoming chronic and worsening all aforementioned changes. Typically, such inflammation leads to the production of cytokines and the activation of matrix metalloproteinases (MMPs), which together with all of the above can destroy conjunctival goblet cells, the main cells responsible for the production of gel mucins. These mucins, due to their water-binding properties, contribute enormously to the muco-aqueous and lubricating properties of the tear film. All these processes contribute to the instability of the tear film and restart the cycle again (**Fig. 8**).

Among the "entry points", i.e. the etiological factors of DED, one of the most common causes of DED is meibomian gland dysfunction (MGD), which has its own vicious cycle. Another epidemiologically-important etiology is Sjögren's syndrome (also known as Gougerot-Sjögren syndrome in French speaking countries). These two etiologies will be discussed in depth in the following sections. Other factors such as ocular surgery (especially refractive surgery), side effects of topical (eyedrop preservatives) and systemic drugs, contact lens wear, steroid hormone-related factors, inflammatory pathological episodes such as allergies and viral or bacterial conjunctivitis, and environmental factors such as low humidity and high airflow provide alternative inputs to the cycle (**Fig. 8**). Finally, the “neurotrophic” entry point, suggesting the importance of corneal nerves in the vicious cycle, has been the object of specific focus in our team (Baudouin, 2007; Baudouin et al., 2013; Baudouin et al., 2016) and was one of the aims of the present research project.

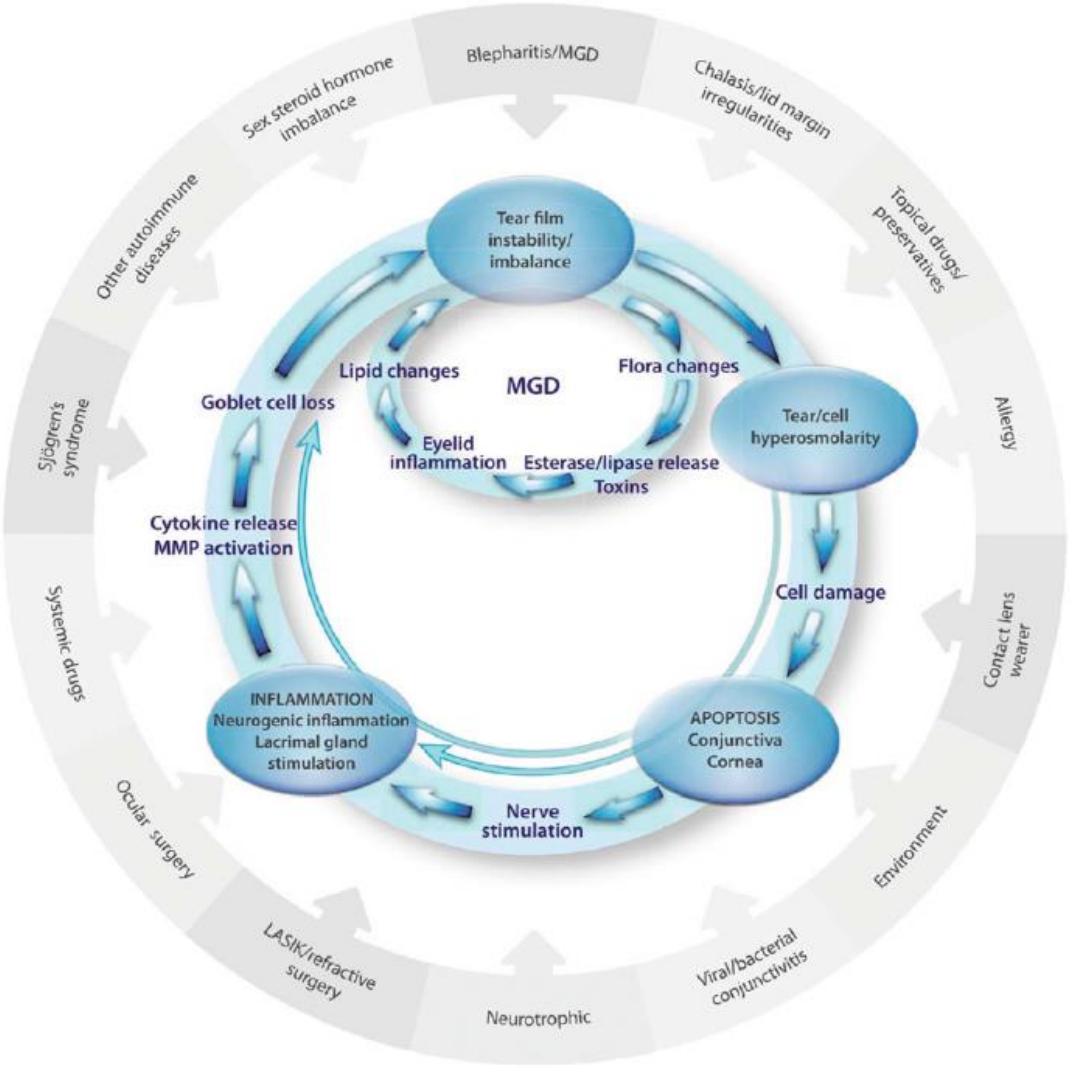


**Figure 8: The vicious cycle of Dry Eye Disease (DED) and Meibomian Gland Dysfunction (MGD).** DED and MGD are two interconnected vicious circles with a great variety of entry points (grey). *From Baudouin et al., 2016.*

Finally, in 2017 the TFOS-DEWS revised the definition of DED, in a second meeting (TFOS-DEWS II), as follows:

***"Dry eye is a multi-factorial disease of the ocular surface characterized by a loss of homeostasis of the tear film, and accompanied by ocular symptoms, in which tear film instability and hyper-osmolarity, ocular surface inflammation and damage, and neuro-sensory abnormalities play etiological roles."*** *(Craig et al., 2017)*

New elements and changes are highlighted below:

- It is maintained that DED is a multi-factorial disease of the ocular surface (in a broad sense, as explained in section "II. The homeostatic ocular surface") but the term "tear film instability" is replaced by the broader term "loss of homeostasis of the tear film".
- Ocular symptoms are not specified in the definition but ocular discomfort and visual disturbance remain.
- Several processes that have already been linked to DED are established as having an etiological value: tear film instability and hyper-osmolarity and ocular surface inflammation and damage.
- Finally, and this is of importance for the present research project, the term "**neuro-sensory abnormalities**" appears as a novel etiological factor: pathology at the level of the nervous system may be triggering dry eye. On this topic, we published a review (Guerrero-Moreno et al., 2020).

While the aim of TFOS-DEWS II was to propose a broad definition for global application in several settings including research, its practical utility in the clinics was not so straightforward. Therefore, an international group of expert ophthalmologists recently proposed an adapted definition of DED for clinical diagnostic use (Tsubota et al., 2020):

*"Dry eye is a multi-factorial disease characterized by a **persistently unstable and/or deficient tear film** causing **discomfort and/or visual impairment**, accompanied by variable degrees of ocular surface epitheliopathy, inflammation and neuro-sensory abnormalities."*

This definition is in line with that provided by TFOS-DEWS II in 2017 but clearly specifies the minimum parameters to be considered for diagnosing DED, with the aim of making them accessible to any practitioner in the world:

1. "Persistently unstable and/or deficient tear film": It can be qualitatively assessed with simple slip lamp examination and fluorescein staining.
2. "Discomfort and/or visual impairment": Questionnaires are the main way to quantify symptoms.

The other terms in the definition (ocular surface epitheliopathy, inflammation and neuro-sensory abnormalities) can and must also be assessed in the clinics.

## V.2 Etiologies of dry eye disease

As previously mentioned, numerous diseases can take part in the vicious cycle of dry eye disease, as illustrated in **Fig. 8**. Each specific disease induces dry eye by one or more distinct mechanisms, often different from the other DED-inducing conditions. Considering the major mechanisms implicated in DED, the TFOS-DFEWS II committee has subdivided DED etiologies between aqueous-deficient dry eye (ADDE) and evaporative dry eye (EDE).

### A. Aqueous-deficient dry eye (ADDE)

An ADDE can be established when a decrease in tear volume is detected (Schirmer test ≤ 4 mm/5 min, (Jones et al., 2017). ADDE has been further subdivided into 2 main groups: Sjögren's syndrome dry eye (SSDE) and non-Sjögren's syndrome dry eye (NSDE), depending on whether the systemic disease has been diagnosed or not.

**Sjögren syndrome dry eye (SSDE)**

Sjögren's syndrome (SS) is a chronic, systemic autoimmune disease characterized by an infiltration of immune cells in exocrine glands. SS is associated with systemic complications such as peripheral neuropathy, myelitis and meningitis, due to autoantibody production and lymphocytic infiltration (Akpek et al., 2019). Symptoms of chronic dry eye and dry mouth are a major feature of SS that are a result of infiltration of the salivary and lacrimal glands by T and B lymphocytes, dendritic cells, macrophages and other mononuclear cells, leading to tissue dysfunction or destruction. Patients with SS usually present with the most severe DED phenotype, appearing in younger individuals and with a faster aggravation (Bron et al., 2017).

**Non-Sjögren syndrome dry eye (NSDE)**

NSDE encompasses congenital and acquired forms of DED with decreased tear volume but without SS diagnosis. Since this group arises from an exclusion diagnosis, it is rather heterogeneous and of very limited practical utility, both clinically and scientifically. This section will focus only on age-related ADDE as it comprises most cases. Epidemiological data suggest that this condition appears from the age of 50 onwards, its progression is quite attenuated and severe cases are less common than in SSDE. The origin of this form of DED is secondary to ageing that affects the LFU leading to the entry into the DED vicious circle. The

most common sign of age-related NSDE has been conjunctival inflammation that may spread to other elements of the ocular surface and/or lead to goblet cell loss (Bron et al., 2017).

### B. Evaporative dry eye (EDE)

EDE emerges when the mechanisms that prevent tear hyper-evaporation fail. Depending on the mechanism that fails, EDE can be sub-classified in different subtypes. Among EDE the most common origin is Meibomian gland dysfunction (MGD) which is also the most common cause of DED overall. EDE can also occur as a consequence of blink-related disorders.

**Meibomian Gland Dysfunction (MGD)**

Meibomian gland dysfunction (MGD) was defined in the International Workshop on Meibomian Gland Dysfunction as *a "chronic, diffuse abnormality of the meibomian glands, commonly characterized by terminal duct obstruction and/or qualitative/quantitative changes in the glandular secretion. This may result in alteration of the tear film, symptoms of eye irritation, clinically apparent inflammation, and ocular surface disease"* (Nelson et al., 2011).

According to this definition, the main consequence of MGD is the pathological change in meibomian secretion. This change may consist of hyper-secretion, leading to what is known as meibomian seborrhea (high meibum delivery state), although reduced secretion (low meibum delivery state) is much more common. In turn, low meibum delivery states are sub-classified depending on whether this is a consequence of gland obstruction or not. In the absence of obstruction, it is called hypo-secretory MGD, while if there is evidence of obstruction, it is diagnosed as obstructive MGD (Nelson et al., 2011). Obstructive MGD is documented to be the most common subclass not only of MGD and EDE, but of DED overall (Stapleton et al., 2017).

This condition is well characterized, with specific pathological mechanisms although in practice it is intertwined with DED. This pathology is characterized by a reduction in the fluidity of the meibum, a consequence of bacterial proliferation that releases lipases and esterases that represent the new vicious cycle, as they continue to increase the melting point of the meibum. This deficiency in lipids leads to tear film instability which triggers the DED cycle (Baudouin et al., 2013).

It is known that low delivery states can occur as a consequence of the ageing process, as meibomian gland acini are lost due to decreased meibocyte production and increased orifice blockage (Bron et al., 2017). This clinical entity is known as age-related MGD.

**Blink-related disorders**

Blink-related disorders represent a heterogeneous group, the most common cause being inadequate eyelid seal (lagophtalmos). Also, DED can be triggered by activities involving a decrease in the blink rate such as those related to states of attention (*e.g.* being in front of a screen). These and other circumstances result in increased tear evaporation which could lead to DED (Bron et al., 2017).

### C. Hybrid forms of ADDE and EDE

As indicated above and reflected in (Craig et al., 2017), most actual cases of DED are not purely EDE or ADDE, but have characteristics of both, more often when the disease progresses. For example, severe ADDE can trigger a tear breakup leading to an evaporative component. Another common example of hybrid DED is SS in which many cases of patients developing MGD have been found clinically. Hybrid subtypes of DED are detailed in **Table 1** (Bron et al., 2017).

**Table 1: Hybrid subtypes of dry eye disease**

| ***Subtype*** | ***Example*** |
|---|---|
| Organic ADDE due to lacrimal gland pathology, combined with anorganic MGD-dependent EDE | Sjögren's syndrome |
| A combination of an organic ADDE, MGD-dependent EDE and EDE secondary to ocular surface disease | Graft-versus-host disease (Appenteng Osae and Steven, 2021) or to varying degrees, other forms of cicatrizing conjunctivitis. There is obstruction to the lacrimal gland ducts, cicatrizing MGD and ocular surface disease secondary to the primary systemic disease. |
| Organic ADDE with a functional EDE | In severe ADDE there is defective spreading of the TFLL and a predicted functional EDE. |
| Organic EDE with a functional ADDE | When DED is severe, there is a decrease in corneal sensitivity. It is predicted that, in EDE, this leads to a loss of compensatory, sensory drive to the lacrimal gland, and a functional aqueous-deficient state. |
| ADDE evolving to EDE | When tear break-up occurs within the blink interval, the cornea is subjected to excessive evaporation at the site of the break-up. Thus, any ADDE of sufficient severity is |

| | |
|---|---|
| | predicted to be converted to an EDE. Tear proteins of lacrimal origin should be at a normal level. |

## V.3 Assessment of symptoms and signs of DED

Diagnosis, assessment and monitoring of the progression of DED in patients are based on different clinical tests and tools which quantify disease **symptoms** and **signs**. It is important to clarify that there is no pathognomonic sign of DED. Instead, the diagnosis and monitoring of DED will based on the result of different tests performed by the ophthalmologist, whilst aiming to adapt the treatment to the individual case (Wolffsohn et al., 2017).

### A. Assessment of symptoms of DED

The principal clinical tools to quantify symptoms of DED are semi-specific questionnaires. The most used questionnaire is the **Ocular Surface Disease Index** (OSDI), based in different triage questions that assesses the frequency of symptoms, environmental triggers and vision related quality of life. The OSDI is scaled from 0 to 100, with higher scores representing greater disability (Schiffman et al., 2000; Wolffsohn et al., 2017).

There are many other questionnaires available, some focusing on more general aspects of dry eye (as the already mentioned OSDI) and others more specialized in a particular aspect. Of particular note is the recently developed **Ocular Pain Assessment Survey**, a questionnaire designed to specifically quantify ocular pain and associated changes in quality of life (Qazi et al., 2016).

Other approximation is the direct quantification of **pain**. **Visual analog scale** (VAS), a psychometric test based on a straight horizontal line of fixed length (usually 100 mm), is a powerful and easily-applicable approximation for subjective pain quantification. Briefly, patient must mark the point on the line that best corresponds to their pain severity, usually on a scale of 0 to 10, where 0 means "no pain" and 10 means "maximum pain imaginable" (Klimek et al., 2017). The VAS is normally used without specifying the "type of painful sensation", but it should be noted that eye pain can be described by the patient in many ways. A list of terms can be found in **Table 2** (Labetoulle et al., 2017). It is also important to consider the frequency of these symptoms and whether they are associated with activities such as work, especially if it requires maintaining attention on video display terminals, or if it is

evoked by external phenomena such as wind, light (photophobia), low or high humidity or extreme temperatures.

**Table 2: Terms used by patients to refer to their ocular pain sensation in different languages**

| English | Spanish | French | Italian | German |
|---|---|---|---|---|
| ***itchy*** | Picor | Démangeaison /grattent | Prurito | juckend |
| ***sore/irritated*** | Irritante | Irrités | Irritazione | gereizt |
| ***dry/dryness*** | seco/sequedad | Sec | Secchi | trocken |
| ***annoying*** | Molesto | Énervé /dérangeant | Fastidioso | Belästigend |
| ***painful*** | Doloroso | Douloureux | Dolore | Schmerzvoll |
| ***burning*** | quemazón /ardor | Brûlent | Bruciore | Brennend |
| ***discomfort /uncomfortable*** | malestar /incómodo | gene | Disagio | Beschwerend |
| ***sand in eye*** | Arena | Sable | sabia | Sand |
| ***stinging/prickle*** | pinchazos /agujas | Piquer /picotement | pungiglione /pizzicore | Stechend |
| ***(lack of) tears*** | Pegar | Larmes | Lacrimazione | Tränenmangel |
| ***blurred vision*** | visión borrosa | trouble | Offuscata | Sehtrübung |
| ***foreign body*** | cuerpo extraño | corps étranger | Corpoestraneo | Fremdkörper |
| ***scratching*** | Rasposo | Griffer | Graffiano | Kratzend |
| ***sticking*** | Pegajoso | Collage | Appiccicarsi | Klebend |
| ***burdened /heavy*** | carga/pesadez | lourd/fardeau | carico/pesante | Schwerbelastend |
| ***swollen*** | Hinchazón | Enflés /gonflés | Gonfiore | Geschwollen |

*From Labetoulle et al., 2017 .*

## B. Evaluation of clinical signs to establish the diagnosis of DED

Dry eye disease semiology is even more heterogeneous than reported symptomatology. This is reflected in the great variety of clinical tools required for their measurement.

### Corneal and conjunctival epithelial integrity

Epithelial damage can be measured via **ocular surface staining**, the most frequent test performed in many ocular diseases.

The patient's eye is instilled with a dye, commonly sodium fluorescein, rose bengal or lissamine green that stains any disruption in the ocular surface epithelium. Corneal and conjunctival staining is observed by the clinician through the appropriate device such as a slip lamp biomicroscope and then graded accordingly. The most used corneal damage scale is the Oxford scale, based on 5 different levels of increasing severity of punctuate staining (**Fig. 9**). Another scale, the van Bijsterveld scale is also applicable and very relevant for autoimmune-related DED (Wolffsohn et al., 2017). Ocular surface staining is also used in preclinical studies to monitor dry eye disease (Pauly et al. , 2007; Fakih et al., 2019).

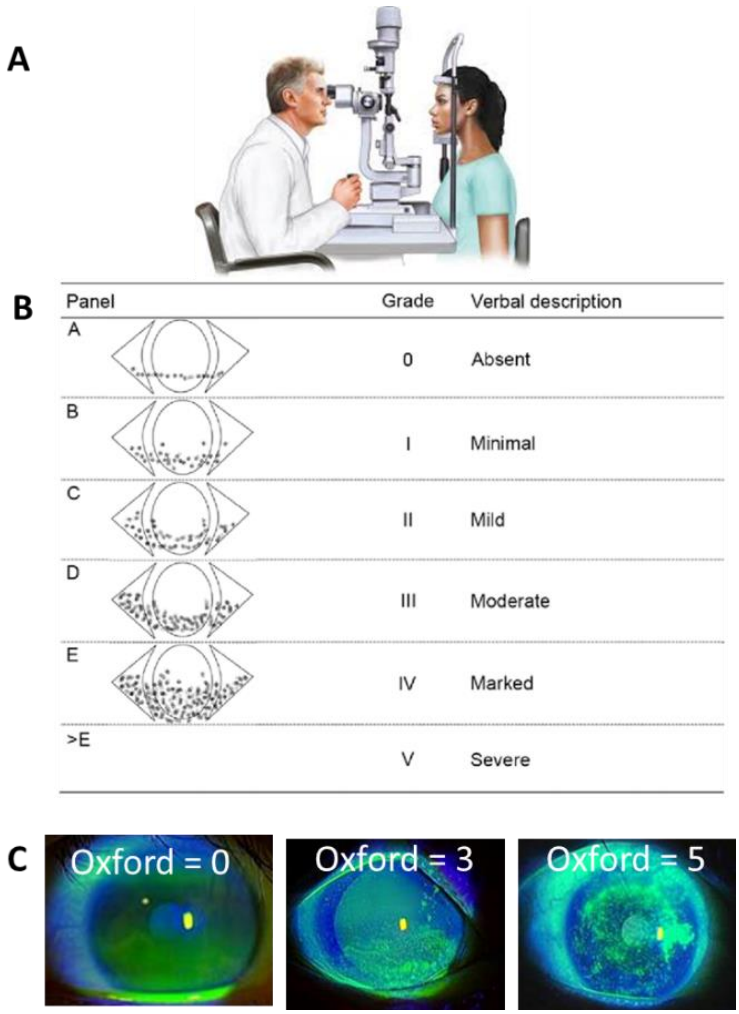


**Figure 9: Ocular surface staining assessment**

**A.** After dye instillation, the patient's ocular surface is observed by slip lamp biomicroscopy. *From Desai, 2016.*

**B.** Oxford grading scale. Ocular surface staining representing cornea and conjunctiva epithelial damage is qualitatively assessed from 0 to 5.

**C.** Examples of ocular surface staining. *From Ogawa et al. , 2013.*

**Tear film instability**

Besides its etiological role in DED, tear film instability represents a measurable sign and a fundamental diagnostic criterion. Studies in patients reveal that decreases in parameters that quantify tear stability may be correlated with the progression of the disease:

- **Tear film breakup time** (TBUT): This is the time interval from a blink and the appearance of the first break in the tear film.
- **Fluorescein breakup time** (FBUT): It is similar to TBUT but instilling the patient with sodium fluorescein to enhance visibility of the tear film. In this approach, the ocular surface of the patient is observed with a slit lamp biomicroscope using a cobalt blue filter and the breakup time is determined by the appearance of the first black spot on the cornea.
- **Non-invasive tear breakup time** (NIBUT): It is becoming a very popular technique as it avoids the effects of fluorescein, temperature, humidity and air-circulation on the obtained result. It is assessed by many of the currently marketed corneal topography systems (videokeratoscopes) and specific software (**Fig. 10**) (Wolffsohn et al., 2017).

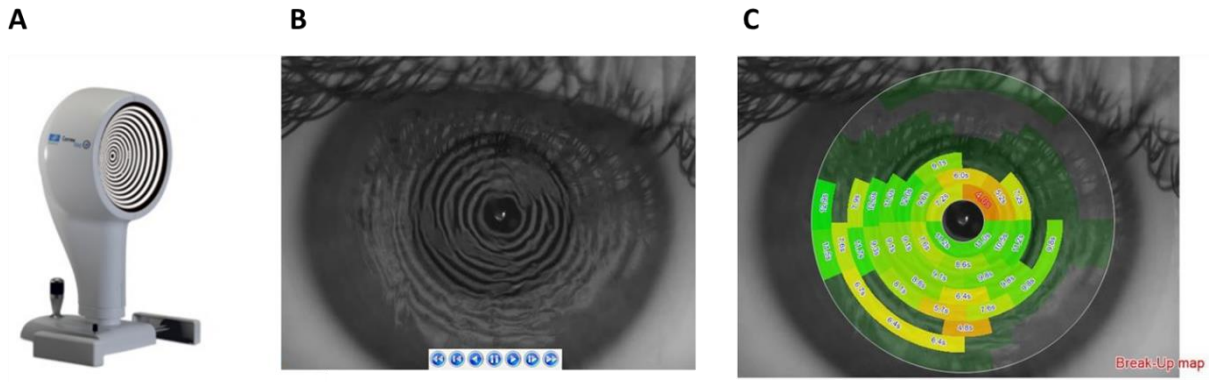


**Figure 10: Non-invasive break-up time**

**A.** Ocular surface tomography device. *From OptometryWeb, 2020* **B.** Dynamic map of the break-up flow. **C.** Graphical map showing numerical values of NIBUTs. *B and C extracted from Muhafiz and Demir, 2022*.

Additionally, there are two other indicators for tear film stability that should be set aside, as they are not as commonly used as the previous ones:

- **Tear evaporation rate**: This parameter can be measured directly on patients by various methods such as vapor pressure gradient and velocity of relative humidity increase within a goggle cup placed over the eye.
- **Thermography**: There is a drop in the temperature of the ocular surface as a consequence of tear evaporation. The measurement of this decrease in temperature with spatial and temporal resolution can be a good parameter to measure this evaporation.

**Tear film hyperosmolarity**

Tear film osmolarity is measured in clinics as a marker of the severity of DED. The most common way to measure it is through the "Tear labTM" device, which after application to the ocular surface gives an absolute measurement (in mOsm/L). It seems to correlate with the severity of clinical DED although some studies states that it is a very variable indicator (Wolffsohn et al., 2017).

**Tear volume**

Tear volume measurement is a good approach for patient stratification once symptomatic DED has been established. Hallmark of aqueous deficient dry eye is decreased tear volume, while in other subtypes of DED it can be in healthy ranges or even elevated (Pflugfelder et al., 2017). Tear volume can be assessed by different methods:

- **Tear meniscus (meniscometry):** The tear menisci refer to tears lying at the junction between the bulbar conjunctiva and the margins of both upper and lower eyelids **(Fig. 1).** As it is the principal reservoir for the pre-corneal tear film, its quantitative assessment (height measurement) represents the most direct approach to measure **tear film volume**. Meniscometry can be assessed by slip lamp biomicroscope or by a specialized meniscometry system. A cutoff of 240 µm in tear meniscus height has been proposed to differentiate aqueous deficient from other DED patients (Pflugfelder et al., 2017).
- **Phenol red thread test**: It consists of a thread that is placed over the ocular canthus (medial or lateral) for a few seconds (10-15s). As a result of the tear rising through the thread by capillarity, it turns red as it contains Phenol red, which is a pH marker. The measurement of the length of the thread that turns red has been established as an indicator of **resting tear volume.** This is the usual way to measure tear volume in small laboratory animals such as mice and rats. However, its use, especially in Europe, is difficult as its commercialization is rather limited.
- **Schirmer test**: It consists in a paper strip (5 x 35 mm) that is placed between the lower eyelid and bulbar conjunctiva for 5 minutes (**Fig. 11**). The wet strip length is then measured, representing the test result. Schirmer test applied without anesthesia is a well standardized test for the measure of **stimulated reflex tear flow**, although it can be applied also with anesthesia (Wolffsohn et al., 2017).

**Figure 11: Schirmer test**
A graduated strip is placed in the lower lid conjunctiva during 5 min. The wet length reflects the tear volume.

**Measurement of corneal sensitivity**

***Non-contact air jet esthesiometer***

The Belmonte non-contact gas esthesiometer allows the measurement of corneal sensory abnormalities following mechanical, thermal, and chemical corneal stimulations, i.e. the detection of polymodal function for both Aδ and C fibers.

***Cochet-Bonnet esthesiometer***

The Cochet-Bonnet contact esthesiometer has been widely used to characterize somatosensory disturbances within the human eye and more specifically for exploring the corneal mechanical nociceptors (Aδ fibers) responses. Cochet-Bonnet is fully extended and applied to the central cornea while its length is reduced gradually. As shorter is the length of the aesthesiometer, as higher is the pressure applied to the ocular surface (**Fig. 12**). The first blink from the patient is recorded as the mechanical threshold. Contrary to what might be thought *a priori,* an increased threshold is equivalent to a lower sensitivity and, conversely, a low threshold would indicate a higher mechanical sensitivity.


**Figure 12: Cochet-Bonnet esthesiometer**
Increasing pressures are applied to the cornea. The first reflex response determines the corneal mechanical threshold.

**Molecular profile of conjunctival epithelium: impression cytology**

Impression cytology refers to the application of a cellulose acetate filter to the ocular surface to collect the superficial layers of the ocular surface epithelium. The collected cells can then

be subjected to molecular (RT-PCR, western blot), histological or immunohistological analyses.

It is worth noting that with this technique HLA-DR over-expression was detected in patients with DED, correlating with the signs and symptoms of the disease (Baudouin et al., 1992; Brignole-Baudouin et al., 2017; Liang et al. , 2019). In a recent study from the team (Nicolle et al., 2018), we demonstrated by RT-qPCR analysis of impression cytology samples from painful DED patients (vs. painless healthy controls) an increase in inflammatory mediators such as HLA-DR, IL-6, CXCR4, CCL2, CCR2 and, most interestingly, proenkephalin, the precursor of Met- and Leu-enkephalin, highlighting the role of the endogenous opioid system in ocular pain, as will be detailed later on.

In recent years, techniques and protocols applicable to these samples have grown considerably, making possible the application of so-called "omics" such as proteomics, lipidomic and metabolomics, which in the future will help to identify novel biomarkers for DED.

### *In vivo* confocal microscopy (IVCM)

#### ***Principles of imaging***

IVCM is a high-resolution non invasive real-time imaging technique allowing layer-by-layer analysis of the cornea at the cellular level in both humans and laboratory animals.

This technique is based on confocal technology: basically, the light coming from a source (laser) passes through a pinhole that focuses the light beam. This beam is focused onto the sample (ocular surface) by means of an objective system. The light from the sample is reflected towards a detection system (photomultiplier), provided with another pinhole allowing 2D images to be acquired of each layer of the cornea **(Fig. 13)**.

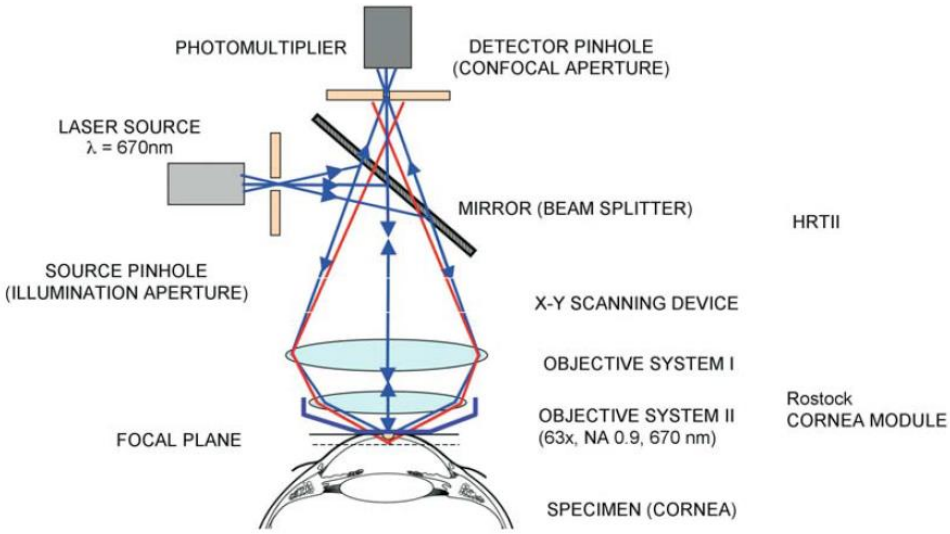


**Figure 13: Principle of confocal laser-scanning microscopy**

*From Guthoff et al., 2006 .*

This reflection is based on the scattering phenomenon that occurs at the interface between objects. In the case of the cornea, this scattering occurs at the junction between cells (cell membrane and/or cytoplasm) and the extracellular medium or between the cell nucleus and the cytoplasm. The amount of back-scattered light depends on the structure of these interfaces as well as their orientation with respect to the light plane (Guthoff et al., 2006). This is the principle that allows imaging at cellular resolution without the use of dyes of corneal epithelial cells differencing between layers, sub-basal nerve plexus, immune cells, stromal keratocytes and endothelial cells (**Fig. 14**).

As the cornea is an easy-accessible and transparent structure, the application of IVCM technology allows imaging with a quality that would be more difficult in other tissues. Therefore, IVCM is an excellent technique not only for the diagnosis of ocular diseases, but also for the *in vivo* study of the cellular events that occur in the ocular surface. An example of the IVCM's ability to image the different layers of the cornea can be found in **Fig.14**.

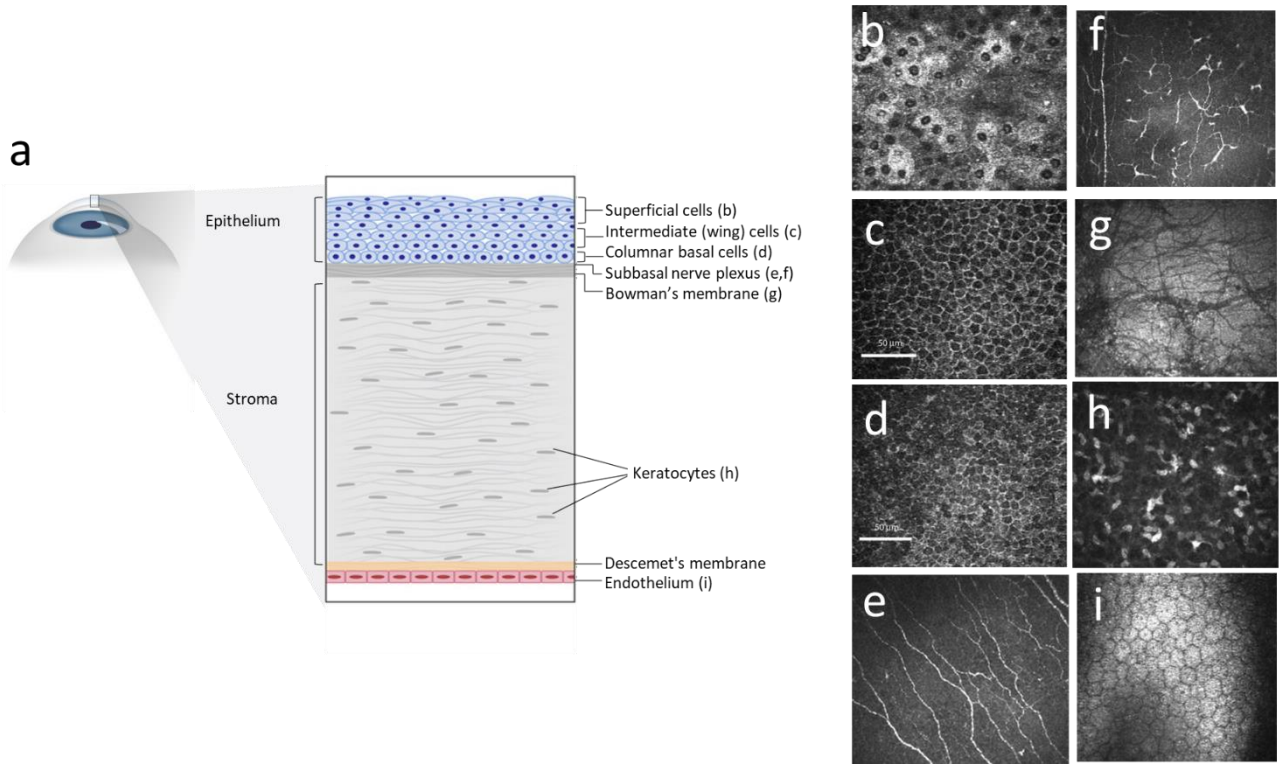


**Figure 14: IVCM exploration of the different corneal layers and cell types**

**a.** Corneal layers and cell types populating each of them. **b-i.** Corneal layers and cell types detected by IVCM **b-d**. Epithelial layers. **e,f.** Sub-basal plexus showing a dense meshwork of nerves (**e**) and dendritiform cells (**f**). **g.** Bowman's membrane. **h.** Stromal keratocytes. **i.** Hexagonal cells from the corneal endothelium. *Images from the lab except for c,d from Guthoff et al., 2006.*

***Morphological abnormalities at the level of the sub-basal layer detected by IVCM***

In addition to the visualization of the different layers of the cornea, IVCM allows the extraction of important information for the diagnosis of DED (Cruzat et al., 2017) as well as to monitor morphological corneal nerve abnormalities at the level of the sub-basal plexus.

**Dendritiform cells** imaged by IVCM correspond to dendritic or Langerhans immune cells. Total number of cells can be quantified and divided between the surface analyzed obtaining their density (cells/mm$^2$). Dendritiform cells density is a marker of corneal inflammation and has been found increased in DED patients. The morphology of those cells can be quantified also as a marker of inflammation as when activated, they elongate their ramifications (elongations/cell) and increase their size (µm$^2$) (Aggarwal et al., 2021) (**Fig. 15**).

Different corneal nerve parameters can also be evaluated from **sub-basal nerves**:

**Sub-basal nerve density** can be assessed by specialized software (NeuronJ plugin for ImageJ) by means of µm/mm$^2$. NeuronJ allows semi-automatic tracing of corneal nerves, meaning that the researcher traces roughly the length of each fiber and the software adjusts the trace to the image more accurately. This allows the trained researcher to trace large numbers of images at high speed. Nerve density has been found decreased in ocular surface diseases including DED (Labbe et al. , 2012; Labbe et al. , 2013; Nicolle et al., 2018). In addition, recovery of nerve density has been reported as a pharmacodynamic biomarker of efficacy of topical treatment in DED (Levy et al., 2017) (**Fig. 15**).

**Sub-basal nerve tortuosity** is a measure based on subjective qualitative scales, typically from 0 to 4 depending on severity of tortuosity (Oliveira-Soto and Efron, 2001). It has been shown to be increased in patients with DED, especially those with painful symptoms (Galor et al. , 2018; Guerrero-Moreno et al., 2020). Such scales used for this measure need to be standardized as each study usually has its own (**Fig. 15**).

**Microneuromas** are another characteristic that can be studied by ICVM. Due to the relevance of this structure in my clinical study (Guerrero-Moreno et al. , 2021b), a specific section about their historical relevance can be found next.

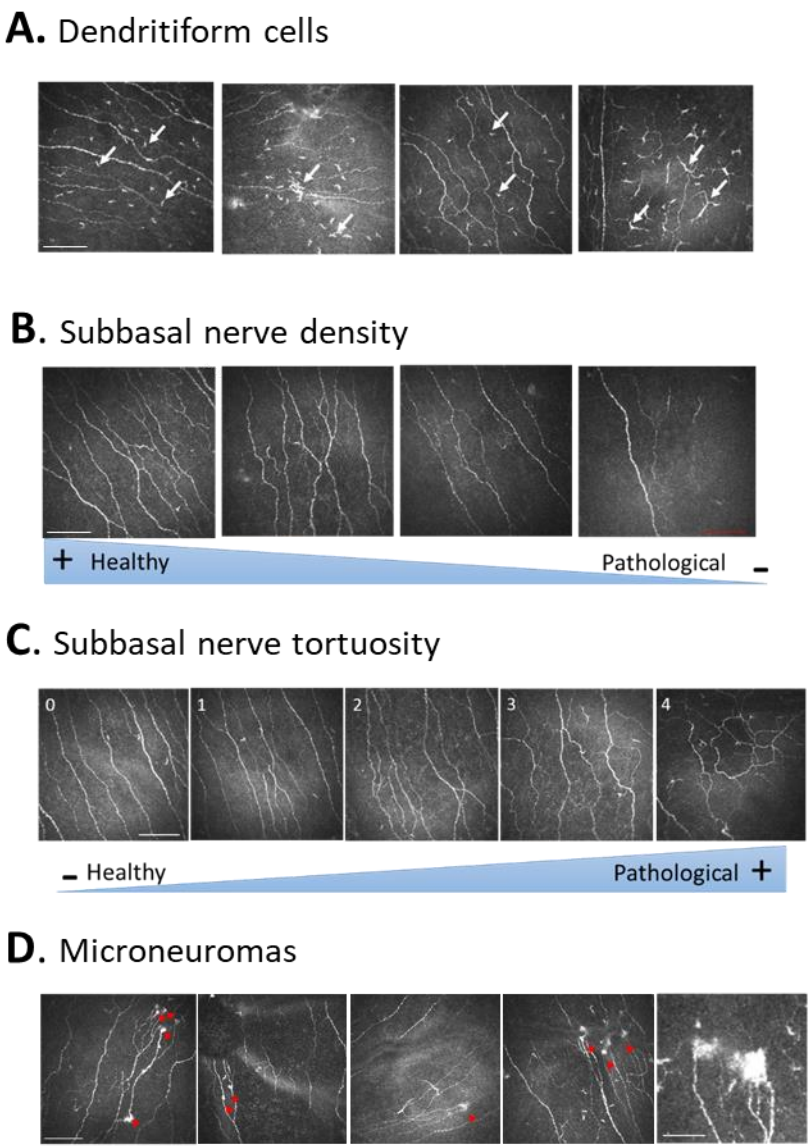


**Figure 15: Cellular and morphological corneal abnormalities studied by IVCM**

**A.** Density of dendritiform cells for monitoring corneal inflammation. **B.** Sub-basal nerve density, known to decrease in many ocular surface diseases including DED. **C.** Sub-basal nerve tortuosity, which increases in painful ocular surface diseases. **D.** Microneuromas, evidenced as abrupt nerve swellings.

***Microneuromas: a biomarker of neuropathic corneal pain?***

Microneuromas detected in cornea by IVCM have received increasing attention in ocular surface research these past years. These structures are given various names and definitions depending on the study, although their molecular and cellular function and identity are still unclear. The uniting characteristic of these structures is that they do not have a clearly defined shape and that they are associated with corneal nerves.

In the following section, studies that have considered these structures are listed in chronological order using the bibliography of a recent systematic review as a guide (Chinnery et al., 2021). An updated version of the table from (Chinnery et al., 2021) can be found in **Table 3**.

An early reference to the term "neuroma" in the context of the ocular surface can be found in (Belmonte et al., 1997), in which the authors suggest that abnormal firing activity of damaged axons may originate from such structures. Furthermore, in the same context of ocular surface injury, but outside the area of damage, "*the terminal endings of wound-invading neurites formed dense and disorganized neuroma-like fibrillar masses*" as evidenced by gold chloride staining (Rozsa et al. , 1983; Belmonte et al., 1997).

The first study reporting neuromas in 3 healthy human corneas using IVCM was published in 2005 (Patel and McGhee, 2005). The authors reported an irregular structure between 20 to 40 µm in diameter at the level of the inferotemporal mid-peripheral and sometimes central cornea. They were identified as deriving from the perforation of stromal nerves through Bowman's layer while emerging in the subbasal plexus. The same author, a year later (Patel and McGhee, 2006), investigated corneas from 4 patients with keratoconus. In this case, two types of abnormal structures were found at the subbasal level: The first was found in 2/4 patients and defined as "*irregularly shaped, well defined, areas of hyperreflectivity containing multiple oval-shaped bright objects*" emerging from the stroma but not continuing into the epithelium which were subjectively identified as keratocyte nuclei. The second, only detected in the most severe case of keratoconus (1/4), was defined as "*apparent abrupt terminations of sub-basal nerve fiber bundles*". In this case, it was not confirmed whether or not the structures originate from the stroma and it was therefore suggested that "*they may represent sites of perforation of nerve fiber bundles through Bowman's layer*" or "*correspond to an extension of the nerve degeneration*" (Patel and McGhee, 2006). Another study also found the presence of the "*abrupt terminations*" without further detail in patients with keratoconus (Niederer et al., 2008). This series of studies suggests that these structures may be non-pathological and related to nerve entry points from the stroma to the epithelium when found in healthy controls, and then raises the possibility that they may also be structures related to the pathology of keratoconus.

(Hu et al., 2008) is the first study reporting such structures in DED patients (patients with atopic keratoconjunctivitis and dry eye symptomatology). According to the authors, abrupt sub-basal nerve endings were found in 10/24 observed eyes. They suggested that they corresponded to stroma-epithelium entry sites or regenerating nerve sites, without further validation.

In (Vera et al., 2009), corneal nerve abnormalities were studied in patients with toxic epidermal necrolysis and Stevens-Johnson syndrome, two diseases characterized by severe muco-cutaneous reactions related to an adverse drug event. In 4 eyes of 3 different patients out of the total of 26 DED eyes analyzed by IVCM, nerve sprouting was found with a similar shape to those later commonly referred to as microneuromas (Vera et al., 2009), Fig 2, B).

In the study by (Lagali et al., 2009), IVCM images of a phototherapeutic keratectomy patient recapitulated the clinical history of the sprouting of sub-basal nerves and regenerating nerves that may occur after the surgery.

Rao et al., 2010 showed another clinical case history of herpes zoster ophthalmicus-related neurotrophic keratopathy treated with autologous plasma. The IVCM images showed how a basal state showing the lack of subbasal plexus evolved after treatment in the presence of "*nerves with beading*" indicative of regenerating axons.

In 2011, a study provided a detailed anatomical description of these structures. It clearly establishes they are found both in healthy controls (Al-Aqaba et al., 2011) and in patients with Fuchs dystrophy, a dysfunction of the corneal endothelium. It is also pointed out, for the first time, that these structures can be found in the nerve trunks at the corneal stroma level and not only in the sub-basal plexus. The stromal microneuromas were found only in Fuchs dystrophy patients. The authors hypothesized that microneuromas at the sub-basal plexus level are physiological but those found in the stromal level they may have a pathological nature associated with Fuch dystrophy. Those stromal structures were positive for acetylcholinesterase, suggesting that they could represent sympathetic fibers. Another study on rabbit corneas demonstrated that acetylcholine-responding neurons were not activated by mechanical or thermal stimuli, reinforcing this hypothesis (Tanelian, 1991).

The following year Deng et al., 2012 studied neuromas in patients who underwent LASIK surgery (during which a laser cuts corneal nerves to form a corneal flap). Authors found the appearance of "*dilated head ends*" right at the site of the laser incision in 2/26 cases 1 month

after surgery and in 5/26 cases 3 months after surgery. It is unclear whether these structures were regenerating axons or sources of ectopic neuronal activity. A case-series by (Borsook and Rosenthal, 2011) described for the first time 5 painful patients without any objective signs of ocular surface damage (*i.e.* "pain without stain"), suffering from neuropathic corneal pain (NCP).

Patients with the same pathology were also studied in (Aggarwal et al., 2015). This is the first of a total of 6 papers that have been published to date using microneuromas as an imaging biomarker of NCP. In this article, the term "neuroma" was used for the first time to refer to a series of structures detected on IVCM images from patients suffering from ocular pain that consisted of "*stumps of severed nerves and were identified as abrupt endings of a nerve fiber*". This article directly linked neuromas as nerve structures correlated with painful ocular pathology. Definition of neuropathic pain requires detection of nerve damage and these neuromas represent excellent candidates. They were not only presented as imaging biomarkers for NCP diagnosis, but also as treatment-response biomarkers, as these structures disappear in painful patients following autologous serum tears. Two subsequent reviews by the same group reinforce this concept (Cruzat et al., 2017; Dieckmann et al. , 2017). Another study (Giannaccare et al., 2017) pointed to the same direction in which 20 patients with painful DED (VAS score: 8.9 ± 0.9) were treated with cord blood serum eye drops. The treatment not only reduced the ocular pain (VAS score: 3.2 ± 2.0) but also the percentage of patients presenting neuromas in IVCM from 32% to 20%.

In parallel, another clinical study (Parissi et al., 2016) demonstrated with impressive mosaics reconstructing a large part of the sub-basal plexus that structures designated as "penetration points" appeared as a result of fibers entering the subbasal plexus from patients with keratoconus. This resulted from collagen cross-linking, a treatment that enables these patients to regenerate the plexus lost as a consequence of the disease. This article partially supports the initial hypothesis: these structures could actually be stroma-epithelium entry points, but of newly regenerated fibers.

Three other articles led by Pr. P. Hamrah were then published in the following years with somewhat contradictory conclusions. In the first (Cavalcanti et al., 2018), microneuromas were observed in patients with Herpes Zoster Ophthalmicus. The only reference to a quantification noted that all patients had a similar frequency of microneuromas (41.6%),

however the study was composed of 14 patients with ocular pain and 10 without. The following article (Morkin and Hamrah, 2018), which dealt with patients suffering from NCP, did not contain any reference to microneuromas in the results section, although the images presented in the second figure, seem to suggest the presence of microneuromas, although not specified. The third article (Aggarwal et al., 2019) is in line with previously published studies (Aggarwal et al., 2015; Giannaccare et al., 2017). The authors reported that microneuromas were found in 100% of 16 patients with NCP, while they were not detected in healthy controls. Similarly to (Aggarwal et al., 2015), NCP patients were treated with autologous serum tears which decreased pain scores and the percentage of patients with microneuromas to 6%.

Al-Aqaba and colleagues, who proposed neuromas as entry points in Fuchs' dystrophy (Al-Aqaba et al., 2011), published a review (Al-Aqaba et al., 2019) in which they defined neuromas as "*bulb-like structures*". They provide additional information by combining acetyl cholinesterase technique and electron microscopy to point that these structures detected by IVCM are none other than the aforementioned stroma-epithelium entry points.

The same authors were also able to differentiate patients with peripheral NCP from patients with central NCP (Ross et al., 2020). Contrary to previous publications quantifying microneuromas at the sub-basal level, here the authors quantified microneuromas in the stroma, at the level of the neural trunks. They differentiated three types of stromal microneuromas: "*spindle neuromas*", "*lateral neuromas*" and "*stump neuromas*". Interestingly, the number of these structures per patient was significantly higher in patients with peripheral NCP compared to patients with central NCP (9.3±2.8 vs. 2.95±1.15).

In another paper (Shen et al., 2019), sub-basal nerve sprouts were found in 2 of 10 patients with episodic migraine. It is noteworthy that the sub-basal nerve density was found to be increased in those patients as compared to healthy controls, contrary to what is usual in DED and other ocular surface diseases.

In 2020, another study lead by Pr P. Hamrah (Moein et al., 2020) reported sub-basal microneuromas in 100% (n=25) of patients with NCP, while were not detected in painless DED patients (n=30) or in healthy controls. Therefore, based on these data, microneuromas are established as a diagnostic imaging biomarker for NCP. In another study by the same group

(Yavuz Saricay et al., 2021) microneuromas were detected in 6/7 patients with painful neurotrophic keratopathy, which are therefore considered as suffering from NCP.

More recently, Dermer and colleagues (Dermer et al., 2022) continued to investigate the link between microneuromas and NCP. The study enrolled a larger population of DED patients (119 who did not underwent refractory surgery + 16 who did) and 18 healthy controls. No difference in terms of neuroma proportion was found in the 3 cohorts. Next, all subjects in the study were grouped according to whether or not they had microneuromas and a wide range of parameters were compared: demographics, psychiatric conditions, comorbidities, ocular history, systemic and topical medications and parameters related to DED symptoms and signs, including sub-basal nerve parameters assessed by IVCM. None of the wide variety of parameters studied differed between patients with and without microneuromas. **This study, therefore, suggests that microneuromas cannot be used as an imaging biomarker for NCP and, in fact, do not seem to correlate with any other aspect in these patients**.

An interesting review on the topic (Stepp et al., 2020) established that the so-called "neuromas" and "microneuromas" are, as already indicated in previous publications, stroma-epithelium entry points. The authors provided IVCM images from a depth volume scan, together with immunostained human corneal nerves reinforcing the “entry point” hypothesis. This study suggests that these structures are probably derived from other cell types such as nonmyelinating Schwann cells, endoneurial cells, corneal epithelial cells, immune cells or even collagen produced by the endoneurial fibroblasts and extracellular matrix from the epithelial basement membrane. Thus, from this publication, a new hypothesis arose: these structures could be stroma-epithelial nerve penetration sites and their cellular entity is non-neuronal cells. A study in patients with multiple myeloma (Koschmieder et al., 2020), a hematologic malignancy, showed that sub-basal microneuromas were detected in 18/25 patients, all of them with such symptoms of neuropathy, pointing to the hypothesis of microneuromas as a marker of ocular pain.

Finally, the last published study related to corneal microneuromas deals with SARS-CoV-2 infection. This study enrolled 23 patients who had been infected by SARS-CoV-2 (Barros et al. , 2022) with mild or asymptomatic COVID-19 and 46 healthy controls. In the SARS-CoV-2 infected group, 8 developed DED (OSDI>13), 6 had some symptoms of DED (OSDI: 6-12) while 9 did not develop DED. The presence of microneuromas was found in 75% of patients with

DED, 35% of patients with DED symptoms and 45% of patients who did not develop DED, while microneuromas were detected in 2/46 healthy controls. Another interesting finding is that the percentage of microneuromas varied depending on age of the patient post-COVID with 45% patients less than 35 years, 80% of patients between 36 and 55 years and 65% of patients older than 55 years.

**Table 3: Updated literature on microneuromas in IVCM corneal images and their characteristics**

| First author, year | Research question type and study design | Journal | Participants/ Population | Corneal nerve plexus evaluated | Representative corneal IVCM image provided in paper? | Corneal region where nerve feature(s) noted | Number of corneal nerve IVCM images analyzed per participant; IVCM scan mode | Masking of IVCM method: image selection; image analysis | Keyword(s) present (Pathological or Physiological context) |
|---|---|---|---|---|---|---|---|---|---|
| Patel and McGhee, 2005 | Methodological – retrospective cohort | Invest Ophthalmol Vis Sci | Normal eyes (n=3) | Sub-basal | Yes (Figure 5) of "probable sites of perforation of nerves through Bowman's layer" | Inferotemporal midperiphery | >373 for each participant; section scan mode | NA | • Perforation (Physiological) |
| Patel and McGheem, 2006 | Methodological – retrospective cohort | Invest Ophthalmol Vis Sci | Eyes with keratoconus (n=4) | Sub-basal | Yes (Figure 4) of "apparent abrupt terminations of sub-basal nerve fiber bundles" | "Region of the cone" | NR; section scan mode | NA | • Abnormalities<br>• Abrupt<br>• Perforation (all Pathological) |
| Hu et al., 2008 | Etiology – case control | Ophthalmol | Patients with atopic keratoconjunctivitis (n=21) and healthy controls (n=19) | Sub-basal and stromal | Yes (Figure 6) of "abrupt terminations" in sub-basal plexus | Central | "3 clearest images"; sequence scan mode | Selection – NR; Analysis - Yes | • Abnormalities<br>• Abrupt<br>• Bifurcation<br>• Sprout (all Pathological) |
| Niederer et al., 2008 | Etiology – cross-sectional | Invest Ophthalmol Vis Sci | Patients with keratoconus (n=52) and age-matched controls (n=52) | Sub-basal and stromal | Yes (Figure 2), but not of nerve features of interest per se | Central | 3 images; section scan mode | Selection – NR; Analysis - NR | • Abruptly (Pathological) |
| Zhao et al., 2008 | Etiology – cross-sectional | Klin Monatsbl Augenheilkd | Patients with various types of polyneuropathy (n=18) and agematched controls (n=15) | Sub-basal and stromal | Yes (Figure 1) of "abundant sprouting of sub-basal nerve bundles"; (Figure 2B), large hyperreflective, round features in the sub-basal nerve plexus are shown, but are referred to as "beads". | Central | 3 to 5 images; "full layer corneal scans" | Selection – Yes; Analysis - Yes | • Sprouting (Pathological) |
| Lagali et al., 2009 | Etiology – prospective cohort | Invest Ophthalmol Vis Sci | Patients who underwent PTK (n=13) | Sub-basal and stromal | Yes (Figure 3) of "presumed sprouting subbasal nerves" and "presumed sprouts… and mildly tortuous regenerated subbasal nerves" | Scanned "several millimeters of central cornea" | 6 images; "crosssectional images" ; and additional confocal scans obtained across a 3- to 4-mm central region of each cornea" | NA | • Presumed sprout/ing (Pathological) |

| | | | | | | | | | |
|---|---|---|---|---|---|---|---|---|---|
| Vera et al., 2009 | Etiology – cross-sectional | Cornea | Patients with secondary DED (n=25) | Sub-basal | Yes (Figure 2) of "nerve sprouting" | Central and peripheral | NR; NR | NA | • Sprouting (Pathological) |
| Rao et al., 2010 | Intervention – prospective cohort | Br J Ophthalmol | Eyes of patients with neurotrophic keratopathy (n=6) | Sub-basal | Yes (Figure 2) of "nerve stumps" and (Figure 4) of "nerve sprouts" | Central | 4 randomly selected images; "sequential" imaging | Selection – NR; Analysis - NR | • Sprout<br>• Stump (all Pathological) |
| Al-Aqaba et al., 2011 | Etiology – case series | Am J Ophthalmol | Eyes (n=25) of bullous keratopathy (n=25) and eyes (n=6) of normal controls (n=6) | Sub-basal and stromal | Yes (Figure 1) of "bulbous terminations of sub-basal nerves"; "; and (Figure 2) "localized nerve excrescences or thickenings ...suggestive of early sprouting)" | "Central and paracentral (approximately 7mm x 7mm)" | NR, although states "approximatel y 7x7mm of cornea"; "scanned through all layers" | Selection – NR; Analysis - NR | • Bifurcations (Physiological) • Thickening (Pathological)<br>• Bulb-like (Physiological)<br>• Bulbous termination (Physiological)<br>• Perforation (Physiological)<br>• Sprout/ing (Pathological) |
| Zheng et al., 2011 | Etiology – cross-sectional | Invest Ophthalmol Vis Sci | Patients with unilateral PXF (n=27) and normal controls (n=27) | Sub-basal | Yes (Figure 4) of "nerve sprouts" | Central | "3 best focussed images"; sequence scan mode | Selection – NR; Analysis - Yes | • Sprout (Pathological) |
| Deng et al., 2012 | Intervention – prospective cohort | Neural Regen Res | Myopic patients (n=26) who underwent LASIK | Sub-basal and stromal | Yes (Figure 5) of "dilated head ends" | "From the margin of the ablation zone to the center at each four quadrants (superior, inferior, nasal and bitemporal)" | NR; section scan mode | Selection – NR; Analysis - NR | • Ends<br>• Stump (Pathological) |
| Shaheen et al., 2014 | Review | Surv Ophthalmol | NA | Sub-basal and stromal | Yes (Figure 3), but not of nerve features of interest per se | NR | NA | NA | • Abrupt (Pathological)<br>• Bifurcate/bifurcation (Physiological)<br>• Endings (Physiological)<br>• Microneuroma (Pathological)<br>• Sprout (Pathological) |
| Aggarwal et al., 2014 | Intervention – retrospective case-control | Ocular Surface | Patients with neuropathy-induced severe photoallodynia (n=16) and normal controls (n=16) | Sub-basal | Yes (Figures 1 and 3) of "neuromas" | Central | "3 images most representative of the subbasal nerve plexus"; sequence mode | Selection – Yes; Analysis - Yes | • Abrupt<br>• Endings<br>• Neuroma<br>• Sprouting<br>• Stump<br>• Swelling (all Pathological) |

| | | | | | | | | | |
|---|---|---|---|---|---|---|---|---|---|
| Parissi et al., 2016 | Etiology – prospective cohort | JAMA Ophthalmol | Patients with keratoconus who underwent CXL (n=19) and agematched healthy controls (n=19) | Sub-basal | Yes (Figure 5) of "abrupt orientation changes after penetration" | Central | 3 images meeting quality criteria; sequence scan mode | Selection; NR; Analysis - Yes | • Abrupt<br>• Penetration point (Pathological) |
| Cruzat et al., 2017 | Review | Ocular Surface | NA | Sub-basal and stromal | Yes (Figure 10) of "neuromas" | Central | NA | NA | • Abrupt<br>• Endings<br>• Microneuroma<br>• Neuroma<br>• Sprouting<br>• Swelling (all Pathological) |
| Dieckmann et al., 2017 | Review | Ophthalmology | NA | Sub-basal | Yes (Figure 4) of "microneuromas" | NR | NA | NA | • Endings<br>• Microneuromas<br>• Swelling (all Pathological) |
| Giannaccare et al., 2017 | Intervention – single-arm open label | Cornea | Patients with ocular surface disease (n=20) | Sub-basal | Yes (Figure 1) of "neuromas" | NR | "3 images most representative" ; sequence scan mode | Selection; Yes; Analysis - Yes | • Abrupt<br>• Endings<br>• Neuroma<br>• Stumps (all Pathological) |
| Cavalcanti et al., 2018 | Etiology – casecontrol | Ocular Surface | Patients with unilateral HZO (n=24) and the contralateral normal eyes, and 24 normal volunteers as controls | Sub-basal | Yes (Figure 5) of "neuromas" | Central | "minimum of 3 representative images" from "at least 50 good quality images"; sequence scan mode | Selection; Yes; Analysis - Yes | • Microneuroma<br>• Neuroma (all Pathological) |
| Morkin and Hamrah, 2018 | Intervention – retrospective case series | Ocular Surface | Patients with neuropathic corneal pain who received self-retained cryopreserved amniotic membrane (PROKERA) (n=9) | Sub-basal | Yes (Figure 2), but not of nerve features of interest per se | Central | "4 representative images"; "full thickness coronal corneal scans" | Selection – Yes; Analysis - Yes | • Abrupt endings<br>• Microneuroma (all Pathological) |
| Aggarwal et al., 2019 | Intervention – retrospective case-control | Ocular Surface | Patients with severe neuropathic corneal pain (n=16) and controls (n=12) | Sub-basal | Yes (Figures 1 and 3) of "micro-neuromas" | Central | "3 images most representative of the subbasal nerve plexus" from 50-100 acquired images; sequence scan mode | Selection – Yes; Analysis - Yes | • Micro-neuroma<br>• Stump (all Pathological) |

| | | | | | | | | | |
|---|---|---|---|---|---|---|---|---|---|
| **Al-Aqaba et al., 2019** | Review | Prog Ret Eye Res | NA | Sub-basal and stromal | Yes (Figures 12 and 24) of "bulb-like termination of sub-basal nerves" | NR | NA | NA | • Bifurcations (Physiological)<br>• Bulb-like termination (Physiological)<br>• Endings (Physiological)<br>• Microneuroma (Pathological)<br>• Perforation (Physiological)<br>• Sprouting (Pathological)<br>• Swelling (Physiological)<br>• Thickened (Pathological) |
| **Ross et al., 2019** | Etiology – cross-sectional | Br J Ophthalmol | NCP patients (n=14 patients, 27 eyes), and 14 eyes from 7 healthy controls | Sub-basal and stromal | Yes (Figure 4) of "microneuromas" and "nerve sprouts" in the stroma, and (Figure 5) of "fusiform neuroma" | Central and paracentral | NR; "scanned through all corneal layers" | NA | • Abnormalities<br>• Hyperreflective<br>• Microneuromas<br>• Neuromas<br>• Stump<br>• Swelling (all Pathological) |
| **Shen et al., 2019** | Etiology – case control | J Pain Research | Patients with episodic migraine (n=10) and age and sex-matched controls (n=10) | Sub-basal | Yes (Figure 1) of "nerve sprouts" | Central | "3 high quality images"; "scanned through all the corneal layers" | Selection - NR; Analysis - Yes | • Injury<br>• Sprouts (all Pathological) |
| **Moein et al., 2020** | Etiology, case-control | Ocular Surface | Patients with clinical diagnosis of NCP (n = 25), DED (n = 30), and age- and sex-matched healthy controls (n = 16), | Sub-basal | Yes (Figure 1) of "microneuromas" | Central | To analyze nerve morphology (microneuromas and nerve beading), multiple full-thickness IVCM volume scans, as well as sequence scans comprised of an average 100 images per scan from all layers of the cornea were screened for each selected eye. | Selection - no; analysis - Yes | • Microneuromas<br>• Nerve beading (all Pathological) |
| **Dermer et al., 2022** | Etiology, cross-sectional | Br J Ophthalmol | Control subjects without DE symptoms or history of refractive surgery (n=18), patients with DE symptoms and no | Sub-basal | Yes (Figure 1) of "microneuromas" | Central | Up to three images of different regions of subbasal plexus | Selection - yes; analysis - Yes | • Microneuromas (Pathological/physiological) |

| | | | | | | | | | |
|---|---|---|---|---|---|---|---|---|---|
| | | | history of refractive surgery (n=119) and individuals with DE symptoms and a history of refractive surgery (n=16). | | | | | | |
| **Koschmieder et al., 2020** | Etiology, cross-sectional | Bioscience Reports | multiple myeloma patients (n=25) | Sub-basal | Yes (Figure 1) of “microneuromas” | Central | NR; "At least three scans" | NR | • Microneuromas (Pathological/physiological) |
| **Yavuz Saricay et al., 2021** | Etiology, case series | Ocular Surface | 7 cases of ocular pain patients | Sub-basal | Yes (Figure 3) of “microneuromas” | NR | three most representative images | Selection - yes; analysis - Yes | • Microneuromas (Pathological/physiological) |
| **Guerrero-Moreno et al., 2021b** | Etiology, case-control | Biomedicines | Painless AIDE (n=8), AIDE-NCP (n=7), painless MGD (n=8), MGD-NCP (n=11), controls (n=10) | Sub-basal | Yes (Figure 3 and 6A) of “microneuromas” | Central | median (range): 77 (31–193) images/patient | NR | • Microneuromas (Pathological/physiological) |
| **Barros et al., 2022** | Etiology, case-control | Ocular Surface | Patients with mild or asymtomathic Sars-CoV-2 (n=23), controls (n=46) | Sub-basal | Yes (Figure 2) of “neuromas” | central and paracentral cornea | five selected images from each subject | NR | • Neuromas • axon beads (Pathological/physiological) |

References in red were added to the version in Chinnery et al., 2021.

### V.4 Dry eye disease-related neuropathic corneal pain: *When signs and symptoms do not correlate*

For the majority of DED patients, there is some correlation between clinical signs and symptoms. However, there exist a significant proportion of patients who have seemingly conflicting signs and symptoms (Baudouin et al., 2014). It is therefore common to find clinical cases where patients present with signs of DED without symptoms, which could be related to corneal hypoesthesia as a consequence of chronic untreated DED. Other possibility for patients presenting signs without symptoms is a case of presymptomatic form of DED, which will require preventive management, especially if ophthalmological treatments known to aggravate it are to be performed in the near future. Conversely, patients can present with important symptomatology (e.g. severe ocular pain) in the absence of any significant ocular damage, often referred to as ***"pain with no stain"***. This is thought to reflect **neuropathic corneal pain** (Craig et al., 2017).

As defined before, neuropathic pain results from damage or disease of the somatosensory system. Any morphological or functional alteration of the corneal nerve terminals may explain the painful symptoms of some patients. In addition to the DED, various inflammatory diseases, neurological diseases, and surgical interventions can lead to corneal neuropathic pain, as summarized in **Table 4** . (Rosenthal and Borsook, 2016; Dieckmann et al., 2017; McMonnies, 2017; Aggarwal et al., 2019).

**Table 4: Possible etiologies of neuropathic corneal pain**

| ***Type*** | ***Example*** |
|---|---|
| Chronic ocular surface disease | • DED<br>• Recurrent corneal erosions<br>• Chemical burns<br>• Ocular surface neoplasia |
| Post-surgical | • Kerato-refractive surgery<br>• Cataract surgery<br>• Corneal transplant surgeries |
| Infections | • Herpes simplex keratitis<br>• Herpes zoster keratitis |
| Toxic Keratopathy | • Topical – preservatives containing benzalkonium chloride |

| | |
|---|---|
| | • Systemic – Isotretinoin |
| Radiation and ultraviolet light exposure | |
| Systemic neuropathies | • Diabetes<br>• Small fiber neuropathy<br>• Multiple sclerosis |
| Trauma | |
| Miscellaneous | • Trigeminal neuralgia<br>• Fibromyalgia |

Triggers that lead to corneal nerve damage result in corneal neuropathy, such as damage to nerves during refractive surgeries, ocular surface diseases such as chronic dry eye disease, recurrent corneal erosions, corneal neuropathic infections such as herpetic simplex and zoster, systemic neuropathic conditions such as diabetes, exposure to topical and systemic drugs, radiation keratopathy and chemotherapy (Theophanous et al. , 2015; Rosenthal and Borsook, 2016). *Adapted from Ophthalmology, 2022.*

Regarding the NCP associated with DED, patients develop no obvious signs of ocular surface damage (i.e. "pain without stain") (Rosenthal et al. , 2009; Galor et al., 2018). Pain does not resolve with commonly used DED treatments. For these patients, especially if peripheral NCP is suspected, the use of IVCM has been proposed to correlate morphological biomarkers of corneal abnormalities with NCP. Unfortunately, this is a clinical entity that has only recently been described on the ocular surface and its diagnosis is still the subject of much debate in the research field. In an attempt to better characterize these patients, we have investigated the corneal nerve morphological abnormalities in patients with NCP using IVCM (Guerrero-Moreno et al., 2021b)

The role of NCP in patients with high pain but low clinical signs could be clear, but, the idea that highly symptomatic patients with ocular surface stain (*i.e.* signs of epithelial damage) may also have a neuropathic component to their pain, should not be ruled out.

Treating NCP is highly challenging, and there is still a current lack of available topical nerve-targeted treatment to alleviate ocular pain. This is very relevant as it represents a debilitating condition that can dramatically affect the quality of life of the patient.

### V.5 Assessment and treatment of DED and DED-related NCP

For the treatment of DED and its possible neuropathic component, a number of factors must be considered. Firstly, the signs and symptoms of DED should be assessed with the tools previously described, to treat the patient according to his or her specific type of DED. If a neuropathic component is suspected, *i.e.* the symptoms are very severe compared to the signs, or if IVCM markers of NCP are found (reduced sub-basal nerve density, abundance of microneuromas, increased sub-basal nerve tortuosity), it is recommended to perform a proparacaine challenge test. This test consists of instilling a drop of proparacaine 0.5% on the painful eye. If the painful symptoms decrease considerably, a peripheral origin can be considered, *i.e.* peripheral neuropathic pain. Otherwise, one should consider a possible mixed neuropathic corneal pain (peripheral & central) or pure central neuropathic corneal pain (Dieckmann et al.,2017; Ross et al., 2020; Guerrero-Moreno et al., 2021b).

With this in mind, the following treatments can be considered.

#### A. Ocular lubricants ("artificial tears")

Ocular lubricants are the first line treatment of choice, especially useful in mild cases of DED. It is a short-term symptomatic treatment based on the compensation of the lacking tear film volume. Those formulations are comprised of an abundant aqueous phase supplemented by other ingredients like viscosity-enhancing agents (polyacrylic acid, carboxymethyl cellulose, dextran, hyaluronic acid, hydroxypropyl methylcellulose etc.) (Jones et al., 2017). Formulations without preservatives, specially devoid of benzalkonium chloride, are preferred in order to avoid their possible toxic effects on the ocular surface. Those formulations can be beneficial in all DED subtypes and also for patients suffering from NCP. However, their principal disadvantage is their short lived efficacy requiring regular topical administration and their lack of specific pharmacological action targeting any pathophysiological aspect of the ocular surface disease. Therefore, as DED and NCP becomes more severe, other treatments must be considered.

#### B. Topical anti-inflammatory therapy

Topical anti-inflammatory drugs can be considered as second-line treatment for DED. As DED implies a chronic inflammation of the ocular surface, targeting it offers interesting prospects in terms of management of DED (Jones et al., 2017). It has been demonstrated that chronic

inflammation triggers sensitization of sensitive nerves so decreasing inflammation is also a good approach to treat NCP. There are different topical anti-inflammatory drugs that can be used, which can be grouped according to their mechanism of action.

**Topical non-glucocorticoid immunomodulators**

They are drugs capable of reducing/modulating the immune response via a non-steroid hormone-based mechanism. Among them, Ciclosporin A, the prototypical second-line treatment for DED, stands out in Europe. Ciclosporin A is a fungal peptide which prevents T cell activation by inhibiting cytokine production including interleukin-2 (IL-2). In other countries, such as United States, other non-glucocorticoid immunomodulators are also available, such as Lifitegrast. It is a synthetic small molecule designed to inhibit the biding between LFA-1 expressed by activated T cells and ICAM-1 expressed by epithelial cells under inflammatory conditions.

**Topical glucocorticosteroids**

They are based on the activation of the quasi ubiquitous glucocorticoid receptor. It is implicated, among other functions, in the attenuation of the immune response confirming their usefulness to decrease ocular inflammation. Hydrocortisone is one of the most widely used in Europe (Messmer et al., 2023). However, the necessary long period of application in DED and NCP patients must be accompanied by careful monitoring by the ophthalmologist, as long exposure time can trigger steroid-related complications such as glaucoma and cataract.

### C. Topical and oral secretagogues

These drugs aim to increase tear production. Topical secretagogues such as Diquafosol are indicated for aqueous deficient dry eye as they are capable of stimulating water and mucin secretion from epithelial and goblet cells.

SS is characterized by the production of auto-antibodies targeting the muscarinic acetylcholine receptors. For those patients, oral secretagogues consisting on cholinergic agonist as pilocarpine and cevimeline can revert that inhibition, increasing the tear production. (Jones et al., 2017)

### D. Topical neuroregenerative therapy

Peripheral NCP can be treated with topical therapies aiming to promote nerve regeneration. This approach must be considered for patients with reduced nerve density in IVCM and/or not responding to other topical therapies (Aggarwal et al., 2019, Alio et al., 2017). They are based on the action of nerve growth factor that reduces allodynia and hyper-algesia in those patients. NGF can be applied to the ocular surface by specific formulations or through blood-derived preparations. The most widespread form of this therapy is autologous serum tears (AST) that contain different concentrations of NGF and other growth factors as insulin-like growth factor-1 and vitamins (Dieckmann et al., 2017). Among the disadvantages of AST is the lack of standardization as different dilutions are applied and they depend considerably on the patient's systemic health.

### E. Amniotic membrane graft

Self-retained cryo-preserved amniotic membrane application on the ocular surface contributes to the treatment of severe DED and NCP through anti-inflammatory, anti-fibrotic and neuro-trophic effects. It brings a symptomatic alleviation and improvement of the ocular surface signs (John et al., 2017). However, their application in NCP patients with severe hyper-algesia is not indicated as they may not tolerate the polycarbonate ring used to fix the membrane to the ocular surface.

### F. Systemic Pharmacotherapy

Until now, the treatments proposed can promote some beneficial effects in patients suffering from peripheral NCP. For patients with a clear mixed or central NCP and/or not responding to those treatments, systemic pharmacotherapy has been suggested. However, before applying this approach, it has to be taken in account that clinical studies are still scares for their use in NCP, so co-management between the pain specialist and the ophthalmologist is important. In this line, in (Dieckmann et al., 2017), three lines of treatments have been proposed:

**First line treatments**

***Tricyclic Antidepressants (TCAs)*:**

They have been used effectively in the treatment of neuropathic pain and could be applied to NCP patients (Ozmen et al., 2020). TCAs exert their action by inhibiting pre-synaptic reuptake

of serotonin and norepinephrine, as well as by blocking cholinergic, histaminergic, and sodium channels. However, common side effects of these drugs include dry mouth, constipation, and sedation, considerably limiting its applicability in DED patients.

***Carbamazepine***

Carbamazepine is a sodium channel blocker indicated for trigeminal neuralgia (Kobayashi et al., 2020). NCP patients may benefit from its actions; however, its side effects include drowsiness, headache, and dizziness.

**Second line treatments**

***Oral low-dose Naltrexone***

Naltrexone is an antagonist of the μ-opioid and κ-opioid receptor used to treat acute opioid intoxication. However, their use with lower concentrations can be effective to treat central NCP (Dieckmann et al., 2021). However, common side effects include headache, tachycardia, and vivid dreams.

***Tramadol***

Tramadol is a weak μ-opioid receptor agonist and norepinephrine and serotonin reuptake inhibitor. As with other opioids, it can be used for the treatment of pain but, it has associated side effects as nausea, vomiting, constipation, sedation and can produce dependence in the patient.

**Third line treatments**

***α2-δ calcium channel ligands***

These drugs inhibit the release of glutamate, norepinephrine and substance P in CNS neurons. Gabapentin and pregabalin are some examples of those drugs that have been used to treat neuropathic pain (Small et al. , 2020; Ongun and Ongun, 2021). Common side effects include dizziness; somnolence, dry mouth and constipation. Their efficacy in NCP has been demonstrated in some studies (Pakravan et al. , 2012, Small et al., 2020, Tei et al. , 2022).

***Serotonin and norepinephrine reuptake inhibitors***

Commonly used to treat major depression, those drugs increase the endogenous levels of serotonin and norepinephrine by inhibiting their degradation. Some examples are duloxetine

and venlafaxine but their use is limited by their side effects of nausea, dry mouth, headache, decreased libido, dizziness, somnolence, and insomnia.

### G. Surgical approaches

If patient's quality of life is seriously affected by the ocular surface disease and the previous indicated treatments are not effective, surgical approaches must be considered. Among them, some examples include punctual occlusion, tarsorrhaphy or minor salivary gland transplantation (Dieckmann et al., 2017, Jones et al., 2017; Galor et al., 2018) .

## V.6 Preclinical modeling and evaluation of DED and DED-related pain

### A. Measurement of corneal sensitivity and ocular discomfort in mice models

**Spontaneous ocular discomfort: ocular aperture ratio**

The well-known and widely used "*mouse grimace scale*" (Langford et al., 2010) states, in its first item, that orbital tightening is a measure of pain expression and establishes a 3-value scale to rank it: not present, moderate, severe. The **ocular aperture ratio,** also known as spontaneous **eye closing ratio (**Fakih et al., 2019**,** 2020**,** 2021**)** or **palpebral opening** (Mecum et al., 2020) is basically a refined and more quantitative measure of this same phenomenon. It consists of taking a photograph of the awake animal (immobilized or not) in which the position of the eyelids in relation to the eye must be clearly visible. Then, using imaging software such as ImageJ, the length between the internal and external canthus (x) and the distance between the edge of the upper and lower eyelids (y) are measured. Finally, y/x is divided and a value between 0 and 1 is obtained, where 0 is equivalent to the eye completely closed and 1 to the eye completely open (**Fig. 16**).

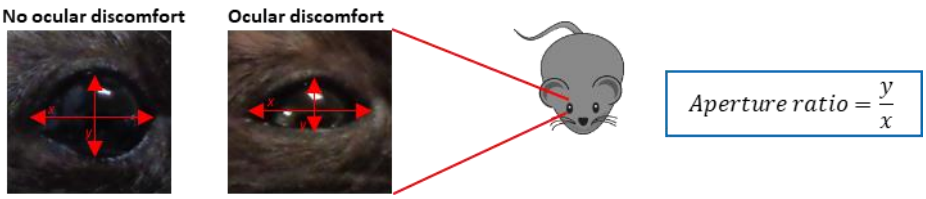


**Figure 16: Aperture ratio for ocular discomfort quantification**

When taking the picture, it is important that the surface of the camera lens be parallel to the ocular surface to prevent the effect of tilt from affecting the final result. As indicated above, this test can be performed in an immobilized animal, so it is important that the animals are accustomed to the experimenter and the room where the experiment is performed. Another approach is record a video in which key clips are selected, but this makes less easy to obtain images at the correct angle and generally increases the time needed to apply this test. As with any behavioral test, mice stress can affect this measure so thorough habituation is necessary before the test.

The ocular aperture ratio test, firstly described in (Fakih et al., 2019) has started to be used during the last few years in mouse models of DED where the main objective was the study of symptoms. It is currently used to monitor ocular discomfort and to test the analgesic effects of drugs (Fakih et al., 2019; Mecum et al., 2020; Fakih et al., 2020; Fakih et al., 2021).

**Corneal cold sensitivity: *menthol challenge test***

The sensitivity of cold receptors can also be assessed in rodents. For this purpose, the natural TRPM8 agonist menthol is used. The test consists of topically applying a drop of menthol (in concentrations ranging from 50 µM to 50 mM) and measuring the ocular aperture ratio during 5 min post-instillation (Fakih et al., 2020) or the nocifensive behavior of the mice (Robbins et al., 2012).

Menthol challenge determines the sensitivity of the ocular surface as a whole, as the drop spreads over the entire ocular surface (cornea, conjunctiva and eyelids).

**Corneal mechanical sensitivity: *von Frey filaments test***

Similarly to humans, corneal mechanical sensitivity can be assessed in laboratory animals. For this purpose, von Frey filaments are applied to the center of the cornea. Instead of being a single filament like the Cochet-Bonnet esthesiometer, a set of filaments is applied from the thinnest (lower pressure) to the widest (higher pressure) **(Table 5)**. Similarly to Cochet-Bonnet esthesiometry, the value of the first filament that elicits a blink reflex response will be taken as the mechanical threshold value. It is important to note that for the correct application of this test a preliminary training (a minimum of 5 days is required) of animals is mandatory. Among the disadvantages of this behavioral test, is that it only assesses the part of the cornea in contact with the filament which is in the millimeter range. This can be compensated by

applying the filament always in the center of the cornea, but applying the filament exactly in the same place is technically impossible. Another disadvantage of this test is that the values are concrete, as filaments with fixed pressure values are used.

Still, von Frey filaments test, combined with other behavioral and sensitivity tests, is a useful test for monitoring corneal mechanical sensitivity.

**Table 5: von Frey filaments used to measure corneal mechanical sensitivity in mice: filament diameter and corresponding mechanical force applied**

| Size (mm) | 1.65 | 2.36 | 2.44 | 2.83 | 3.22 |
|---|---|---|---|---|---|
| Force (g) | 0.008 | 0.02 | 0.04 | 0.07 | 0.16 |

**Corneal chemical sensitivity: *capsaicin challenge test***

The sensitivity from poly-modal nociceptors can also be measured in mice. Similarly to menthol challenge test, the natural TRPV1 agonist capsaicin is used for this purpose. A drop (10 µL) of capsaicin (10 µM to 100 µM) is instilled in the center of the eye. At this point, the mouse closes the eye, and is then immediately placed in a cage and observed for 5 minutes. The time that the animal takes to reopen completely the eye corresponds to the palpebral closure time. Contrary to the mechanical threshold, an increase in time is indicative of an increase in sensitivity. This test has been shown to be sensitive to the possible effect of experimental DED treatments in experimental models (Reaux-Le Goazigo et al., 2019; Fakih et al., 2021). Capsaicin test, together with other sensitivity measurements, yields important outputs in characterizing the effectiveness of new treatments for the challenging eye pain.

**Corneal chemical sensitivity: *eye-wiping test (NaCl 2M)***

Ocular chemical sensitivity can also be assessed using topical application of hypertonic solutions. As it is a hypertonic solution, it should be expected that all the corneal receptors to be activated by affecting their membrane potential. If not all, at least the cold receptors are activated by this challenge as they are sensitive to changes in osmolarity. This test, similar to the previous ones, consists of immobilizing the mouse with one hand and applying a drop (10 µL) of 2M NaCl. The mouse is then left in a transparent cage and the number of "wipes", *i.e.* the number of times the animal tries to wipe its eye with the ipsilateral forepaw during a

period of 30s, is counted. Only obvious wipes should be counted as grooming is common in these circumstances but does not represent an effective wipe. It is a robust test for measuring sensitivity in mice before and after a treatment or procedure (Farazifard et al., 2005).

### B. Animal models of DED and ocular pain

To improve the knowledge of corneal pain pathophysiology in relation to DED, along with molecular biomarkers of disease progression, animal models mimicking human DED are required. The ocular surface represents a complex system composed of very heterogeneous tissue populations including sensitive neurons, immune cells, epithelial cells, but also lacrimal and lipidic glands. It is a very dynamic structure whose homeostasis is frequently challenged due to environmental insults. Blinking and tear production from both lipid and aqueous glands are the principal actors of such homeostasis. Although the molecular characteristics of DED can be emulated *in vitro*, animal models are required to better recapitulate the characteristics of DED.

DED is a complex, multi-factorial disease and this is reflected in the variety of animal models trying to mimic the disease. To this day, there is not a single model recapitulating all aspects of the disease and this is partially a consequence of the multiple etiologies and grades of severity among patients. For review, see (Chang et al., 2021, Rahman et al., 2021) .

**Environmental desiccating stress and parasympathetic blockade**

A well-established murine model for DED is the desiccating environmental stress (DES) accompanied by muscarinic receptor blockade using scopolamine (Dursun et al., 2002). DES involves exposure to a combination of low humidity and increased airflow giving rise to inflammation and ocular surface damage in association with scopolamine mediated-inhibition of lacrimal gland secretion via its parasympatholytic effect (Bron et al., 2017, McKay et al. , 2019).

Interestingly, animals subjected to DES + scopolamine or only chronically treated with scopolamine showed reduced corneal nerve density and mechanosensitivity (Simsek et al., 2018; Stepp et al., 2019). Another study showed that female DES + scopolamine treated mice showed higher values of ocular surface staining, reduced goblet cell number and overall more

severe DED than males due to an increase in effector T cells ($T_H1$ and $T_H17$) and a decrease in regulatory T cells (Gao et al., 2015).

A DES setup allowed a DED phenotype to be elicited without the need for scopolamine (Chen et al., 2014), also triggering ocular chemical hypersensitivity in the animals as quantified by eye-wiping test (hypertonic saline stimulation) (Chen and Dana, 2023).

These different modalities are thought to recapitulate innate and adaptative immunological responses of DED.

**Genetic models of Sjögren's syndrome**

Several genetic mouse models of Sjögren's syndrome (SS) have contributed to our current understanding of immunopathologic mechanisms underlying the disease such as TSP-1 deficient, TGF- β1 deficient, non-obese diabetic (NOD), F1 hybrids of New Zealand Black and New Zealand White (NZB/NZW F1) and IQI/Jic or NFS/sld mice. Although these models address glandular aspects of SS pathology, their impact on ocular surface tissues is addressed only in a few models such as TSP-1 deficient, C57BL/6.NOD.*Aec1Aec2*, NOD.H2$^b$, NOD.Aire KO, and IL-2Rα (CD25) KO mice. A review has been recently published on mouse models of Sjögren's Syndrome with ocular surface disease (Masli and Dartt, 2020).

Studies have focused on inflammatory cell infiltration and destruction of the lacrimal gland tissue as the etiopathogeny of DED (Barabino and Dana, 2004, Chang et al., 2021).

**Animal models of Meibomian Gland Dysfunction**

MGD is the most common cause of DED and some mouse and rat models have been used to mimic this pathology. An experimental approach is the obstruction of the glands by cauterization (Dong et al., 2018) which leads to DED ocular signs in cauterized animals. Aging has been associated with MGD in humans and this is also true for C57BL/6 mice which develop DED at the age of 1 year, with evident MGD at 2 years. Some genetic models also recapitulate aspects of MGD like the *Sod1*$^{-/-}$and the *ApoE*$^{-/-}$ mice based on the increased oxidative stress and altered lipid metabolism, respectively. For an exhaustive review of mouse models of MGD, please check (Sun et al., 2020).

**Chemically-induced Dry Eye Disease model: *topical benzalkonium chloride***

Benzalkonium chloride (BAK) is a quaternary ammonium compound with biocide properties. It is the most common preservative in topical ophthalmic solutions due to its detergent properties through bacterial walls and membranes (Baudouin et al., 2010). Safe concentrations range from 0.004% to the most commonly used concentration of 0.01%. However, experimental and clinical studies have found that long-term use of topical drugs with BAK may alter ocular surface integrity and trigger tear film instability, inflammation, loss of goblet cells, conjunctival squamous metaplasia, epithelial apoptosis and subconjunctival fibrosis (Rahman et al., 2021). Altogether, repeated BAK instillations trigger DED symptoms in patients and laboratory animals (Baudouin et al., 2010).

In preclinical studies, BAK 0.2% is chronically instilled on the ocular surface of laboratory animals to recapitulate some aspects of DED. Although it had already been used in rabbits and rats, the first descriptions of the mouse homologue model were led by Dr Liu (Lin et al., 2011; Xiao et al. , 2012; Xiao et al. , 2013; Lin et al. , 2014; Zhang et al. , 2014). These studies used male BALB/c mice and established it as a DED model recapitulating signs (Lin et al., 2011; Xiao et al., 2013; Lin et al., 2014) and inflammatory markers (Lin et al., 2011; Zhang et al., 2014) of the disease, as well as its use to test topical treatments (Xiao et al., 2012; Lin et al., 2014). In other studies, the BAK model is characterized by a reduction in goblet cells, a typical hallmark of DED (Barabino et al. , 2014; Portal et al. , 2017; Yang et al. , 2017). This ocular surface damage was shown to be dose-dependent, showing a clear toxicological profile (Yang and Zheng, 2017; Zhang et al. , 2020b). An interesting study compared two mouse strains (Yang et al., 2017) and found that although the severity increased with the concentration of BAK used (from 0.25% to 2%), this aggravation was more severe in C57BL/6 than in BALB/c. The most commonly used concentration of BAK applied to the ocular surface was 0.2% in a regimen of two instillations per day for 7 days (Lin et al., 2011; Launay et al. , 2016) or 14 days (Kim et al. , 2016; Bang et al. , 2019; Wang et al. , 2022). Although most studies applied BAK unilaterally (Lin et al., 2014; Qu et al. , 2019), some applied it bilaterally (Xiao et al., 2012; Matynia et al., 2015,). No study has provided evidence of sexual dimorphism in this mouse model of dry eye disease.

Regarding corneal sensitivity, male C57BL/6 mice receiving 0.2% BAK for 7 days developed an increased hypertonic saline-evoked eye-wiping behavior and mechanical allodynia (Launay et al., 2016; Reaux-Le Goazigo et al., 2019). It correlated with an increase in c-Fos (neuronal

activation), ATF-3 (neuronal damage) and Iba1 (macrophage) immunoreactivity in the ipsilateral trigeminal ganglion of BAK-treated mice, as well as increase in mRNA of inflammatory markers (TNF-α and IL-6) (Launay et al., 2016). This neuroinflammation spreads to the central nervous system, in the spinal trigeminal nuclei, where afferents from primary corneal sensory neurons synapse with secondary sensory neurons, with an increase in the mRNA expression of proinflammatory (TNF-α, IL-6, CCL2) and neuronal (Fos and ATF-3) markers at this level.

**Corneal inflammatory pain model: *corneal scraping associated with lipopolysaccharide instillation***

The corneal scraping and lipopolysaccharide installation model aims to emulate the corneal damage and inflammation observed in DED.

LPS is a bacterial endotoxin able to trigger inflammation as an agonist of innate immunity receptor TLR4 expressed, among others, on the surface of macrophages. This model was first described in rabbits by scraping the corneal epithelium, followed by topical application of LPS (Liang et al., 2007). Rabbits developed an increased infiltration of Ki 67$^{+}$ proliferating cells, TUNEL$^{+}$ apoptotic cells and TNF-α$^{+}$, TNFR1$^{+}$, TLR4/MD2$^{+}$, ICAM-1$^{+}$, RLA-DR$^{+}$, CD11b$^{+}$ and CD11c$^{+}$ inflammatory cells in eyes that received LPS compared to those that received saline (Liang et al., 2007).

In mice, the cornea is mechanically de-epithelialized using a trephine and an interdental brush. A drop (10 µL) of lipopolysaccharide (LPS, 50 µg) is instilled into the injured area. This allows corneal nerve sensitization by two means: first, the direct damage to the intraepithelial terminals provoked by the mechanical disruption and then the inflammatory environment in the affected area, both by direct injury to the epithelium and by the LPS that potentiates the acute inflammatory response (Belkouch et al., 2011; Reaux-Le Goazigo et al., 2019; Joubert et al. , 2020). A second instillation of LPS (50 µg/10 µL) must be performed on day 3 to prevent re-epithelialization and to maintain the inflammatory response. Mice are monitored for a total of 5 days (Reaux-Le Goazigo et al., 2019; Joubert et al., 2020). As shown in Joubert et al., 2019, corneal scraping without LPS instillation was alone able to increase sensitivity to hypertonic solutions and increase the frequency of spontaneous ciliary nerve activity 24 hours

after damage. However, these animals did not show any mechanical allodynia and a decrease in the ciliary nerve firing frequency evoked after a $CO_2$ pulse (Joubert et al., 2019), which is known to activate mechanosensitive terminals by physical action of the gas as well as polymodal receptors as a consequence of the acidification of the medium. 5 days after scraping (without any LPS instillation), mechano-sensitivity and sensitivity to capsaicin challenge were found to be increased (Reaux-Le Goazigo et al., 2019). For the animals challenged with scraping and LPS instillation, mechanical allodynia was similarly observed at day 5 (Reaux-Le Goazigo et al., 2019; Joubert et al., 2020), as well as an increase in the frequency of spontaneous ciliary nerve activity (Joubert et al., 2020). Regarding the firing frequency evoked after $CO_2$ pulse, contrary to the acute model (24 h after scraping), no differences with control animals were detected. A possible explanation for the differences between the acute (24h post-scraping) and the complete model (5 days post-scraping + LPS) in terms of mechanical sensitivity and ciliary activity after $CO_2$ stimulation is that axotomy of the corneal nerves acutely produces an hypoesthesia to the stimulus, whereas 5 days later, the nerves had regenerated and were sensitized following longer exposure to the inflammatory environment.

**Lacrimal gland excision models**

Various mouse, rat and rabbit models of lacrimal gland excision have been developed to mimic DED, that can be separated according to the number and the nature of the excised glands:

- Simultaneous excision of extra-orbital lacrimal gland and infra-orbital lacrimal gland;
- Unilateral or bilateral excision of the extra-orbital lacrimal gland only;
- Excision of extra-orbital lacrimal gland and harderian gland.

***Simultaneous excision of the extra-orbital and infra-orbital lachrimal glands***

Male C57BL/6J mice developed aqueous deficient dry eye following unilateral removal of extra-orbital and infra-orbital lacrimal glands: corneal fluorescein staining score increased 2 weeks post-surgery and remained elevated until 10 weeks post-surgery. Inflammation in the cornea, conjunctiva and meibomian glands was detected at 4 and 8 weeks post-surgery (Shinomiya et al., 2018).

***Unilateral or bilateral excision of the extra-orbital lacrimal gland only***

The bilateral extra-orbital lacrimal gland excision model was shown to result in a DED phenotype (evidencing via corneal staining) and activation of $T_H17$ cells superior to that elicited by the DES + scopolamine model (Stevenson et al., 2014). These $T_H17$ cells inhibit regulatory T cells responsible for self-antigen tolerance and are therefore thought to play an important role in the initiation of the immune response in DED. Regulatory T cells, when activated by an antigen, prevent the immune response against it. Interestingly, regulatory T cells in the bilateral extra-orbital lacrimal gland excision model were unable to restore antigen tolerance if activated more than 4 days post-surgery (Guzman et al., 2016).

The sex of the animal used in this model seems to impact the outcome of the experiment. In C57BL/6J mice, the ocular fluorescein score was found to be higher in females both in the case of unilateral or bilateral extra-orbital lacrimal gland excision (Mecum et al., 2019). The number of apoptotic and proliferating corneal cells tended to be higher in bilaterally operated females than in males (Mecum et al., 2019). Notably, the percentage of dendritic cells ($CD45^+$ $CD11b^+$) in unilaterally operated female mice was higher than in males of the same condition and comparable to the percentage in bilaterally operated animals of both sexes at one week post-surgery (Mecum et al., 2019).

In terms of DED symptoms, there were also differences between sexes. When extra-orbital lacrimal gland excision was unilateral, only females showed a decrease in palpebral opening ratio, a measure of eye discomfort, while the reduction happened in both sexes with bilateral gland surgery (Mecum et al., 2020). Surprisingly, the chemical sensitivity (capsaicin test) and the cold sensitivity (menthol test) were only significantly increased compared with the control in the unilaterally operated female mice but not in either sex operated bilaterally. Both sexes showed a decrease in exploratory behavior (open-field test) and an increase in anxiety-like behavior (open-arms test) when operated bilaterally. However, this was only true for females and not for males in the unilaterally operated animals (Mecum et al., 2020). All together it seems to indicate that female mice are predisposed to signs and symptoms of DED, similarly to that seen in epidemiological human studies.

***Excision of extra-orbital lacrimal gland and Harderian gland***

The surgical excision of extra-orbital lacrimal gland and Harderian gland in mice to induce severe DED has been recently developed in our laboratory. This mouse model is characterized by a persistent and severe reduction of tear production, a corneal inflammation and a reduction of intraepithelial corneal nerves at D21 post-surgery. Mice also develop mechanical corneal hypersensitivity accompanied by higher spontaneous activity of corneal nerves. Interestingly, the corneal inflammation, evidenced using neuro-inflammatory and neuronal/glial activation markers (such as c-Fos, ATF-3, NOS2, NOX4 and GFAP), spreads to the trigeminal ganglion (Fakih et al., 2019, Guerrero-Moreno et al. , 2021a).

### C. Usefulness of the double excision model to study the cellular and molecular changes related to severe DED (*Review 2 - Guerrero-Moreno et al. Neural Reg Res. 2021*)

The aforementioned unilateral extra-orbital lacrimal gland and harderian gland double excision model has allowed a detailed investigation of the cellular and molecular changes associated with persistent DED, reviewed in Guerrero-Moreno et al., 2021a, presented hereafter.

# How does chronic dry eye shape peripheral and central nociceptive systems?

**Adrian Guerrero-Moreno, Darine Fakih, Stéphane Melik Parsadaniantz, Annabelle Réaux-Le Goazigo***

Dry eye disease (DED) is a multifactorial disease characterized by a loss of homeostasis of the tear film and accompanied by ocular symptoms, in which tear film instability and hyperosmolarity, ocular surface inflammation and damage, and neurosensory abnormalities play etiological roles (Belmonte et al., 2017).

Interestingly, DED shares common characteristics with neuropathic pain, which is defined as pain caused by damage or disease affecting the somatosensory nervous system. Ocular pain, more commonly called corneal pain, has gained recognition due to its increasing prevalence, morbidity, and resulting social burden (Belmonte et al., 2017). To date, the management of chronic corneal pain still represents a therapeutic challenge. A better understanding of the molecular and cellular mechanisms participating in the transition from acute to chronic pain are crucial issues for developing the effective management and a therapeutic strategy to alleviate this debilitating condition. Today, much of the knowledge of neuroinflammation-neuropathic pain processing comes from data from the spinal cord, but a comparatively small number of investigations have been carried out in the corneal trigeminal pain pathway.

**Corneal nociceptive pathway: from the cornea to the brain:** The cornea is the most densely innervated tissue in the body, with 300–600 times the sensory innervation density of the skin (7000 nociceptors/mm$^2$). The sensory innervation of the cornea is provided by ciliary nerves, a subdivision of the nasociliary branch, which originates from the ophthalmic branch of the trigeminal ganglion (TG) (Belmonte et al., 2017). Sensory inputs from the cornea are conveyed to the ophthalmic branch of the TG by first-order neurons, which only represent 1% to 3% of the total population of trigeminal neurons (Launay et al., 2015). Then, the central axons of corneal sensory neurons make synapses in two discrete regions of the trigeminal brainstem sensory complex: the transition region between the subnucleus interpolaris (Vi) and caudalis (Vc) and the Vc/rostral spinal cord cord junction, which constitutes the first relay of somatosensory information.

**Corneal nerve damage, inflammation and peripheral sensitization after chronic dry eye:** Understanding the pathophysiology of corneal neuropathic pain observed in patients suffering from DED is essential for the development of new therapeutic strategies and implies the development of relevant preclinical models that best mimic the human disease. In that context, we recently developed a model of chronic dry eye in mice, consisting of the excision of the extraorbital lachrymal gland (responsible for the aqueous constituent of the tear film) and Harderian gland (which produces lipids of the tear film). Glands removal markedly reduced tear production over time and induced corneal nerve abnormalities in the superficial epithelium (Fakih et al., 2019). The reduced number of intra-epithelial corneal nerve endings in DED mice 3 weeks after the surgery was consistent with previous animal (Kovacs et al., 2016) and clinical studies (Labbe et al., 2012; Hamrah et al., 2017). In addition to corneal nerve abnormalities, a mechanical allodynia (decreased mechanical threshold) and inflammatory responses also developed at the cornea level.

Several lines of evidence support the idea that neuroimmune and neuronal–glial interactions play a major role in the chronification of pain at both spinal and trigeminal levels (Grace et al., 2014). Indeed, the activation of immune cells participates in the peripheral sensitization mechanism, which is characterized by a change in the excitability of nociceptors (decreased threshold); an increase in spontaneous stimuli evoked the firing rate of the sensory neurons, leading to spontaneous pain and hyperalgesia.

Considering that, we further evaluated changes in the spontaneous corneal nerve fiber activity of the ciliary nerve in our preclinical model of persistent dry eye. Electrophysiological recordings of the ciliary nerve fibers revealed a 100% increase of action potential frequency between sham and dry eye mice on day 21. These data confirm that corneal inflammation and nerve damage are able to modify the characteristics of trigeminal afferent neurons, resulting in their hyperexcitability and increased ongoing activity (Acosta et al., 2013; Kovacs et al., 2016; Fakih et al., 2019) (**Figure 1**). These results are of importance because they link corneal nerve abnormalities, the upregulation of the ongoing activity of the corneal nerve and persistent pain. Such morphological and functional alterations of the corneal nerve may indeed explain the painful state of patients suffering from chronic DED.

The total tear suppression observed following the excision of the extraorbital lachrymal gland and Harderian gland could be considered as a severe dry eye model. Other mild and moderate preclinical models through reducing tear volume have been developed. For example, controlled environment chamber model using exposure to low humidity and constant airflow, as well as its combination with lachrymal gland insufficiency generated by systemic application of scopolamine, are well established murine model of DED mimicking the human pathology.

**Corneal inflammation spreads to the TG:** Inflammatory responses and neuronal and glial activations have been reported in the ipsilateral TG (containing first-order neurons) in various models of corneal injury. For example, in an acute model of alkali burn or in mouse models of benzalkonium chloride-induced corneal neurotoxicity, corneal inflammation triggers trigeminal inflammation which is characterized by an increase of Iba1 positive (monocytes/macrophages) cells and an increase in the gene expression of proinflammatory cytokines tumor necrosis factor α and interleukin (IL)-6, substance P and its receptor NK1 (Ferrari et al., 2014; Launay et al., 2016). We also observed that the mRNA levels of neuronal activation (Fos proto-oncogene), neuronal injury (activating transcription factor 3), astrocyte (glial fibrillary acidic protein), and oxidative (inducible nitric oxide synthetase type 2 and NOX4) markers increased significantly three weeks after gland excisions in the ipsilateral TG (Fakih et al., 2019). In addition to the upregulation of the gene expression of proinflammatory mediators, persistent dry eye pain induces an upregulation of Iba1 (monocyte/macrophages), GFAP (satellite glial cells), and ATF3 (neuronal injury marker) immunoreactivity in the ipsilateral TG, revealing glial and neuronal dysregulation (**Figure 1**). These cumulative molecular and cellular changes also provide a much better understanding of interactions of the neuronal, glial and immune systems in the context of persistent corneal pain. In addition, there is increasing evidence that unilateral nerve injury may evoke contralateral responses and such phenomenon also occurs at the level of the eye-TG axis. In fact, clinical and preclinical studies have shown that unilateral corneal injury triggers inflammatory responses in the contralateral eye and TG (Ferrari et al., 2014; Launay et al., 2015). The release of proinflammatory mediators, such as IL-1β, tumor necrosis factor α and substance P, has been proposed to mediate these bilateral effects, although further study is required to decipher underlying mechanisms.

**Chronic corneal pain triggers neuroinflammatory responses and presynaptic changes in the central nervous system:** Proinflammatory mediators are known to play an important role not only in peripheral sensitization but also in the transfer of nociceptive information from the periphery to the central nervous system (Melik Parsadaniantz et al., 2015). Indeed, it has been well described that persistent peripheral inflammation as well as peripheral nerve damage may generate extensive changes in pain processing in the central nervous system by triggering maladaptive neuroplasticity (neuroplastic changes and hyperexcitability of central nociceptive neurons). Maladaptive neuroplasticity in a chronic pain condition is referred to as central sensitization. Indeed, non-neuronal cells—i.e., glial cells in the central nervous system, namely astrocytes and microglia—become aberrantly activated in response to sustained activation under peripheral nerve injury (Grace et al., 2014). Moreover, synaptic efficacy also plays a key role in central sensitization in response to activity, inflammation, and neural injury. Although the cellular and molecular mechanisms that occur in the central nervous system in the context of pain have been elegantly described and investigated in the spinal cord, research into corneal pain has remained very patchy for a long time. Thus, our recent research works aim to decipher the neurobiological mechanisms of chronic ocular pain.

Activated microglial cells, which are known to release proinflammatory cytokines,

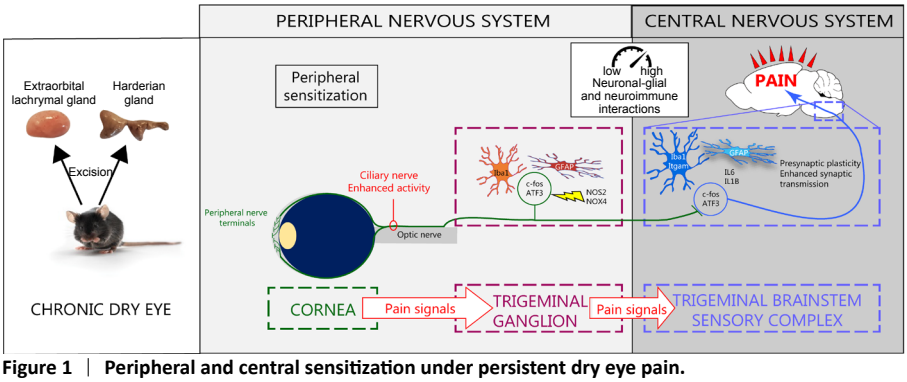


**Figure 1** | **Peripheral and central sensitization under persistent dry eye pain.**
After the removal of the Harderian gland and extraorbital gland in adult mice, nerve abnormalities, inflammation and sensitization of the corneal nerves developed. These mechanisms trigger the activation of primary sensory neurons, immune and glial cells in the ipsilateral trigeminal ganglion. This peripheral neuroinflammation spreads to the trigeminal brainstem sensory complex, leading to persistent ocular pain. ATF3: Activating transcription factor 3; c-fos: Fos proto-oncogene; IL: interleukin; NOS: nitric oxide synthase.

neurotrophic factors and chemokines, contribute to neuronal excitability and central sensitization mechanism during chronic pain states (Melik Parsadaniantz et al., 2015). We found higher Iba1-immunopositive cells and CD68 and Itgam mRNA levels in the trigeminal brainstem complex, confirming the activation of microglial cells in acute (7 days) and persistent (21 days) ocular pain (Launay et al., 2016; Fakih et al., 2019). Aside from immune cell activation, astrocyte activation (astrogliosis) was also confirmed by a robust astrocyte reaction (higher levels of GFAP immunoreactivity) and the upregulation of GFAP mRNA expression in the ipsilateral trigeminal brainstem sensory complex. Proinflammatory responses also occurred in this brain structure three weeks after gland excisions; proinflammatory cytokines (IL-6 and IL-1β), oxidative stress enzyme (iNOS2) and neuronal (ATF3 and FOS) markers were increased, confirming a dysregulation in glial cells activation in the central nervous system (Fakih et al., 2019; **Figure 1**). Overall, this study highlights neuronal–glial and neuroinflammatory interactions which may account for the development and persistence of the ocular pain reported in DED patients.

Accumulating evidence has also suggested that chronic changes of activity in primary afferent neurons induce synaptic rearrangements in the central nervous system and lead to the functional remodeling of presynaptic sites. With regard to the synaptic mechanisms of chronic inflammatory and neuropathic pain, it has been proposed that changes in presynaptic function play an essential role; however, until now, nothing has been known about the possible presynaptic changes during a persistent ocular pain state. Piccolo, one of the components of the presynaptic zone, plays a key role in synaptic plasticity by facilitating/managing the secretion of synaptic vesicles. A significant finding in our study was the increased levels of Piccolo immunoreactivity in the trigeminal brainstem sensory complex induced by chronic dry eye pain. The upregulated expression of Piccolo demonstrates that a persistent corneal nociceptive activity triggers neuronal plasticity in the central nervous system, which may participate in the enhancement in the excitability of pain circuits.

Such cellular rearrangement (enhancement of excitatory synaptic transmission in the trigeminal brainstem complex) is in line with a previous study from Rahman et al. (2015), reporting that persistent (2-week) tear deficiency in rats caused the sensitization of ocular-responsive neurons at multiple regions of the caudal trigeminal brainstem.

In summary, the cellular modifications we reported in the context of chronic corneal pain include changes in proinflammatory gene expression, changes in cell morphology (cell activation), and a reorganization of neural nociceptive networks in the central nervous system. Many experiments are still required to further characterize the precise nature of this central neuronal plasticity linked to pain.

To conclude, a better understanding of the sequence and nature of the events that drive these neurobiological mechanisms will offer significant promise for the discovery of new approaches and targets for the management of chronic ocular pain. We predict that this will be an exciting area of new investigations. Further fundamental and clinical studies using functional and morphological magnetic resonance imaging studies may help to depict how chronic corneal pain can shape the brain and identify the morphological changes that may occur during persistent corneal pain. An elegant *in vivo* magnetic resonance imaging study has already reported macrophage infiltration in the TG after corneal alkali burn in mice (Ferrari et al., 2014). Although our knowledge of the mechanisms involved in corneal pain has progressed over the last decade, our efforts must be continued for the identification and validation of new therapeutic targets, which are currently sorely lacking.

*We apologize to all colleagues and contributors to this field who were not included or cited due to space limitations.*

*This work was completed with the support of the Programme Investissements d'Avenir IHU FOReSIGHT (ANR-18-IAHU-01).*

**Adrian Guerrero-Moreno, Darine Fakih, Stéphane Melik Parsadaniantz, Annabelle Réaux-Le Goazigo***
Sorbonne Université, INSERM, CNRS, Institut de la Vision, Paris, France
***Correspondence to:** Annabelle Réaux-Le Goazigo, PhD, annabelle.reaux@inserm.fr.
https://orcid.org/0000-0003-3855-9523
(Annabelle Réaux-Le Goazigo)

**Received:** March 9, 2020
**Peer review started:** March 11, 2020
**Accepted:** April 26, 2020
**Published online:** August 24, 2020

**https://doi.org/10.4103/1673-5374.290895**
**How to cite this article:** *Guerrero-Moreno A, Fakih D, Parsadaniantz SM, Réaux-Le Goazigo A (2020) How does chronic dry eye shape peripheral and central nociceptive systems? Neural Regen Res 16(2):306-307.*


## References

Acosta MC, Luna C, Quirce S, Belmonte C, Gallar J (2013) Changes in sensory activity of ocular surface sensory nerves during allergic keratoconjunctivitis. Pain 154:2353-2362.
Belmonte C, Nichols JJ, Cox SM, Brock JA, Begley CG, Bereiter DA, Dartt DA, Galor A, Hamrah P, Ivanusic JJ, Jacobs DS, McNamara NA, Rosenblatt MI, Stapleton F, Wolffsohn JS (2017) TFOS DEWS II pain and sensation report. Ocul Surf 15:404-437.
Fakih D, Zhao Z, Nicolle P, Reboussin E, Joubert F, Luzu J, Labbe A, Rostene W, Baudouin C, Melik Parsadaniantz S, Reaux-Le Goazigo A (2019) Chronic dry eye induced corneal hypersensitivity, neuroinflammatory responses, and synaptic plasticity in the mouse trigeminal brainstem. J Neuroinflammation 16:268.
Ferrari G, Bignami F, Giacomini C, Capitolo E, Comi G, Chaabane L, Rama P (2014) Ocular surface injury induces inflammation in the brain: in vivo and ex vivo evidence of a corneal-trigeminal axis. Invest Ophthalmol Vis Sci 55:6289-6300.
Grace PM, Hutchinson MR, Maier SF, Watkins LR (2014) Pathological pain and the neuroimmune interface. Nat Rev Immunol 14:217-231.
Hamrah P, Qazi Y, Shahatit B, Dastjerdi MH, Pavan-Langston D, Jacobs DS, Rosenthal P (2017) Corneal nerve and epithelial cell alterations in corneal allodynia: an in vivo confocal microscopy case series. Ocul Surf 15:139-151.
Kovacs I, Luna C, Quirce S, Mizerska K, Callejo G, Riestra A, Fernandez-Sanchez L, Meseguer VM, Cuenca N, Merayo-Lloves J, Acosta MC, Gasull X, Belmonte C, Gallar J (2016) Abnormal activity of corneal cold thermoreceptors underlies the unpleasant sensations in dry eye disease. Pain 157:399-417.
Labbe A, Alalwani H, Van Went C, Brasnu E, Georgescu D, Baudouin C (2012) The relationship between subbasal nerve morphology and corneal sensation in ocular surface disease. Invest Ophthalmol Vis Sci 53:4926-4931.
Launay PS, Godefroy D, Khabou H, Rostene W, Sahel JA, Baudouin C, Melik-Parsadaniantz S, Reaux-Le Goazigo A (2015) Combined 3DISCO clearing method, retrograde tracer and ultramicroscopy to map corneal neurons in a whole adult mouse trigeminal ganglion. Exp Eye Res 139:136-143.
Launay PS, Reboussin E, Liang H, Kessal K, Godefroy D, Rostene W, Sahel JA, Baudouin C, Melik Parsadaniantz S, Reaux Le Goazigo A (2016) Ocular inflammation induces trigeminal pain, peripheral and central neuroinflammatory mechanisms. Neurobiol Dis 88:16-28.
Melik Parsadaniantz S, Rivat C, Rostene W, Reaux-Le Goazigo A (2015) Opioid and chemokine receptor crosstalk: a promising target for pain therapy? Nat Rev Neurosci 16:69-78.
Rahman M, Okamoto K, Thompson R, Katagiri A, Bereiter DA (2015) Sensitization of trigeminal brainstem pathways in a model for tear deficient dry eye. Pain 156:942-950.

*C-Editors: Zhao M, Li JY; T-Editor: Jia Y*

## VI. Towards novel therapeutic strategies for chronic ocular pain: *could topical opioids be the key?*

As previously discussed, dry eye disease can be of complex management, especially in cases of associated neuropathic corneal pain. Some patients will require systemic treatments of variable efficacy and often accompanied by bothersome untoward effects that can significantly alter their quality of life. New more effective and better tolerated treatments are thus needed. Considering the easy access to the cornea and the corneal nerves, topical administration of analgesic compounds could be a promising strategy.

In this context, our team has previously demonstrated that inhibition of endogenous enkephalinases at the level of the ocular surface using topical administrations of PL265, a dual enkephalinase inhibitor, could provide significant ocular pain relief by increasing the concentration of local endogenous opioids (Reaux-Le Goazigo et al., 2019).

Therefore, targeting the opioid system at the level of the cornea using topical compounds could provide a new avenue towards innovative ocular pain management.

### VI.1 Pain and the opioid system

Heroin, morphine, and other opiates trace their origins to a single plant—the opium poppy. Cultivation of this plant dates back to the earliest periods of human civilization, and opium use was common in ancient Mesopotamia. Opium derivatives, including morphine, became widely used analgesics, particularly since the 1800s.

The term opioid refers to all compounds that bind to opiate receptors. Conventionally, the term opiate can be used to describe those opioids that are alkaloids derived from the opium poppy (morphine and codeine). Opioids include semi-synthetic opiates, *i.e.* drugs that are synthesized from naturally occurring opiates (such as heroin from morphine and oxycodone from thebaine), as well as synthetic opioids such as methadone, fentanyl, and propoxyphene.

There have been many advances in the use of opioids for moderate-to-severe pain control in recent years. The position of morphine as the gold standard became gradually more questioned, mostly because of serious adverse effects and the availability of novel -more potent- opioids and new formulations of existing opioids.

### A. Endogenous opioids

Endogenous opioid peptides, naturally produced in the body, include enkephalins, dynorphins, and endorphins. These peptides have in common the C-terminal amino acid sequence Tyr-Gly-Gly-Phe-Met/Leu, known as the opioid motif **(Table 6)** (Stein., 2018). A fourth family of opioid ligands with pro-nociceptive functions was recently discovered and named nociceptin/orphanin FQ (Donica et al., 2013). It does not contain the opioid motif **(Table 6)** but shares other characteristics with the other three families **(Fig. 17)**.

Another common feature of opioid peptides is that they are not translated into their active form but are produced as precursors that are enzymatically modified into their active form, thus allowing modulation of their activity. Briefly, the cleavage of proopiomelanocortin (POMC) gives rise to various molecules including β-endorphins, preproenkephalin (pre-PENK) gives rise to Met- or Leu-enkephalin, prodynorphin (pro-dyn) gives rise to various forms of dynorphins and processing of pre-pronociceptin produces nociceptin (Donica et al., 2013; Corder et al. , 2018a; Stein, 2018a).

Endogenous opioids have selectivity for some types over others **(Table 6)**. Thus, β-endorphins show a preference for MOR, enkephalins for MOR and DOR, dynorphins for KOR and nociceptin for nociceptin receptor (Ozawa et al., 2015). Interestingly, the action of opioids does not depend on the type of ligand, but on the activated receptor and the cells where it is expressed (**Fig 18**).

**Table 6: Endogenous opioid peptides**

| Family | Precursor | Opioid peptide | Amino acid sequence | Opioid receptor target(s) |
|---|---|---|---|---|
| **Enkephalins** | Pre-PENK | Leu-enkephalin | **YGGFL** | DOR, MOR |
| | | Met-enkephalin | **YGGFM** | DOR, MOR |
| | | Metorphamide | **YGGFM**RRV-$NH_2$ | DOR, MOR |
| **Endorphins** | POMC | α-Endorphin | **YGGFM**TSEKSQTPLVT | MOR |
| | | β-Endorphin | **YGGFM**TSEKSQTPLVTL FKNAIIKNAYKKGE | MOR, DOR |
| | | γ-Endorphin | **YGGFM**TSEKSQTPLVTL | MOR |
| **Dynorphins** | Pro-Dyn | Dynorphin A | **YGGFL**RRIRPKLKWDNQ | KOR |
| | | Dynorphin $A_{1-8}$ | **YGGFL**RRI | KOR, MOR (partial agonist of DOR) |
| | | Dynorphin B | **YGGFL**RRQFKVVT | KOR |
| **Nociceptin** | Pre -pronociceptin | Nociceptin | FGGFTGARKSARKLANQ | NOR |

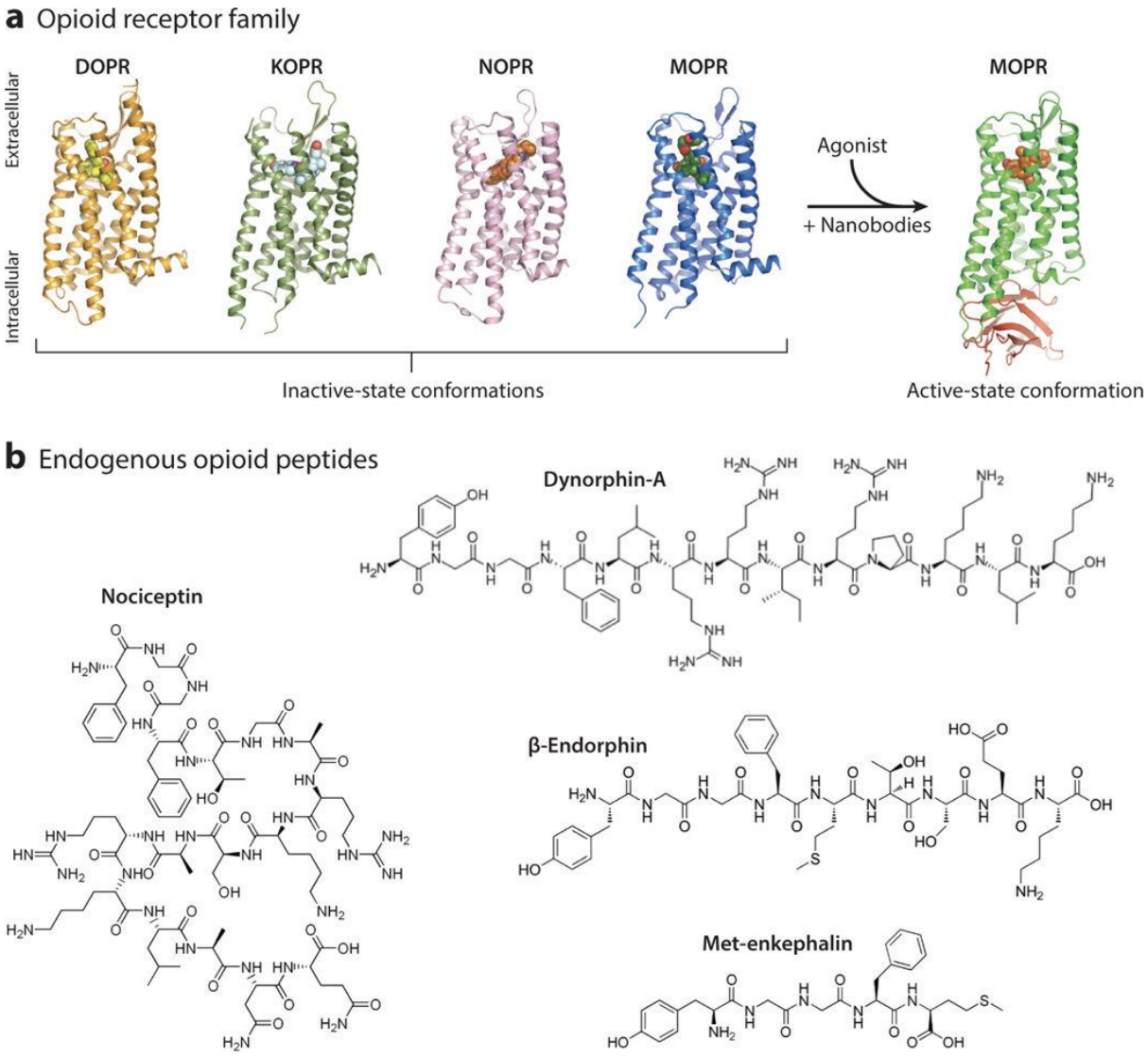


**Figure 17: The endogenous opioid system**
**(a)** Crystal structures of the inactive state of all four opioid receptors (DOPR, KOPR, NOPR, and MOPR). When an opioid agonist enters the binding pocket of its cognate receptor, a conformational change in the transmembrane domains allows for intracellular effector molecules to bind and activate signaling cascades that modulate neural function. The addition of stabilizing nanobodies to the crystal preparation has elucidated the active state of MOPR.
**(b)** Chemical structures of the four main classes of opioid peptides: met-enkephalin, dynorphin-A, nociceptin, and β-endorphin. Abbreviations: DOPR, delta opioid receptor; KOPR, kappa opioid receptor; MOPR, mu opioid receptor; NOPR, nociceptin opioid receptor. *From Corder et al. , 2018b.*

### B. Exogenous opioids

Opioid receptors, in addition of being activated by endogenously produced opioid peptides, can be targeted by exogenous opioids **(Fig. 18)**. The best known is morphine, a MOR agonist, the gold standard for pain treatment and opioid-based therapy itself. Since the emergence of morphine, many others opioids have been developed, mostly targeting MOR. For example,

**oxycodone** (14-hydroxy-7,8-dihydrocodeinone) is a semi-synthetic derivative of thebaine that binds to MOR and KOR, exhibiting a comparable analgesic efficacy to that of morphine. **Methadone**, a synthetic opioid, is very potent as it develops additional effects as an N-methyl-D-aspartate (NMDA) receptor antagonist and serotonin reuptake inhibitor. **Fentanyl** is a MOR agonist initially developed specifically for anesthetic use, because of its high potency and rapid onset of action (McMahon, 2013).

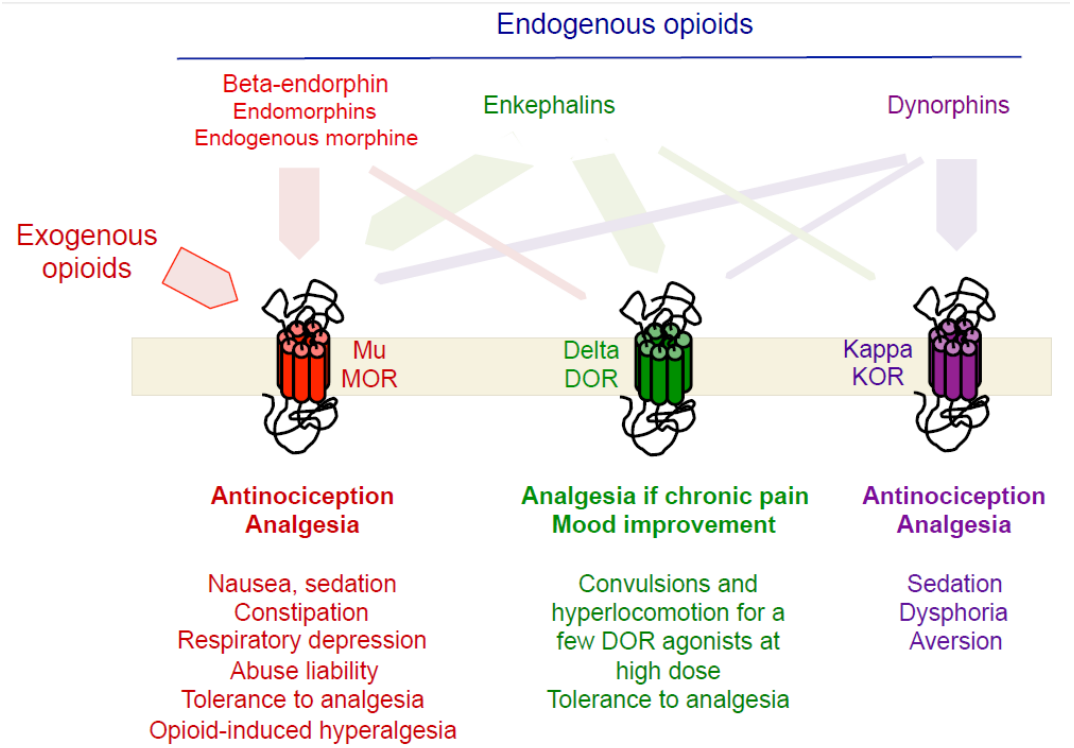


**Figure 18: Opioid receptor activation by exogenous and endogenous opioids**
Opioid ligands activate with various selectivity MOR, DOR and KOR. Endomorphins have more affinity for MOR, while enkephalins show selectivity for MOR and DOR and dynorphins for KOR. Once activated, they trigger beneficial (bold) or adverse effects (pale). *From Stein and Gaveriaux-Ruff 2020.*

In addition to these drugs, a large number of MOR-, DOR- and KOR-specific synthetic agonists and antagonists have been developed and used in preclinical and clinical studies for the treatment of pain and other diseases. For review see (Stein, 2018b)

**DAMGO** ([D-Ala2, N-Me-Phe4, Gly5-ol]-enkephalin) is a selective and specific MOR agonist. DAMGO, unlike morphine, was shown to induce MOR internalization, limiting its ability to induce tolerance (Arden et al. , 1995; Keith et al. , 1996). Peripheral application of DAMGO was shown to decrease pain in models of neuropathic pain secondary to sciatic nerve ligation,

unlike systemic administration of similar concentrations of MOR agonists (Truong et al., 2003; Obara et al. , 2004).

**SNC-80** is a highly potent and selective synthetic DOR agonist (Varga, 2003). SNC-80 was shown to promote analgesia and anxiolytic effects in several models of pain; however some studies reported analgesic tolerance following repeated administrations (Chu Sin Chung and Kieffer, 2013).

**Naloxone methiodide**, is a nonselective synthetic receptor antagonist which does not cross the blood–brain barrier (Lewanowitsch and Irvine, 2002). In research, Naloxone methiodide is commonly used to decipher the effects of exogenous (Kremer et al., 2020) or endogenous (Baddack-Werncke et al., 2017) opioid peptides in various preclinical models of pain.

### C. Opioid receptors

The opioid receptors belong to the superfamily of the seven-transmembrane G protein-coupled receptors (GPCRs). Opioid receptors consist of the classical μ-, δ-, and κ-opioid receptors (MOR, DOR, KOR) and a fourth member, the nociceptin/orphanin FQ receptor (NOP). Each receptor is encoded by a unique gene (*Oprm1, Oprd1, Oprk1 and Oprl1 respectively*) sharing upward of 60% of its amino-acid composition (Stein, 2018). The NOP receptor shares high structural homology with the other opioid receptors but do not bind opioids. On the other hand, its ligand, nociceptin/orphanin FQ, shows no affinity for the classical μ-, δ-, and κ-opioid receptors.

Delineating the crystal structures of opioid receptors (**Fig. 17**) has been pivotal for understanding receptor function and providing new avenues for drug design. When opioid receptors are activated by systemically-administered exogenous agonists, they give rise to different effects, both therapeutic and untoward, depending on the receptor activated:

- Activation of MOR triggers analgesia as therapeutic effect but also sedation, dependence, respiratory distress, euphoria and opioid-induced hyperalgesia.
- Activation of DOR mediates analgesia, antidepressant and anti-convulsant effects but also tolerance and dependence.
- Induction of KOR is involved in analgesia but unfortunately also depression, sedation, stress but also dissociative and hallucinogenic effects.

**Opioid receptor signaling**

As described before, the endogenous opioid peptides exhibit different affinity and selectivity for the various opioid receptor subtypes **(Table 6)**. Agonist binding and subsequent receptor activation initiate a cascade of events that result in a varied array of biological effects. Both classical opioid receptors (MOR/ DOR/ KOR) and the non-classical NOP opioid receptor couple to inhibitory G-proteins. These include suppression of adenylate cyclase activity by Gα subunits, thereby reducing cyclic AMP production, and inhibition of voltage-gated calcium channels (VGCC) as well as activation of G protein-gated inwardly rectifying potassium (GIRK) channels by Gβγ subunits thus promoting neuronal hyper-polarization **(Fig. 19)**. Overall, this results in reduced neuronal cell excitability leading to a reduction in transmission of nerve impulses along with the inhibition of neurotransmitter release. Additionally, they can act by inhibiting $Na^+$, $I_h$ currents or TRPV1 directly, totally blocking the nociceptive message in primary sensory neurons.

A growing number of studies have found that opioid receptors can form heterodimers composed of different opioid receptors, which offers the potential to develop bivalent ligands with unique pharmacological properties (Hommes, 1966; Drieu la Rochelle et al., 2018; Zhang et al., 2020a). Moreover, heterologous desensitization between opioids and chemokine receptors has been reported in rodents (Benard et al. , 2008; Melik Parsadaniantz et al., 2015). Finally, biased opioid receptor ligands have been discovered, that stabilize receptor conformations preferentially activating either the underlying G protein or β-arrestin pathway, thus opening a new promising field of research aimed at designing drugs with better potency and fewer side effects (depending on the predominance of G protein or β-arrestin bias).

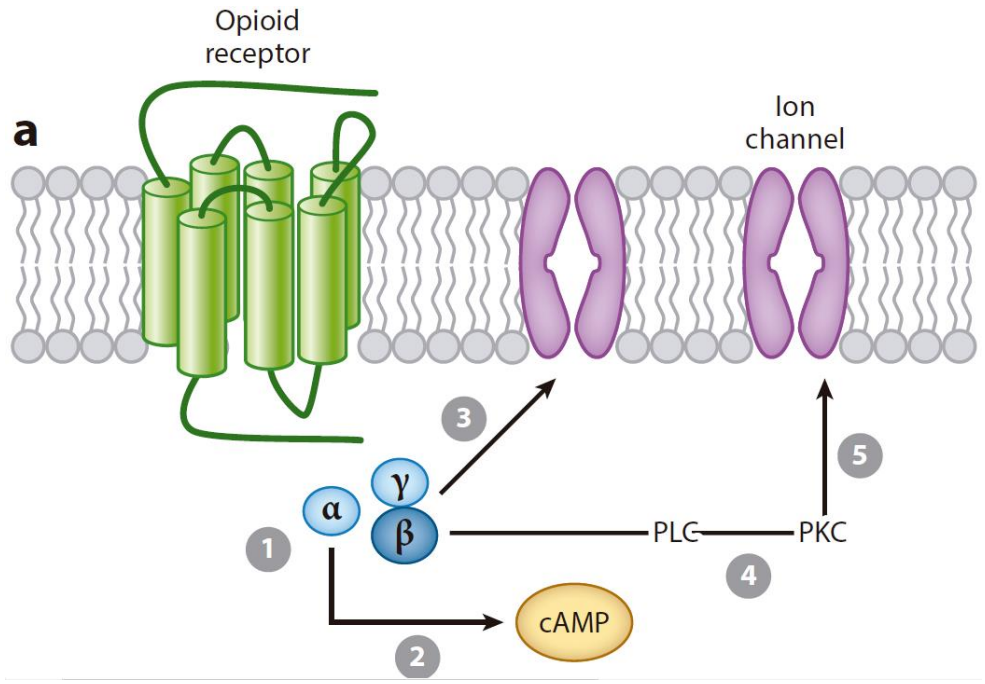


**Figure 19: Opioid receptor signaling and recycling**

Opioid receptors are bound by their ligands inducing the coupling and activation of G-proteins. The effects of receptor activation are mediated by G-proteins (1) via different signaling processes: (2) inhibition of adenylyl cyclase reducing cyclic adenosine monophosphate (cAMP) production; (3) direct inhibition of voltage-gated $Ca^{2+}$ channels or activation of rectifying $K^{+}$ channels; (4-5) indirect inhibition of ion channels through phosphokinase C (PLC) and protein kinase C (PKC) activation. (Stein, 2016)

### Distribution of opioid receptors

The different opioid receptors are widely distributed throughout the peripheral and central nervous systems that explains the large pharmacological responses observed following administration of opioid agonists. Opioid receptors are specifically expressed in all nociception-related sites, including primary sensory neurons, specific neuronal populations in the CNS as well as immune and glial cells as described below.

#### ***Neuronal expression of opioid receptors***

There is evidence that MOR, DOR, KOR and NOR are expressed in primary sensory neurons in the TG (MOR: Bai et al. , 2020; MOR,DOR: Buzas and Cox, 1997; KOR: Schafer et al., 1994; NOP: Hou et al., 2003) and dorsal root ganglion (MOR, DOR: Buzas and Cox, 1997; KOR: Schafer et al., 1994; NOP: (Ozawa et al., 2015). Activation of opioid receptors by exogenous or endogenous opioids on these primary sensory neurons, both at the nerve terminal and

soma level, inhibits the nociceptive pathway (**Fig. 20**) (Stein, 2013; Melik Parsadaniantz et al., 2015; Stein, 2018b; Machelska and Celik, 2020).

Opioid receptors have also been detected in second-order sensory neurons. The activation of these receptors, via endogenous opioid production by inter-neurons or microglia, is the second point at which opioids mediate analgesia (**Fig. 20**) (Corder et al., 2018). A well-known mechanism of opioids for the modulation of the nociceptive message at the CNS level is the so-called "descending modulatory system". This system is formed by neurons in the periaqueductal grey matter (PAG) and the rostral ventromedial medulla (RVM) both sensitive to opioids. The PAG sends efferences to the RVM, a cerebral structure rich in pre-PENK. After the appropriate cleavage and transport of pre-PENK to RVM terminals, enkephalins are released at the dorsal horn level, modulating the nociceptive message (**Fig. 20**).

Finally, the opioid system plays a key role in higher brain structures such as the anterior cingulate cortex (ACC), nucleus accumbens (NAc), ventral tegmental area (VTA) and basolateral amygdala. These structures, integrated in the limbic system, are responsible for the affective aspects of the painful experience. The activation of these structures is probably related to the addictive character of exogenous opioids, which will be explained later on.

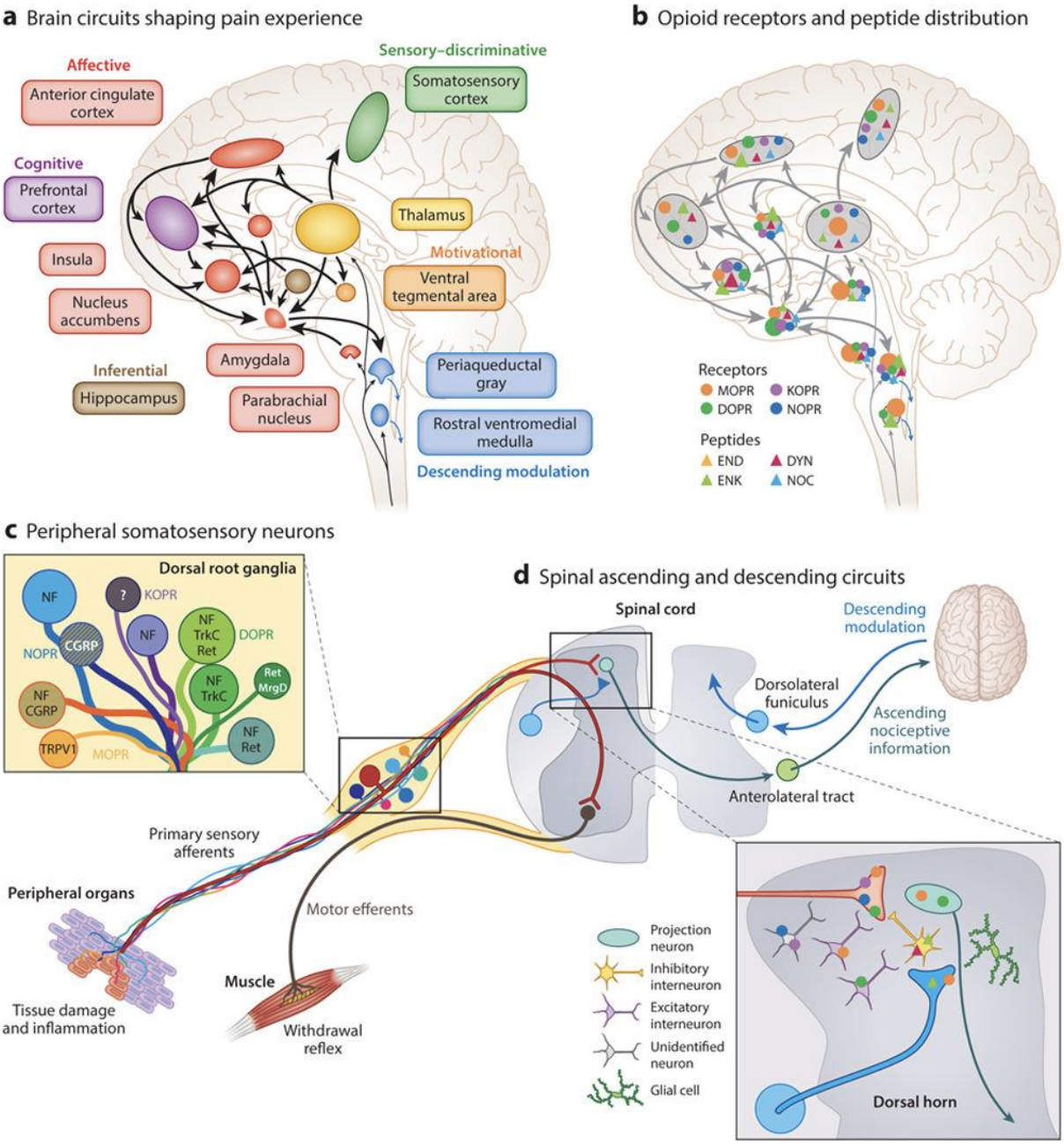


**Figure 20: Neuroanatomical substrates of pain perception and remodeling by opioids**

**(a)** A large interconnected neural network of supraspinal brain circuits transforms nociceptive information ascending from the spinal cord into an aversive, painful experience.

**(b)** The opioid system is well positioned within this brain network to modify the perception of pain. The different opioid receptors and peptides are distinctively, though broadly, expressed in different sites, the function of which is under intense investigation. Relative opioid receptor (circles) and peptide (triangles) expression levels are denoted by the size of the shapes.

**(c,d)** Opioid receptor types and peptides are also distributed in distinct subpopulations of (c) DRG neurons, identified with the indicated markers such as TRPV1, and (d) second-order spinal cord dorsal horn neurons. NF marks large-diameter DRG neurons with myelinated axons. Striped neurons co-express different opioid receptor types. Abbreviations: CGRP, calcitonin gene-related peptide; DRG, dorsal root ganglion; DOPR, delta opioid receptor; DYN, dynorphin; END, p-endorphin; ENK, enkephalin; KOPR, kappa opioid receptor; MOPR, mu opioid receptor; MrgD, Mas-related G protein-coupled receptor member D; NF, neurofilament; NOC, 99ociception/orphanin FQ; NOPR, 99ociception

opioid receptor; Ret, Ret proto-oncogene; TrkC, tropomyosin receptor kinase C; TRPV1, transient receptor potential cation channel subfamily V member 1. *Extracted from Corder et al., 2018*

Furthermore, the generation of transgenic mice expressing MOR mCherry and DOR eGFP allows the generation of a detailed map of MOR and DOR co-expression in the whole mouse brain. This work showed that Sp5i (Spinal trigeminal subnucleus interpolaris) contained second-order nociceptive neurons co-expressing both receptors (Erbs et al., 2015). Other brain areas related to pain such as the RVM, lateral parabrachial nucleus and spinal cord also showed MOR/DOR co-expression. Interestingly, the PAG showed no co-expression of MOR/DOR. Cerebral cortex was also devoid of MOR/DOR co-expression except in the piriform cortex, a structure mediating odor processing (Erbs et al., 2015). The same study provides an online atlas of MOR and DOR expression in the whole mouse brain (**Fig. 21,** http://mordor.ics-mci.fr/).

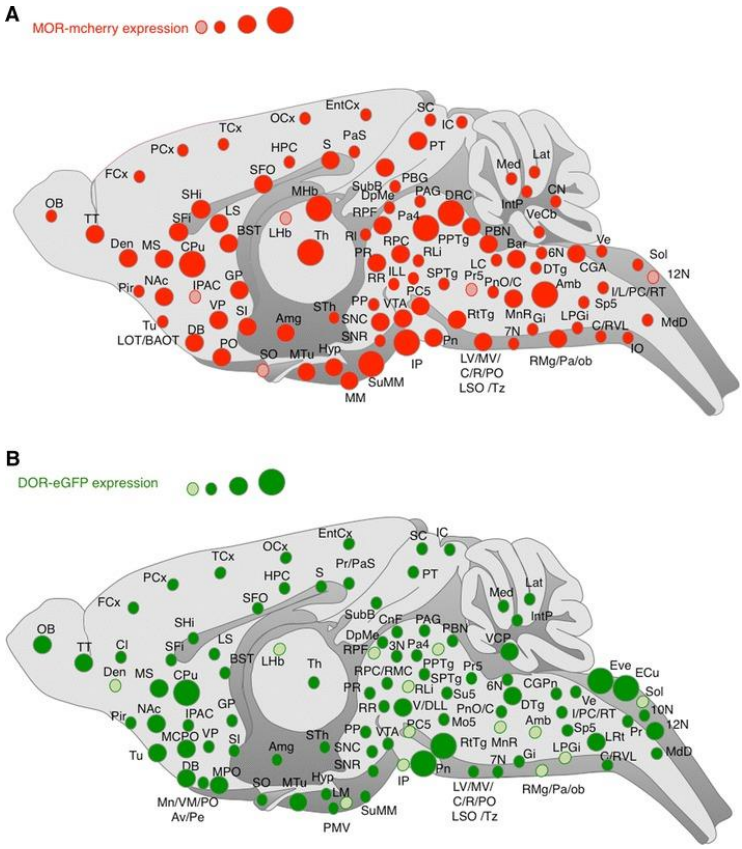


**Figure 21: Distribution of μ and δ opioid receptors in the nervous system**

**a.** Brain distribution of the MOR-mCherry construct. The size of the red circle is indicative of the abundance of the receptor in then given area. A pink circle indicates low expression level. **b.** Brain distribution of the DOR-eGFP construct. The size of the green circle is indicative of the abundance of

the receptor in the given area. A pale green circle indicates low expression level. *Extracted from Erbs et al., 2015*.

***Opioid Receptors in peripheral immune cells and Glial Cells***

A recent review (Eisenstein, 2019) analyzed the expression and role of opioid receptors in peripheral immune cells and glia in the modulation of pain. All four opioid receptors have been identified at the mRNA and protein levels in immune cells (lymphocytes, granulocytes, monocytes, macrophages) in humans, rhesus monkeys, rats and mice. In that line, opioid treatment was reported to suppress Natural Killer cell activity, responses of T and B cells to mitogens, antibody formation and phagocytic activity of neutrophils and macrophages but also cytokine and chemokine production by macrophages, microglia, and astrocytes (Eisenstein, 2019). Another study (Celik et al., 2016) reported that activation of leukocyte MOR, DOR, and KOR receptors could attenuate pain following nerve injury in mice.

MOR mRNA or protein were not detected in spinal cord microglia of naïve transgenic mice with fluorescently-labeled microglia (CX3CR1-eGFP) or with fluorescently-tagged MOR receptors (MOR-mCherry) (Corder et al., 2017). In contrast, analysis of multiple datasets of brain RNA expression revealed that Oprm1 (MOR coding gene) is expressed in specific microglial populations both in mice and human tissues (Maduna et al., 2018). In the same study, a double mutant mouse expressing reporter genes GFP in microglial cells and mCherry in MOR-expressing cells, allowed the detection of MOR expression in microglial cells from frontal cortex, NA, central amygdala, VTA and PAG (Maduna et al., 2018). Interestingly, the population of VTA microglial cells expressing MOR-mCherry was higher in males (50 ± 14%) than in females (35 ± 4%, $p<0.05$) (Maduna et al., 2018). The microglial MOR in those cells was localized in cis and trans-Golgi organelles, suggesting local production (Maduna et al., 2018). Although still subject to debate, MOR might be expressed in microglia and astrocytes, but more well-controlled studies are needed to verify the presence of DOR, KOR, and NOR receptors in native glia. Such discrepancy has been reviewed in (Machelska and Celik, 2020). As previously indicated, glial cells, especially microglia, have an important role in pain modulation at the central level (Ji et al. , 2013, Ji et al. , 2016). Bidirectional communication between CNS neurons and glial cells has been demonstrated by means of cytokines such as CCL2 and CX3CL1 and other inflammatory mediators such as ATP, DAMPs, TNF, IL-1β or IFN-γ (Grace et al., 2014). This communication occurs in both homeostatic and pathological conditions and could contribute both to exacerbation and reduction of pain (Grace et al.,

2014). In this context, recent studies point to an important role for the opioid system (Machelska and Celik, 2020).

However, starting in the last decade, an unexpected hypothesis has emerged, namely, that morphine activates glia, and that glial activation via the release of pro-inflammatory cytokines mediates morphine tolerance (Watkins et al. , 2005; Eisenstein, 2019). This fact could also suggest that these cells may mediate the addiction process or be involved in withdrawal symptoms. This may be true for high-dose opioid cases or for chronic applications, but less so for acute treatments with appropriate dosing. These studies identified activation of innate immunity receptor TLR4, as a mechanism for inflammatory activation of microglia rather than classical activation. However attempts to replicate this finding have failed as reported in (Eisenstein, 2019).

### D. Latent pain sensitization

Chronic pain in patients is often characterized by painful episodes that alternate with bouts of remission rather than constant pain sensation. These episodes can occur after the recovery from the primary insult. One hypothesis to explain this phenomenon is the **latent pain sensitization** that can be recapitulated in rodents. This chronic pain hypothesis/model is based in the counterbalance of two biological system: the antinociceptive and the pronociceptive systems and consists of the following steps:

1. An initial equilibrium (homeostasis) between the systems is disturbed by an episode increasing the nociceptive processes by means of nociceptor sensitization. Typical examples of those stimulus are chronic opioid application, inflammation or neuropathic damage.
2. After the initial insult, hyperalgesia/allodynia ceases but sensitization of the pronociceptive system is still present. In this new equilibrium, the antinociceptive system has increased its activity to compensate for the pronociceptive system, giving rise to a new equilibrium that is truly known as "latent sensitization".
3. This new balance may mask this latent sensitization, but any new stimulus that decreases the activity of the antinociceptive system will give rise to a new episode of hyperalgesia/allodynia, in the absence of the initial damage that caused the sensitization.

Latent sensitization has been demonstrated in different preclinical models of pain. In this context, the best studied element of the antinociceptive system is MOR. An abnormal constitutive activation of this receptor has been detected after the initial insult. Application

of an inverse agonist, able to silence constitutive activity of MOR, triggers the episode of hyperalgesia/allodynia (step 3). Pro-dynorphin, pro-enkephalin and pro-opiomelanocortin KO mice showed “normal” latent pain sensitization, highlighting that is a process mediated by constitutive activation of MOR.

Preclinical studies related to latent pain sensitization have been focusing mostly on central phenomena (central sensitization), but this process can also occur in the peripheral nervous system. Indeed, a recent publication explored this process in a model of ocular neuropathic pain induced by an acute alkali burn (NaOH 0.75M) (Cho et al., 2019). In this model, hyperalgesia to topical administration of an hyperosmolar solution (NaCl 2M) subsided 42 days after the burn (D42). A quantitative study of corneal innervation showed a decrease in nerve density in all layers (epithelial, sub-basal and stromal) at D2. Nerve density returned to baseline values at D42 at epithelial and stromal level, but remained decreased in the sub-basal plexus, while quantification of mean fiber length showed longer nerves at epithelial level and shorter at the sub-basal level. Interestingly, structures designated as neuromas were found at central epithelial level at D42. Altogether, those morphological data suggest a “new state” of nociceptive corneal innervation that could correspond to the latent peripheral sensitization. To unmask the latent sensitization, mice were treated systemically at D49 with naltrexone, an opioid antagonist, which not only unmasked the hyperalgesia to the hyperosmolar solution but also increased the number of p-ERK$^{+}$ cells (a marker of sensitization) in the ophthalmic branch of the trigeminal ganglion demonstrating a latent pain sensitization. However, the most interesting point was that at D112, topical instillation with naloxone methiodide, a peripheral opioid antagonist, provoked hyperalgesia to the hyperosmolar solution, confirming the peripheral latent sensitization (Cho et al., 2019).

In a mouse model of chemotherapy-induced neuropathic pain, a latent sensitization was found, dependent on both MOR and DOR. Interestingly, unmasking of latent pain sensitization was also elicited by the systemic application of a specific interfering peptide (DOR carboxyl tail mimic peptide) blocking MOR/DOR heteromerization. This phenomenon also occurred in a model of incision-evoked pain, confirming that heteromerization of MOR and DOR molecules mediates the maintenance of pain remission. All those data were similar in both male and female animals (Inyang et al., 2021).

### E. Side effects of systemic opioids

As previously introduced, systemic opioids are known to mediate unwanted effects in addition to their analgesic activity. The most reported are constipation and nausea, which are usually easily managed and thus of little consequence. More serious is the case of respiratory depression which can be fatal. Furthermore, chronic opioid use leads to tolerance, defined as a decrease in the drug efficacy (for the same dose). It's possible to reproduce such phenomenon *in vitro* when cellular models expressing ORs are exposed to agonists; in that situation, a decrease of signaling is observed and is designated as OR desensitization.

A paradoxical situation is opioid-induced hyperalgesia (OIH), a phenomenon whereby opioid treatment, far from treating pain, triggers hypersensitivity.

The emergence of OIH instead of desired analgesic effect seems to depend on a plethora of factors such as the pharmacology of the opioids used, administration route, dose and regimen, genetic background and sex (Roeckel et al., 2016). Cellular and molecular players which have demonstrated importance in OIH are the same as for chronic pain and latent pain sensitization (Roeckel et al., 2016). MOR is among the most important molecular players as, depending on the splicing isoform, intracellular traffic triggered and heteromerization, it can mediate either hyperalgesic or analgesic processes (Roeckel et al., 2016). The cellular and molecular mechanisms associated with OIH has been nicely reviewed by Roeckel and colleagues (Roeckel et al., 2016). A summary of the mechanisms involved is illustrated in **Fig. 22**.

One of the ways suggested to avoid such untoward effects produced by systemically-administrated opioids is to resort to topical administration of opioids, possible in the context of ocular pain, as detailed hereafter.

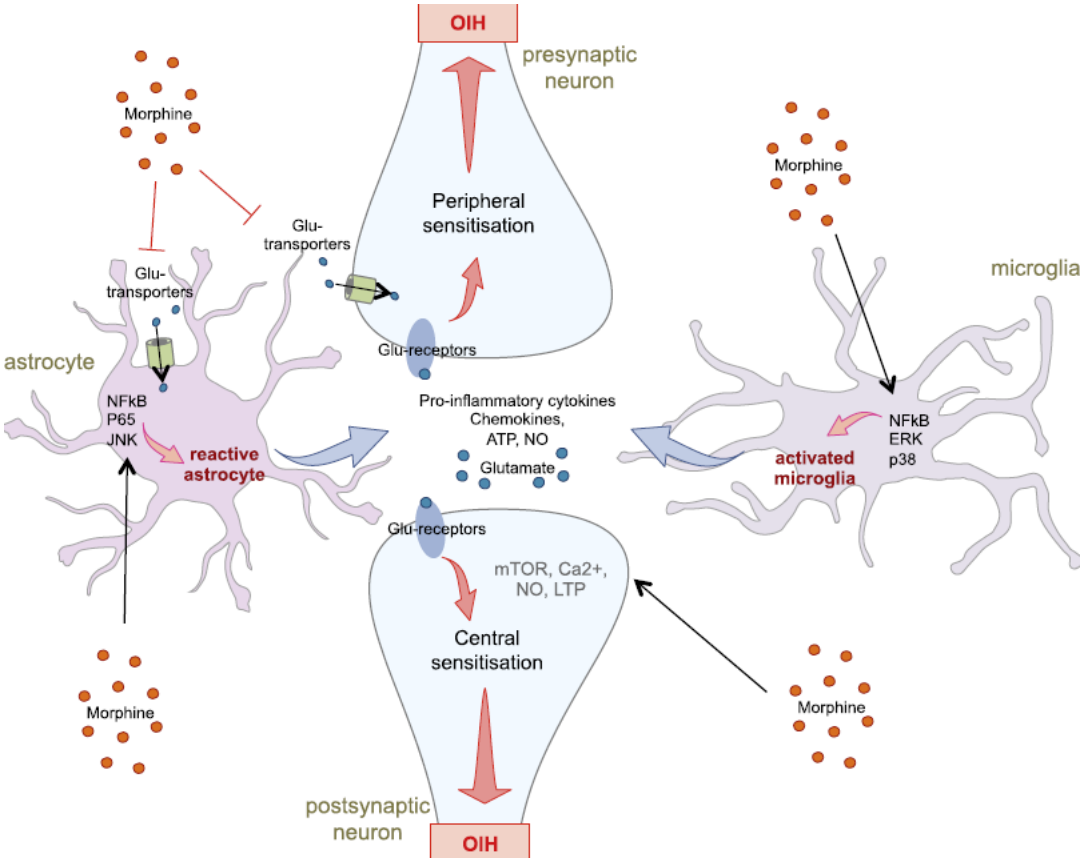


**Figure 22: Tetrasynapse activation contributes to OIH**
Morphine activates neurons, astrocytes and microglia by inhibiting glutamate recapture and inducing production of pro-inflammatory molecules. In response to its activation, each cell will produce more excitatory substances such as proinflammatory chemokines, cytokines, ATP or NO contributing to the establishment and the maintenance of OIH. ERK, Extracellular signal-regulated kinase; mTOR, mammalian target of rapamycin; NFkB, nuclear factor kappa B; NO, nitric oxide; LTP, long-term potentiation. *Adapted from Roeckel et al., 2016.*

### VI.2 Peripheral mechanisms of opioid analgesia: targeting peripheral opioid receptors

The literature in recent years has led to the suggestion that a good alternative for peripheral inflammatory pain management is topical application of opioid receptor agonists. Opioids exert greater analgesic effects in inflamed tissues than in non-inflamed tissues, limiting its action to damaged areas. This is explained by different findings triggered by peripheral inflammation:

- An up-regulation of opioid receptor expression is induced in somas of the primary sensory neurons innervating the affected region at the level of DRG and TG respectively.

- The transport of opioid receptors from the soma to the terminals is increased in inflammatory conditions.
- The perineurial barrier can be disrupted, facilitating the access of opioids.
- Inflammation is characterized by low pH, increasing the agonist efficacy due to facilitated receptor-G-protein signaling.

The result is a higher density and activity of opioid receptors at peripheral nerve terminals which potentiate ligands efficacy, both exogenous or endogenously released by inflammatory cells in the injury site. This effectivity has been demonstrated in models of neuropathic pain secondary to mechanical nerve injury (Stein and Lang, 2009; Stein, 2018a).

The development and application of drugs that do not cross the blood-brain barrier would avoid the unwanted CNS-mediated effects of systemic opioids such as respiratory depression, addiction and hyperalgesia (Stein and Lang, 2009). Still the literature is scares about their use in patients, some peripherally-restricted KOR agonists are currently in clinical trial phase. Two examples are asimadoline for the treatment of atopic dermatitis (Abels and Soeberdt, 2019) and CR845 for postoperative pain and uremic pruritus (Beck et al., 2019).

### VI.3 Targeting corneal opioid receptors

The cornea is a transparent and easy-accessible structure, allowing direct topical treatment and monitoring of efficacity, both in preclinical and clinical studies. As stated before, the cornea is highly innervated by nociceptive nerve fibers representing an excellent tissue for studying peripheral pain and testing new analgesic drugs.

Only a few studies have considered topical morphine as a safe option to alleviate corneal pain. In 1994, a study used 0.5% (6.6 mM) morphine drops in rabbits with corneal abrasion. Rabbits were treated twice a day with either saline solution, morphine 0.5% or proparacaine 0.5%. Wound healing was similar between saline and morphine-treated animals while in the proparacaine group it was severely delayed. Interestingly, proparacaine solution used contained benzalkonium chloride 0.01%. Once the safety of topical 0.5% morphine was confirmed in rabbits, it was evaluated in 7 patients with corneal abrasion. Mechanical hyperalgesia was significantly reduced 10 and 20 minutes after one topical instillation of 0.5% morphine (Peyman et al., 1994). Another study assessing morphine efficacy in dogs with central de-epithelialized corneas showed some conflicting results. Morphine 1% (13.2 mM)

was applied 3 times per day until complete healing at day 4 or 5. Morphine 13.2 mM decreased blepharospasm at day 1, 2 and 3 after surgery. Interestingly, mechanical hyperalgesia, measured by Cochet Bonnet aesthesiometer, decreased after treatment from 2.4 cm to 1.5 cm at day 2 and from 1.6 cm to 1.2 cm at day 3. Those mechanical sensitivity values after treatment were even lower that baseline value (before lesion) (1.8 cm). This study also provided DOR immunostaining in naïve dog corneas at the sub-bepithelial plexus and intraepithelial terminal levels (Stiles et al., 2003).

The first study systematically examining cellular and pharmacological mechanisms of topical morphine treatment was the study of Wenk et al., 2003. They used a rat model of ocular inflammatory pain induced by nitrate cauterization (a model of corneal inflammation and hyperalgesia). Analgesic effects of a single application of topical morphine (from 500 nM to 10 µM) were tested 6h after cauterization by capsaicin challenge test (1 µM). Two minutes after morphine application, the number of blinks elicited by capsaicin were measured during 30 seconds revealing a half maximal effective concentration ($EC_{50}$) of 1.8 µM. Minimal concentration of morphine which significantly reduced chemical hyperalgesia was used for the rest of the study (5 µM). Previous topical application of naloxone, an opioid receptor antagonist, reversed anti-nociceptive effects of morphine, revealing an opioid receptor-mediated effect. Different concentrations of DOR antagonist Naltrindole (from 2 to 200 nM) and MOR antagonist CTAP (from 20 nM to 1 µM) revealed a half maximal inhibitory concentration of 15 nM and 200 nM, respectively, suggesting that anti-nociceptive effects could be mediated by both DOR and MOR. Inflammation kinetic study showed the anti-inflammatory effects of repeated instillation of morphine 5 µM during 24h (every 2 h up to 6 h after injury, and then every 4 h) in inflammatory pain conditions. Histological analysis of different time points revealed that maximum edema in saline-treated rats appeared 12 h after injury while in morphine-treated rats edema had already disappeared at that timepoint in peripheral cornea. Quantification of the number of inflammatory cells, that were identified as neutrophils, showed a significant decrease in morphine-treated corneas 4, 6, 12 and 24 h after injury, clearly demonstrating anti-inflammatory effects. A group of animals were treated also with naloxone 5 µM, naltrindole 200 nM or CTAP 1 µM after morphine and sacrifice 6h after injury. At this timepoint, inhibitory effects of morphine in corneal edema were fully prevented by the three opioid antagonists (naloxone, CTAP and naltrindole). Interestingly,

anti-inflammatory effects of morphine by means of number of inflammatory cells were fully prevented by naloxone, CTAP but only partially by naltrindole, suggesting a more important anti-inflammatory role of MOR over DOR (Wenk et al., 2003).

Finally, another study quantified 0.5% (6.6 mM) morphine topical repeated treatment efficacity in patients following photorefractive keratectomy. Patients received saline or morphine every 2h on the day of surgery, and 4 times/day during the following 2 days. Pain was assessed by questionnaires (visual descriptor, numerical rating, VAS, and oral analgesic consumption) every 2 h while awake during the treatment period. Numeric rating scale score was significantly decreased in morphine-treated patients on postoperative day 1, while VAS score was decreased at postoperative day 1 and 2. No difference between groups was noted in epithelial healing or refractive outcomes (Faktorovich and Basbaum, 2010).

In this line, preclinical studies from our team have focused on the elucidation of cellular and molecular mechanisms of analgesia following the targeting of the ocular opioid system for the management of corneal pain. Recently, we were able to evidence anti-nociceptive and anti-inflammatory properties of PL265, a dual inhibitor of enkephalin-degrading enzymes, topically administrated in BAK and scraping + LPS models of ocular pain (Reaux-Le Goazigo et al., 2019). We showed that repeated administration of PL265 (10 mM) significantly reduced mechanical (von Frey) and chemical (2M NaCl, wiping test) allodynia in the BAK instillation model of ocular pain (**Fig. 23**). Similarly, PL265 reduced mechanical and chemical (capsaicin test) in the scraping + LPS model of inflammatory pain (**Fig. 24).** In the same study, anti-inflammatory effects of PL265 was evidenced by the decreased number of corneal $CD11b^{+}$ dendritic cells in scraping + LPS animals (**Fig. 25**) (Reaux-Le Goazigo et al., 2019).

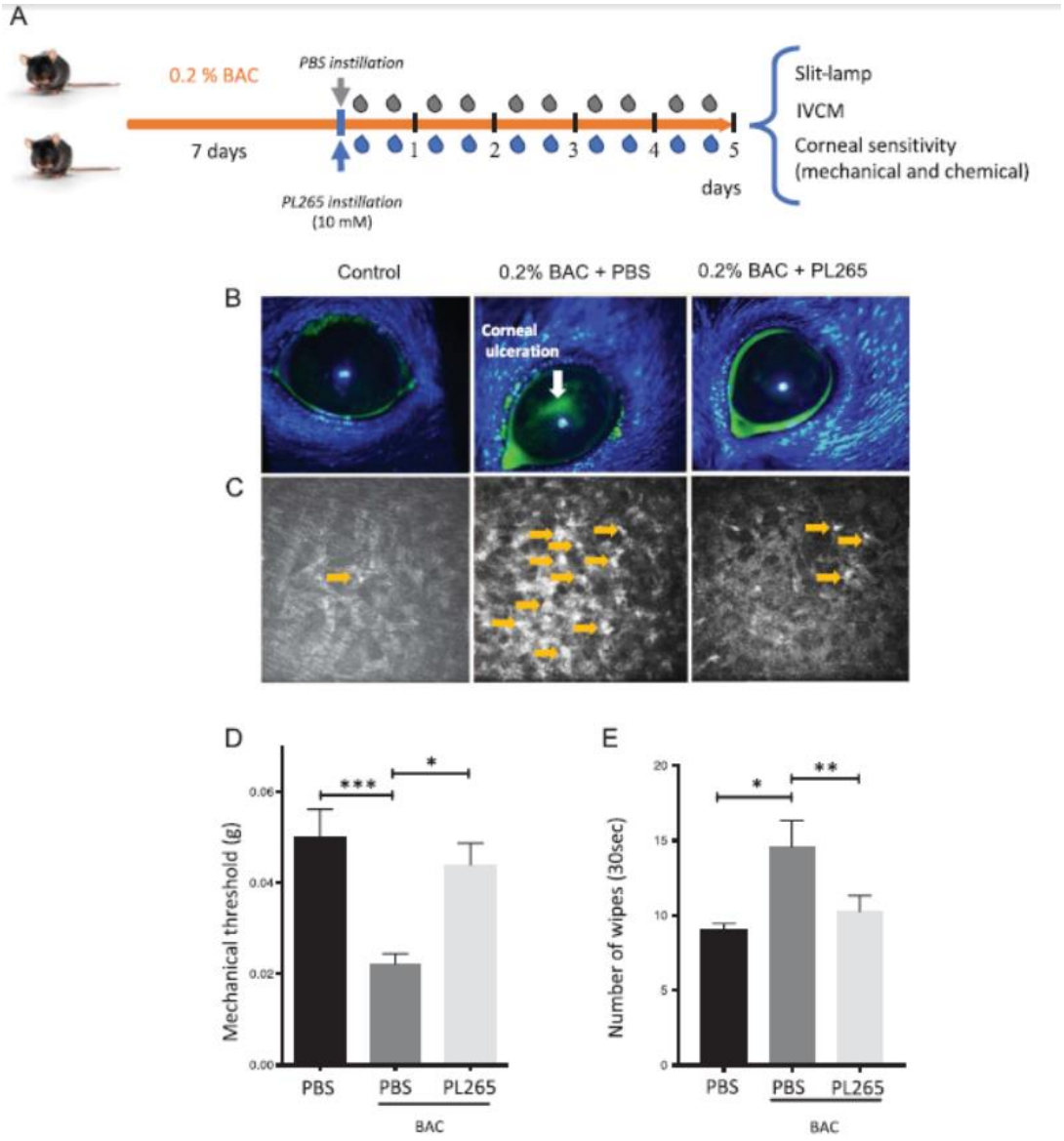


**Figure 23: Topical administration of PL265 reduces corneal injury, inflammation, and corneal hypersensitivity after exposure to benzalkonium chloride**

Schematic diagram of the experimental protocol **(A)**. Fluorescein staining **(B)** confirmed BAC-induced corneal ulceration (white arrow), which was reduced after topical PL265 (10 mM) administration. In vivo confocal microscope images showed **(C)** immune cell infiltration (orange arrows) in the stroma of mice receiving BAC 1 PBS. Note the subsequent anti-inflammatory effect in PL265-treated mice. Mechanical **(D)** and chemical **(E)** sensitivity were measured with von Frey filaments and the eye-wiping test 15 minutes after the last topical administration. A significant antinociceptive effect (an increase of mechanical threshold response and a reduced number of wipes) was observed after topical PL265 compared to PBS. Data were presented as mean ± SEM (n= 10-11 mice per group); differences between groups were analyzed using nonparametric 1-way ANOVA test on ranks (Kruskal and Wallis) followed by Dunn multiple-comparison test. Levels of significance were *p<0.05, **p<0.01, and ***p<0.001, respectively. ANOVA, analysis of variance. *From Reaux-Le Goazigo et al., 2019.*

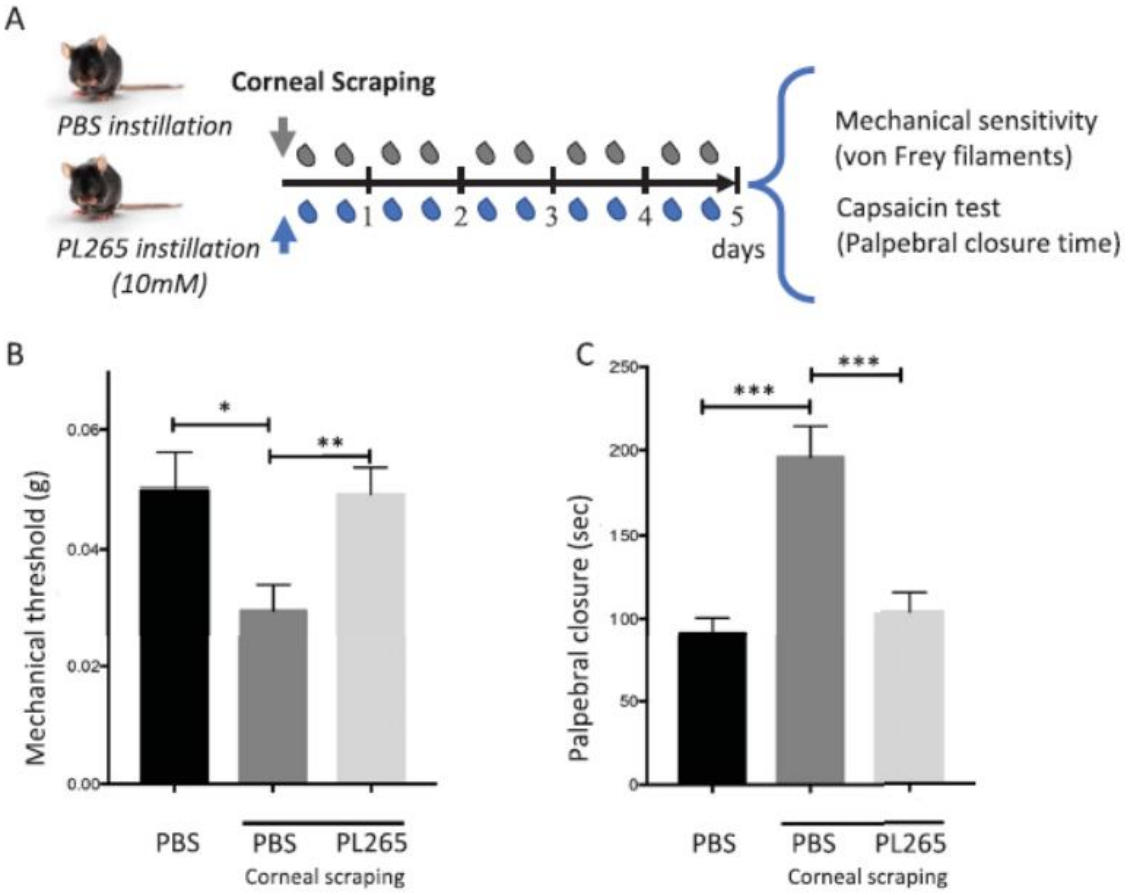


**Figure 24: Antinociceptive effects of topical administration of PL265 after corneal scraping** Schematic diagram of the experimental protocol (A). Mechanical (B) and chemical (C) corneal sensitivity after PBS and PL265 topical administration after corneal scraping. Mechanical sensitivity was measured 15 minutes after the last instillation with von Frey filaments. Animals receiving PBS after corneal scraping showed reduced mechanical threshold response and increased palpebral closure time after capsaicin compared to control PBS animals. Topical PL265 administration had a clear and significant antinociceptive effect using both behavioral tests. Data are expressed as mean±SEM (n=10-11 mice per group). Differences between groups were analyzed using parametric 1-way ANOVA test followed by the Tukey post hoc test. Levels of significance were *p<0.05, **p<0.01, and ***p<0.001, respectively. ANOVA, analysis of variance. *From* *Reaux-Le Goazigo et al., 2019*

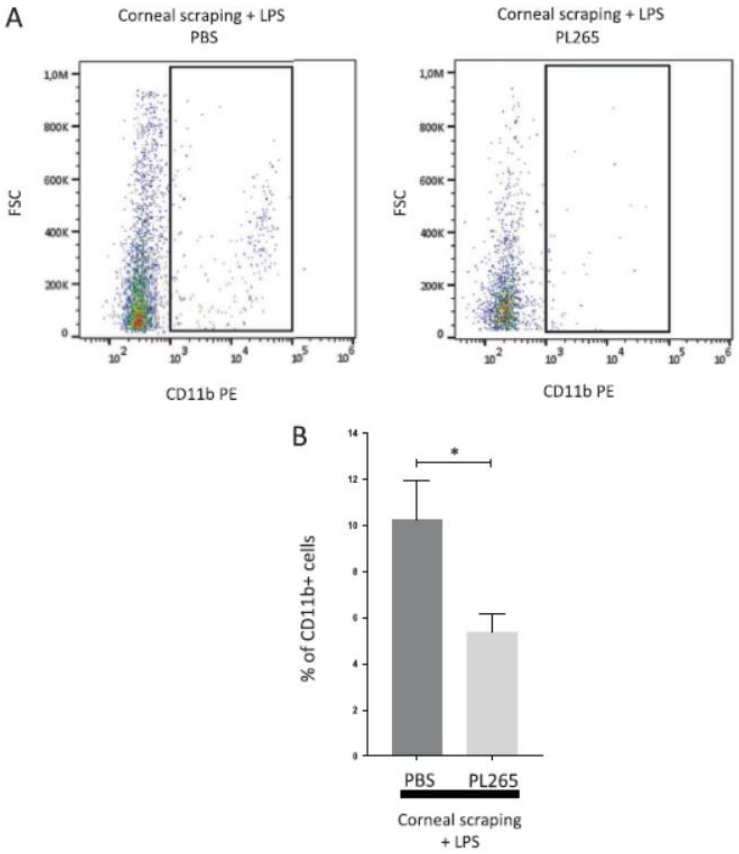


**Figure 25: Topical administration of PL265 decreases corneal inflammation** Representative flow cytometry dot plot for myeloid populations in corneas from different groups of mice with mononuclear phagocytes defined as $CD11b^+$ cells **(A)**. Corneas were extracted at day 5 from mice with a corneal scraping + LPS receiving PBS (left panel) and from mice with a corneal scraping 1 LPS receiving PL265 (right panel). Corneas were dissected at day 5 and digested for flow cytometry analysis by forward-scattered light (FSC) method. Cell suspensions of cornea from individual mice were assessed using anti-CD11b-PE mAb. Graph illustrating the % of $CD11b^+$ cells in the different groups of mice **(B)**. After corneal scraping + LPS, topical PL265 treatment significantly decreased the number of $CD11b^+$ cells in the cornea as compared to the PBS group. Data are presented as mean ± SEM (n = 4 mice per group); difference between groups were analyzed using the nonparametric Mann and Whitney test. Level of significance was *p<0.05. LPS, lipopolysaccharide. *From* *Reaux-Le Goazigo et al., 2019*

Thus, activation of corneal opioid receptors by endogenous enkephalins could be an effective approach for reducing ocular pain (Reaux-Le Goazigo et al., 2019). In the clinical setting, we also found that patients with corneal pain associated with persistent DED had lower enkephalin levels in their ocular surface compared to healthy controls (Nicolle et al., 2018), suggesting a link between endogenous opioids dysregulation and corneal pain.

**In conclusion, peripheral activation of opioid receptors could be a promising strategy to treat corneal pain, as was investigated in the following research project, detailed in the next chapter.**

# Chapter 2: Exploration of novel therapeutic and diagnostic strategies to manage dry eye disease-related corneal pain

As detailed in the previous chapter, DED is a complex disease, often leading to chronic -insufficiently managed- ocular pain.

The research project developed in this thesis thus aimed to better understand, from both a scientific and clinical perspective, the corneal nociceptive system in various ocular surface diseases and more specifically in the context of dry eye disease-related corneal neuropathic pain.

Owing to the multiprofessional environment provided by our research team, we explored new diagnostic and therapeutic strategies to manage DED and DED-related corneal neuropathic pain in both preclinical models and in the clinical setting of a DED patient cohort of the XV-XX national ophthalmological hospital in Paris.

The first part of the PhD project explored the therapeutic potential of targeting the corneal opioid system using topical treatments in a murine model of DED.

The second part of the project assessed potential biomarkers of DED-related corneal neuropathic pain in human patients and novel phenotyping strategies to improve the diagnosis and thus management of corneal neuropathic pain in DED in clinical practice.

## I. MOR as a topical target to manage inflammatory corneal pain (*Study 1 - Joubert et al. Biomed Pharmacotherap. 2020*)

In the first part of the PhD project, we investigated the presence of MOR in the mouse cornea in a preclinical model of acute inflammatory pain (scraping + LPS instillation) to provide the anatomical basis to justify investigating topical opioids as novel treatments for ocular pain (Joubert et al., 2020) .

In this study, we provided the first demonstration that MOR is expressed in mouse corneal nerves and that in inflammatory conditions, MOR mRNA was overexpressed at the level of the TG. Furthermore, in this context chronic topical administration of DAMGO resulted in decreased corneal nerve hyperexcitability, decreased mechanical allodynia and decreased chemical pain **(Fig. 26)**.

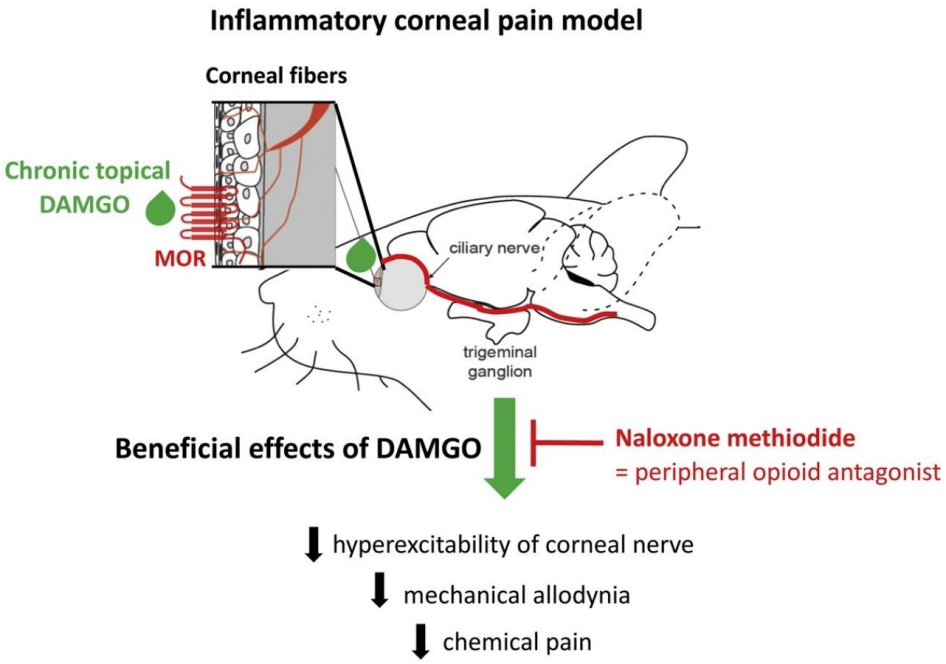


**Figure 26: Graphical abstract of (Joubert et al., 2020)**

In addition, double *in situ* hybridization for TRPV1 and MOR was performed on ipsilateral TG samples from control and scraping-LPS mice and we found that almost all $TRPV1^{+}$ primary sensory neurons at the level of ophthalmic branch ($V_1$) of the TG also expressed MOR. This finding suggests that MOR agonists may act primarily on polymodal sensory neurons.

Biomedicine & Pharmacotherapy 132 (2020) 110794

Contents lists available at ScienceDirect

Biomedicine & Pharmacotherapy

journal homepage: www.elsevier.com/locate/biopha

Original article

# Topical treatment with a mu opioid receptor agonist alleviates corneal allodynia and corneal nerve sensitization in mice

Fanny Joubert [a], Adrian Guerrero-Moreno [a], Darine Fakih [a,b], Elodie Reboussin [a], Claire Gaveriaux-Ruff [c], Maria Carmen Acosta [d], Juana Gallar [d,e], José Alain Sahel [a,f,g,h], Laurence Bodineau [i], Christophe Baudouin [a,f,j], William Rostène [a], Stéphane Mélik-Parsadaniantz [a], Annabelle Réaux-Le Goazigo [a,*]

[a] Sorbonne Université, INSERM, CNRS, Institut de la Vision, 17 Rue Moreau, F-75012, Paris, France
[b] R&D Department, Laboratoires Théa, 12 Rue Louis Biérot, F-63000, Clermont-Ferrand, France
[c] Institut de Génétique et de Biologie Moléculaire et Cellulaire, Université de Strasbourg, CNRS, UMR7104, INSERM U1258, Ecole Supérieure de Biotechnologie de Strasbourg, Illkirch, Strasbourg, France
[d] Instituto de Neurociencias Universidad Miguel Hernández-CSIC, San Juan de Alicante, Alicante, Spain
[e] Instituto de Investigación Sanitaria y Biomédica de Alicante, Alicante, Spain
[f] CHNO des Quinze-Vingts, INSERM-DGOS CIC 1423, 28 Rue de Charenton, F-75012, Paris, France
[g] Fondation Ophtalmologique Rothschild, 29 Rue Manin, F-75019, Paris, France
[h] Department of Ophthalmology, The University of Pittsburgh School of Medicine, Pittsburgh, PA, 15213, United States
[i] Sorbonne Université, INSERM, UMR_S1158 Neurophysiologie Respiratoire Expérimentale et Clinique, F-75013, Paris, France
[j] Department of Ophthalmology, Ambroise Paré Hospital, AP-HP, Paris-Saclay University, F-92100 Boulogne-Billancourt, France

ARTICLE INFO

*Keywords:*
Corneal pain
Inflammation
Opioid receptor
Electrophysiology

ABSTRACT

Corneal pain is considered to be a core symptom of ocular surface disruption and inflammation. The management of this debilitating condition is still a therapeutic challenge. Recent evidence supports a role of the opioid system in the management of corneal nociception. However, the functional involvement of the mu opioid receptor (MOR) underlying this analgesic effect is not known. We first investigated the expression of the MOR in corneal nerve fibers and trigeminal ganglion (TG) neurons in control mice and a mouse model of corneal inflammatory pain. We then evaluated the anti-nociceptive and electrophysiological effects of DAMGO ([D-Ala$^2$,N-Me-Phe$^4$, Gly$^5$-ol] enkephalin), a MOR-selective ligand. MOR immunoreactivity was detected in corneal nerve fibers and primary afferent neurons of the ophthalmic branch of the TG of naive mice. MOR expression was significantly higher in both structures under conditions of inflammatory corneal pain. Topical ocular administration of DAMGO strongly reduced both the mechanical (von Frey) and chemical (capsaicin) corneal hypersensitivity associated with inflammatory ocular pain. Repeated instillations of DAMGO also markedly reversed the elevated spontaneous activity of the ciliary nerve and responsiveness of corneal polymodal nociceptors that were observed in mice with corneal pain. Finally, these DAMGO-induced behavioral and electrophysiological responses were totally blunted by the topical application of naloxone methiodide, an opioid receptor antagonist. Overall, these results provide evidence that topical pharmacological MOR activation may constitute a therapeutic target for the treatment of corneal pain and improve corneal nerve function to alleviate chronic pain.

## 1. Introduction

Ocular pain, in particular, cornea-driven pain, is considered to be a core symptom of inflammatory and traumatic disorders of the ocular surface. Pain is a frequently reported symptom in dry eye disease, which has gained recognition as a public health problem, given its increasing prevalence (5–30% of the population aged ≥ 50 years), morbidity, and associated social burden [1–4]. The management of chronic corneal pain still represents a therapeutic challenge. The cornea is one of the most densely innervated and sensitive tissues in the body [5,6]. Its sensory innervation is supplied by ciliary nerves derived from ophthalmic division of the trigeminal ganglion (TG) [7–9]. The cornea is exclusively

* Corresponding author.
*E-mail address:* annabelle.reaux@inserm.fr (A. Réaux-Le Goazigo).

https://doi.org/10.1016/j.biopha.2020.110794
Received 6 August 2020; Received in revised form 17 September 2020; Accepted 19 September 2020
Available online 6 October 2020

innervated by C- and A-delta fibers, including mechano-nociceptors, which are triggered by noxious mechanical stimulation, polymodal nociceptors, which are excited by mechanical, chemical, and thermal stimuli, and cold thermoreceptors, which are activated by cooling [10–12].

Inflammatory pain refers to increased sensitivity due to the inflammatory response associated with tissue damage. Corneal inflammation is a reaction of the immune system to pathogens or injuries, whereas the triggers of ocular inflammation in the clinic may be different (dry eye disease, breakdown of corneal epithelium, uveitis, *etc.*). However, they produce similar symptoms, including pain. Pain can be modulated by endogenous (enkephalins, endorphins, and dynorphins) and exogenous (opium alkaloids) opioids, which activate mu-(MOR), delta-(DOR) and kappa-(KOR) opioid receptors expressed throughout the peripheral and central nervous systems [13–16]. Although systemic opioids are still the gold standard for treating pain, common side effects include respiratory depression, nausea, constipation, hyperalgesia, addiction, tolerance, and dependence [17]. In ophthalmology, oral opioids are used for post-operative pain [18] and for alleviating corneal neuropathic pain in dry-eye patients [19,20], but side effects are often reported. Topical ocular drug administration offers a number of advantages over systemic administration, including direct targeting of the corneal nerves by the drugs and minimizing centrally mediated side-effects. We recently reported that repeated instillation of PL265, a dual enkephalinase inhibitor, which increases the endogenous levels of enkephalins, mediates antinociceptive effects in corneal pain models [21]. Moreover, studies have considered topical morphine as a safe alternative to alleviate corneal nociception in rats [22], cats [23], dogs [24], and patients [25,26]. However, these studies did not evaluate the functional implication of the MOR underlying this analgesic effect, nor its expression in corneal nerves and trigeminal neurons or the electrophysiological effects of a topical MOR agonist on corneal nerve activity.

Given that selective MOR agonists can be particularly effective for the treatment of inflammatory pain [27], we hypothesized that targeting corneal MOR by topical agonists could be an efficient means to alleviate corneal inflammatory pain in mice and modulate corneal nerve-fiber activity.

Herein, we report increased expression of the MOR in corneal nerve fibers and trigeminal sensory neurons in a mouse model of inflammatory corneal pain. We further demonstrate numerous beneficial effects of multiple instillations of DAMGO ([D-Ala$^2$,N-Me-Phe$^4$,Gly$^5$-ol] enkephalin), a MOR-selective ligand, on mechanical and chemical corneal allodynia, as well as on spontaneous and evoked-ciliary nerve-fiber activity. Finally, through the use of the pharmacological antagonist, naloxone methiodide, we confirmed that these effects are specifically mediated by peripheral MORs. Our experiments have important implications for the potential role of MOR agonists as anti-allodynic drugs and for understanding how mu opioid agonists modulate corneal nerve-fiber activity in the context of corneal pain.

## 2. Materials and methods

### 2.1. Animals

Six-week-old adult male C57BL/6 mice (Janvier Labs, Le Genest Saint Isle, France) were randomly assigned to cages (5 mice/cage) and maintained on a 12 h light–dark cycle with free access to food and water. All experiments were approved by the Charles Darwin Ethics Committee for Animal Experimentation (Ce5/2011/05) and carried out in accordance with Directive 2010/63/EU of the European Parliament and the Council of 22 September 2010 and French law (2013/118). They were also validated by the "Service Protection et Santé Animales", APAFIS #1501 2015081815454885 v2. All efforts were made to minimize the number of animals used and their suffering. All experiments were performed in strict accordance with the recommendations of the Weatherall Report regarding good animal practice.

### 2.2. Drugs: pharmacological agents

DAMGO ([D-Ala$^2$,N-Me-Phe$^4$,Gly$^5$-ol] enkephalin), naloxone methiodide, capsaicin, and lipopolysaccharide (LPS; from *Escherichia coli* O111:B4) were obtained from Sigma-Aldrich (Saint-Quentin Fallavier, France). DAMGO, naloxone methiodide and LPS were dissolved in 0.1 M phosphate-buffered saline (PBS; pH 7.4). Capsaicin (Sigma-Aldrich) was dissolved in 100 % ethanol (1 M solution) and then diluted in isotonic saline to obtain a 10 μM solution.

### 2.3. Preclinical mouse model of corneal inflammatory pain (corneal scraping + LPS administration)

Mice were anesthetized by isoflurane inhalation (2%). A drop of ophthalmic gel was used to maintain hydration of the left eye during the surgery. On day 1 (D1), the topical anesthetic oxybuprocaine (Théa laboratories, Clermont Ferrand, France) was applied to the ocular surface and corneal scraping was performed on the right eye using an interdental brush to remove the superficial corneal epithelium. Ten microliters LPS (5 mg/mL) was applied to the right scraped cornea immediately after corneal injury (D1), and a second LPS application was performed on D3, as previously described [21] (Supplementary Fig. 1A).

### 2.4. Topical ocular administrations: pharmacological studies

The effect of topical DAMGO (50 μM), a selective MOR ligand, was determined in a corneal inflammatory pain model. For topical ocular administration, the cage order was randomized daily. Animals received repeated instillation of PBS or naloxone methiodide (100 μM), followed by either PBS or DAMGO (50 μM) 10 min after, twice daily, for five consecutive days. Behavioral experiments and electrophysiological recordings were performed on D5, before ($t_0$) and 15 min ($t_{15}$) after the last drug instillation (Supplementary Fig. 1B).

### 2.5. In vivo confocal microscopy

Corneal integrity was examined by *in vivo* confocal microscopy (IVCM, Heidelberg Retina Tomography (HRT) II/Rostock Cornea Module [RCM; Heidelberg Engineering GmbH, Heidelberg, Germany]) as previously described [10,28]. The first layer of the superficial epithelium, the sub-basal plexus, and the stroma were observed. A minimum of 50 serial TIFF images (400 × 400 μm) were acquired per animal.

### 2.6. Electrophysiological experiments: Recording of spontaneous and stimulus-evoked ciliary nerve-fiber activity

Electrophysiological experiments were performed on the control and injured corneas on D5. The mice were sacrificed by cervical dislocation. Their eyes were enucleated and the connective tissue and extraocular muscles at the back of the eye carefully removed to expose and isolate the ciliary nerves. The eye was then placed in a two-compartment chamber (divided by a Sylgard-coated plastic wall) to isolate the cornea from the back of the eye, as previously described [10,29,30]. The cornea was continuously superfused with a deoxygenated physiological saline solution (133.4 mM NaCl, 4.7 mM KCl, 2 mM $CaCl_2$, 1.2 mM $MgCl_2$, 16.3 mM $NaHCO_3$, 1.3 mM $NaH_2PO_4$, 7.8 mM glucose) at a rate of 2 mL/min at 33 ± 1 °C. It was then saturated with $O_2$ and adjusted to pH 7.4 by bubbling with 95 % $O_2$ and 5% $CO_2$. The posterior compartment of the chamber was filled with physiological saline. The extracellular multi-unit electrical activity of the ciliary nerve was recorded using a suction electrode (Ag/AgCl). The signal was filtered (300−5000 Hz), amplified (x 10000) (A–M Systems, Sequim, USA), and digitalized using Spike 2 data analysis and acquisition software (CED Micro1401, Cambridge Electronic Design) at a sampling frequency of 10,000 Hz. A threshold corresponding to a +50 % peak to peak of the background noise was determined to distinguish the spike from noise, as previously

described [10]. The cornea was superfused with physiological saline for 30 min to stabilize the preparation before performing the electrophysiological recordings. The area of the corneal surface innervated by the recorded ciliary nerve (receptive field) was identified using mechanical stimulation with a fine paint brush, as previously described [10]. The following firing parameters were calculated: a) *Spontaneous activity*: after the stabilization period, the frequency of spontaneous activity was assessed as impulses per second (imp/s) for 1 min before any corneal stimulation; b) *Responsiveness to chemical ($CO_2$) stimulation*: the following parameters were analyzed to describe the $CO_2$ pulse-evoked firing discharge: *i)* the mean firing frequency, expressed as the number of impulses per second (imp/s) for a 30-s $CO_2$ pulse and *ii)* the latency of the impulse discharge, in seconds, between the beginning of the $CO_2$ pulse and the first detected $CO_2$-evoked nerve impulse.

Drugs were added to the physiological saline solution followed by incubation for 2 min, *i.e.,* either 1x PBS or DAMGO (50 μM) alone or naloxone methiodide (100 μM) followed by DAMGO (50 μM). The spontaneous and CO2-evoked activity were recorded and the perfusion then returned to a normal physiological saline solution. The spontaneous activity and corneal responsiveness to chemical stimulation at $t_0$ and $t_{15}$ after the last drug administration were compared (Supplementary Fig. 1B). Electrophysiological traces were analyzed in a blinded manner, the experimenter was blinded to the treatment (PBS, DAMGO, DAMGO + Naloxone Metiodide), as well as the group of mice analyzed (operated or naive).

### 2.7. Behavioral studies

Experiments were carried out during the light period (between 10:00 and 17:00). For behavioral tests, mice were placed in the testing room (at least 30 min before the start of the experiments) and the order of testing was randomized. The experimenter was blinded to the treatment group. Mice were trained a week before the surgery (surgery considered as D1 in this study). The immobilization (handling- restraint) lasted a maximum of 20 s to reduce any potential stress and anxiety.

*Corneal mechanical sensitivity*: von Frey filaments (Bioseb, Vitrolles, France) were used to evaluate corneal sensitivity in response to corneal mechanical stimulation [21,30]. The mechanical threshold response was determined by assessing the first blinking response evoked by calibrated von Frey filaments of increasing force (0.08 – 0.7 mN) applied to the central cornea of immobilized mice. The mechanical corneal sensitivity was determined on D1, before the surgery, to obtain the basal threshold. The $t_0$ value determined on D5 corresponded to the mechanical threshold measured before the last daily PBS or DAMGO instillation. The $t_{15}$ value corresponded to the threshold measured 15 min after the last topical administration of the drugs (Supplementary Fig. 1B).

*Corneal sensitivity to capsaicin*: The chemical corneal sensitivity to capsaicin was assessed by applying 10 μL of a 10 μM capsaicin solution to the cornea 15 min after the PBS or drug instillation, as previously described [21]. The animals were immediately placed in an individual cage and the palpebral closure time measured by the investigator. The same experimenter performed all experiments in a test room close to the colony room to minimize stress (Supplementary Fig. 1B).

### 2.8. Immunohistological studies

#### 2.8.1. Tissue preparation

Mice were deeply anesthetized with a 300-μL mixture of ketamine (80 mg/kg) and xylazine (8 mg/kg), which was injected intraperitoneally. Mice were then perfused with a 0.9 % NaCl solution, followed by a 4% (mice) paraformaldehyde (PFA) solution. The eyes were enucleated and frozen in liquid nitrogen until use. The TG were carefully dissected, post-fixed for 24 h in 4% PFA and placed in a 30 % sucrose solution in PBS for 48 h before being frozen at −20 °C in 7.5 % gelatin and 10 % sucrose. Corneal and TG frozen sections were prepared using a Cryostat (Leica Microsystems, Wetzlar, Germany). The sections were mounted on Superfrost™ slides and stored at −20 °C for subsequent use (Table 1).

#### 2.8.2. Double immunofluorescence labelling in the cornea and TG

The suppliers, reference, and dilutions of the primary and secondary antibodies used for immunohistochemistry are listed in Table 1. Neuronal markers (PGP 9.5, anti-beta III tubulin and Milli-Mark Pan Neuronal Marker) were used to identify corneal nerves and trigeminal neurons. They are all suitable for detecting myelinated and nonmyelinated nerve fibers in peripheral tissues and are commonly used to identify all nerve fibers in the cornea [7,31–33]. We carefully checked that all of the neuronal markers showed classic morphological patterns and normal distribution of nerve fibers in the cornea tissues. Moreover, the beta III tubulin antibody stained cells exhibiting the classic morphology and distribution of neurons and their fibers in TG sections from mice.

The specificity of the MOR antibody: rabbit recombinant anti-Mu opioid receptor monoclonal antibody [UMB3, ab134054, abcam], has been previously well characterized [34]. This antibody was raised against a synthetic peptide corresponding to amino acids of human MOR aa 350–450 (the intracellular C-terminus). It is considered to be an excellent tool for assessing MOR protein expression in mice, rats, and human tissues and is widely used [15,35]. This antibody has also been knockout validated, as western-blot analysis of mouse brain homogenates from wild-type mice resulted in a broad band of ~70−80 kDa but not those from MOR knockout mice [34]. In addition, it provides specific staining of MOR-transfected cells and wild-type mouse brain and the translocation of MOR immunostaining after agonist exposure [34]. The absence of non-specific staining by the secondary antibody was demonstrated by incubating corneal and TG sections from naive and scraped/LPS-treated animals with a purified rabbit IgG Isotype control (Biorad, PRABP01) using the same concentration as that used with UMB3 for the corneal and TG sections. This was followed by incubation with the appropriate secondary antibodies and detection reagents (as described above). The sections were then analyzed in a blinded manner (Supplementary Fig. 2). Negative controls were included in which the primary antibodies were omitted to confirm secondary antibody specificity (data not shown).

Corneal sections: Sequential immunostaining was performed on whole-mount corneas and frozen corneal sections (12-μm cryostat sections). The corneas were rinsed in phosphate-buffered saline-0.1 % Triton (PBS-T 0.1 %) and blocked for 2 h at room temperature (RT) with PBS-T 0.1 % containing 10 % normal goat serum (NGS). The corneas were first incubated with monoclonal mouse anti-PGP 9.5 (ab8189, Abcam, Cambridge, UK, 1:500) (free-floating cornea) or an antibody against the pan neuronal marker (MAB2300, Millipore, 1:500) (cryostat sections) in PBS-T 0.5%–3% NGS overnight at 4 °C. The corneas were then rinsed in PBS-T 0.1 % and incubated with goat anti-mouse Alexa 488 (Invitrogen, 1:1000) and DAPI (1:1000) in PBS-T 0.5 %–3 % NGS for 2 h at RT. The corneas were washed in PBS-T 0.1 % and next incubated with rabbit monoclonal anti-MOR (UMB-3, ab134054, Abcam, Cambridge, UK, 1:250) in PBS-T 0.5 %–3 % NGS for 24 (cryostat sections) or 36 h (free-floating cornea) at 4 °C. The tissues were rinsed and incubated with donkey anti-rabbit Alexa 594 (Invitrogen, 1:1000) in PBS-T 0.5 %–3 % NGS for 2 h at RT. Free-floating corneas were mounted onto Superfrost™ slides and the slides cover slipped with Fluoromount Aqueous Mounting Medium (Sigma Aldrich).

TG sections: frozen TG sections were rinsed in PBS-T 0.1 % and blocked for 2 h with PBS-T 0.1 % containing 3% normal horse serum (NHS). The sections were incubated with a solution containing a mixture of primary antibodies (rabbit monoclonal anti-MOR, 1:500; mouse monoclonal anti-beta III tubulin antibody, ab78078, Abcam; 1:500) in PBS-T 0.5 % with 3% NHS for 48 h. The sections were rinsed in PBS-T 0.1 % and the slides incubated with biotinylated goat anti-rabbit immunoglobulin (Vector Laboratories, 1:1000) and donkey anti-mouse Alexa 488 antibody (Invitrogen, 1:500) in PBS-T 0.5 % for 2 h at RT. Then, TG

**Table 1**
Suppliers, references, and dilutions of the primary and secondary antibodies used for immunohistochemistry.

| Sample | Sectioning | Primary Antibody (target, ref#, company) | Concentration | | Secondary Antibody | Ratio | Amplification |
|---|---|---|---|---|---|---|---|
| | | | Used | Real | | | |
| Cornea | No (whole-mount) | PGP 9.5, ab8189, Abcam | 1:500 | 2 ug/mL | goat anti-mouse Alexa 488, Invitrogen | 1:1000 | |
| | | MOR, UMB-3, ab134054, Abcam | 1:250 | 0,176 ug/mL | donkey anti-rabbit Alexa 594, Invitrogen | 1:1000 | |
| | Cryostat (14 μm) | Pan Neuronal marker, MAB 2300, Millipore | 1:500 | Unknown | goat anti-mouse Alexa 488, Invitrogen | 1:1000 | |
| | | MOR, UMB-3, ab134054, Abcam | 1:250 | 0,176 ug/mL | donkey anti-rabbit Alexa 594, Invitrogen | 1:1000 | |
| TG | Cryostat (16 μm) | MOR, UMB-3, ab134054, Abcam | 1:50 | 0,88 μg/mL | goat anti rabbit biotinylated, Vector Laboratories | 1:1000 | Streptavidin Alexa 594 conjugated, Invitrogen (1:1000) |
| | | beta III Tubulin, ab78078, Abcam | 1:500 | 2 ug/mL | donkey anti-mouse Alexa 488, Invitrogen | 1:500 | |

sections were incubated with Alexa 594-conjugated streptavidin (Invitrogen, 1:1000) and DAPI (1:1000) in PBS-T 0.5 % for 2 h at RT. The sections were washed, mounted onto Superfrost™ slides, and cover slipped with Fluoromount.

### 2.9. Fluorescent in situ hybridization for Mu opioid receptor mRNA in mouse TGs

Mouse TGs were dissected and post-fixed in 4% PFA for 24 h at 4 °C. The tissues were immersed in 10 %, 20 %, and 30 % sucrose solutions (in PBS) for 12–24 h at each step. The tissues were placed at an optimal cutting temperature (OCT), frozen in liquid nitrogen, and stored at -80 °C. Then, the TG were cut using a cryostat (Leica CM 3050 S) to make 12-μm sections, which were mounted on Superfrost slides. Fluorescent *in situ* hybridization studies were performed using the RNAscope Fluorescent Multiplex Reagent kit v2 assay, according to the protocol for fixed frozen tissue (Advanced Cell Diagnostics, Newark, CA). Briefly, the sections were washed with 1X PBS, treated with hydrogen peroxide (RNAscope, ref# 322335) for 10 min at RT and then washed in distilled $H_2O$. Using a steamer, the tissues were treated with distilled $H_2O$ for 10 s at 99 °C and then moved to RNAscope 1X target Retrieval Reagent (RNAscope, ref# 322000) and incubated for 5 min at 99 °C. The tissues were washed with distilled $H_2O$, transferred to 100 % ethanol for 3 min and treated with RNAscope Protease III (RNAscope, ref#322337) for 30 min at 40 °C. A species-specific target probe for MOR, Oprm1-C3 (ref# 315841-C3), was diluted (1:50) with probe diluent (RNAscope, ref#300041). The sections were then incubated with the Oprm1-C3 probe and negative (ref# 320871) and positive (ref# 320881) control probes (provided by the manufacturer). The probes were hybridized for 2 h at 40 °C in a humidified oven (RNAscope HybEZ oven, with an HybEZ humidity control tray from Advanced Cell Diagnostics). A series of incubations was then performed to amplify the hybridized probe signal and label the target probe for the assigned fluorescence detection channel (PerkinElmer, Opal 650 Reagent, Ref# FP1496A; dilution 1:200). The nuclei were stained using a DAPI nuclear stain (RNAscope Ref# 323108) for 30 s at RT. The slides were then mounted using ProLong Gold Antifade Mounting reagent (Ref# P36934) onto glass sides and cover slipped.

Expression of the MOR gene and protein was quantified by examining the corneal and TG sections with a Zeiss M1 epifluorescence microscope (Axio ImagerM1; Carl Zeiss) equipped with a digital camera (Axio Cam HRC; Carl Zeiss) and image acquisition software (Zen; Carl Zeiss). The microscope settings were established using a control section and remained unchanged for all subsequent acquisitions. TIFF images were recorded. Three to five sections were used for the cornea and TG for each animal. Images (grayscale 8-bits) were then analyzed using Fiji (ImageJ) software. The thresholding function was used to discriminate objects of interest from the surrounding background and the total surface occupied by immunoreactive structures (*i.e.,* the total stained pixels) above the set threshold was estimated within a standard area, as previously reported [21]. A summation of all grey values for the entire image was extracted for the TG sections.

### 2.10. Microscopic analysis

Tissue sections were examined with an inverted Olympus FV1000 confocal microscope equipped with an argon (488 nm) ion laser and laser diodes (405 and 559 nm). The images were acquired sequentially, line-by-line, to reduce excitation and emission crosstalk. The step size was defined according to the Nyquist–Shannon sampling theorem (1024*1024 pixels). A PlanApoN (20/1.42 NA, oil immersion) objective lens (Olympus) was used and TIFF images were obtained. A single investigator analyzed all data from the microscopic analysis in a blinded manner.

### 2.11. Statistical analysis

The data are expressed as the mean ± SEM and were analyzed using GraphPad Prism7 (GraphPad, San Diego California USA). The normality of the data distribution was verified using the Kolmogorov–Smirnov test. Paired or unpaired *t* tests or Mann–Whitney tests were used to assess differences for the inflammatory corneal injury model. For the DAMGO experiments, a Kruskal–Wallis test, followed by Dunn's post hoc least squares differences (PLSD) correction, or one-way or two way ANOVA, followed by Bonferroni's PLSD correction, was performed, depending on which was appropriate. The differences were considered significant for $p < 0.05$.

## 3. Results

### 3.1. MOR is expressed in the corneal nerve fibers and trigeminal primary sensory neurons in mice

We carried out immunohistochemistry experiments to determine whether MOR is expressed in the corneal nerve fibers and primary afferent neurons of the ophthalmic branch of the TG in control mice. MOR immunoreactivity was clearly detectable in PGP9.5-positive nerve fibers in mouse cornea (Fig. 1A). We also found MOR immunoreactivity in numerous primary sensory neuron somata (positive for beta III tubulin), located in the ophthalmic branch of the TG in mice (Fig. 1B). Moreover, MOR immunoreactivity was predominantly detected in primary sensory neurons of small (diameter < 25 μm) to medium (25−45 μm) size. The presence of the MOR in the corneal nerve fibers and afferent primary neurons of the ophthalmic branch of the TG under physiological conditions led us to further investigate the functional role of this receptor under conditions of inflammatory corneal pain.

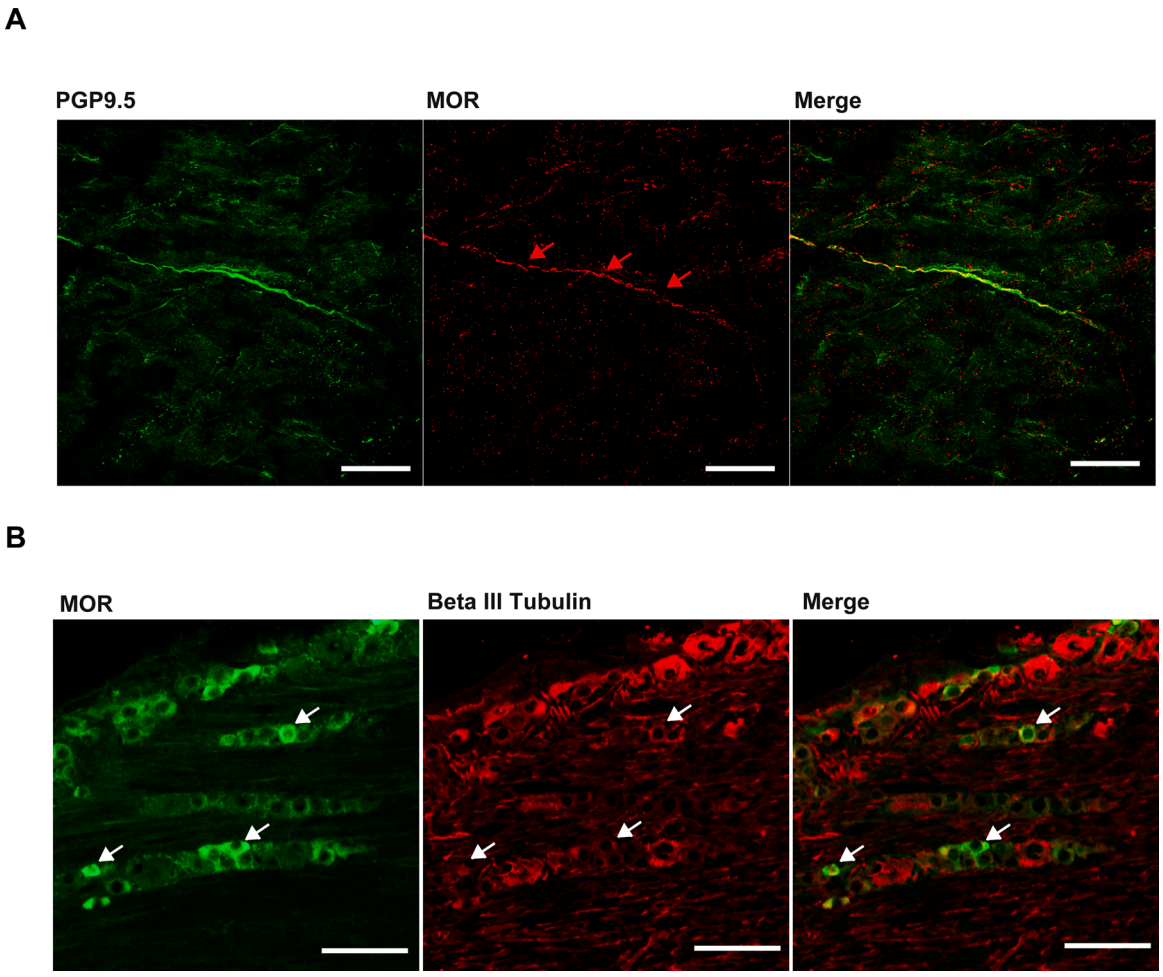


**Fig. 1.** Mu opioid receptor immunoreactivity in corneal nerves and primary afferent neurons in the TG of control mice.
(**A**) Confocal images showing MOR immunoreactivity in mouse corneal nerve fibers immuno-stained with the PGP9.5 neuronal marker (red arrows). Scale bar: 25 μm. (**B**) Images showing immunofluorescent staining for the MOR and beta III tubulin in the ophthalmic branch of the TG. Arrows indicate afferent TG sensory neurons labelled by the MOR UMB3 antibody. Note the presence of MOR immunoreactivity in small- and medium-sized neurons. Scale bar: 100 μm.

### *3.2. Scraping/LPS animals exhibit alterations of the corneal integrity, mechanical corneal sensitivity, and ciliary nerve fiber activity*

We modelled corneal inflammatory pain using the scraping/LPS model that we previously developed and characterized [21]. Corneal scraping (*i.e.*, corneal nerve damage) was performed on day 1 (D1), combined with two instillations of LPS (50 μg) on D1 and D3, as previously described [21]. On D5, corneal integrity was evaluated in control and scraping/LPS mice by *in vivo* confocal microscopy (IVCM) (Fig. 2A). IVCM images taken on D5 for the corneal scraping/LPS mice clearly confirmed the presence of numerous hyper-reflective inflammatory cells in the corneal stroma (Fig. 2B, red arrows) and corneal inflammation in this model. We then evaluated mechanical corneal sensitivity using von Frey filaments for both groups of animals. On D1, before corneal scraping, the baseline mechanical threshold response was 0.30 ± 0.04 mN and was significantly lower than the basal values for the scraping/LPS-treated mice on D5 (0.17 ± 0.02 mN *vs* 0.30 ± 0.04 mN, $p < 0.05$, Fig. 2C), demonstrating the development of mechanical allodynia. We further evaluated whether inflammatory pain provoked changes of corneal nerve activity. Electrophysiological recordings of the ciliary nerve fibers showed differences between the control (Fig. 2D) and scraping/LPS (Fig. 2E) corneas. Indeed, quantification of the electrophysiological recordings showed significantly higher spontaneous ciliary nerve activity on D5 for scraping/LPS mice than control animals (40.1 ± 5.8 imp/s *vs* 27.4 ± 1.9 imp/s, $p < 0.05$; Fig. 2D, E, and F). Next, we investigated the responsiveness of polymodal corneal nociceptors using 30-s $CO_2$ pulses applied to control and scraping/LPS corneas. The latency of the impulse discharge evoked by the $CO_2$-pulse was significantly shorter for the scraping/LPS (4.7 ± 1.3 s) than control corneas (10.0 ± 1.2 s, $p < 0.05$; Fig. 2G, H, and I), indicating greater corneal responsiveness following corneal injury. There was no statistical difference in the firing frequency evoked by the stimulus between groups (5.6 ± 1.0 imp/s in control corneas *vs* 3.6 ± 0.9 imp/s in scraping/LPS corneas, Fig. 2J**).**

### *3.3. Inflammatory corneal pain induces the upregulation of MOR expression in the cornea and trigeminal ganglion*

Previous studies focusing on the spinal cord and dorsal root ganglia reported an increase in the peripheral expression of the MOR following inflammatory pain [36]. We investigated whether such modulation of the MOR also occurs in the corneal nerve fibers and trigeminal neurons of mice with corneal inflammatory pain (Fig. 3A). DAPI staining clearly confirmed alteration of the cornea, with cell infiltration in the stroma (red arrows) of the scraping/LPS mice relative to control corneas (Fig. 3B). This result corroborates *in vivo* confocal microscopy images of the cornea (see Fig. 3B) and is consistent with our previous results [21]. MOR immunoreactivity was higher in scraping/LPS than control corneas (Fig. 3**B and C**). Semi-quantitative analysis of MOR staining showed the stained area to be significantly greater in scraping/LPS than control

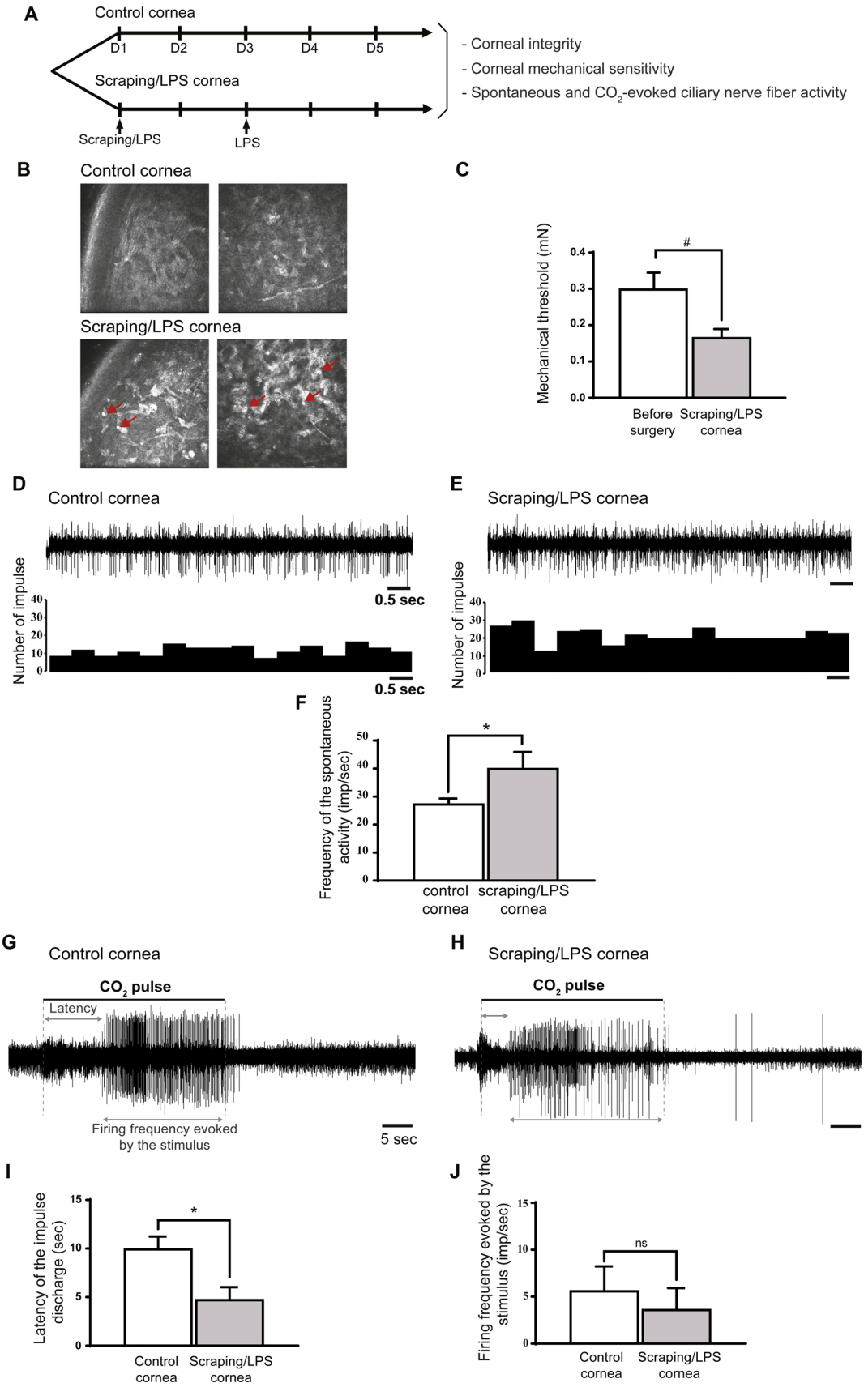


(caption on next page)

**Fig. 2.** Corneal inflammatory pain induces mechanical allodynia and increases the spontaneous and evoked activity of ciliary nerve fibers.
(**A**) Schematic diagram of the experiments. (**B**) *In vivo* confocal images (400 μm/400 μm) of the control and scraping/LPS corneas on D5. Damage to the superficial epithelium and inflammatory cells (red arrows) was observed in the scraping/LPS corneas relative to the control (non-injured) corneas. (**C**) Histogram showing the corneal mechanical sensitivity threshold, measured using von Frey filaments, which elicited a different blink response before surgery (white bar) and 5 days (D5) after corneal scraping/LPS (grey bar). (**D-E**) Traces illustrating the multiunit spontaneous ciliary nerve activity in the control (**D**) and scraping/LPS (**E**) corneas. (**F**) Histogram showing the mean value of the multiunit spontaneous firing frequency of the ciliary nerve fibers in the control corneas (white bar) and on D5 after corneal scraping/LPS (gray bar). (**G-H**) Traces illustrating the corneal responsiveness to a 30-s $CO_2$ pulse in control (**G**) and scraping/LPS (**H**) corneas. The black horizontal line represents the duration of the $CO_2$ pulse. (**I-J**) Histograms showing the latency of the impulse discharge (**I**) and the mean firing frequency evoked by the $CO_2$ stimulus (J) in the control corneas (white bars) and 5 days after corneal scraping/LPS (grey bars). N = 7–10 mice per group. Differences were analyzed using paired *t* or Mann-Whitney tests, depending on which was appropriate. * indicates a significant difference between the control and scraping/LPS groups. * $p < 0.05$.

corneas (3.55 ± 0.40 % *vs* 1.35 ± 0.06 %, $p < 0.001$, Fig. 3D). We hypothesized that corneal inflammation may also increase gene expression of MOR mRNA in the ophthalmic part of the TG. We thus investigated the expression of MOR mRNA in the ipsilateral ophthalmic branch of the TG using RNAscope® *in situ* hybridization on control and scraping/LPS mice (Fig. 4**A, B**). Images of fluorescent *in situ* hybridization showed abundant red punctate dots, corresponding to RNAscope MOR probes, in numerous trigeminal primary sensory neurons (Fig. 4B). *In situ* hybridization also confirmed that MOR mRNA expression was found in small- and medium-sized sensory neurons. Moreover, we detected MOR mRNA expression in the cytoplasm of primary sensory neurons, suggesting that MOR mRNA is readily available to be translated into protein.

We next performed semi-quantitative analysis of MOR expression in the ophthalmic part of the TG to determine whether corneal pain affects trigeminal MOR expression. Semi-quantitative analysis of the area covered by the MOR mRNA probe, as well as staining intensity, showed MOR mRNA expression to be significantly higher in the TG from scraping/LPS mice than those of control animals (intensity: $1.5 \times 10^6 \pm 0.2 \times 10^6$ AU *vs* $0.9 \times 10^6 \pm 0.1 \times 10^6$ AU, $p < 0.05$; area: 7.6 ± 0.8 % *vs* 4.8 ± 0.8 %, $p < 0.05$; Fig. 4C). Overall, these results show upregulation of the MOR in TG under conditions of corneal inflammatory pain.

### 3.4. Repeated topical treatment with DAMGO reduces spontaneous and stimulus-evoked ciliary nerve-fiber activity in the inflammatory corneal pain model

We further evaluated the chronic effects of *in vivo* instillation of DAMGO twice a day for five days on spontaneous (ongoing) ciliary nerve-fiber activity on the last day (D5) **(**Fig. 5**A). On D5, before the last instillation of PBS or DAMGO alone (50 μM), or naloxone methiodide (100 μM)/DAMGO (50 μM), the eyes were prepared for electrophysiological recordings. The basal spontaneous activity ($t_0$ values) on D5 was significantly lower in the *in vivo* DAMGO-treated scraping/LPS than PBS-treated scraping/LPS corneas (32.0 ± 4.5 imp/s *vs* 48.4 ± 5.5 imp/s, $p < 0.05$) (Fig. 5**B). The last DAMGO exposure did not modify the spontaneous ciliary nerve activity, which remained significantly lower than that of PBS-superfused corneas ($t_{15}$ values: 28.7 ± 5.1 imp/sec and 54.9 ± 7.2 imp/sec, $p < 0.01$; Fig. 5**B, C, and D**). Repeated topical naloxone methiodide administration prevented the inhibitory effects of DAMGO at $t_0$ (51.2 ± 2.7 imp/s *vs* 32.0 ± 4.5 imp/s, $p < 0.01$, Fig. 5B) and the effect was also observed 15 min after the last naloxone methiodide superfusion (45.6 ± 2.3 imp/s *vs* 28.7 ± 5.1 imp/s, $p < 0.05$, Fig. 5**B and E**). These results confirm the involvement of opioid receptors at the ocular surface in the effects mediated by DAMGO.

The responsiveness of the polymodal corneal nerve fibers to chemical stimulation was thereafter evaluated on D5 at $t_0$ and $t_{15}$ after the last administration of either PBS, DAMGO (50 μM), or naloxone methiodide (100 μM)/DAMGO (50 μM) **(**Fig. 6**A, B, and C). At $t_0$, there was no significant difference in the latency between DAMGO- and PBS-treated animals (5.4 ± 0.7 s *vs* 3.2 ± 0.7 s, Fig. 6**B). In contrast, the latency was significantly higher 15 min after the last DAMGO application than for the PBS group (11.5 ± 2.9 s *vs* 3.3 ± 1.1 s, $p < 0.01$; Fig. 6**B, D, and E). Furthermore, the $t_{15}$ value for the DAMGO group was significantly higher than the $t_0$ value (11.5 ± 2.9 s *vs* 5.4 ± 0.7 s, $p < 0.01$), confirming an additional effect of topical DAMGO on corneal nerve activity. Finally, although there was no difference in the latency at $t_0$ between the corneas treated with DAMGO and those treated with DAMGO and naloxone methiodide- (3.7 ± 0.8 s *vs* 5.4 ± 0.7 s), naloxone methiodide exposure markedly blunted the increase of latency induced by DAMGO at $t_{15}$ (3.9 ± 1.1 s *vs* 11.5 ± 2.9 s, $p < 0.001$; Fig. 6**B, E, and F).**

The firing frequency induced by a 30-s $CO_2$ pulse before the last drug application ($t_0$) was not significantly different between DAMGO- and PBS-treated corneas (2.4 ± 0.6 imp/s *vs* 4.2 ± 0.6 imp/s, respectively, Fig. 6C). However, the last DAMGO application ($t_{15}$) significantly reduced the firing frequency relative to that of PBS-treated corneas (1.9 ± 0.4 imp/s *vs* 5.2 ± 1.3 imp/s relative to PBS superfusion, $p < 0.05$; Fig. 6**C, D, and E).** The application of naloxone methiodide completely prevented the effects of DAMGO, both at $t_0$ (5.7 ± 1.1 imp/s *vs* 2.4 ± 0.6 imp/s, $p < 0.05$, Fig. 6C) and 15 min after the drug superfusion (5.9 ± 1.2 imp/s *vs* 1.9 ± 0.4 imp/s, $p < 0.05$; Fig. 6**C, E, and F**).

### 3.5. Repeated topical treatment with DAMGO reduces mechanical and chemical hypersensitivity of scraping/LPS mice

We then explored whether chronic administration of topical DAMGO could alleviate the corneal mechanical allodynia associated with scraping/LPS. The mechanical threshold response was measured using von Frey filaments, before surgery (basal values in naïve mice) and on D5 (at $t_0$ and $t_{15}$ after the last drug instillation) (Fig. 7**A). Before surgery (naïve animals), there was no significant difference in the mechanical threshold between the animals (0.31 ± 0.03 mN, 0.27 ± 0.03 mN, and 0.26 ± 0.03 mN for the PBS, DAMGO, and naloxone methiodide/DAMGO groups, respectively) (Fig. 7**B). Although the mechanical threshold was similar between DAMGO-treated mice and those of the PBS group at $t_0$ on D5 (0.30 ± 0.03 mN *vs* 0.22 ± 0.02 mN) (**Fig. 7**B), the mechanical threshold after the last DAMGO administration was significantly higher (less mechanical allodynia) 15 min. after its topical instillation than that of PBS (0.46 ± 0.05 mN *vs* 0.24 ± 0.02 mN, $p < 0.001$) (Fig. 7**B). Further pharmacological experiments proved the involvement of corneal opioid receptors, as naloxone methiodide exposure completely blunted the effect of DAMGO at $t_{15}$ (0.25 ± 0.03 mN *vs* 0.46 ± 0.05 mN, $p < 0.001$; Fig. 7B). Finally, we tested whether DAMGO is also able to reduce the nociceptive response induced by chemical stimulation by applying capsaicin (10 μM), the ligand of the transient receptor potential vanilloid 1 (TRPV1) channel, 15 min after the last instillation of PBS, DAMGO, or naloxone methiodide/DAMGO on D5. At D5, repeated topical DAMGO application resulted in significantly lower (by -25 %) palpebral closure time, an index of ocular discomfort/pain, than for animals receiving PBS (217.2 ± 1 3.4 s *vs* 287.8 ± 16.5 s, $p < 0.05$, Fig. 7C). The topical instillation of naloxone methiodide completely prevented the antinociceptive effects of DAMGO (332.8 ± 32.9 s *vs* 217.2 ± 13.4 s, $p < 0.01$, Fig. 7C), thus demonstrating that the analgesic effect of this mu opioid agonist on capsaicin-evoked responses was mediated by opioid receptors expressed at the ocular surface. 4. Discussion

Here, we show that (1) the MOR is detected in the corneal nerve fibers and trigeminal primary sensory neurons of mice, (2) inflammatory corneal pain induces upregulation of MOR expression in the cornea and TG, (3) topical administrations of DAMGO, a MOR-selective agonist, reduces mechanical allodynia and topical capsaicin-induced corneal

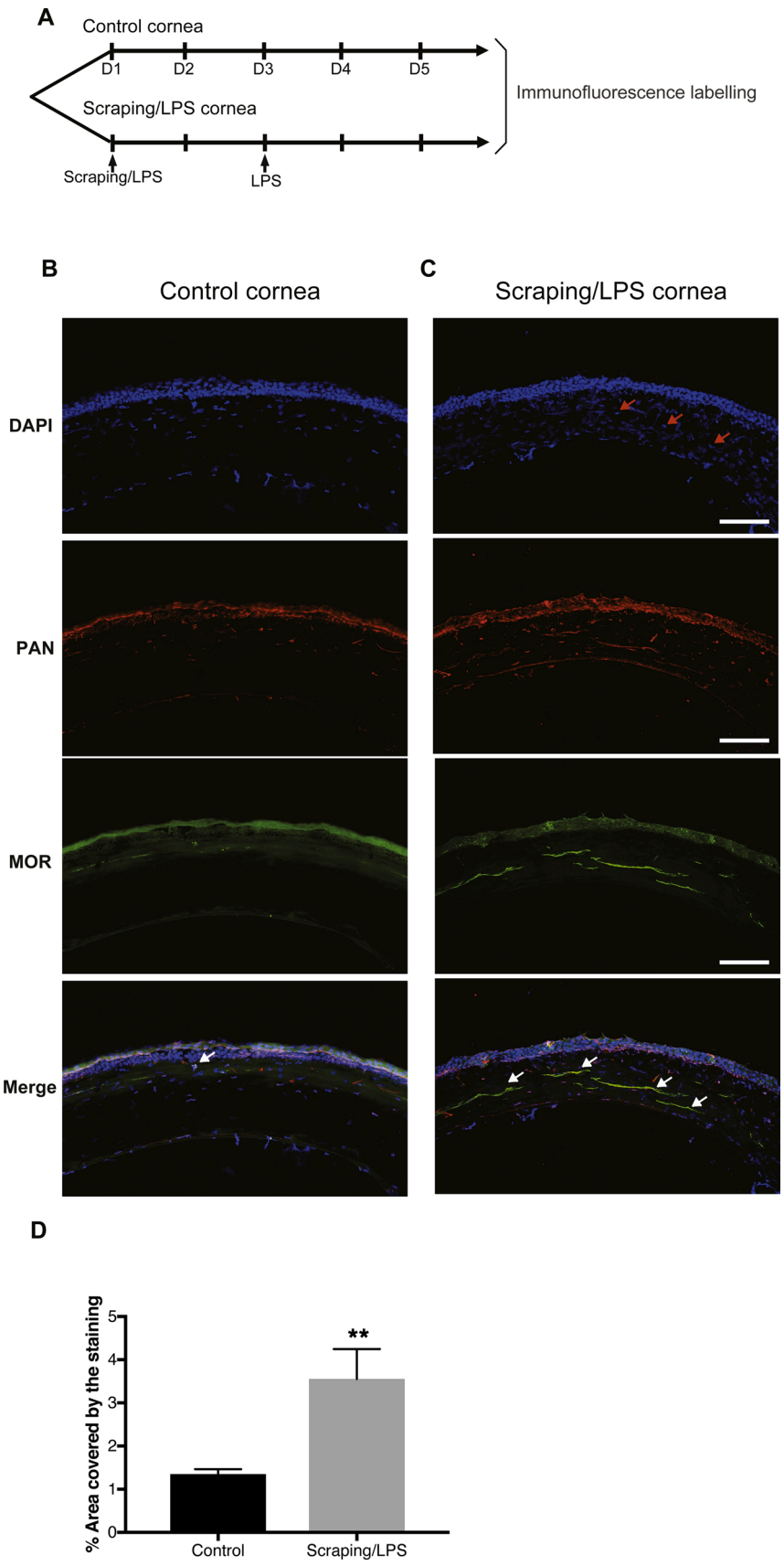


**Fig. 3.** MOR immunoreactivity increased in cornea under corneal pain conditions.

(**A**) Schematic diagram of the experiments. (**B-C**) Confocal images of control (B) and scraping/LPS (C) corneas stained with DAPI (blue), the PAN neuronal marker (red), and MOR antibodies (green). DAPI staining showed cell infiltration in the corneal stroma for the scraping/LPS mice (**C,** red arrows) relative to the control animals (**B**). Note that MOR immunoreactivity is higher in the inflamed (**C**, white arrows) than control cornea (**B**). Histograms showing the semi-quantitative analysis of the percentage of the area covered by MORs in control and scraping/LPS corneas (D). The difference between groups was analyzed using the unpaired *t* test. ** indicates a significant difference between the control and scraping/LPS groups. **$p < 0.01$. Scale bar: 100 μm

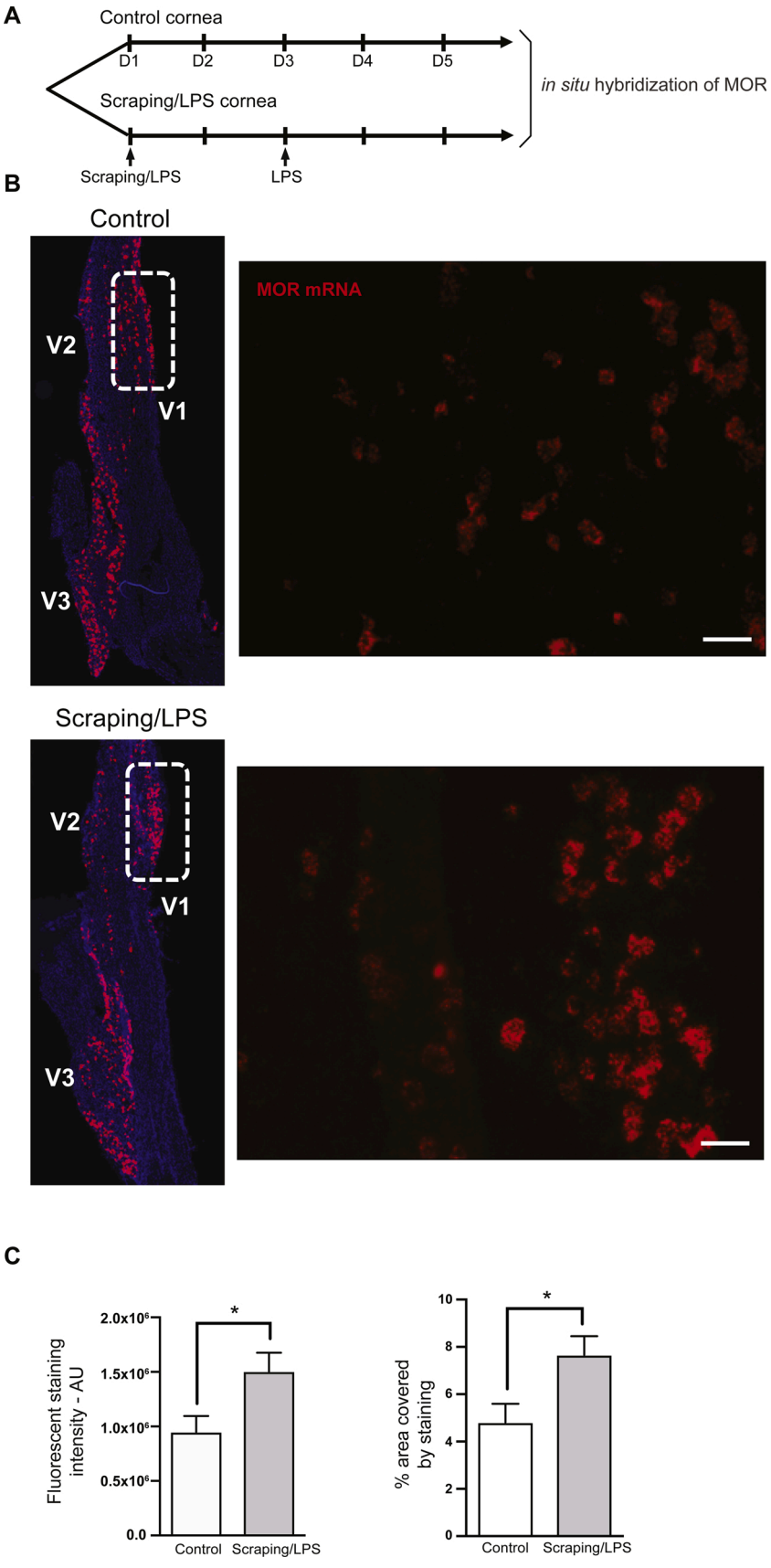


**Fig. 4.** Mu opioid receptor RNA expression increases in the trigeminal ganglion during inflammatory corneal pain.
(**A**) Schematic diagram of the experiments. (**B**) MOR mRNA levels were evaluated by *in situ* hybridization RNAscope technology. Images for MOR mRNA (red) and nuclei counterstained with DAPI (blue) in the TG from control and scraping/LPS mice are shown. The dashed-line rectangle represents the ophthalmic branch (V1) of the TG. The high magnification shows the primary sensory neurons that express MOR mRNA in the ophthalmic branch of TG. Scale bars: 50 μm. (**C**) Histograms showing the semi-quantitative analysis of the fluorescence staining intensity of MOR (left graph) and the percentage of area covered by MOR (right graph) in the ophthalmic branch of TG in control mice (white bars) and scraping/LPS animals (grey bars). MOR mRNA levels were analyzed using Fiji (ImageJ). N = 5 mice per group. The difference between groups was analyzed using an unpaired *t* test. * indicates a significant difference between the control and scraping/LPS groups. * $p < 0.05$. V1: ophthalmic branch, V2: maxillary branch, V3: mandibular branch of the TG.

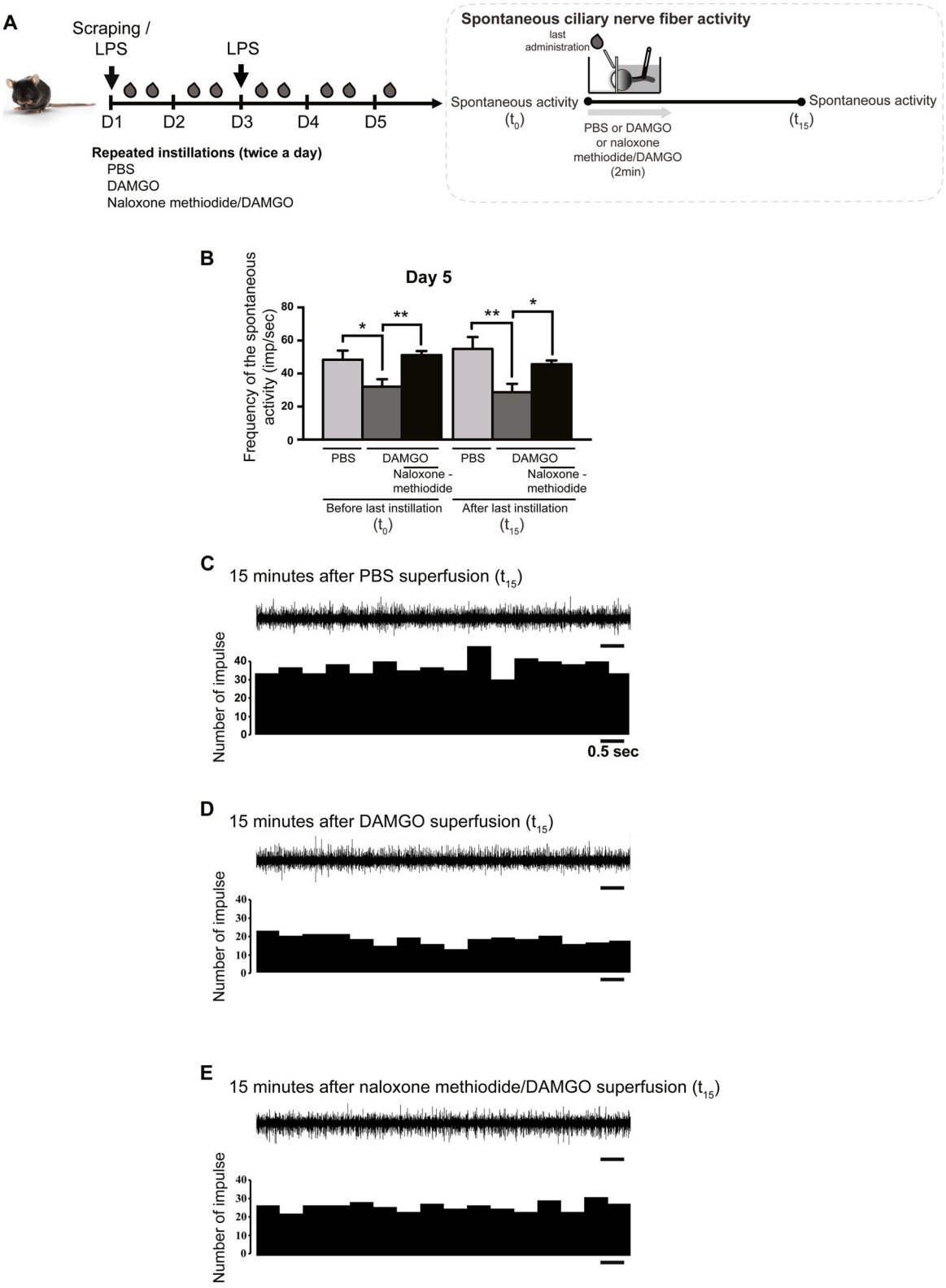


**Fig. 5.** Repeated topical instillations of DAMGO prevents the increase in spontaneous activity of ciliary nerve fibers induced by corneal pain.
(**A**) Schematic diagram of the experiments. Spontaneous ciliary nerve-fiber activity was determined before ($t_0$) and 15 min ($t_{15}$) after the last drug exposure. (**B**) Histogram showing the mean value of the spontaneous firing frequency of ciliary nerve fibers on D5 at $t_0$ and $t_{15}$ after the last instillation of PBS (light grey bars), DAMGO (dark grey bars), or naloxone methiodide followed by DAMGO (black bars). **(C–E)** Traces illustrating the spontaneous ciliary nerve-fiber activity on D5 at $t_{15}$ after the last instillation of PBS (C), DAMGO (D), or naloxone methiodide followed by DAMGO **(E).** N = 5–10 mice per group. The differences between groups were analyzed by one-way ANOVA. * indicates a significant difference between DAMGO and PBS alone or naloxone methiodide followed by DAMGO. *$p < 0.05$, **$p < 0.01$.

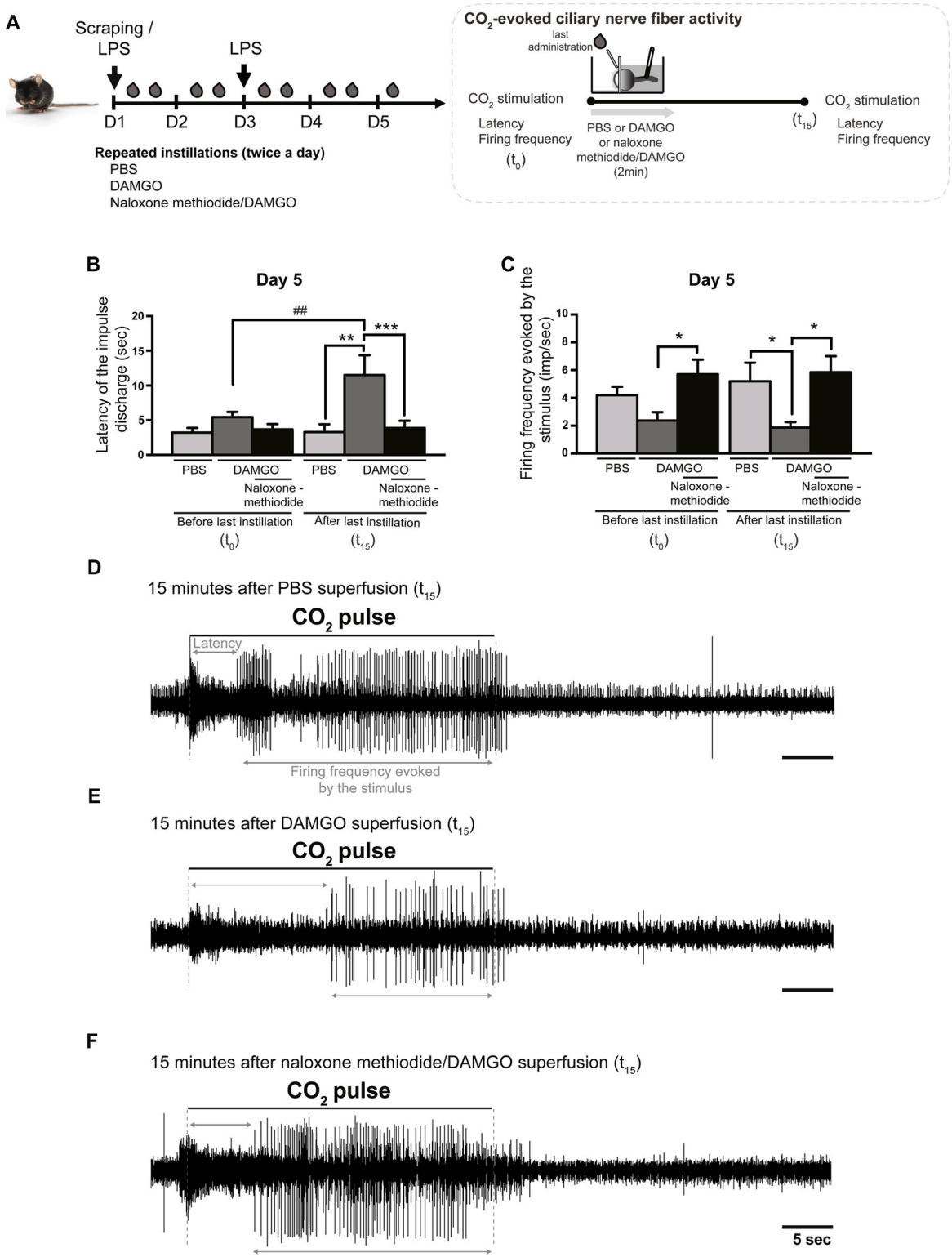


**Fig. 6.** Repeated instillations of DAMGO reduces the responsiveness of ciliary nerves to chemical stimulation in the inflammatory corneal pain model.
(**A**) Schematic diagram of the experiments performed 5 days after scraping/LPS treatment. Time 0 ($t_0$) and $t_{15}$ values correspond to the latency of the impulse discharge or the firing frequency evoked by the stimulus, measured before and 15 min after drug superfusion, respectively. **(B–C)** Histograms showing the latency of the impulse discharge **(B)** and the mean firing frequency evoked by the $CO_2$ pulse stimulus **(C)** on D5 at $t_0$ and $t_{15}$ after PBS (light grey bars), DAMGO alone (dark gray bars), or naloxone methiodide followed by DAMGO (black bars) administration **(D–F)** Traces illustrating the corneal responsiveness to chemical stimulation, with a 30-s $CO_2$ pulse, 15 min after the superfusion of PBS (**D**), DAMGO (**E**), or naloxone methiodide followed by DAMGO (**F**). The black line represents the duration of the $CO_2$ pulse. N = 5–10 mice per group. The differences between groups were analyzed by one-way ANOVA, Kruskal and Wallis tests, or two-way ANOVA, depending on which was appropriate. * indicates a significant difference between the DAMGO and PBS alone or naloxone methiodide followed by DAMGO. $^{\#}$ indicates a significant difference between $t_0$ and $t_{15}$ after DAMGO instillation. *$p < 0.05$, **$p < 0.01$, ***$p < 0.001$, $^{\#\#}p < 0.01$.

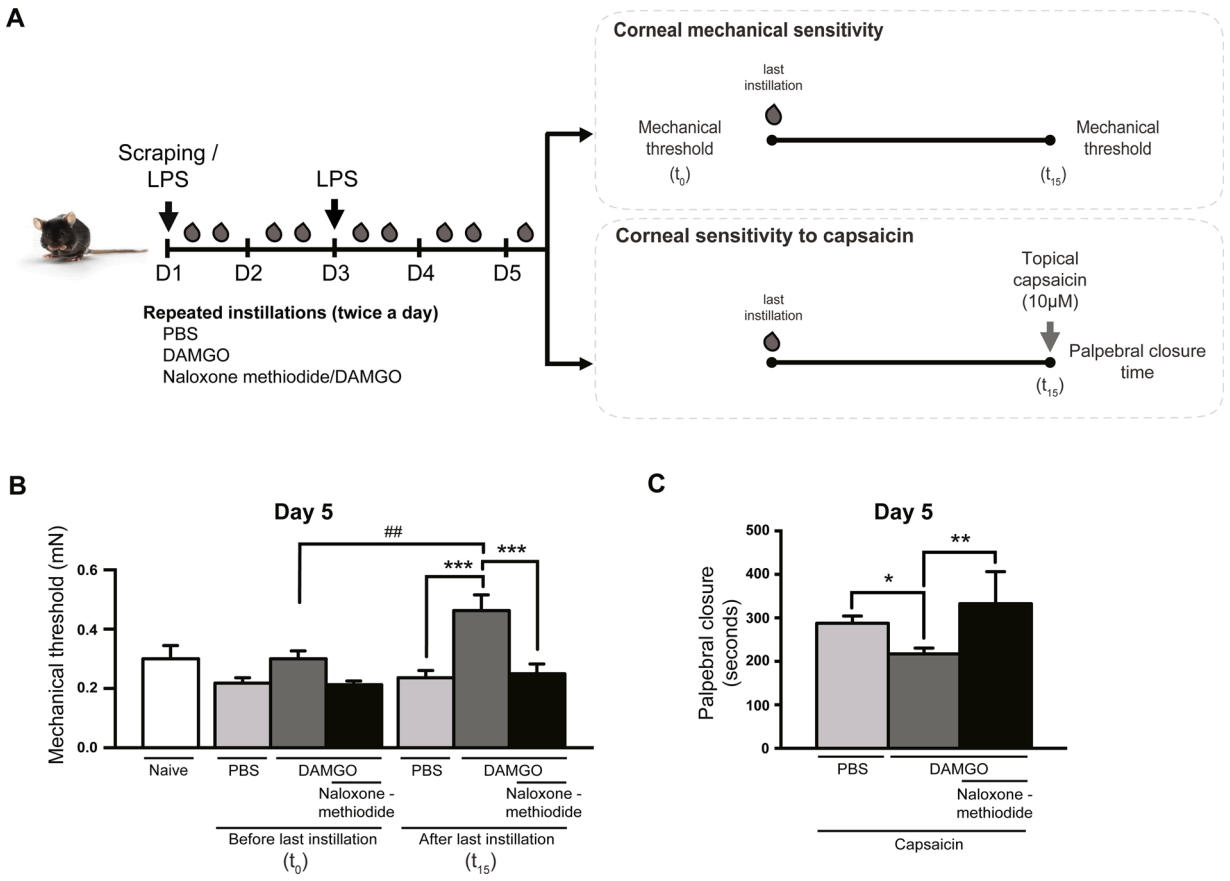


**Fig. 7.** Repeated topical instillations of DAMGO induces analgesic effects by decreasing the mechanical allodynia and pain induced by topical capsaicin. (**A**) Schematic diagram of the experiments. (**B**) Mechanical corneal sensitivity in naive mice (white bar) and on D5 after corneal scraping/LPS, before ($t_0$) and 15 min ($t_{15}$) after the last instillation of PBS (light gray bars), DAMGO alone (dark gray bars), or naloxone methiodide followed by DAMGO (black bars). (**C**) The palpebral closure time after deposition of a drop of capsaicin onto the cornea on D5, at $t_{15}$ after the last instillation of PBS (light gray bar), DAMGO alone (dark gray bar), or naloxone methiodide followed by DAMGO (black bar). N = 8–11 mice per group for mechanical corneal sensitivity 5–6 per group for the capsaicin test. The differences between groups were analyzed by one-way or two-way ANOVA, depending on which was appropriate. * indicates a significant difference between the PBS, DAMGO, and naloxone methiodide/DAMGO groups. # indicates a significant difference between $t_0$ (before) and $t_{15}$ after DAMGO instillation. *$p < 0.05$, **$p < 0.01$, ***$p < 0.001$, ##$p < 0.01$.

pain, and (4) topical instillation of DAMGO prevents the increase of the spontaneous activity of ciliary nerve fibers associated with corneal inflammatory pain.

The management of ocular pain is still a therapeutic challenge and no specific pharmacological approaches to treat corneal pain are yet available. In the clinic, topical anesthetics are used to reduce acute pain, but their long-term use is not recommended due to their shortcomings (*e.g.*, corneal ulceration) [37,38]. We recently demonstrated that repeated ocular administration of PL265, a dual inhibitor of the enkephalin-degrading enzymes, neutral endopeptidase and aminopeptidase N, exerts anti-nociceptive effects in several models of corneal pain [21]. This study revealed that targeting opioid receptors could be an effective approach to reduce corneal pain. However, it did not assess the contribution of the MOR, the potential changes of MOR expression in the cornea and TG neurons, or the beneficial effects of ocular administration of MOR agonists on corneal nerve-fiber activity and pain-like behavior.

Our anatomical data demonstrate, for the first time, that the MOR can be detected in the corneal nerves of mice. This observation is consistent with the study of Zollner, who reported MOR immunoreactivity of corneal nerves in the human cornea [39]. Moreover, clear staining was found in the small- and medium-sized neurons located in the ophthalmic branch of the TG. This is consistent with a previous finding of Ichikama, in which MOR immunoreactivity was also not found in small or medium-sized trigeminal neurons [40].

Several studies have reported that the expression of opioid receptors increases under pathological conditions, such as injury and inflammation, leading to improved agonist efficacy of peripheral nerve terminals [36,41]. We observed a quantitative increase in MOR expression in the cornea and ophthalmic branch of TG under conditions of pain. These changes in MOR expression provide novel clues about the involvement and activation of the endogenous opioid system during inflammatory corneal pain.

Corneal sensory information is relayed by myelinated A-delta and unmyelinated C-fibers [33,42,43], which have a small diameter and respond to chemical, mechanical, and thermal noxious stimulation of the cornea. The presence of MORs, both in corneal nerves and the small afferent neurons of TG, provides an anatomical basis to support the possible modulation of MOR activity by MOR agonists. Although a large number of studies have proven that MOR agonists, such as DAMGO, reduce pain in various peripheral pain models [44,45], the topical analgesic effects of DAMGO in a corneal pain model are still unknown. Here, we provide evidence for the antinociceptive effects of DAMGO by showing reduced mechanical corneal allodynia and capsaicin-induced thermal hyperalgesia in mice. This last result is consistent with those of the study of Wenk [22], who reported that topical application of morphine attenuated capsaicin-induced blinking in acute chemical injury in rats.

Previous *in vivo* and whole-cell patch-clamp studies on dorsal root neurons have demonstrated that MOR activation decreases pain responses and capsaicin-induced TRPV1 currents in a naloxone-sensitive

manner [46]. Currently, it is difficult to determine whether MOR activation modifies TRPV1 currents in corneal nerve terminals, as previously reported in the primary sensory neuron in dorsal root ganglia. Further studies are necessary to test this hypothesis. Moreover, complete reversion of the antinociceptive effects of DAMGO by naloxone methiodide (a non-selective antagonist of opioid receptors that does not cross the blood-brain barrier [47]) confirms that the DAMGO-induced analgesic effects are mediated by peripheral MOR activation. The marked antinociceptive effect of DAMGO instillation, together with the increased expression of MOR in TG neurons, reinforces the hypothesis that the MORs within these structures are involved in the peripheral modulation of inflammatory pain noxious inputs.

*Ex vivo* and *in vivo* behavior (pain-like behavioral tests) demonstrated that mice treated with repeated topical ocular DAMGO do not develop exacerbated excitability of corneal afferents or mechanical hypersensitivity. This is in contrast to studies that observed increased sensitivity to pain after peripheral MOR activation and that repeated injection of DAMGO at the site of mechanical nociception testing (hind paw) produced changes in nociceptor function [48–50]. The differences between the aforementioned study and ours could be explained by the nature of the tissue (skin *versus* cornea) and the nociceptive pathways involved (dorsal root ganglion *vs* trigeminal ganglion).

A link between corneal nerve damage, inflammation, and the ongoing activity of corneal nerve fibers has been previously reported in various mouse models of corneal injury [10,30,51]. Here, we used a preclinical model of corneal inflammatory pain consisting of the combination of corneal scraping (corneal nerve damage) and LPS administration [21,51]. The two instillations of LPS at D1 and D3 were used to maintain the release of inflammatory mediators that activate and sensitize the nociceptive system. Both factors (inflammation and corneal nerve damage) are important for studies on the pathophysiological mechanisms of ocular inflammatory pain. In addition, this model is characterized by infiltration of the inflammatory monocyte/macrophage population ($CD11b^+$ cells) in the cornea [21], as confirmed by *in vivo* confocal microscopy. These recruited inflammatory cells ultimately release a number of proinflammatory cytokines, *i.e.*, IL-1, IL-6, and TNF-alpha [28,52], in the proximity of the corneal fibers. These local inflammatory responses could explain the increase of the nociceptive mechanical and chemical (capsaicin) sensitivity found in our scraping/LPS model. The infiltration of inflammatory cells is known to affect the activity of corneal nerve terminals, contributing to the sensitization of nociceptors and reducing the responsiveness of cold thermoreceptors [28,52]. Peripheral sensitization is characterized by a specific change in the excitability of these nerve fibers by an increase in their ongoing and stimulus-evoked nerve activity [2,53]. Thus, the increased ongoing firing activity of the ciliary nerve, observed in the scraping/LPS corneas on D5, may have largely resulted from changes in the excitability of the cold-sensitive nerve fibers induced by corneal injury. This is a condition that triggersTRPM8 channel expression and thus increases ongoing firing activity [2,51,54].

Another important finding from our experiments is that repeated topical instillation of DAMGO modulates the electrophysiological properties and activity of corneal neurons. Previous studies have reported that exogenous and endogenous opioids are able to attenuate the excitability or propagation of the action potentials of peripheral nociceptors [55,56]. Injection of DAMGO into the brainstem (Vc/C1 region) was shown to reduce the response of second-order corneal neurons to $CO_2$ stimulation of the cornea in rats [4]. Here, we demonstrate, for the first time, that repeated administration of DAMGO diminishes the increased spontaneous ciliary nerve activity associated with corneal pain, as well as the corneal polymodal response to $CO_2$ stimulation. The functional changes of the corneal polymodal nociceptors and cold thermoreceptors induced by DAMGO were entirely blunted by naloxone methiodide, demonstrating that the effects of DAMGO are directly mediated by MORs expressed by the corneal nerves. Importantly, these electrophysiological changes corroborate the analgesic effects (decreased mechanical allodynia and topical capsaicin-induced pain) that we report here.

## 4. Conclusions

We demonstrate that MOR expression increases in corneal nerve fibers and trigeminal neurons under conditions of corneal pain, as well as the beneficial effects of repeated ocular administration of DAMGO on corneal nerve hyperactivity and corneal allodynia. Our findings contribute to a literature suggesting that topical opioid agonists could be repurposed for the treatment of ocular pain. Thus, pharmacological activation of corneal MORs may be a potential therapeutic target for the treatment of inflammatory ocular pain.

## Author contributions

F. Joubert designed and performed the experiments, analyzed and interpreted the data, generated the figures, discussed the results and their significance, and wrote the manuscript. A. Guerrero-Moreno performed the immunohistochemistry experiments and analyzed the *in situ* experiments. D. Fakih performed the RNAscope experiments. E. Reboussin performed the confocal image acquisition. C. Gaveriaux-Ruff provided scientific input and commented on the manuscript. MC. Acosta and J. Gallar helped in the acquisition and analysis of the electrophysiological recordings and commented on the manuscript. JA. Sahel provided scientific input. L. Bodineau helped in the electrophysiological experiments and commented on the manuscript. C. Baudouin discussed the results and their significance and commented on the manuscript. W. Rostène discussed the results and their significance and commented on the manuscript. S. Melik-Parsadaniantz interpreted the data, discussed the results and their significance, and commented on the manuscript. A. Réaux-Le Goazigo designed and supervised all experiments, obtained the funding, interpreted the data, discussed the results and their significance, and wrote the manuscript. All authors approved the final version of the article.

## Declaration of Competing Interest

The authors report no declarations of interest.

## Acknowledgements

We thank Stéphane Fouquet (imagery platform) and the staff of the animal house facilities at the Institut de la Vision and Institut du Cerveau et de la Moelle for their help. We also thank Yanis Merabet for technical assistance with the UMB3 staining in the cornea and Katia Marazova for fruitful discussions. This work was supported by the Sorbonne Université and the Institut National de la Santé et de la Recherche Médicale, the ANR, LabEx LIFESENSES (ANR-10-LABX-65), and IHU FOReSIGHT (ANR-18-IAHU-01). Fanny Joubert was supported by a Fondation de France post-doc fellowship grant. Adrian Guerrero Moreno was funded by a H2020-MSCA-ETN program (IT-DED$^3$) (Grant Agreement 765608). The text has been edited for English by Alex Edelman & Associate.

## Appendix A. Supplementary data

Supplementary material related to this article can be found, in the online version, at doi:https://doi.org/10.1016/j.biopha.2020.110794.

## References

[1] F. Stapleton, M. Alves, V.Y. Bunya, I. Jalbert, K. Lekhanont, F. Malet, K.S. Na, D. Schaumberg, M. Uchino, J. Vehof, et al., TFOS DEWS II epidemiology report, Ocul. Surf. 15 (2017) 334–365.

[2] A.E. Levitt, A. Galor, A.R. Chowdhury, E.R. Felix, C.D. Sarantopoulos, G.Y. Zhuang, D. Patin, W. Maixner, S.B. Smith, E.R. Martin, R.C. Levitt, Evidence that dry eye

represents a chronic overlapping pain condition, Mol. Pain 13 (2017), 1744806917729306.
[3] A. Galor, H.R. Moein, C. Lee, A. Rodriguez, E.R. Felix, K.D. Sarantopoulos, R. C. Levitt, Neuropathic pain and dry eye, Ocul. Surf. 16 (2018) 31–44.
[4] H. Hirata, S. Takeshita, J.W. Hu, D.A. Bereiter, Cornea-responsive medullary dorsal horn neurons: modulation by local opioids and projections to thalamus and brain stem, J. Neurophysiol. 84 (2000) 1050–1061.
[5] A.J. Rozsa, R.W. Beuerman, Density and organization of free nerve endings in the corneal epithelium of the rabbit, Pain 14 (1982) 105–120.
[6] C.F. Marfurt, R.E. Kingsley, S.E. Echtenkamp, Sensory and sympathetic innervation of the mammalian cornea. A retrograde tracing study, Invest. Ophthalmol. Vis. Sci. 30 (1989) 461–472.
[7] J.J. Ivanusic, R.J. Wood, J.A. Brock, Sensory and sympathetic innervation of the mouse and guinea pig corneal epithelium, J. Comp. Neurol. 521 (2013) 877–893.
[8] C.F. Marfurt, D.R. Del Toro, Corneal sensory pathway in the rat: a horseradish peroxidase tracing study, J. Comp. Neurol. 261 (1987) 450–459.
[9] P.S. Launay, D. Godefroy, H. Khabou, W. Rostene, J.A. Sahel, C. Baudouin, S. Melik-Parsadaniantz, Reaux-Le Goazigo A: combined 3DISCO clearing method, retrograde tracer and ultramicroscopy to map corneal neurons in a whole adult mouse trigeminal ganglion, Exp. Eye Res. (2015).
[10] F. Joubert, M.D.C. Acosta, J. Gallar, D. Fakih, J.A. Sahel, C. Baudouin, L. Bodineau, S. Melik Parsadaniantz, Reaux-Le Goazigo A: effects of corneal injury on ciliary nerve fibre activity and corneal nociception in mice: a behavioural and electrophysiological study, Eur. J. Pain 23 (2019) 589–602.
[11] M.C. Acosta, C. Luna, S. Quirce, C. Belmonte, J. Gallar, Corneal sensory nerve activity in an experimental model of UV keratitis, Invest. Ophthalmol. Vis. Sci. 55 (2014) 3403–3412.
[12] S. Gonzalez-Rodriguez, M.A. Quadir, S. Gupta, K.A. Walker, X. Zhang, V. Spahn, D. Labuz, A. Rodriguez-Gaztelumendi, M. Schmelz, J. Joseph, et al., Polyglycerol-opioid conjugate produces analgesia devoid of side effects, Elife (2017) 6.
[13] C. Stein, M. Schafer, A.H. Hassan, Peripheral opioid receptors, Ann. Med. 27 (1995) 219–221.
[14] E. Erbs, L. Faget, G. Scherrer, A. Matifas, D. Filliol, J.L. Vonesch, M. Koch, P. Kessler, D. Hentsch, M.C. Birling, et al., A mu-delta opioid receptor brain atlas reveals neuronal co-occurrence in subcortical networks, Brain Struct. Funct. 220 (2015) 677–702.
[15] D. Wang, V.L. Tawfik, G. Corder, S.A. Low, A. Francois, A.I. Basbaum, G. Scherrer, Functional divergence of Delta and mu opioid receptor organization in CNS pain circuits, Neuron 98 (2018) 90–108, e105.
[16] C. Gaveriaux-Ruff, Opiate-induced analgesia: contributions from mu, delta and kappa opioid receptors mouse mutants, Curr. Pharm. Des. 19 (2013) 7373–7381.
[17] P. Richebe, A. Cahana, C. Rivat, Tolerance and opioid-induced hyperalgesia. Is a divorce imminent? Pain 153 (2012) 1547–1548.
[18] V.B.P. Pereira, R. Garcia, A.A.M. Torricelli, A. Mukai, S.J. Bechara, Codeine plus acetaminophen for pain after photorefractive keratectomy: a randomized, double-blind, placebo-controlled add-on trial, Cornea 36 (2017) 1206–1212.
[19] G. Dieckmann, S. Goyal, P. Hamrah, Neuropathic corneal pain: approaches for management, Ophthalmology 124 (2017) S34–S47.
[20] A.N. Siedlecki, S.D. Smith, A.R. Siedlecki, S.M. Hayek, R.R. Sayegh, Ocular pain response to treatment in dry eye patients, Ocul. Surf. 18 (2020) 305–311.
[21] A. Reaux-Le Goazigo, H. Poras, C. Ben-Dhaou, T. Ouimet, C. Baudouin, M. Wurm, Melik Parsadaniantz S: dual enkephalinase inhibitor PL265: a novel topical treatment to alleviate corneal pain and inflammation, Pain 160 (2019) 307–321.
[22] H.N. Wenk, M.N. Nannenga, C.N. Honda, Effect of morphine sulphate eye drops on hyperalgesia in the rat cornea, Pain 105 (2003) 455–465.
[23] S.M. Thomson, J.A. Oliver, D.J. Gould, M. Mendl, E.A. Leece, Preliminary investigations into the analgesic effects of topical ocular 1% morphine solution in dogs and cats, Vet. Anaesth. Analg. 40 (2013) 632–640.
[24] J. Stiles, C.N. Honda, S.G. Krohne, E.A. Kazacos, Effect of topical administration of 1% morphine sulfate solution on signs of pain and corneal wound healing in dogs, Am. J. Vet. Res. 64 (2003) 813–818.
[25] G.A. Peyman, M.H. Rahimy, M.L. Fernandes, Effects of morphine on corneal sensitivity and epithelial wound healing: implications for topical ophthalmic analgesia, Br. J. Ophthalmol. 78 (1994) 138–141.
[26] E.G. Faktorovich, A.I. Basbaum, Effect of topical 0.5% morphine on postoperative pain after photorefractive keratectomy, J. Refract. Surg. 26 (2010) 934–941.
[27] R. Moshourab, C. Stein, Fentanyl decreases discharges of C and A nociceptors to suprathreshold mechanical stimulation in chronic inflammation, J. Neurophysiol. 108 (2012) 2827–2836.
[28] P.S. Launay, E. Reboussin, H. Liang, K. Kessal, D. Godefroy, W. Rostene, J.A. Sahel, C. Baudouin, S. Melik Parsadaniantz, A. Reaux Le Goazigo, Ocular inflammation induces trigeminal pain, peripheral and central neuroinflammatory mechanisms, Neurobiol. Dis. 88 (2016) 16–28.
[29] M.C. Acosta, C. Luna, S. Quirce, C. Belmonte, J. Gallar, Changes in sensory activity of ocular surface sensory nerves during allergic keratoconjunctivitis, Pain 154 (2013) 2353–2362.
[30] D. Fakih, Z. Zhao, P. Nicolle, E. Reboussin, F. Joubert, J. Luzu, A. Labbe, W. Rostene, C. Baudouin, S. Melik Parsadaniantz, A. Reaux-Le Goazigo, Chronic dry eye induced corneal hypersensitivity, neuroinflammatory responses, and synaptic plasticity in the mouse trigeminal brainstem, J. Neuroinflammation 16 (2019) 268.
[31] F. Bech, O. Gonzalez-Gonzalez, E. Artime, J. Serrano, I. Alcalde, J. Gallar, J. Merayo-Lloves, C. Belmonte, Functional and morphologic alterations in mechanical, polymodal, and cold sensory nerve fibers of the Cornea Following Photorefractive Keratectomy, Invest. Ophthalmol. Vis. Sci. 59 (2018) 2281–2292.
[32] J. He, T.L. Pham, A.H. Kakazu, H.E.P. Bazan, Remodeling of substance P sensory nerves and transient receptor potential melastatin 8 (TRPM8) cold receptors after corneal experimental surgery, Invest. Ophthalmol. Vis. Sci. 60 (2019) 2449–2460.
[33] A. Alamri, R. Bron, J.A. Brock, J.J. Ivanusic, Transient receptor potential cation channel subfamily V member 1 expressing corneal sensory neurons can be subdivided into at least three subpopulations, Front. Neuroanat. 9 (2015) 71.
[34] A. Lupp, N. Richter, C. Doll, F. Nagel, S. Schulz, UMB-3, a novel rabbit monoclonal antibody, for assessing mu-opioid receptor expression in mouse, rat and human formalin-fixed and paraffin-embedded tissues, Regul. Pept. 167 (2011) 9–13.
[35] Y. Cui, S.B. Ostlund, A.S. James, C.S. Park, W. Ge, K.W. Roberts, N. Mittal, N. P. Murphy, C. Cepeda, B.L. Kieffer, et al., Targeted expression of mu-opioid receptors in a subset of striatal direct-pathway neurons restores opiate reward, Nat. Neurosci. 17 (2014) 254–261.
[36] C. Stein, S. Kuchler, Targeting inflammation and wound healing by opioids, Trends Pharmacol. Sci. 34 (2013) 303–312.
[37] J.P. Harnisch, F. Hoffmann, L. Dumitrescu, Side-effects of local anesthetics on the corneal epithelium of the rabbit eye, Albrecht Von Graefes Arch. Klin. Exp. Ophthalmol. 197 (1975) 71–81.
[38] G. Rocha, I. Brunette, M. Le Francois, Severe toxic keratopathy secondary to topical anesthetic abuse, Can. J. Ophthalmol. 30 (1995) 198–202.
[39] C. Zollner, S. Mousa, A. Klinger, M. Forster, M. Schafer, Topical fentanyl in a randomized, double-blind study in patients with corneal damage, Clin. J. Pain 24 (2008) 690–696.
[40] H. Ichikawa, S. Schulz, V. Hollt, Z. Mo, M. Xiang, T. Sugimoto, Effect of Brn-3a deficiency on primary nociceptors in the trigeminal ganglion, Neurosci. Res. 51 (2005) 445–451.
[41] R. Weibel, D. Reiss, L. Karchewski, O. Gardon, A. Matifas, D. Filliol, J.A. Becker, J. N. Wood, B.L. Kieffer, C. Gaveriaux-Ruff, Mu opioid receptors on primary afferent nav1.8 neurons contribute to opiate-induced analgesia: insight from conditional knockout mice, PLoS One (2013) 8, e74706.
[42] A. Nakamura, T. Hayakawa, S. Kuwahara, S. Maeda, K. Tanaka, M. Seki, O. Mimura, Morphological and immunohistochemical characterization of the trigeminal ganglion neurons innervating the cornea and upper eyelid of the rat, J. Chem. Neuroanat. 34 (2007) 95–101.
[43] C. Belmonte, J.J. Nichols, S.M. Cox, J.A. Brock, C.G. Begley, D.A. Bereiter, D. A. Dartt, A. Galor, P. Hamrah, J.J. Ivanusic, et al., TFOS DEWS II pain and sensation report, Ocul. Surf. 15 (2017) 404–437.
[44] P. Armenian, K.T. Vo, J. Barr-Walker, K.L. Lynch, Fentanyl, fentanyl analogs and novel synthetic opioids: a comprehensive review, Neuropharmacology 134 (2018) 121–132.
[45] H. Beaudry, D. Dubois, L. Gendron, Activation of spinal mu- and delta-opioid receptors potently inhibits substance P release induced by peripheral noxious stimuli, J. Neurosci. 31 (2011) 13068–13077.
[46] J. Endres-Becker, P.A. Heppenstall, S.A. Mousa, D. Labuz, A. Oksche, M. Schafer, C. Stein, C. Zollner, Mu-opioid receptor activation modulates transient receptor potential vanilloid 1 (TRPV1) currents in sensory neurons in a model of inflammatory pain, Mol. Pharmacol. 71 (2007) 12–18.
[47] S. Van Dorpe, A. Adriaens, I. Polis, K. Peremans, J. Van Bocxlaer, B. De Spiegeleer, Analytical characterization and comparison of the blood-brain barrier permeability of eight opioid peptides, Peptides 31 (2010) 1390–1399.
[48] D. Araldi, L.F. Ferrari, J.D. Levine, Hyperalgesic priming (type II) induced by repeated opioid exposure: maintenance mechanisms, Pain 158 (2017) 1204–1216.
[49] D. Araldi, L.F. Ferrari, J.D. Levine, Repeated mu-opioid exposure induces a novel form of the hyperalgesic priming model for transition to chronic pain, J. Neurosci. 35 (2015) 12502–12517.
[50] G. Corder, D.C. Castro, M.R. Bruchas, G. Scherrer, Endogenous and exogenous opioids in pain, Annu. Rev. Neurosci. 41 (2018) 453–473.
[51] R. Pina, G. Ugarte, M. Campos, A. Inigo-Portugues, E. Olivares, P. Orio, C. Belmonte, J. Bacigalupo, R. Madrid, Role of TRPM8 channels in altered cold sensitivity of corneal primary sensory neurons induced by axonal damage, J. Neurosci. 39 (2019) 8177–8192.
[52] H. Liang, F. Brignole-Baudouin, A. Labbe, A. Pauly, J.M. Warnet, C. Baudouin, LPS-stimulated inflammation and apoptosis in corneal injury models, Mol. Vis. 13 (2007) 1169–1180.
[53] M. Costigan, A. Moss, A. Latremoliere, C. Johnston, M. Verma-Gandhu, T. A. Herbert, L. Barrett, G.J. Brenner, D. Vardeh, C.J. Woolf, M. Fitzgerald, T-cell infiltration and signaling in the adult dorsal spinal cord is a major contributor to neuropathic pain-like hypersensitivity, J. Neurosci. 29 (2009) 14415–14422.
[54] I. Kovacs, C. Luna, S. Quirce, K. Mizerska, G. Callejo, A. Riestra, L. Fernandez-Sanchez, V.M. Meseguer, N. Cuenca, J. Merayo-Lloves, et al., Abnormal activity of corneal cold thermoreceptors underlies the unpleasant sensations in dry eye disease, Pain 157 (2016) 399–417.
[55] Q. Cai, C.Y. Qiu, F. Qiu, T.T. Liu, Z.W. Qu, Y.M. Liu, W.P. Hu, Morphine inhibits acid-sensing ion channel currents in rat dorsal root ganglion neurons, Brain Res. 1554 (2014) 12–20.
[56] B. Oehler, M. Mohammadi, C. Perpina Viciano, D. Hackel, C. Hoffmann, A. Brack, H.L. Rittner, Peripheral interaction of resolvin D1 and E1 with opioid receptor antagonists for antinociception in inflammatory pain in rats, Front. Mol. Neurosci. 10 (2017) 242.

## II. Translational potential of corneal MOR: *exploration of MOR immunoreactive in corneal nerve fibers and sensory neurons in non-human primates* (*Guerrero-Moreno et al., in preparation*)

After demonstrating that MOR is detected in corneal nerve fibers and TG primary sensory neurons in mice (Joubert et al., 2020), we further investigated if similar distributions exist in a non-human primate, as a means of further exploring the translational potential of aforementioned results.

### II.1 Materials and methods

#### A. Animals

Two cynomolgus macaques (*Macaca fascicularis*) were euthanized under deep anesthesia with an intravenous injection of sodium pentobarbital and were perfused with 0.9% NaCl followed by a 4% PFA solution. These animals had been used previously for other purposes by other researchers, and the cornea and TGs of these macaques were unaffected by the experiments. Furthermore, the animals did not exhibit any ocular surface pathology. All experiments were performed in strict accordance with the recommendations of the Weatherall Report regarding good animal practice.

#### B. Tissue preparation and sectioning

Eyes were extracted, post-fixed in PFA 4% and 40 µm-thick sections were obtained using a Vibratome (Leica CT1000S). The TGs were carefully dissected, post-fixed in 4% PFA and placed in a 30% sucrose solution in PBS before being frozen at -20°C in 7.5 % gelatin and 10 % sucrose. 16 µm-thick TG frozen sections were prepared using a Cryostat (Leica Microsystems, Wetzlar, Germany). The sections were mounted on Superfrost™ slides and stored at – 20°C for subsequent use.

#### C. Double immunofluorescence labelling in cornea and TG from macaques

**Macaque cornea**

Free floating macaque corneal sections were rinsed in PBS-Triton (PBS-T) 0.1% and blocked 2 hours with PBS-T 0.1% - Normal Horse Serum (NHS) 3% at room temperature (RT). Corneal sections were then incubated with rabbit monoclonal anti-MOR (UMB-3, ab134054, abcam, 1:50, 0,88 µg/mL) and mouse monoclonal anti-beta III Tubulin antibody (ab78078, Abcam;

1:500, 2 µg/ml) in PBS-T 0.5% - NHS 3% for 48h. Sections were rinsed in PBS-T 0.1% and incubated with horse anti-rabbit biotinylated antibody (Vector Laboratories, 1:500) and donkey anti-mouse Alexa 488 Antibody (Invitrogen, 1:500) in PBS-T 0.5% for 2 hours at RT. Then, sections were incubated with streptavidin Alexa 594 conjugated (Invitrogen, 1:1000) and DAPI (1:1000) in PBS-T 0.5% for 2 hours at RT. Sections were washed, mounted onto Superfrost slides and coverslipped with Fluoromount. Tissue sections from cornea were examined with an inverted Olympus FV1000 confocal microscope equipped with an argon (488 nm) ion laser and laser diodes (405 and 559 nm). The images were acquired sequentially, line-by-line, to reduce excitation and emission crosstalk. The step size was defined according to the Nyquist–Shannon sampling theorem (1024*1024 pixels). TIFF images were obtained.

**Macaques TG**

TG sections were rinsed in PBS, placed in a blocking solution containing normal goat serum (NGS) 5% and PBS-T 0.1% for 2 hours at RT and incubated with a rabbit monoclonal anti-MOR (UMB-3, ab134054, Abcam) at 1:500 (0,088 µg/mL) and mouse anti-beta III Tubulin antibody (ab78078, Abcam) at 2 µg/mL (1:500) overnight at 4°C. After PBS washes, sections were incubated with biotinylated goat anti rabbit immunoglobulin (Vector Laboratories, Newcastle, UK; 1:1000) and donkey anti-mouse Alexa 594 Antibody (Invitrogen,1:500) for 2 hours at RT, following an incubation with streptavidin-Alexa Fluor 488 (Invitrogen, 1:500) and DAPI (1:2000) for 1 hour. Finally, sections were coverslipped using Fluoromount Aqueous Mounting Medium (Sigma Aldrich). TG sections were examined with a Zeiss M1 epifluorescence microscope (Axio ImagerM1; Carl Zeiss) equipped with a digital camera (Axio Cam HRC; Carl Zeiss) and image acquisition software (Zen; Carl Zeiss). TIFF images were recorded.

## II.2 Results: MOR is detected in corneal nerve fibers and trigeminal sensory neurons of macaques

MOR immunoreactivity was clearly found in corneal nerves co-stained with beta III tubulin antibody. As illustrated in **Figure 27**, MOR immunoreactivity was punctate. At the level of the ophthalmic branch of the TG, MOR immunoreactivity was found in numerous sensory neurons co-stained with beta III tubulin. Both small-sized (<30 µm diameter) and medium-sized (30-40 µm diameter) neurons expressed MOR (**Fig. 27**).

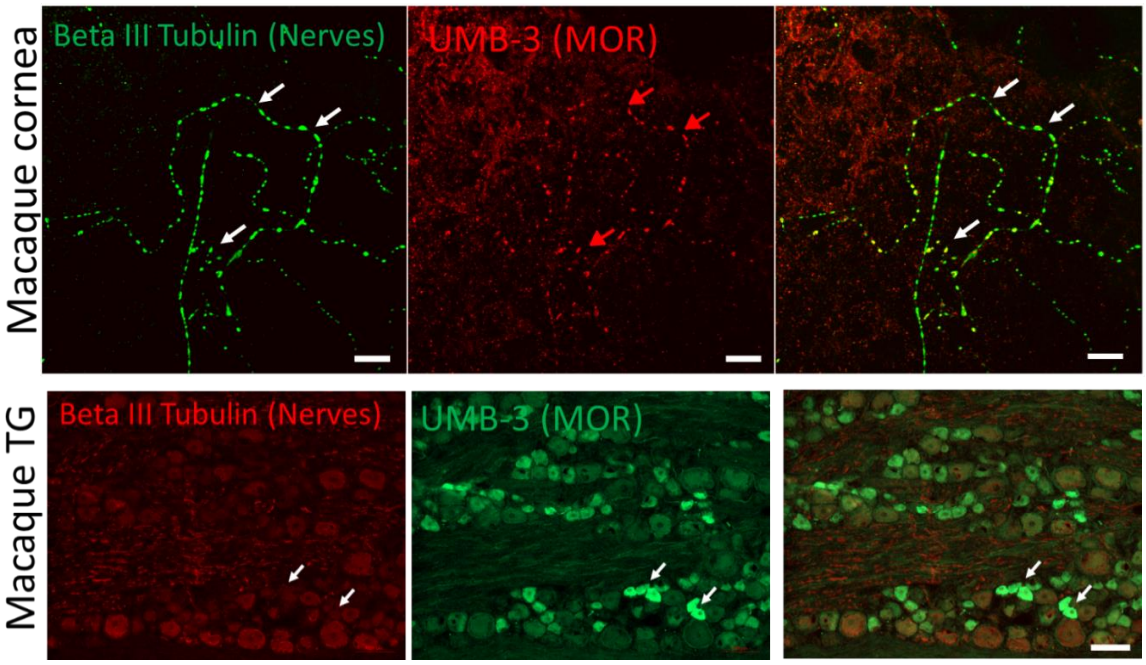


**Figure 27: MOR immunoreactivity can be detected in corneal nerves and primary sensory neurons in TG from cynomolgus macaques**
**Upper panels:** Representative confocal images showing MOR immunoreactivity (red) in corneal nerve fibers immuno-stained with Beta III tubulin (green) in macaques (arrows). Scale bar: 25 µm.
**Bottom panels:** Epifluorescence images showing the staining for MOR (green) and Beta III Tubulin (red) in the ophthalmic branch of the macaque TG. The presence of MOR immunoreactivity in small- and medium-sized neurons should be noted (arrows). Scale bar: 100 µm.

Our anatomical studies demonstrated for the first time the MOR immunoreactivity in corneal nerves of non-human primates (macaques). This observation is in line with the study of Zollner reporting MOR immunoreactivity on nerve fibers in human cornea (Zöllner et al., 2008). Moreover, the expression of MOR was further confirmed in small-sized or medium-sized trigeminal neurons at the level of the ophthalmic branch.

## III. Exploring MOR/TRPV1 co-expression in an acute inflammatory context (*Guerrero-Moreno et al., in preparation*)

In additional experiments, we investigated the expression of MOR in TRPV1$^+$ primary sensory neurons in an acute inflammatory context.

### III.1 Materials and methods: *In situ hybridization for MOR and TRPV1 in TG from scraping/LPS and control animals*

Mouse TGs were dissected and post-fixed in 4% PFA for 24 h at 4 ◦C. The tissues were immersed in 10 %, 20 % and 30 % sucrose solutions (in PBS) for 12–24 h at each step. The tissues were placed at an optimal cutting temperature (OCT), frozen in liquid nitrogen, and stored at -80°C. Then, the TG were cut using a cryostat (Leica CM 3050 S) to make 12-µm sections, which were mounted on Superfrost slides. Fluorescent *in situ* hybridization studies were performed using the RNAscope Fluorescent Multiplex Reagent kit v2 assay, according to the protocol for fixed frozen tissue (Advanced Cell Diagnostics, Newark, CA). Briefly, the sections were washed with 1X PBS, treated with hydrogen peroxide (RNAscope, ref# 322335) for 10 min at RT and then washed in distilled $H_2O$. Using a steamer, the tissues were treated with distilled $H_2O$ for 10 s at 99°C and then moved to RNAscope 1X target Retrieval Reagent (RNAscope, ref# 322000) and incubated for 5 min at 99°C. The tissues were washed with distilled $H_2O$, transferred to 100 % ethanol for 3 min and treated with RNAscope Protease III (RNAscope, ref#322337) for 30 min at 40°C. Species-specific target probes for MOR (Oprm1-C3, ref#315841-C3) and TRPV1 (Trpv1, ref# 31331) were combined. The sections were then incubated with the mix of probes and negative (ref# 320871) and positive (ref# 320881) control probes (provided by the manufacturer). The probes were hybridized for 2h at 40°C in a humidified oven (RNAscope HybEZ oven, with an HybEZ humidity control tray from Advanced Cell Diagnostics). A series of incubations was then performed to amplify the hybridized probe signal and label the target probe for the assigned fluorescence detection channel Opal 650 (Ref# FP1496A, dilution 1:200, Akoya) for channel 3 (MOR) and Opal 520 (Ref# FP1487A, dilution 1:200, Akoya) for channel 1. The nuclei were stained using a DAPI nuclear stain (RNAscope Ref# 323108) for 30s at RT. The slides were then mounted using ProLong Gold Antifade Mounting reagent (Ref# P36934) onto glass sides and cover slipped. Images were taken with Zeiss M1 epifluorescence microscope (Axio ImagerM1; Carl Zeiss)

equipped with a digital camera (Axio Cam HRC; Carl Zeiss) and image acquisition software (Zen; Carl Zeiss). The microscope settings were established using control sections (positive and negative) and remained unchanged for all subsequent acquisitions. TIFF images were recorded. Three images belonging to the $V_1$ branch of two or three TG sections per animal were used. Analysis of co-expression were made through manual counting of the expressing cells ($MOR^+TRPV1^+$, $MOR^+TRPV1^-$ and $MOR^-TRPV1^+$ cells) using ImageJ Software.

### III.2 Results: *MOR is expressed in TRPV1⁺ primary sensory neurons in the $V_1$ branch of TG in control and inflammatory pain conditions*

After detecting MOR both in corneal fibers (immunostaining, Fig. 1 in (Joubert et al., 2020) and primary sensory neurons in the $V_1$ region of the TG (immunostaining, Fig. 1 *in situ* hybridization, Fig. 4 in (Joubert et al., 2020), we wanted to further characterize this population of neurons in an inflammatory pain condition (scraping + LPS instillation). Repeated instillations of DAMGO, a peripherally restricted MOR agonist, increased the latency and reduced the frequency of the activity of ciliary nerve fibers after a $CO_2$ pulse (Fig. 6 in Joubert et al., 2020) and reduced the palpebral closure time after instillation of capsaicin (Fig. 7 in (Joubert et al., 2020). Both phenomena are presumably mediated by polymodal neurons which express the chemosensory channel TRPV1, so we wanted to confirm that those neurons do express MOR. Although local translation of mRNA in peripheral terminals is possible (Khoutorsky and Price, 2018), most of the process is located in the neuronal soma. For this reason, we focused our analysis in the ophthalmic branch ($V_1$) region of the TG to describe the expression of MOR in polymodal neurons ($TRPV1^+$).

Co-expression between MOR and TRPV1 was observed following fluorescent *in situ* hybridization by the RNAscope probes targeting MOR and TRPV1 in trigeminal sensory neurons soma (**Fig. 28A**, arrows). Quantitative analysis of MOR/TRPV1 co-expression was done in the ophthalmic part of the TG for both groups of animals (scraping + LPS vs. controls) in order to evaluate the percentage of these populations expressing MOR and whether the pain condition affects their co-expression. For MOR/TRPV1 co-expression, the number of $TRPV1^+MOR^+$, $TRPV1^+MOR^-$ and $TRPV1^-MOR^+$ cells were quantified. Analysis of co-expression indicated that around two thirds of $MOR^+$ cells were also $TRPV1^+$ (69.1% in control vs 66.9% in Scraping/LPS mouse, **Fig. 28B**) and almost all $TRPV1^+$ neurons were also $MOR^+$ (98.5% in

control vs 96.5 % in LPS/Scraping mouse, **Fig. 28B**). No significant difference was detected between study groups.

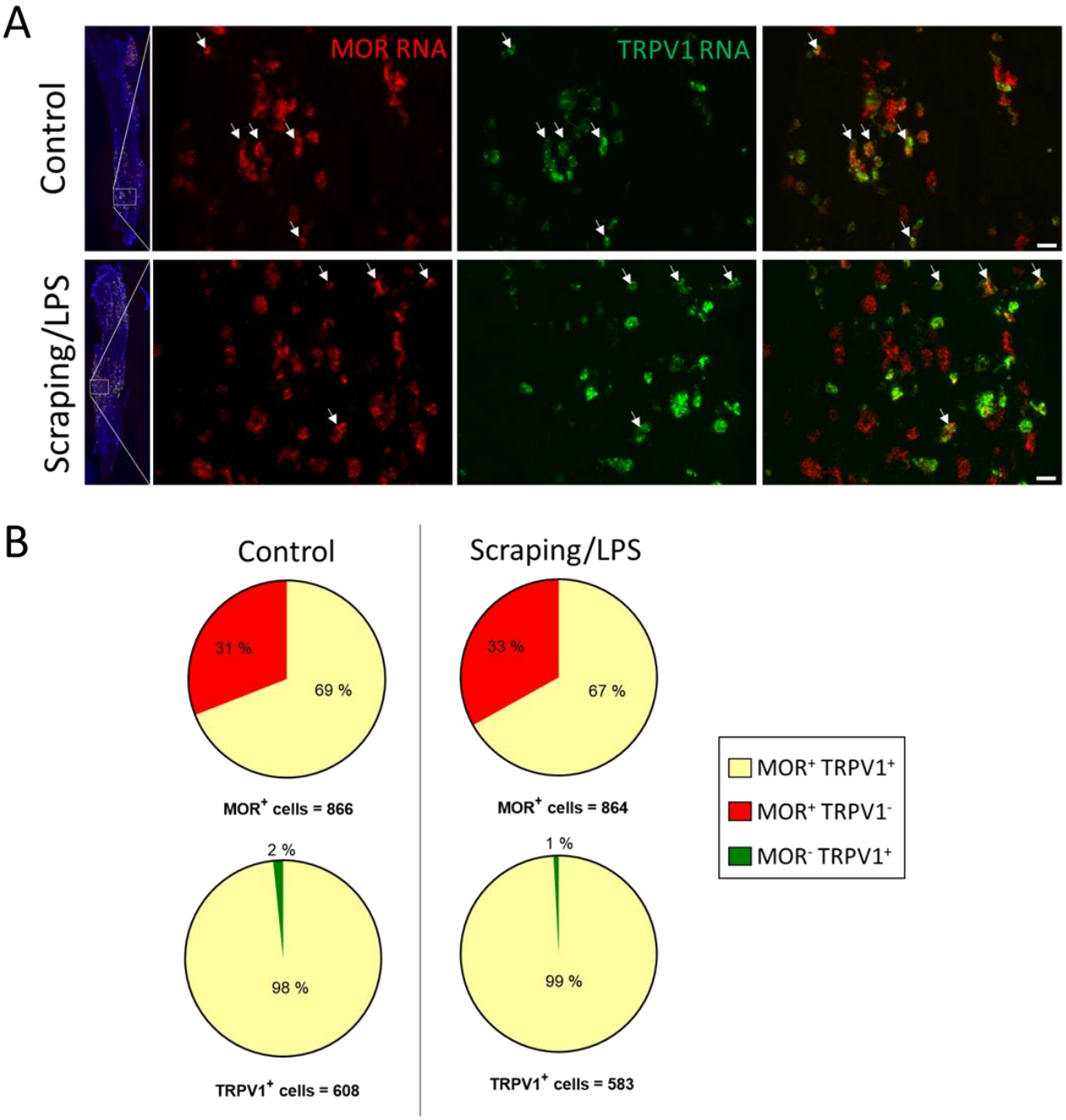


**Figure 28: MOR is expressed in TRPV1$^+$ afferent neurons under normal and painful conditions in the trigeminal ganglion**

**A.** Left: Overview of the MOR RNA expression (red), TRPV1 RNA (green) and nuclei counterstained with DAPI (blue) in the TG from control vs scraping/LPS mouse. Right: Extension of the zone delimited by a square in the left image, showing the expression of MOR mRNA (red), TRPV1 mRNA (green) in the ophthalmic branch ($V_1$) of TG. Notice the co-expression between MOR and TRPV1 (arrows). Scale bars: 50 µm.

**B.** Co-expression of MOR mRNA with TRPV1 mRNA in primary sensory neurons in V1 branch of TG in control and scraping/LPS conditions. Data were grouped by populations of cells: MOR-expressing cells (up) and $TRPV1^+$ neurons (bottom).

Although it was not possible to show phenotypic plasticity in neurons expressing MOR under an acute inflammatory pain condition, it is obvious that almost all polymodal neurons express MOR, representing two thirds of the MOR-expressing cells in $V_1$ branch region of TG. Thus, although experiments with retrograde tracers placed at the level of corneal terminals will be necessary to confirm such data, it could be expected that polymodal neurons in the cornea express MOR.

## IV. MOR as a topical target to manage chronic corneal pain secondary to severe DED (*Guerrero-Moreno et al. in preparation*)

As explained in the previous section, we recently found that MOR expression is overexpressed in corneal nerve fibers and primary sensory neurons in an acute (5 days) inflammatory corneal pain model (corneal scraping and LPS instillation). We demonstrated that repeated topical ocular administration of 50µM DAMGO ([D-Ala2,N-Me-Phe4,Gly5-ol]-enkephalin), a MOR-selective ligand, markedly reduced the mechanical corneal hypersensitivity as well as the spontaneous activity of corneal nerve triggered by inflammatory pain. Altogether, these data reinforce the concept that corneal MOR can be targeted to alleviate acute corneal pain (Joubert et al., 2020).

Despite the current evidence for the potent analgesic effects of topical MOR agonist in acute inflammatory ocular pain model, more research is needed to evaluate their use in DED-associated pain. In this context, we recently developed a chronic DED model in mice, which is obtained after the unilateral surgical removal of the extra-orbital lacrimal gland and Harderian gland (Fakih et al., 2019) as previously described. We observed a marked reduction of tear production and the development of corneal inflammation at D21 post-surgery and a reduction of intraepithelial corneal nerve terminals. Behavioral and electrophysiological studies showed in this model that animals developed time-dependent mechanical corneal hypersensitivity accompanied by increased spontaneous ciliary nerve fiber electrical activity. At D21, mRNA levels of Fos, ATF3, NOS2 and NOX4 and GFAP markers increased significantly in the ipsilateral trigeminal ganglion.

Thus, this preclinical model of chronic DED is an excellent model to determine whether MOR could serve as a therapeutic target in the management of pain secondary to severe DED.

## IV.1 Materials and methods

### A. Experimental Animals

8- to 10-week-old adult male C57BL/6 mice (Janvier Labs, Le Genest Saint Isle, France) were maintained under controlled conditions (22 ± 1 °C, 60% ± 10% relative humidity, 12/12 h (hour) light/dark cycle, food and water *ad libitum*. All animal procedures were performed in strict accordance with institutional guidelines for the care and use of experimental animals approved by the European Communities Council Directive 2010/63/UE (APAFIS #20186 2019040812404058 v5).

### B. Surgical Procedures

DED was induced by unilateral (right) excision of the harderian gland (HG) and extra-orbital lacrimal gland (ELG), under ketamine (80 mg/kg intraperitoneal (i.p.)) and xylazine (8 mg/kg i.p.) anesthesia, as recently described (Fakih et al., 2019). Before surgery, a drop of lacrimal gel (Lubrithal™, Hamilton, Canada) was applied to both eyes. Under an operative microscope (Leica-Alcon II, Wetzlar, Germany), an 8 mm skin incision was made on the temporal side to expose and remove the ELG. After dissociating the conjunctival tissue above the orbital cavity near the internal canthus, the HG was carefully removed. Complete removal was verified by inspecting the surgical area for any remaining glandular tissue. The skin incision was then sutured using 6-0 braided silk sutures (6-0 Vicryl, Ethicon, Dulmen, Germany). A drop of iodine solution was applied to the incision to avoid bacterial infection. For sham mice, an incision was made in the same skin zone and the conjunctival tissue above the orbital cavity was dissociated without affecting the glands. The mice were placed in thermostatic cages (30°C) to recover from the surgery.

### C. Drugs

DAMGO ([D-Ala2,N-Me-Phe4,Gly5-ol] enkephalin), naloxone methiodide and capsaicin were purchased from Sigma-Aldrich (Saint-Quentin Fallavier, France). DAMGO and naloxone methiodide was dissolved in 0.1 M phosphate-buffered saline (PBS; pH 7.4) to obtain a final concentration of 50 µM and 100 µM, respectively. Capsaicin (Sigma-Aldrich) was dissolved in 100 % ethanol (1 M solution) and then diluted in PBS to obtain a 10 µM solution.

### D. Experimental design of treatment and behavioral tests

Twice per day, DED mice received ocular instillations of PBS, DAMGO (50 µM), or naloxone methiodide (100 µM) followed 15 min later by DAMGO (50 µM) from day 7 post-surgery (D7) until D21 (**Fig. 29**). Untreated sham and DED mice were monitored daily. The same experimenter performed all experiments, administrated the study treatment and performed the behavioral studies.

**Tear volume**

Tears were measured using cotton phenol red threads (Zone-Quick, Tokyo, Japan). In the room dedicated to behavioral tests, awake mice were immobilized and the top of the phenol red threads was placed on the lateral canthus of the eye for 30 s. The thread is yellow in color (acidic), but changes to light red when exposed to tears. After 30s, the length (in millimeters) of the color change was determined using a scale. Tear volume was calculated by measuring the length of thread wetting as previously described (Fakih et al., 2019).

**Behavioral tests**

Behavioral tests were carried out during the light period, between 16h and 18h by the same experimenter, 15 min after the last instillation of PBS or DAMGO in the day. Mice were habituated to the behavioral room, experimenter and immobilization (handling-restraint) techniques for at least 7 days before the first behavioral test. Any excessive stress or injuries were reported and in such case animals were excluded from the analysis (7 animals were excluded from a total of 65 used).

***Corneal mechanical sensitivity***

von Frey filaments (Bioseb, Vitrolles, France) were used to evaluate corneal sensitivity in response to corneal mechanical stimulation (Fakih et al., 2019; Joubert et al., 2019; Reaux-Le Goazigo et al., 2019; Fakih et al., 2021). The mechanical threshold response was determined by assessing the first reflex response evoked by calibrated von Frey filaments of increasing force (0.008 g, 0.02 g, 0.04 g, 0.07 g and 0.16 g) applied to the central cornea of immobilized mice. The mechanical corneal sensitivity was determined on day 0 (D0) (before the surgery) and on D7, D14 and D21.

***Ocular discomfort: spontaneous eye aperture***

Spontaneous eye aperture is an accurate index for monitoring spontaneous eye pain (Fakih et al., 2020; Fakih et al., 2021) and is one of the quantitative measures of the grimace scale,

which is used to monitor spontaneous pain behavior (Langford et al., 2010; Matsumiya et al. , 2012). Eye aperture was measured for the ipsilateral (right) eye based on photographs of the ocular surface of mice that were awake and i mmobilized but visibly calm. The aperture ratio was calculated dividing the height between the width. The width is the distance between the internal and external canthus and the height, the distance between the edge of the upper and lower eyelids, going through the center of the cornea. Images were captured by a digital camera. Ocular discomfort was determined on D0 ( before the surgery) and on D7, D14 and D21.

***Corneal sensitivity to capsaicin:***

The chemical corneal sensitivity to capsaicin was assessed by applying 10µL of a 10µM capsaicin (TRPV1 agonist) solution to the ipsilateral (right) cornea 15 min after the last PBS, DAMGO or naloxone methiodide (100 µM) + DAMGO (50 µM) instillation at D21, as previously described (Joubert et al., 2019; Reaux-Le Goazigo et al., 2019). The animals were immediately placed in an individual cage and the palpebral closure time measured with a timer.

### E. Histological studies

**Tissue preparation**

At D21, mice were deeply anesthetized with a 300µL solution of ketamine (80 mg/kg) and xylazine (8 mg/kg), which was injected intraperitoneally. Mice were then perfused with a 0.9 % NaCl solution, followed by a 4% paraformaldehyde (Klimek et al., 2017) solution. Eyes were enucleated and fixed directly in PFA 4% during 15 min and washed twice with PBS during 5 min. Then cornea samples were excised from the rest of the eye and postfixed with PFA 4% during 30 min. Corneas were rinsed with PBS and keep at 4°C in PBS with azide 0.1%. Head of the mice were postfixed during 24h in 4% PFA at 4°C under agitation and ipsilateral TG were carefully dissected the next day. Cryoprotection of TG samples were performed through sucrose gradient (10%, 20% and 30%) in PBS for 24 h each step. TG samples were embedded at Neg-50™ Frozen Section Medium (#6502, Fisher scientific), frozen in liquid nitrogen, and stored at -80°C. Then, the TG were cut using a cryostat (Leica CM 3050 S) to make 12-µm sections, which were mounted on Superfrost slides.

**Fluorescent in situ hybridization for MOR, TRPV1 and TRPM8 mRNA in ipsilateral TGs**

Fluorescent *in situ* hybridization studies were performed using the RNAscope Fluorescent Multiplex Reagent kit v2 assay, according to a modified version of the protocol for fixed frozen tissue (Advanced Cell Diagnostics, Newark, CA). Briefly, the sections were washed with 1X PBS, treated with hydrogen peroxide (RNAscope, ref# 322335) for 10 min at RT and then washed in distilled $H_2O$. Samples were dehydrated by ethanol gradient (50%, 70% and 100%) in water for 3 min each step. Then samples were left during 2h to allow complete dying. A hydrophobic barrier was applied around the tissue in the slices and treated with RNAscope Protease III (RNAscope, ref#322337) for 30 min at 40°C. Mouse-specific target probes for MOR mRNA (Oprm1-C2, ref#315841-C2), TRPV1 mRNA (Trpv1, ref#313331) and TRPM8 mRNA (Trpm8-C3, ref# 420451-C3) were diluted (1:50). The sections were then incubated with the mix of probes or with negative (ref# 320871) or positive (ref# 320881) controls. The probes were hybridized for 2h at 40°C in a humidified oven (RNAscope HybEZ oven, with an HybEZ humidity control tray from Advanced Cell Diagnostics). A series of incubations was then performed to amplify the hybridized probe signal and label the target probe for the assigned fluorescence detection channel: Opal 520 (Ref# FP1487A, dilution 1:100, Akoya) for channel 3 (TRPM8), Opal 570 (Ref# FP1488A, dilution 1:100, Akoya) for channel 1 (TRPV1) and Opal 650 (Ref# FP1496A, dilution 1:100, Akoya) for channel 2 (MOR). The nuclei were stained using a DAPI nuclear stain and cover slipped with Fluoromount.

**Double immunofluorescence labelling for nerves, macrophages and dendritic cells in mouse whole-mount cornea**

Fixed corneas from naïve, sham, untreated DED and DED treated with PBS or DAMGO, were rinsed in phosphate buffered saline 0.5% Triton (PBS-T 0.5%) and blocked for 2h at room temperature (RT) with PBS-T 0.5%- saponin 0.15% containing 3% normal donkey serum. Them, corneas were stained with mouse monoclonal anti-beta III tubulin antibody (ab78078, Abcam; 1:400) and goat anti-Iba1 (ab5076, Abcam; 1:500) in PBS-T 0.5%- saponin 0.15%-NDS 1% during 66 h at 4°C. The corneas were then rinsed in PBS-T 0.5 % and incubated with DAPI (1:1000), donkey anti-mouse Alexa Fluor 594 (1:500) and donkey anti-goat Alexa Fluor 647 (1:500) in PBS-T 0.5%- saponin 0.15% at RT during 24h. Free-floating corneas were flattened through radial cuts and mounted onto Superfrost™ slides and cover slipped with Fluoromount Aqueous Mounting Medium (Sigma Aldrich).

### F. Microscopic imaging

Image stacks from whole-mounted corneas were performed on an Olympus FV3000 laser-scanning confocal microscope equipped with high-sensitivity GaAsP detectors. DAPI (nuclear staining), AlexaFluor-594 (nerves), AlexaFluor-647 (macrophages and dendritic cells) were excited by using 405 nm, 559 nm, 635 nm laser diodes, respectively. The objective used was an Olympus UPLXAPO20X NA 0.8 WD 0.6. Image acquisition were conducted by using Olympus Fluoview software FV31S Version 2.61.243 at a resolution of 1024×1024 pixels, with a scan rate of 4 µs.pixel$^{-1}$ without zoom. Images were acquired sequentially, line by line, in order to reduce excitation and emission crosstalk, step-size was defined according to the Nyquist-Shannon sampling theorem. Exposure settings that minimized oversaturated pixels in the final images were used.

To perform image mosaics, the Multi Area Time lapse (MATL) module from Fluoview software was used to program 10% overlap between each tile. Montage was then processed using Fluoview software or ImageJ stitching plugins (Preibisch et al., 2009) or Bitplane Imaris Stitcher 9.3.1.

TG sections were examined using a Zeiss M1 epifluorescence microscope (Axio ImagerM1; Carl Zeiss). The epifluorescence microscope was equipped with a digital camera (ORCA-Flash4.0 LT+ Digital CMOS; Hamamatsu) and image acquisition software (Zen; Carl Zeiss). Three TG slices with the three branches anatomically visible were selected in each animal. Two or three high quality images per TG slice covering the entire $V_1$ branch were taken in TIFF format. The microscope settings were established using control sections (positive and negative) and remained unchanged for all subsequent acquisitions.

### G. Image analysis

**Cell density, volume and intensity of Iba1$^+$ macrophages and dendritic cells in mouse central and peripheral cornea**

3D images from Iba1-stained corneas were processed for analysis in Imaris 9.3 Software. Whole-mounted corneas were divided into five zones. The peripheral zones were defined as four 0.14 mm$^3$ regions (a 1000 x 1000 x 140 µm) whose peripheral borders were ~100 µm away from the limbus internal border. The central zone was defined as a 0.14 mm$^3$ region, not overlapping with the peripheral boxes (see **Fig. 31A**). Surface mode of Imaris 9.3 Software

was used for baseline subtraction and median filter to reduce fluorescent background. Then, surface analysis was applied for the three-dimensional automatic detection of objects positive for Iba1. The detected objects were filtered in order to represent only cells of a size compatible with macrophages and dendritic cells (area between 500 and 3500 $\mu m^2$). Parameters as number of cells, mean intensity, surface and volume were extracted.

**Levels of MOR mRNA in $V_1$ branch region of mouse TGs**

Expression of the MOR mRNA were quantified by automatically detecting the number of spots, representing the number of individual mRNA molecules in the TG samples. Images (grayscale 8-bits format) were analyzed using Fiji (ImageJ, United States National Institutes of Health) software. Background were subtracted using a rolling ball of 50 pixels radius and auto local threshold (Bernsen method, radius=15) were applied (Sezgin and Sankur, 2004; Vatani and Enayatifar, 2015) . After watershed treatment, particles were detected through "Analyze Particles" tool and quantified in number of spots/image and number of spots/$mm^2$, corresponding to the density of mRNA particles.

**Co-expression of MOR, TRPV1 and TRPM8 in $V_1$ branch region of mouse TGs**

Number of cells expressing at least one of three markers (MOR, TRPV1 or TRPM8) were quantified in the TG images. *Cell counter plugin* from Fiji (ImageJ, United States National Institutes of Health) allowed manual quantification of the number of $MOR^+$ $TRPV1^+$ $TRPM8^+$, $MOR^+$ $TRPV1^+$ $TRPM8^-$, $MOR^+$ $TRPV1^-$ $TRPM8^+$, $MOR^+$ $TRPV1^-$ $TRPM8^-$, $MOR^-$ $TRPV1^+$ $TRPM8^+$, $MOR^-$ $TRPV1^+$ $TRPM8^-$ and $MOR^-$ $TRPV1^-$ $TRPM8^+$ cells in each slice (**Table 7**). Results are expressed in number of cells/$mm^2$.

**Table 7: Labels used in Fiji Software to quantify co-expression of MOR, TRPV1 and TRPM8 mRNA**

| | Label used | | | | | | |
|---|---|---|---|---|---|---|---|
| | 1 | 2 | 3 | 4 | 5 | 6 | 7 |
| MOR Mrna | + | + | + | + | - | - | - |
| TRPV1 mRNA | + | - | + | - | + | - | + |
| TRPM8 mRNA | - | + | + | - | - | + | + |

### H. Statistical analysis

Data are expressed as mean ± SEM and were analyzed using GraphPad Prism7 (GraphPad, San Diego California USA). 2-way ANOVA was used to assess differences in tear volume, ocular discomfort, mechanical sensitivity and different expression of molecular markers in TG (MOR, TRPV1, TRPM8), one-tail unpaired *t*-test for chemical (capsaicin) sensitivity between study groups and two-tailed unpaired t-test for number, volume and mean intensity of $Iba1^+$ cells. Data is presented as mean ± SEM. The differences were considered significant for $p < 0.05$.

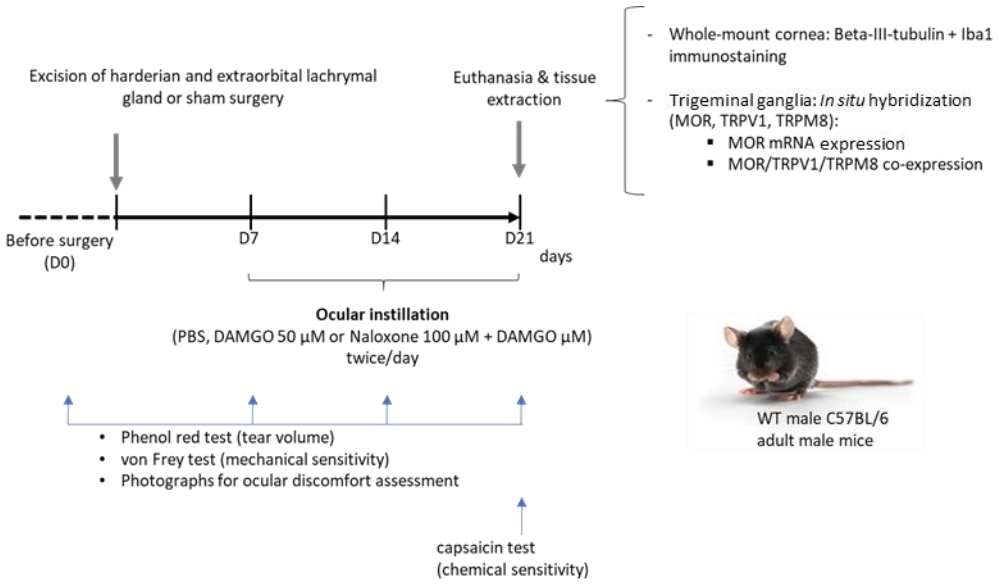


**Figure 29: Schematic diagram of the experiments**

### IV.2 Results

***Excision of the extra-orbital lachrymal gland and Harderian gland markedly reduces tear production***

Tear volume was similar before surgery for the sham and DED mice (2.80 ± 0.41 mm/30 s *vs* 2.50 ± 0.63, $P > 0.05$) (Fig. **30**). However, there was a rapid and significant reduction in tear production in DED mice by D7 (5.60 ± 0.93 *vs* 0.75 ± 0.16, $p < 0.05$), which remained significantly lower until D21 (5.40 ± 0.40 *vs* 0.70 ± 0.20, $p < 0.001$ at D14, and 3.60 ± 0.70 *vs* 0.30 ± 0.20, $p < 0.05$, at D21) (Fig. **30**) respect sham animals. Those data are in line with those reported in Fakih, 2019.

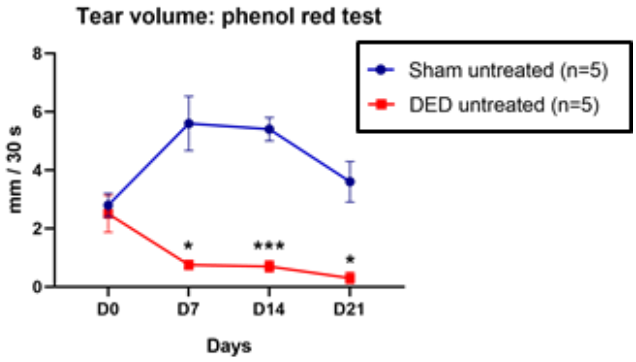


**Figure 30: Excision of ELG and HG in mice induced a persistent reduction of tear production**
Evaluation of tear volume for sham and DED untreated mice assessed by phenol red threads. Data represented as mean ± SEM. Statistical comparations by two-way ANOVA; *: $p < 0.05$, ***: $p < 0.001$.

**Does topical DAMGO modify corneal Iba1$^+$ macrophage and dendritic cell morphology in chronic DED?**

A previous study from our team has reported that topical PL265, a dual enkephalinase inhibitor, decreased the number of corneal CD11b$^+$ dendritic cells in a preclinical model of inflammatory corneal pain (Reaux-Le Goazigo et al., 2019). This suggests that modulating the endogenous opioid system (specifically increasing the levels of endogenous enkephalins) at the ocular surface level reduced corneal inflammation associated with corneal pain. We thus hypothesized that such anti-inflammatory effect could also occur following topical treatment with a MOR agonist in a model of chronic ocular pain associated with DED. To validate this hypothesis, we quantified corneal Iba1$^+$ cells, corresponding to macrophages and dendritic cells, in samples from DED mice treated with PBS or DAMGO. As the density of immune cells in the cornea decreases from the periphery towards the center (Yamagami et al. , 2005; Hattori et al., 2016; Frutos-Rincon et al., 2022). Therefore, for proper analysis and interpretation of the results, peripheral and central corneal regions were analyzed independently and compared between PBS- and DAMGO-treated DED mice.

3D images from Iba1-stained corneas were processed for analysis in Imaris 9.3 Software and Iba-1 immunostaining detected in peripheral and central whole-mount cornea (**Fig. 31A**) of DED mice treated with PBS or DAMGO. Parameters of cell density, volume and fluorescence intensity were obtained. Cell density and volume of Iba1$^+$ were not different between PBS- and DAMGO-treated DED mice neither in the peripheral nor in the central cornea (**Fig. 31B,C**). Fluorescence intensity of Iba1$^+$ cells was significantly decreased in the central cornea, while

in the peripheral cornea it was significantly increased in DAMGO-treated DED mice (**Fig. 31D**). This suggests that topical DAMGO could affect the central and peripheral cornea differently but further morphological analyses are necessary to confirm this.

These anatomical results were obtained as part of an ongoing collaboration with the laboratory of Dr. Juana Gallar (Neurosciences Institute, Alicante, Spain) in which the PhD student Almudena Íñigo Portugués analyzed the 3D images of whole-mount corneas stained with Iba-1 and beta III tubulin antibodies. Corneas from the other study groups (sham, DED untreated, DED PBS and DED DAMGO) were also stained with both markers and analyses are ongoing. Preliminary images are illustrated in **Fig. 36**. Comparations between control and study groups will allow us to uncover the morphological changes triggered by persistent DED and then the effects of DAMGO on nerve morphology or density and its possible anti-inflammatory effect.

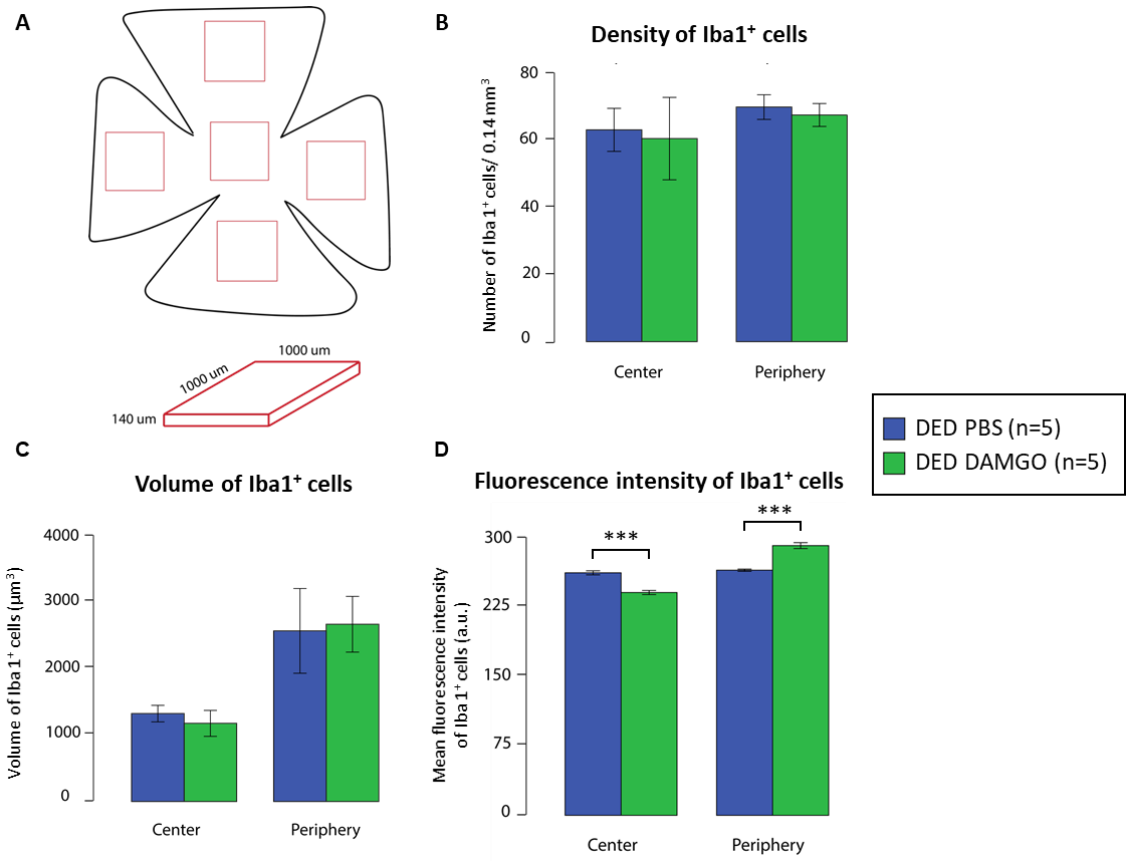


**Figure 31: Topical DAMGO treatment affects Iba1 staining intensity differently in central and peripheral cornea**

Quantification of macrophages and dendritic cells parameters in 3D images from whole-mount corneas stained with Iba1 antibody. **A.** Schematic representation of the areas analyzed in the whole-mount cornea. **B.** Density of Iba1$^+$ cells per region analyzed (Number of Iba1$^+$ cells/0.14 mm$^2$). **C.** Volume of individual Iba1$^+$ cells (µm$^3$). **D.** Mean fluorescence intensity of Iba1 staining in the detected cells.***: p<0.001.

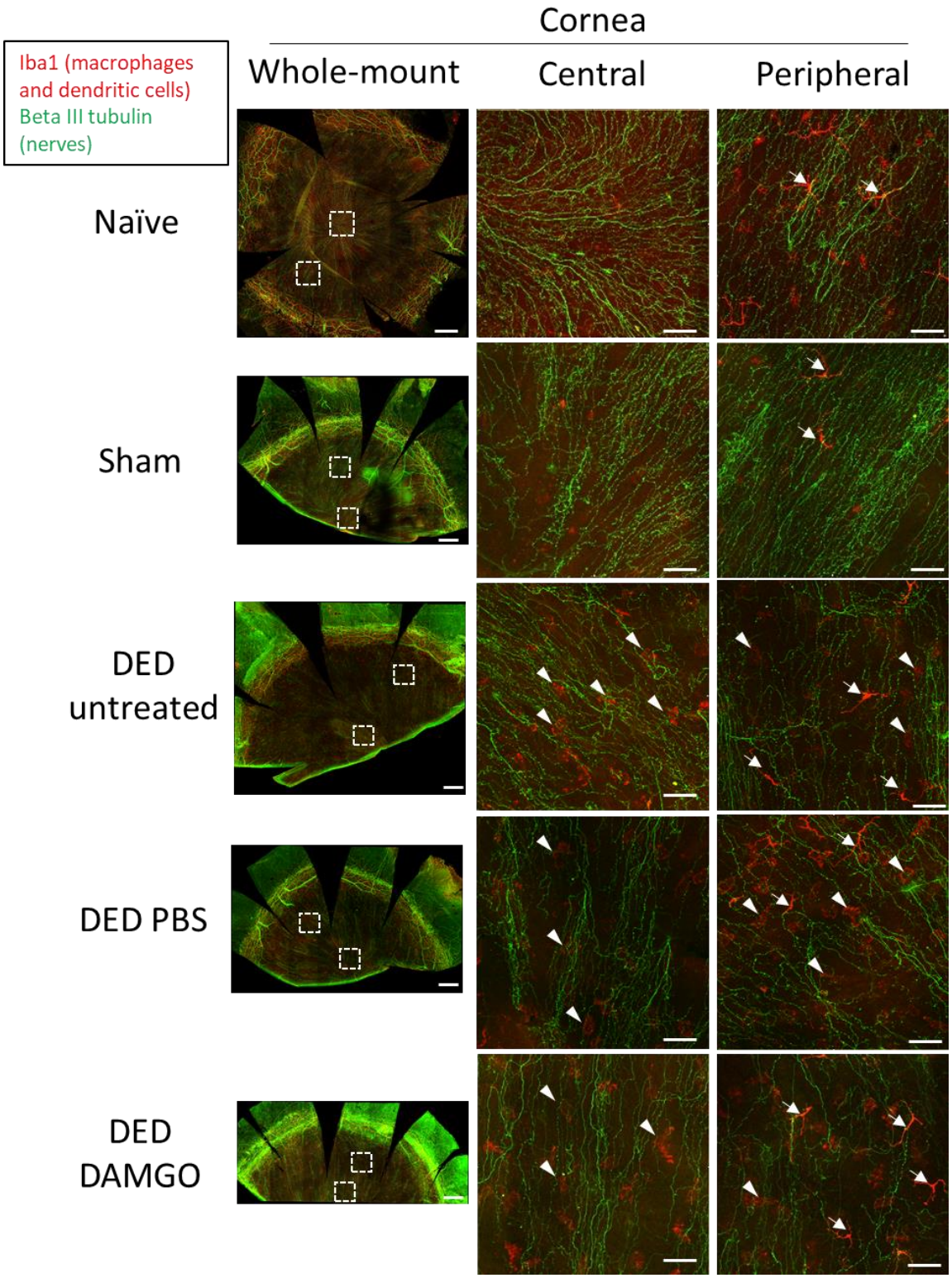


**Figure 32: Preliminary results: Whole-mount corneas stained with beta III tubulin and Iba1**
Confocal images of whole-mount corneas from naïve mice and at D21 after sham surgery or excision of Harderian and extra-orbital lachrymal gland (DED) untreated or treated with PBS or DAMGO. Immunostaining for nerves (beta III tubulin) in green and macrophages and dendritic cells (Iba1) in red (arrows). Left panels: Confocal full-thickness mosaics representing the cornea and conjunctiva of all study groups. Center and right panels: higher magnification view of the regions indicated by dashed lines in the left panels representing central and peripheral cornea. Scale bars: left panels: 350 µm; center and right panels: 50 µm.

**DED-related corneal pain induces upregulation of MOR mRNA in $V_1$ branch region of TG**

At D21, TG from sham and DED animals were extracted for *in situ* hybridization. Images showed abundant grey punctate spots, each spot corresponding to individual MOR mRNA molecules **(Fig. 33A).** Quantitative analysis of the number of spots showed MOR mRNA expression to be significantly higher in the $V_1$ branch region of TG from DED untreated mice (1067 ± 127 spots/image, 9584 ± 1145 spots/mm$^2$), than those of sham mice (651 ± 145 spots/image, 5847 ± 1313 spots/mm$^2$; **Fig. 33B**) confirming an upregulation of MOR expression in TG under chronic corneal pain.

Co-expression of MOR, TRPV1 (molecular marker of polymodal nociceptors) and TRPM8 (marker of cold thermoreceptors) mRNA was then studied using multiple-labelled *in situ* hybridization. Images from $V_1$ branch region of TG revealed co-expression between MOR and TRPV1 (**Fig. 33C**, arrows), MOR and TRPM8 (**Fig. 33C**, arrow-heads) and a triple co-expression of TRPV1, TRPM8 and MOR (**Fig. 33C**, asterisk) in both groups. Manual counting of primary sensory neuron somas showed that most TRPV1$^+$ primary sensory neurons expressed MOR both in sham (88 ± 3 %) and DED mice (86 ± 3 %). Populations of cells expressing or not the three markers (MOR, TRPV1 and TRPM8) were not statistically different between sham and DED animals **(Fig. 33D)**. Altogether, these findings confirm the expression of MOR in primary polymodal and cold receptor sensory neurons in TG.

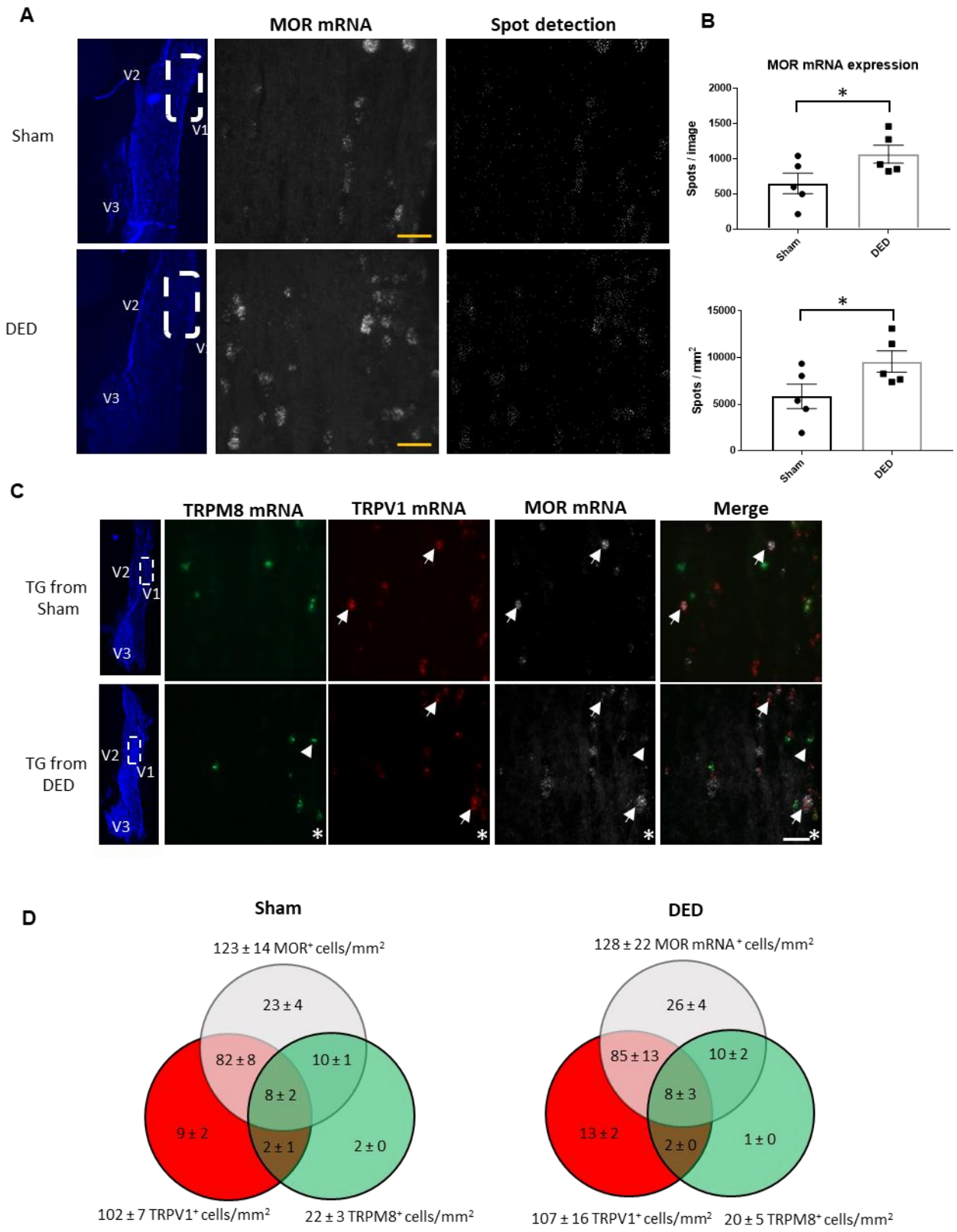


**Figure 33: MOR mRNA expression increases after chronic DED and is expressed in TRPV1⁺ and TRPM8⁺ primary sensory neurons in $V_1$ region of the TG**

**(A)** MOR mRNA levels were evaluated by *in situ* hybridization RNAscope technology. Images for MOR mRNA (grey) in the TG from sham and DED untreated mice are shown. The dashed-line rectangle represents the ophthalmic branch ($V_1$) region of the TG. The high magnification shows the primary sensory neurons that express MOR mRNA in the ophthalmic branch region of TG. Scale bars: 50 µm.

(**B**) Histograms showing the quantitative analysis of the spots representing individual MOR mRNA molecules. The number of spots per image (upper graph) and per $mm^2$ (lower graph) in sham and DED untreated mice were detected using Fiji (ImageJ). N = 5 mice per group. The difference between groups was analyzed using one-tailed unpaired t test. *: $p<0.05$. **(C)** MOR co-expression in $TRPV1^+$ and $TRPM8^+$ in the $V_1$ branch region from TG of sham and DED mice. Epifluorescence images showing TRPM8 (green), TRPV1 (red) and MOR (grey) mRNA detection by *in situ* hybridization (RNAscope) in cryostat sections of the $V_1$ branch region of ipsilateral TG (dashed-line rectangle). Some cells were co-expressing TRPV1 (red) and MOR mRNA (gray, arrows), TRPM8 (green, arrows) and MOR mRNA (grey, arrowheads) or the three markers (TRPM8, TRPV1, MOR mRNA) at the same time (asterisk). Scale bar: 50 µm. (**D**) Number of cells/$mm^2$ expressing MOR (grey circle), TRPV1 (red circle) and/or TRPM8 (green circle) mRNA at the $V_1$ level from TG in sham and DED conditions. Values at the intersections of the circles represent the percentage of cells expressing more than one marker. The difference between groups was analyzed using 2-way ANOVA. N= 5 for sham and N=6 for DED mice.

### *Repeated topical treatment with DAMGO alleviates corneal discomfort and allodynia in the chronic DED model*

To corroborate that chronic DED induced allodynia and ocular discomfort, mice were monitored during 21 days after ELG and HG excision or sham surgery. As expected, there were no differences between sham and DED untreated mice at baseline (before surgery, sham vs. DED untreated: **D0**: **von Frey test**: 0.033 ± 0.003 g vs. 0.030 ± 0.004 g; **aperture ratio**: 0.74 ± 0.02 vs 0.77 ± 0.02, **Fig. 34A,B**). However, mechanical sensitivity and aperture ratio remained significantly lower at all time points analyzed after the surgery, confirming mechanical allodynia and ocular discomfort triggered by the chronic DED (sham vs DED untreated: **von Frey test**: **D7**: 0.024 ± 0.003 g vs 0.013 ± 0.001 g, $p < 0.05$; **D14**: 0.035 ± 0.005 g vs 0.020 ± 0.002 g, $p < 0.05$; **D21**: 0.028 ± 0.003 g vs 0.017 ± 0.002 g, $p < 0.05$; **aperture ratio: D7:** 0.71 ± 0.02 vs 0.57 ± 0.04, < 0.05; **D14**: 0.71 ± 0.02 vs 0.61 ± 0.02; **D21:** 0.72 ± 0.02 vs 0.62 ± 0.02, **Fig. 34A,B**).

The ocular pain model is based on chronic desiccation of the ocular surface. Therefore, repeated application of any aqueous solution may contribute to an improvement of the corneal sensitivity, as occurs in DED patients treated with ocular surface lubricants. To test the effect of the diluent of DAMGO on the ocular surface, we applied PBS topically. As expected, there were no differences between sham and DED PBS mice at **D0** (sham vs. DED PBS: **von Frey test:** 0.033 ± 0.003 g vs 0.028 ± 0.006 g; **aperture ratio:** 0.74 ± 0.02 for sham vs 0.71 ± 0.02 for DED PBS, **Fig. 34A,B**). Animals developed mechanical allodynia after surgery (sham vs. DED PBS: **D7**: 0.024 ± 0.003 g vs 0.013 ± 0.002 g, $p < 0.05$; **D14:** 0.035 ± 0.005 g 0.017 ± 0.003 g, $p < 0.05$; **D21:** 0.028 ± 0.003 g 0.018 ± 0.002 g, $p < 0.05$; **Fig. 34B**). However, DED mice treated with topical PBS showed a decrease in aperture ratio compared with sham

animals that was significant only before to start PBS treatment at **D7** (0.71 ± 0.02 vs. 0.58 ± 0.03, p< 0.01, **Fig. 34B**), but not at D14 and D21 (sham vs. DED PBS: **D14**: 0.71 ± 0.02 vs. 0.66 ± 0.04; **D21:** 0.72 ± 0.02 vs. 0.62 ± 0.02). This finding demonstrate that repeated instillation of PBS alone is enough to reduce ocular discomfort but not sufficient to reduce mechanical allodynia in DED mice.

Previous data have reported that topical application of DAMGO was effective reducing ocular allodynia in models of inflammatory pain (Joubert et al., 2020). However, its effectivity in a DED-related chronic pain scenario is not known. In order to further evaluate the beneficial effects of topical DAMGO in persistent dry eye pain, animals were treated with DAMGO twice/day from D7 for 2 weeks. Mechanical allodynia, ocular discomfort and chemical corneal sensitivity to capsaicin were assessed as previously explained (**Fig. 33**). As expected, there were no differences in mechanical sensitivity neither ocular discomfort before the surgery (**D0:** sham vs. DED DAMGO: von Frey test: 0.033 ± 0.003 g vs. 0.034 ± 0.006 g; aperture ratio: 0.74 ± 0.02 vs. 0.79 ± 0.02, **Fig. 34A,B**). At **D7**, before beginning of DAMGO treatment, DED DAMGO animals showed mechanical allodynia (0.024 ± 0.003 g for sham vs. 0.013 ± 0.003 g for DED DAMGO, p < 0.05, **Fig. 34B**). At **D14**, after one week of two instillations per day of DAMGO, DED animals still had a decreased mechanical threshold (0.035 ± 0.005 g for sham vs. 0.017 ± 0.002 g for DED DAMGO, p < 0.01, **Fig. 34B**) but not statistically significant difference in ocular discomfort (0.71 ± 0.02 for sham vs. 0.65 ± 0.03 for DED DAMGO, **Fig. 34A).** Finally, after 2 weeks of DAMGO treatment, DED animals showed a recovery of basal mechanical sensitivity, not significantly different from sham (0.028 ± 0.003 g for sham vs. 0.022 ± 0.002 g for DED DAMGO, **Fig. 34B**) and an increased aperture ratio that was not different than sham animals but statistically increased compared with DED PBS mice (0.72 ± 0.02 for sham; 0.63 ± 0.04 for DED PBS vs. 0.75 ± 0.03 for DED DAMGO, p< 0.01, **Fig. 34A**). Moreover, we found a significant reduction of the palpebral closure time after capsaicin challenge (99.8 ± 27.9 s for DED PBS vs. 39.6 ± 8.0 s for DED DAMGO, p < 0.05, **Fig. 34C**). Altogether, these findings demonstrated the beneficial effects of 2 weeks of topical instillation of DAMGO, alleviating mechanical and chemical allodynia and ocular discomfort in a model of DED-associated chronic pain in mice.

In previous preclinical studies investigating topical MOR agonists on the ocular surface, naloxone methiodide, a nonselective opioid receptor antagonist, was used 15 minutes before

topical instillation of the topical drug (Reaux-Le Goazigo et al., 2019; Joubert et al., 2020). Similarly, in our study, naloxone methiodide (100 µM) was applied to the ocular surface of DED animals 15 min before DAMGO instillations, expecting a remission of its beneficial effects. Ocular discomfort and mechanical sensitivity was similar between all groups before the surgery. Those animals did not showed significantly different ocular discomfort or mechanical sensitivity compared with sham or DED DAMGO mice at **D7**, before the beginning of the treatment (ocular aperture ratio: 0.71 ± 0.02 for sham, 0.58 ± 0.04 for DED DAMGO, 0.71 ± 0.04 for DED naloxone methiodide + DAMGO; von Frey: 0.024 ± 0.003 for sham, 0.013 ± 0.003 for DED DAMGO, 0.015 ± 0.003 for DED naloxone methiodide + DAMGO, **Fig. 34A,B**). Similarly, ocular aperture ratio remained elevated after one week (D14) and two weeks (D21) of naloxone methiodide + DAMGO treatment in DED animals and not significantly different from sham animals or DED DAMGO (sham vs. DED naloxone methiodide +DAMGO: **D14**: sham: 0.71 ± 0.02, DED DAMGO: 0.65 ± 0.03, DED naloxone methiodide: 0.77 ± 0.04; **D21**: sham: 0.72 ± 0.02, DED DAMGO: 0.75 ± 0.03, DED naloxone methiodide: 0.77 ± 0.04; **Fig. 34A).** However these animals showed mechanical allodynia at **D14** (0.035 ± 0.005 g for sham vs. 0.018 ± 0.002 g for DED naloxone methiodide + DAMGO, $p < 0.05$) and **D21** (0.028 ± 0.003 g for sham vs. 0.015 ± 0.003g for DED naloxone methiodide + DAMGO, $p < 0.05$). Animals showed no significant difference in palpebral closure time after capsaicin challenge comparing with DED PBS animals or DED DAMGO (99.8 ± 27.9 s for DED PBS, 39.6 ± 8.0 s for DED DAMGO, 63.6 ± 13.9 s for DED naloxone methiodide + DAMGO, **Fig. 34C**). At D21, our results showed that inhibition of ocular MOR reversed the beneficial effects of DAMGO on mechanical and chemical allodynia, confirming a direct effects of DAMGO through µ opioid receptors.

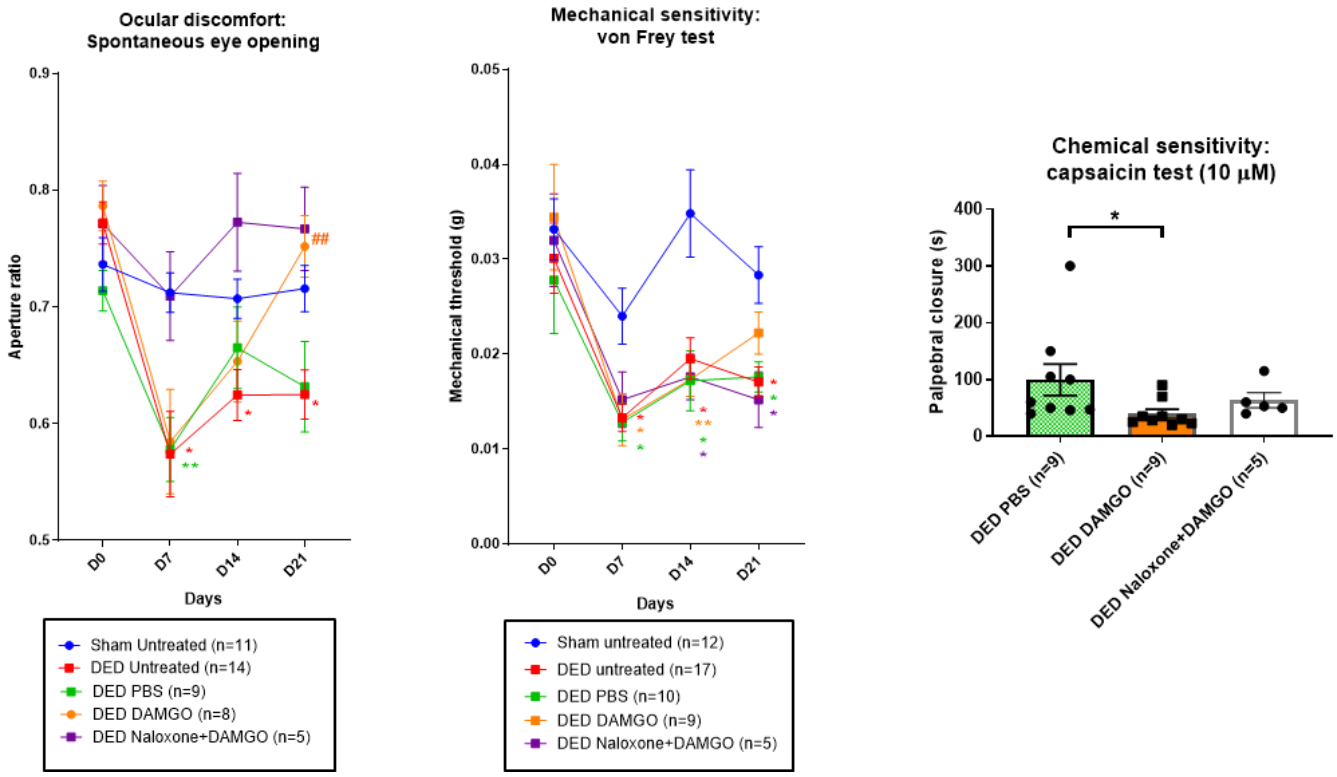


**Figure 34: Repeated topical instillations of DAMGO prevents mechanical allodynia and ocular discomfort in chronic DED mice**

Ocular discomfort was evaluated with the aperture ratio from photographs of the ocular surface (**A**) and mechanical corneal threshold was assessed by von Frey test (**B**) in 5 groups (sham, DED untreated, DED PBS , DED DAMGO and DED naloxone + DAMGO-treated DED mice). (**C**) Chemical allodynia in DED mice treated with DAMGO or PBS quantified by capsaicin challenge test (palpebral closure time). Statistical comparations by two-way ANOVA (**A**, **B)** or one-tailed unpaired *t*-test (**C**). Data represented as mean ± SEM. *: Significant difference with sham group. #: Significant difference with DED untreated group. Statistical significance is illustrated based on number of signs as follows: one sign = $p < 0.05$, two signs = $p < 0.01$, three signs = $p < 0.001$.

In conclusion, extra-orbital lacrimal gland and harderian gland excision in mice triggered a significant reduction in tear volume and an increase in mechanical and chemical corneal allodynia and ocular discomfort, attesting of its relevance as a preclinical model for the study of DED-associated ocular pain.

DED animals were treated with DAMGO or PBS from D7 during 2 weeks. Previous publications showed that repeated treatment aiming to activate corneal MOR decreased inflammation in preclinical models of inflammatory pain (Wenk et al., 2003; Reaux-Le Goazigo et al., 2019). In this study, we were unable to evidence an anti-inflammatory effect to repeated instillation DAMGO, although the analysis, for the moment, only took into account the density and

volume of Iba1$^+$ cells. Fine analysis of Iba1$^+$ morphology could shed some light as dendritic cells typically display elongated shapes while macrophages are rounder.

Our animals showed an increase in MOR mRNA levels at the $V_1$ branch region of the TG, region containing the soma of primary sensory neurons of one third of the head, including the cornea. In the same region, we found that most TRPV1$^+$ (polymodal) primary sensory neurons expressed MOR (88 ± 3 % in sham, 86 ± 3 % in DED mice). Similarly, most TRPM8$^+$ neurons were positive for MOR in both sham (79 ± 3 %) and DED (87 ± 4 %) conditions. Altogether, the increase in MOR mRNA levels are not a consequence of phenotypic plasticity as the populations were not different in sham and DED mice. On the contrary, it would be the same populations that already expressed MOR in basal conditions that increase their mRNA expression levels in conditions of DED-associated pain.

## V. Investigating other topical targets to management DED-related ocular pain: *the example of TRPV1 blockade (Study 2 - Fakih et al. J Neurinfla. 2021)*

Considering the aforementioned role of local inflammation and peripheral sensitization in the development of chronic DED in ELG/HG excision models, our team has also investigated other topical targets for the management of DED-related ocular pain, notably TRPV1 antagonists, as detailed in the following published study (Fakih et al., 2021).

Fakih et al. Journal of Neuroinflammation (2021) 18:111
https://doi.org/10.1186/s12974-021-02162-7

Journal of Neuroinflammation

RESEARCH Open Access

# Capsazepine decreases corneal pain syndrome in severe dry eye disease

Darine Fakih[1,2], Adrian Guerrero-Moreno[1], Christophe Baudouin[1,3,4], Annabelle Réaux-Le Goazigo[1†] and Stéphane Mélik Parsadaniantz[1*†]

## Abstract

**Background:** Dry eye disease (DED) is a multifactorial disease of the ocular surface accompanied by neurosensory abnormalities. Here, we evaluated the effectiveness of transient receptor potential vanilloid-1 (TRPV1) blockade to alleviate ocular pain, neuroinflammation, and anxiety-like behavior associated with severe DED.

**Methods:** Chronic DED was induced by unilateral excision of the Harderian and extraorbital lacrimal glands of adult male mice. Investigations were conducted at 21 days after surgery. The mRNA levels of TRPV1, transient receptor potential ankyrin-1 (TRPA1), and acid-sensing ion channels 1 and 3 (ASIC1 and ASIC3) in the trigeminal ganglion (TG) were evaluated by RNAscope in situ hybridization. Multi-unit extracellular recording of ciliary nerve fiber activity was used to monitor spontaneous and stimulated (cold, heat, and acid) corneal nerve responsiveness in ex vivo eye preparations. DED mice received topical instillations of the TRPV1 antagonist (capsazepine) twice a day for 2 weeks from d7 to d21 after surgery. The expression of genes involved in neuropathic and inflammatory pain was evaluated in the TG using a global genomic approach. Chemical and mechanical corneal nociception and spontaneous ocular pain were monitored. Finally, anxiety-like behaviors were assessed by elevated plus maze and black and white box tests.

**Results:** First, in situ hybridization showed DED to trigger upregulation of TRPV1, TRPA1, ASIC1, and ASIC3 mRNA in the ophthalmic branch of the TG. DED also induced overexpression of genes involved in neuropathic and inflammatory pain in the TG. Repeated instillations of capsazepine reduced corneal polymodal responsiveness to heat, cold, and acidic stimulation in ex vivo eye preparations. Consistent with these findings, chronic capsazepine instillation inhibited the upregulation of genes involved in neuropathic and inflammatory pain in the TG of DED animals and reduced the sensation of ocular pain, as well as anxiety-like behaviors associated with severe DED.

**Conclusion:** These data provide novel insights on the effectiveness of TRPV1 antagonist instillation in alleviating abnormal corneal neurosensory symptoms induced by severe DED, opening an avenue for the repositioning of this molecule as a potential analgesic treatment for patients suffering from chronic DED.

**Keywords:** Trigeminal pain, Nociceptors, Electrophysiology, Dry eye, Behavior, TRPV1 antagonist

* Correspondence: stephane.melik-parsadaniantz@inserm.fr
†Annabelle Réaux-Le Goazigo and Stéphane Mélik Parsadaniantz contributed equally to this work.
[1]Sorbonne Université, INSERM, CNRS, Institut de la Vision, 17 rue Moreau, F-75012 Paris, France
Full list of author information is available at the end of the article

## Background

Dry eye disease (DED) is a multifactorial disease of the ocular surface and tears accompanied by neurosensory abnormalities [1]. Numerous symptoms, such as redness, burning, itching, and pain, have been observed in DED patients [2, 3]. In addition, clinical data have shown that DED is often associated with anxiety and depression syndromes [4, 5]. To date, the management of chronic corneal pain still represents an important therapeutic challenge.

The cornea is the most densely innervated tissue in the body [6, 7]. Corneal nociceptive innervation is provided by ciliary nerves originating from the ophthalmic branch of the trigeminal ganglion (TG) [8, 9]. Different corneal nociceptors coexist at a single sensory nerve ending [10]. Approximately 40% are polymodal nociceptors, sensitive to heat, acidity, and chemical agents; 50% are cold thermoreceptors; and 10% are mechano-nociceptors [11]. Their sensory modalities are linked to the specific expression of ion channels: transient receptor potential vanilloid-1 (TRPV1), TRP ankyrin1 (TRPA1), and acid-sensing ion channels (ASICs 1 and 3) for polymodal nociceptors; TRP melastatin 8 (TRPM-8) for cold thermoreceptors; and piezo-type mechanosensitive ion channel component 2 (Piezo-2) for mechano-nociceptors [10].

Electrophysiological studies of trigeminal neurons in DED models have shown increased nociceptor responsiveness to cold and heat stimulation [12] and corneal nerve endings to acidic and thermal stimulation [13]. Moreover, a TRPV1 antagonist (capsazepine) prevents dry eye sensitization of cold-sensing cells to capsaicin [14]. TRPV1, which is gated by capsaicin, protons, and noxious heat [15], can be activated by hypertonic challenge, causing increased pro-inflammatory cytokine production, underlining its involvement in DED [16, 17]. Increased TRPV1 protein levels in the TG and their role in enhanced nocifensive behavior has been reported for DED rats [18]. In addition, TRPV1 inhibition reduced polymodal responsiveness to acidic stimulation in an allergic eye model [19]. TRPV1 pharmacological blockade decreases substance P release in cold allodynia [20], and DED sensitizes corneal cold nociceptive neurons via TRPV1 [14]. Finally, ocular instillation of tivanisiran, a small interfering oligonucleotide of RNA designed to silence human TRPV1, has been shown to improve ocular hyperemia and tear quality in humans [21].

We aimed to investigate the pharmacological effectiveness of topical TRPV1 antagonist treatment (capsazepine) on abnormal corneal neurosensitivity associated with persistent DED. We used our recently published preclinical mouse model of chronic DED induced by excision of the extraorbital lacrimal gland (ELG) and Harderian gland (HG) [22]. First, we studied polymodal and mechano-nociceptor mRNA expression in the ophthalmic branch of the TG under conditions of DED. Second, we evaluated the spontaneous and evoked electrical activity of the corneal nerves in response to heat, cold, and acid stimulation. Next, we assessed the effectiveness of topical treatment with capsazepine (twice a day for 21 days) on corneal nerve activity in response to heat, cold, and acid stimulation. Finally, we evaluated the beneficial effects of such treatment on nociceptive and anxiety behaviors associated with DED and on the modulation of the expression of genes involved in neuropathic and inflammatory pain in TG.

## Methods

### Experimental animals

Seven- to 8-week-old adult male C57BL/6 mice (average weight 23.48 ± 0.04 g) (Janvier Labs, Le Genest Saint Isle, France) were randomly assigned to cages (5 mice/cage) and maintained under controlled conditions (22 ± 1 °C, 60 ± 10% relative humidity, 12/12 h light/dark cycle, food and water ad libitum). All animal procedures were performed in strict accordance with institutional guidelines for the care and use of experimental animals approved by the European Communities Council Directive 2010/63/UE (APAFIS #1501 2015081815454885 v2). A well-being unit in accordance with ethics guidelines followed all experiments.

### Surgical procedures

Unilateral (right side) ELG and HG excision was performed under ketamine (80 mg/kg intraperitoneal (i.p.)) and xylazine (8 mg/kg i.p.) anesthesia in mice, as recently described [22]. Before surgery, a drop of lacrimal gel (Lubrithal™, Dechra) was applied to both eyes. Under an operative microscope (Leica-Alcon II, Germany), an 8-mm skin incision was made on the temporal side to expose and remove the ELG. After dissociating the conjunctival tissue above the orbital cavity near the internal canthus, the HG was carefully removed. Complete removal was verified by inspecting the surgical area for any remaining glandular tissue. The skin incision was then sutured using 6.0 braided silk sutures (6-0 Vicryl, Ethicon, Scotland). A drop of iodine solution was applied to the incision to avoid bacterial infection. For sham animals, an incision was made in the same zone without touching the glands. The mice were placed in warm (30 °C) cages to recover from the surgery.

### Drugs

Capsazepine (Sigma-Aldrich) was initially dissolved in 99.8% methanol and diluted 1:1325 in sterile endotoxin-free isotonic phosphate-buffered saline (PBS) to obtain a final concentration of 10 μM. Capsaicin (Sigma-Aldrich) was dissolved in 100% ethanol and then diluted 330X in

sterile endotoxin-free isotonic PBS to obtain a 100 μM solution. The vehicle-treated group corresponded to mice treated with sterile endotoxin-free isotonic PBS containing the same proportion of ethanol or methanol as the final capsazepine or capsaicin dilutions, respectively.

### Therapeutic strategy

The topical ocular treatments (vehicle, capsazepine) were randomly assigned to each cage before surgery (sham or DED). Topical ocular instillation, which was only performed in the right eye, with solvent or 10 μM capsazepine started at d7 post-surgery and continued until d21. DED animals were treated twice a day (10 am and 5 pm) in their home cages. Moreover, the cage order was randomized daily for topical ocular administration. All tests were conducted on d21. Behavioral tests were conducted first (eye closing ratio, von Frey, and anxiety). For behavioral tests, mice were placed in the testing room (at least 30–60 min before the start of the experiments), and the order of testing was randomized. The investigator was blinded to the treatment. The animals were then divided into two groups, one for electrophysiological experiments and the other for the measurement of mRNA levels in the TG. Electrophysiological traces were analyzed in a blinded manner, as the experimenter was blinded to the treatment, as well as the group of mice analyzed: operated (sham, DED) or naïve (WT).

For microscopic examination, c-Fos immunostaining was performed on the amygdala of mice from the sham and DED experimental groups in the absence of any eye stimulus; a single investigator analyzed all data in a blinded manner. Analyses were performed only on the right eye and ipsilateral TG.

### Behavioral tests

#### *Measurement of corneal sensitivity to mechanical and chemical stimulation*

Mechanical corneal sensitivity was monitored using von Frey filaments as previously described [22]. Various forces of calibrated von Frey filaments (0.008 to 0.04 g) were applied to the center of the cornea of manually immobilized mice. The mechanical threshold corresponded to the eye-blink response. For corneal chemical sensitivity, 10 μl of 100 μM capsaicin was applied to the right eye. Animals were immediately placed in individual cages, and the palpebral closure time of the right eye was measured for 5 min.

#### *Anxiety tests*

Before the tests, mice were acclimated to the experimental room for a minimum of 60 min. We used a video-tracking system and analyzed behavioral parameters with the Smart 3 software (Harvard Apparatus). The floor and walls of the testing box were cleaned between animal tests with 70% ethanol to avoid any perturbation.

**Elevated plus maze** The animal was placed in the center area of the elevated plus maze (Bioseb in vivo research instruments, France) with its head directed toward a closed arm. Time spent in the open arms (s) was recorded for 5 min [23]. The behavioral parameters were analyzed using the Smart 3 software (Harvard Apparatus).

**Black and white test (light-dark box test)** The animal was placed in the middle of a brightly illuminated chamber of the dark-light box device (Bioseb in vivo research instruments). The time spent in the white zone (%) was recorded for 5 min [24] using the Smart 3 software (Harvard Apparatus).

**Measurement of the eye-closing ratio** Spontaneous eye closure is an accurate index for monitoring spontaneous eye pain [22] and is among the quantitative measures of the grimace scale, which is used to monitor spontaneous pain behavior [25, 26]. The eye closing ratio was measured for the right eye based on photographs of mice that were awake and unconstrained and corresponds to the height/width ratio of palpebral closure. The width is the distance between the internal and external canthus and the height, the distance between the edge of the upper and lower eyelids, going through the center of the cornea. Images were captured by a digital camera using the EyeSuite™ software (Koeniz, Switzerland).

#### *Multi-unit extracellular recording of spontaneous and stimulated activities of ciliary nerve fibers in ex vivo eye preparations*

Spontaneous ciliary nerve fiber activity was determined at d21 as previously reported [22, 27]. Briefly, mice were euthanized, and the right eye (corresponding to the side of the surgery) rapidly and carefully dissected and placed in a two-compartment chamber. The baseline recordings were performed by superfusing the cornea with superfusion saline solution at 33 ± 1°C and pH 7.4. The evoked activity of the ciliary nerve was measured in response to acid or thermal stimulation. Acid stimulation was carried out by changing the pH of the superfusion saline solution from 7.4 to 6 and then 5. Thermal stimulation consisted of modifying the temperature of the superfusion saline solution from 33 ± 1 down to 20 ± 1 °C (cold stimulations) or up to 40 ± 1 °C (heat stimulations) at pH 7.4.

Multi-unit extracellular electrical activity was recorded from the ciliary nerve (composed of a large number of

nerve fibers) using a suction electrode (Ag/AgCl). The signal was filtered (300–5000 Hz), amplified (×10,000) (A-M Systems, Sequim, USA), and digitalized by Spike 2 data analysis (CED Micro1401, Cambridge Electronic Design) at a sampling frequency of 10,000 Hz. The cornea was superfused with superfusion saline solution for 30 min to stabilize the preparation before performing the electrophysiological recordings. Spontaneous extracellular ciliary nerve fiber activity was defined as impulses per second (imp/s).

A thermistor sensor (included in the CL-100 Bipolar Temperature Controller, Warner Instruments) monitored the temperature at the exit of the corneal superfusion. Chemical stimulation was achieved by exposing the cornea to a $CO_2$ (100%) pulse for 30 s.

### RT-qPCR analysis

#### *Tissue preparation for RT-qPCR analysis*

Twenty-one days after surgery, the animals were deeply anesthetized with a 300-μL mixture of ketamine (80 mg/kg) and xylazine (8 mg/kg) and transcardially perfused with 10 mL 0.9% NaCl solution. The ipsilateral TG (corresponding to the eye with LG excisions) was rapidly and carefully dissected and placed at −80°C until use.

#### *RT-qPCR analysis protocol*

RNA extraction from the ipsilateral TG was performed using a NucleoSpin RNA Purification II kit (NucleoSpin RNA S, Germany). RNA quality and concentration were then measured by the NanoDrop method (Thermo Scientific, England). Then, reverse transcription was performed using the iScript cDNA Synthesis Kit (Bio-Rad) according to the manufacturer's instructions. PCR was performed with 300 ng cDNA for each sample. RT-qPCR was performed using SsoAdvanced Universal SYBR® Green supermix (Bio-Rad) and a pain, neuropathic, and inflammatory (SAB Target List) M96-well plate (Bio-Rad; ref 10034393). The GAPDH gene was used as the endogenous reference for each reaction; mRNA levels were calculated after normalizing the results for each sample with those for GAPDH mRNA. The 2-ΔΔCt method was used to analyze the relative differences in specific mRNA levels between groups.

### Tissue preparation for fluorescent in situ hybridization and immunostaining

Twenty-one days after surgery, anesthetized mice were transcardially perfused with 10 mL 0.9% NaCl solution followed by 40 mL 4% (w/v) paraformaldehyde in 1X PBS. Next, TGs were immersed in 10%, 20%, and 30% sucrose in 1X PBS and then conserved in isopentane with liquid nitrogen and stored at −80 °C. Brain (12 μm) and TG (12 μm) thin sections were cut using a cryostat (Leica CM 3050 S) and mounted on Superfrost slides.

### Fluorescent in situ hybridization protocol

Fluorescent in situ hybridization studies were performed according to the protocol for fixed frozen tissue using the RNAscope Fluorescent Multiplex Reagent kit v2 assay (Advanced Cell Diagnostics, Newark, CA, USA). Tissues were washed with 1X PBS and treated with hydrogen peroxide (RNAscope, ref 322335) for 10 min at room temperature and washed in autoclaved distilled water. Using a steamer, tissues were treated with distilled $H_2O$ for 10 s at 99°C and then moved to RNAscope 1X target Retrieval Reagent (RNAscope, ref# 322000) for 5 min at 99°C. Tissues were washed with autoclaved distilled water and transferred to 100% alcohol for 3 min. Then, tissues were treated with RNAscope Protease III (RNAscope, ref 322337) for 30 min at 40°C and washed with autoclaved distilled water. Species-specific target probes TRPV1 C1 (313331 C1), TRPA1 C2 (400211 C2), Piezo-2 C3 (400191 C3), ASIC1 C2 (462381 C2), and ASIC3 C3 (480541 C3) were used. Sections were treated with the probe and negative (ref 320871) and positive (ref 320881) controls and hybridized for 2 h at 40°C in a humidified oven (RNAscope HybEZ oven with HybEZ humidity control tray, Advanced Cell Diagnostics). A series of incubations was then performed to amplify the signal of the hybridized probe and label target probes for the assigned fluorescence detection channel (target probe was labeled for the assigned fluorescence detection channels Opal 520 FP1487001, Opal 570 FP1488001, and Opal 650 FP1496A, PerkinElmer). Nuclei were stained using a DAPI nuclear stain (RNAscope ref 323108) for 30 s at room temperature. The sections were finally mounted with ProLong Gold Antifade Mountant (ref P36934) onto glass sides and coverslipped.

### cFOS immunostaining in the amygdala

Brain sections were rinsed in 0.1M PBS with 3% $H_2O_2$. Then, brain sections were incubated for 1 h in a blocking solution of 0.1M PBS containing 3% normal goat serum and 0.1% triton X-100, followed by incubation with the primary antibody polyclonal guinea pig anti-c-Fos (Synaptic Systems, ref 226 004, 1:1000) at 4 °C for 72 h. All steps following incubation with the primary antibody were performed at room temperature (RT).

Next, brain sections were rinsed in 0.1M PBS-T and incubated with biotinylated goat anti-guinea pig secondary antibody (Vector, ref BA-7000-1.5, 1:500) for 1 h at RT. Samples were washed in PBS and incubated with VECTASTAIN® Elite® ABC HRP (PK-6100, Vector, A reagent 1:250 and B reagent 1:250) in PBS for 1 h at RT. Tissues were rinsed with PBS and then 0.05 M Tris buffer. Revelation was performed in 0.003% $H_2O_2$ with 0.05% 3,3′-diaminobenzidine (DAB) in 0.05 M Tris buffer for 11 min. Frozen sections were dehydrated in an

ethanol series at 50%, 70%, 90%, and 100% and SaveSolv (VWR Q-Path) for 10 min each. Finally, the sections were mounted onto glass slides with Eukitt mounting medium (Sigma Aldrich) and coverslipped.

### Microscopic and NanoZoomer analysis

Brain and ipsilateral TG sections were examined using a NanoZoomer 2.0-HT digital slide scanner (C9600, Hamamatsu Photonics). The area within the field of interest covered by the mRNA profiles relative to the total area of the measured field was analyzed to detect mRNA levels in the ophthalmic branch of the TG. The same gray threshold level was applied to all sections of the same series. For c-FOS staining, the number of positive cells in the amygdala was quantified. TIFF images were analyzed using the NIH ImageJ software.

### Statistical analysis

The data obtained for different groups were compared using the appropriate paired parametric or nonparametric statistical test, as indicated. For statistical analysis, the Kolmogorov–Smirnov test was performed followed by parametric *t*-tests or nonparametric Mann-Whitney or nonparametric Kruskal-Wallis tests using GraphPad Prism version 7.00 (GraphPad Software, La Jolla, CA, USA). All *P* values were considered statistically significant for values < 0.05. All results are presented as the mean ± standard error of the mean (SEM). The unit of analysis was single mouse for all experiments.

## Results

### Chronic DED increases nociceptor mRNA levels in the ophthalmic branch of the TG

We first evaluated the levels of TRPV1, TRPA1, ASIC1, ASIC3, and Piezo-2 mRNA in the ophthalmic branch of the TG of DED and sham animals at d21 by in situ RNA scope hybridization. TRPV1 and TRPA1 mRNA levels in the ophthalmic branch of DED animals were higher than those of sham animals (Fig. 1b, c; white arrows). The percentage of surface stained for TRPV1 and TRPA1 mRNA was 109.38% and 104.07% higher for DED than sham mice, respectively (TRPV1 0.64 ± 0.13 vs. 1.34 ± 0.27, TRPA1 1.72 ± 0.35 vs. 3.51 ± 0.15, $P < 0.05$; Fig. 1b, c). In addition, ASIC1 and ASIC3 mRNA staining in the ophthalmic branch of DED animals was 116.82% and 319.57% higher for DED than sham mice, respectively (ASIC1 1.07 ± 0.13 vs. 2.32 ± 0.53; ASIC3 0.46 ± 0.13 vs. 1.93 ± 0.36, $P < 0.05$; Fig. 1d, e; white arrows). However, Piezo-2 mRNA surface staining showed no significant differences between the two groups (1.79 ± 0.81 vs. 2.94 ± 0.60, $P > 0.05$, Fig. 1f, white arrows).

### Chronic DED induces chemical and mechanical corneal hypersensitivity and anxiety-like behavior

We evaluated corneal chemical sensitivity using the capsaicin test, which consists of the topical application of 100 μM capsaicin (TRPV1 agonist). The palpebral closure time increased by 159% in DED mice over that of sham mice (52.62 ± 2.78 s vs. 136.25 ± 15.46 s, $P < 0.05$, Fig. 2a). The corneal mechanical threshold measured with von Frey filaments was 50% lower for the DED than sham mice (0.028 ± 0.003 g vs. 0.014 ± 0.002 g, $P < 0.05$, Fig. 2b).

We examined the relationship between anxiety and DED-associated pain using two behavioral tests. First, the elevated plus maze test was used to evaluate the time spent in the open arms of the maze. DED mice spent approximately 44.5% less time in the open arms than sham mice (48.25 ± 8.88 s vs. 26.78 ± 4.64 s, $P < 0.05$, Fig. 2c). Then, the black and white test was used to measure the time spent in the white zone. DED mice spent approximately 18% less time in the white zone than sham mice (31.25 ± 2.33 s vs. 25.55 s ± 1.39, $P < 0.05$, Fig. 2d).

Preclinical and clinical studies suggest an important role for the amygdala in the development of chronic anxiety and pain [29, 30]. Thus, we explored changes in cFOS immunoreactivity (a marker of neuronal activation) in this brain structure. We observed greater cFOS immunostaining (black arrows) in the amygdala of DED than sham mice (Fig. 2e). The number of cFos-positive cells in the amygdala was 39% higher in the DED than sham animals (596.91 ± 17.90 cFOS-positive cells vs. 832.72 ± 46.10 cFOS-positive cells, $P < 0.05$, Fig. 2f).

### Chronic DED increases corneal nerve responsiveness

#### *Cold and heat stimulation*

Corneal nerve responsiveness was evaluated at d21 by multi-unit extracellular recording of ciliary nerve fiber activity in ex vivo eye preparations from sham and DED animals. An electrophysiological trace illustrating the extracellular activity of the ciliary nerve fibers for the various heat ramps from 32 to 20°C and 32 to 40°C, with a time scale of 5 s, is shown in Fig. 3a, and histograms representing the number of impulses per second from sham and DED mice are shown in Fig. 3b. The ongoing activity was 54.35% higher in the DED than sham mice at 32°C (59.96 ± 4.77 imp/s vs. 92.55 ± 6.61 imp/s, $P < 0.001$, Fig. 3b). Furthermore, we perfused the cornea with superfusion saline solution at 20°C to activate corneal cold receptors. The frequency of evoked activity was 36.9% higher for the DED than sham mice at 20°C (97.65 ± 5.20 imp/s vs. 133.67 ± 8.09 imp/s, $P < 0.001$, Fig. 3b). The cornea was finally perfused with superfusion saline solution at 40°C to activate polymodal nociceptors. The frequency of firing was 48.4% for the DED than sham mice (64.18 ± 6.80 imp/s vs. 95.24 ± 9.35 imp/s, $P < 0.01$, Fig. 3b). Representative histograms and

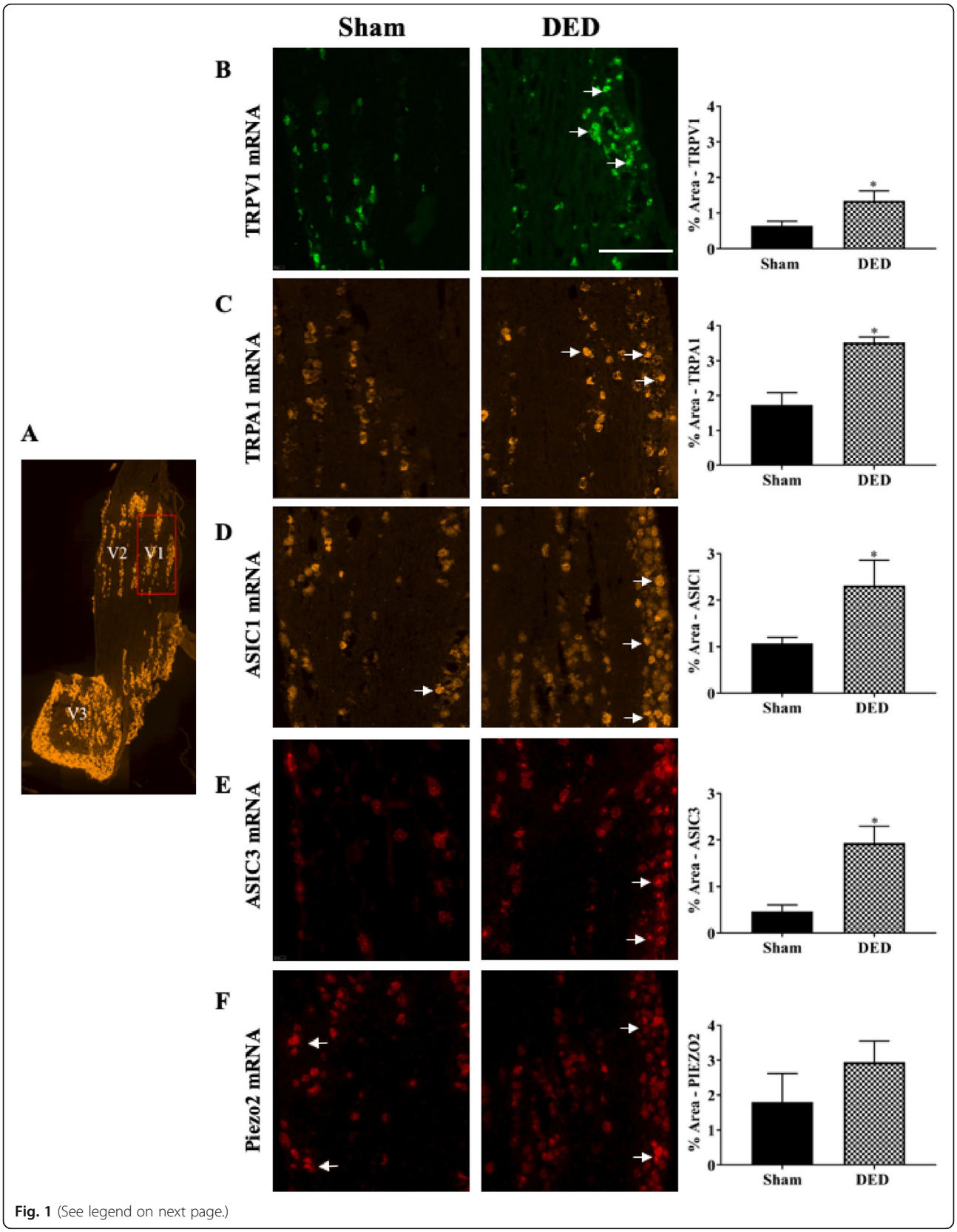


**Fig. 1** (See legend on next page.)

(See figure on previous page.)
**Fig. 1** Evaluation of nociceptor expression in the ophthalmic branch of the trigeminal ganglion (TG) of sham and dry eye disease (DED) animals. **a** Localization of the ophthalmic branch (V1, red rectangle), maxillary branch (V2), and mandibular branch (V3) in a mouse TG using the positive probe of RNAscope (Opal 520). Staining (white arrows) and quantification of mRNA levels by in situ hybridization of (**b**) transient receptor potential vanilloid-1 (TRPV1; Opal 520), (**c**) transient receptor potential ankyrin 1 (TRPA1; Opal 570), (**d**) acid-sensing ion channel 1 (ASIC1; Opal 570), (**e**) ASIC3 (Opal 650), and (**f**) Piezo-2 (Opal 650) in the ophthalmic branch of the TG of sham and DED animals. All experiments were conducted on d21. Total number of mice = 44. Sham and DED animals $n$ = 4–6. Scale bar = 50 μM. *$P < 0.05$ relative to sham group. Results are expressed as the mean ± SEM. For statistical analysis, the Kolmogorov–Smirnov test was performed followed by a parametric $t$-test (TRPV1) or nonparametric Mann-Whitney test (TRPA1, ASIC1, ASIC3, and Piezo-2) using GraphPad Prism version 7.00 (GraphPad Software, La Jolla, CA, USA)

electrophysiological traces of ciliary nerve-fiber activity in ex vivo eye preparations from sham and DED animals at 20, 32, and 40°C are illustrated in Fig. 3 c–h.

#### *Acid stimulation*

We next recorded spontaneous activity while perfusing the cornea with a superfusion saline solution at pH 7.4. The spontaneous activity was 73.15% higher for the DED than sham mice (59.96 ± 4.77 imp/s vs. 92.55 ± 6.61 imp/s, $P < 0.001$, Fig. 3i). Then, acid corneal stimulation was induced by lowering the pH of the superfusion saline solution from 7.4 to 6 and then 5. The firing of evoked ciliary nerve activities was 46.64% higher at pH 6 (81.88 ± 4.97 imp/s vs. 120.07 ± 9.86 imp/s, $P < 0.01$, Fig. 3i) and 52.17% higher at pH 5 (78.50 ± 6.11 imp/s vs. 119.45 ± 13.21 imp/s, $P < 0.01$, Fig. 3i) for the DED than sham mice. Representative histograms and electrophysiological traces of ciliary nerve fiber activity in ex vivo eye preparations from sham and DED animals at pH 5, 6, and 7.4 are presented in Fig. 3 j–o.

#### *Chemical stimulation: $CO_2$*

$CO_2$ gas pulses are a commonly used chemical stimulation to activate corneal polymodal nociceptors [27, 31]. Representative electrophysiological traces and histograms illustrating the number of impulses per second from sham and DED mice during a 30s $CO_2$ pulse are presented in Fig. 4 a and b. The latency of the impulse discharge evoked by $CO_2$ was 36.86% lower for DED than sham mice (10.12 ± 1.03 s vs. 6.39 ± 0.66 s, $P < 0.01$, Fig. 4c).

### Topical treatment with capsazepine decreases the expression of genes related to neuropathic pain and inflammation in the TG of DED animals

We next evaluated the mRNA levels of genes involved in the conduction and modulation of pain in the TG of DED animals relative to that of sham animals and in the TG of DED animals treated with 10 μM capsazepine versus vehicle, taking into consideration that the vehicle hydrates dry corneas and artificial tears are one of the strategies to relieve the symptoms of DED patients.

#### *Glial-inflammatory cell communication*

Neuronal-glial communication mediated by purinergic signaling participates in chronic pain [32]. Adenosine triphosphate (ATP) has been proposed to activate P2X and P2Y purinergic receptors, contributing to inflammation [33, 34]. Moreover, activation of purinergic receptors contributes to acute nociception and the maintenance of nociceptive sensitivity [35]. P2RX3, P2RX7, and P2RY1 mRNA levels were 293%, 54.9%, and 103.96% higher in the TG of DED than sham mice, respectively (P2RX3 1.00 ± 0.03 vs. 1.30 ± 0.11, P2RX7 1.02 ± 0.10 vs. 1.58 ± 0.23, P2RY1 1.01 ± 0.07 vs. 2.06 ± 049, $P < 0.05$, Fig. 5a). There was no difference in P2RX3, P2RX7, or P2RY1 mRNA expression between DED animals treated with 10 μM capsazepine and those treated with the vehicle group (P2RX3 0.88 ± 0.14 vs. 0.81 ± 0.11, P2RX7 1.10 ± 0.25 vs. 0.77 ± 0.074, P2RY1 1.71 ± 0.79 vs. 0.92 ± 0.78, $P > 0.05$, Fig. 5a). However, administration of either capsazepine or vehicle resulted in lower P2RX3 and P2RX7 mRNA expression than in untreated DED animals (P2RX3: DED animals 1.30 ± 0.11 vs. vehicle group 0.88 ± 0.14 vs. 10 μM capsazepine 0.81 ± 0.11, P2RX7: DED animals 1.58 ± 0.23 vs. vehicle group 1.10 ± 0.25 vs 10 μM capsazepine group 0.77 ± 0.074, $P < 0.05$, Fig. 5a).

Brain-derived neurotrophic factor (BDNF) plays a functional role in peripheral and central sensitization processes. Its expression is induced by ATP via purinergic receptors [36]. Here, BDNF mRNA levels were 465% higher in DED than sham animals (1.01 ± 0.09 vs. 5.62 ± 1.52, $P < 0.05$, Fig. 5a). However, chronic treatment with capsazepine did not alter BDNF mRNA expression in DED animals relative to that in the vehicle group (3.30 ± 1.21 vs. 1.60 ± 0.47, $P > 0.05$, Fig. 5a). Nevertheless, BDNF mRNA expression was lower in DED animals treated with 10 μM capsazepine than those that were not (5.62 ± 1.52 vs. 1.60 ± 0.47, $P < 0.05$, Fig. 5a).

#### *Targets related to nociceptive inhibition*

The mu opioid receptor (MOR), cannabinoid receptor 1 (CB1), and proenkephalin (PENK) are known to inhibit nociceptive transmission [37–39]. The mRNA levels of MOR, CB1, and PENK were 149%, 121%, and 149% higher in the TG of DED animals than those of sham

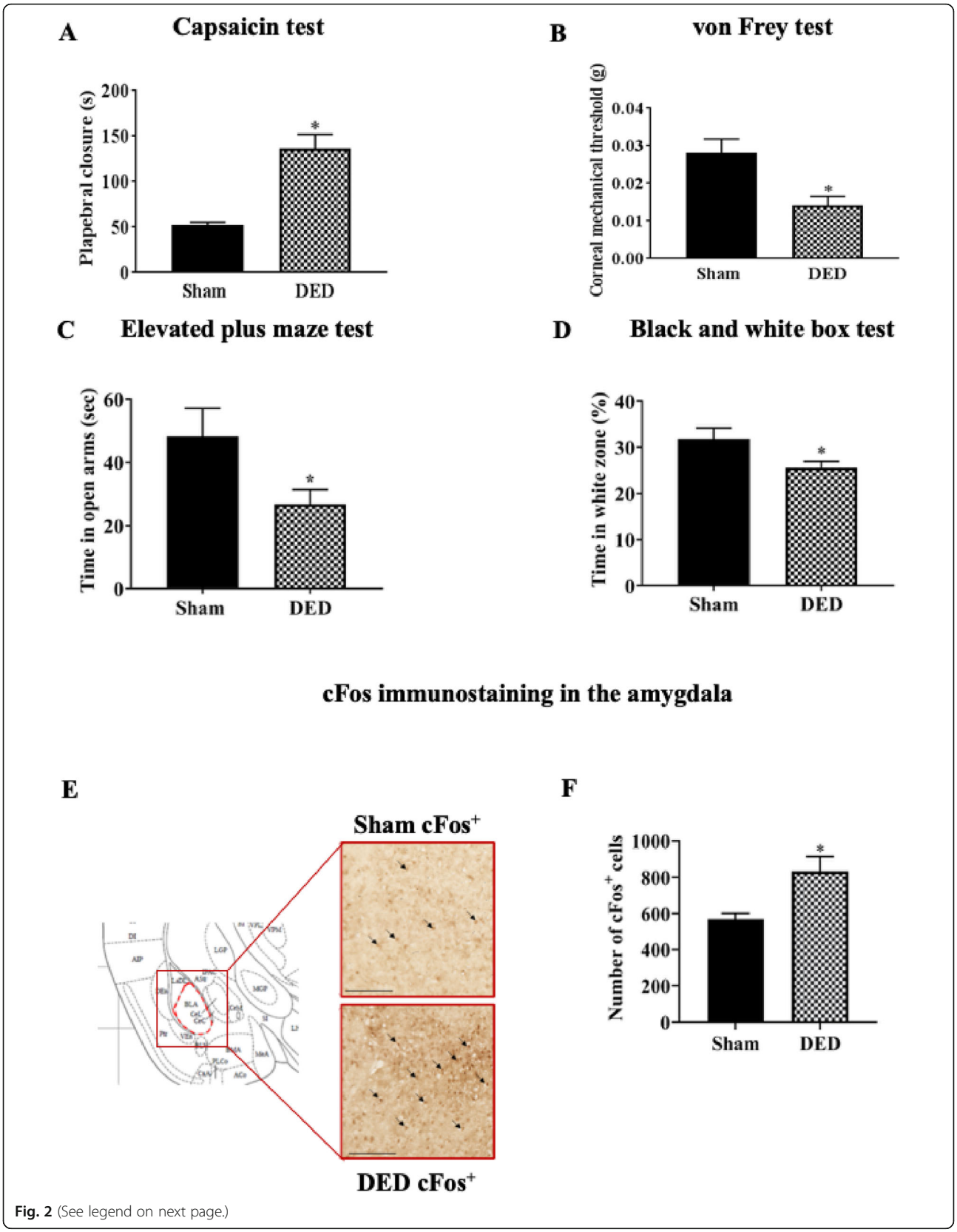


**Fig. 2** (See legend on next page.)

(See figure on previous page.)
**Fig. 2** Evaluation of chemical and mechanical corneal sensitivity and anxiety-like behavior of sham and DED animals on d21. **a** Chemical corneal sensitivity was evaluated using a drop of capsaicin (100 μM) and recording the palpebral closure time for 5 min. **b** The corneal mechanical threshold was measured using von Frey filaments. **c** Elevated plus maze: the mouse was placed in the center area of the maze with its head directed toward a closed arm and time (s) in the open arms was recorded for 5 min. **d** Black and white test: The mouse was placed in the middle of a brightly illuminated chamber and time in the white zone (%) was recorded for 5 min. **e** cFos immunoreactivity in the amygdala of sham and DED mice; $cFos^+$ cells (black arrows). Scale bar = 100 μm. Regions corresponding to the images are depicted in coronal diagrams taken from the Paxinos atlas [28]. **f** Quantification of the number of $cFos^+$ cells in the amygdala of sham and DED animals. Total number of mice = 48. Number of mice included in the analysis = 48. Capsaicin and von Frey test: $n = 6$ sham and DED animals for each test. Elevated plus maze and black and white tests: $n = 15$ sham and DED animals; cFos immunoreactivity in amygdala: $n = 3$ sham and DED animals. *$P < 0.05$ relative to the sham group. Results are expressed as the mean ± SEM. For statistical analysis, the Kolmogorov–Smirnov test was performed followed by a parametric *t*-test (capsaicin test, von Frey test, elevated plus maze test, and black and white test) or nonparametric Mann-Whitney test (quantification of the number of $cFos^+$ cells in the amygdala) using GraphPad Prism version 7.00 (GraphPad Software, La Jolla, CA, USA)

animals, respectively (MOR 1.00 ± 0.05 vs. 2.49 ± 0.33, CB1 1.00 ± 0.05 vs. 2.21 ± 0.21, $P < 0.01$, and PENK 1.00 ± 0.05 vs. 2.49 ± 0.33, $P < 0.05$, Fig. 5b).

CB1 and MOR mRNA expression of DED animals treated with 10 μM capsazepine was 55.93% and 44% lower than that of the vehicle group, respectively (CB1 1.21 ± 0.27 vs. 0.82 ± 0.24, $P < 0.05$; MOR 1.21 ± 0.29 vs. 0.66 ± 0.07, $P < 0.05$; Fig. 5b), whereas there was no significant difference in PENK mRNA expression between the two groups (5.46 ± 2.66 vs. 2.80 ± 0.55, $P > 0.05$, Fig. 5b). Moreover, ocular instillation with capsazepine or vehicle resulted in lower CB1 and MOR mRNA levels in treated than untreated DED animals (CB1: DED animals 2.21 ± 0.21 vs. vehicle group 1.21± 0.27 vs. 10 μM capsazepine group 0.82 ± 0.24, $P < 0.05$; MOR: DED animals 2.49 ± 0.33 vs. vehicle group 1.21 ± 0.29 vs. 10 μM capsazepine 0.66 ± 0.07, $P < 0.05$; Fig. 5b).

### *Intracellular signal transduction*

Mitogen-activated protein kinases (MAPKs) are essential mediators of signal transduction, and their activation contributes to hypersensitivity to pain [40]. MAPK 1, 3, and 8 mRNA levels were 342%, 49%, and 340% higher in the TG of DED than sham animals, respectively (MAPK1 1.02 ± 0.07 vs. 4.51 ± 0.73, MAPK3 1.02 ± 0.04 vs. 1.52 ± 0.14, $P < 0.01$, and MAPK 8 1.01 ± 0.06 vs. 4.45 ± 0.62, $P < 0.001$; Fig. 5c).

Chronic instillation of DED animals with 10 μM capsazepine resulted in MAPK1 and MAPK8 mRNA levels that were 43% and 47% lower, respectively, than those in mice treated with vehicle (MAPKI 2.09 ± 0.58 vs. 1.20 ± 0.33 and MAPK8 2.26 ± 0.58 vs. 1.18 ± 0.28, $P < 0.05$; Fig. 5c). MAPK3 mRNA expression was not significantly different in DED animals treated with 10 μM capsazepine relative to that of the vehicle group (0.86 ± 0.26 vs. 0.60 ± 0.17, $P > 0.05$, Fig. 5c). In addition, corneal instillation with capsazepine or vehicle resulted in lower MAPK1 and MAPK8 mRNA levels in the treated than untreated DED animals (MAPKI: DED animals 4.51 ± 0.73 vs. vehicle 2.09 ± 0.58 vs. 10 μM capsazepine 1.20 ± 0.33 and MAPK8: DED animals 4.45 ± 0.62 vs. vehicle 2.26 ± 0.58 vs. 10 μM capsazepine 1.18 ± 0.28, $P < 0.05$, Fig. 5c).

### *Voltage-gated ion channels*

Electrical excitation of peripheral somatosensory nerves is controlled by potassium and sodium ion channels [41, 42]. We found potassium channel 2 (KCJN6) mRNA levels to be 136.63% higher in DED than sham animals (KCJN6 1.01 ± 0.07 vs. 2.39 ± 0.58, $P < 0.05$, Fig. 5d). In addition, sodium channel 1.8 (Nav1.8) and 1.7 (Nav1.7) mRNA levels were 166% and 293% higher in DED than sham animals, respectively (Nav1.8 1.00 ± 0.05 vs. 2.66 ± 0.40, Nav1.7 1.00 ± 0.06 vs. 3.93 ± 0.53, $P < 0.01$, Fig. 5d).

Capsazepine treatment resulted in Nav1.8 and Nav1.7 mRNA levels that were 40% and 62% lower, respectively, than in animals treated with vehicle (Nav1.8 1.29 ± 0.27 vs. 0.78 ± 0.19, Nav1.7 2.23 ± 0.70 vs. 0.84 ± 0.05, $P < 0.05$, Fig. 5d). We observed no significant difference of KCJN6 mRNA expression in the TG of DED animals treated with 10 μM capsazepine relative to those treated with vehicle (KCJN6 1.13 ± 0.21 vs. 1.34 ± 0.17, $P > 0.05$, Fig. 5d). However, both treatments resulted in lower Nav1.8 and Nav1.7 mRNA levels in both groups than in untreated DED animals (Nav1.8: DED 2.66 ± 0.40 vs. vehicle group 1.29 ± 0.27 vs. 10 μM capsazepine 0.78 ± 0.19, $P < 0.05$; Nav1.7: DED 3.93 ± 0.53 vs. vehicle 2.23 ± 0.70, $P < 0.05$ vs. 10 μM capsazepine 0.84 ± 0.05, $P < 0.01$; Fig. 5d).

### *Synaptic transmission*

Increased electrical excitation increases synaptic transmission. We investigated serotonin and glutamate receptor expression in the TGs of DED and sham animals. The levels of 5-hydroxytryptamine receptor 2A (HTR2A) and glutamate (NMDA) receptor subunit zeta-1 (GRIN1) mRNA were 109% and 79% higher in the TG of DED than sham animals, respectively (HTR2A 1.00 ± 0.06 vs. 2.09 ± 0.17, $P < 0.001$; GRIN1 1.00 ± 0.05 vs. 1.79 ± 0.18, $P < 0.01$; Fig. 5e).

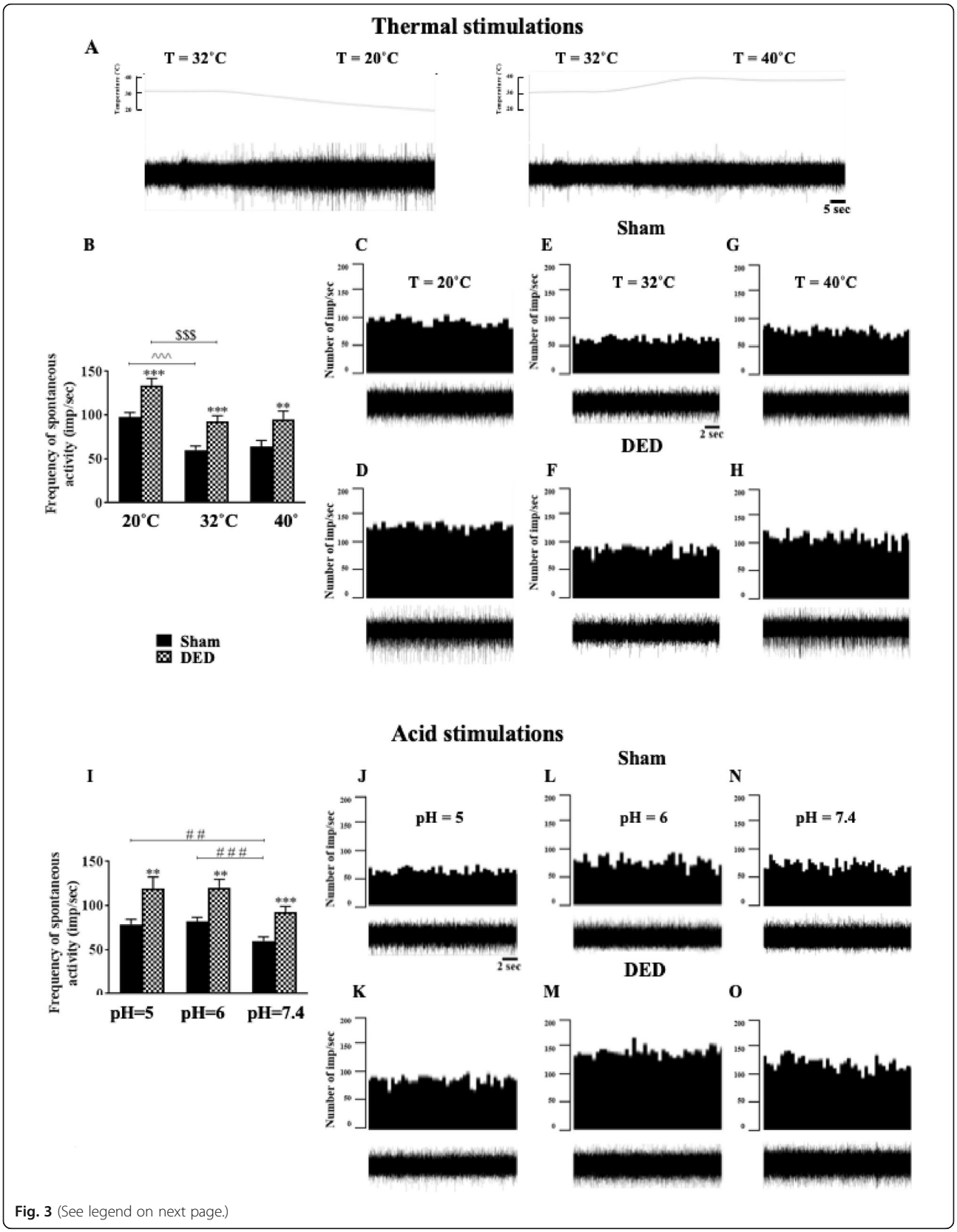


**Fig. 3** (See legend on next page.)

(See figure on previous page.)
**Fig. 3** Ex vivo evaluation of spontaneous and evoked activities of the ciliary nerve from sham and DED mice. **a** Electrophysiological trace illustrating the extracellular activity of the ciliary nerve fiber with the various heat ramps; time scale = 5 s. Histograms showing the mean value of spontaneous (32°C) and evoked (20°C and 40°C) firing frequency of ciliary nerves: **b** at 20, 32, and 40°C. Representative histograms and electrophysiological traces to illustrate extracellular activity of the ciliary nerve: **c**, **d** at 20°C; **d**, **f** at 32°C; and **g**, **h** at 40°C in sham and DED mice; time scale = 2 s. Histograms showing the mean value for the spontaneous firing frequency of ciliary nerves: **i** at pH 5, 6, and 7.4 in both groups. Representative histograms and electrophysiological traces to illustrate extracellular activity of the ciliary nerve: **j**, **k** at pH 5; **l**, **m** at pH 6; and **N**, **O** at pH 7.4 in sham and DED mice; time scale = 2 s. All experiments were conducted on d21. Total number of mice = 27. Number of mice included in the analysis = 26. Thermal stimulation: $n$ = 13 sham and DED animals; acid stimulation: $n$ = 10 sham and DED animals. All experiments were conducted on d21. $^{**}P < 0.01$, $^{***}P < 0.001$ relative to the sham group. ^^^ < 0.001 sham at 20°C and 32°C. $$$ < 0.001 DED at 20°C and 32°C. ## < 0.01 sham at pH 5 and 7.4. ### < 0.001 sham at pH 6 and 7.4. Results are expressed as the mean ± SEM. For statistical analysis, the sham vs DED groups were compared for each condition using the Kolmogorov–Smirnov test, followed by the parametric $t$-test, using GraphPad Prism version 7.00 (GraphPad Software, La Jolla, CA, USA)

Chronic ocular treatment with capsazepine did not alter HTR2A and NMDA mRNA levels in DED animals relative to the vehicle group (HTR2A 1.10 ± 0.25 vs. 0.68 ± 0.13, GRIN1 0.96 ± 0.05 vs. 0.97 ± 0.16, $P > 0.05$; Fig. 5e). HTR2A mRNA levels were, however, lower in capsazepine- and vehicle-treated than untreated DED animals (HTR2A: DED 2.09 ± 0.17 vs. vehicle 1.10 ± 0.25, $P < 0.05$ vs. 10 μM capsazepine 0.68 ± 0.13, $P < 0.001$, Fig. 5e). Moreover, capsazepine treatment resulted in lower NMDA mRNA levels in DED animals treated with 10 μM capsazepine than in untreated DED animals (GRIN1 1.79 ± 0.18 vs. 0.97 ± 0.16, $P < 0.05$, Fig. 5e).

### *Inflammation*

The mRNA levels of prostaglandin-endoperoxide synthase 2 (PTGS2), also known as cyclooxygenase-2 (COX-2), prostaglandin E synthase 3 (PTGES3), and prostaglandin E receptor 3 (PTGER3), were 502%, 500%, and 342% higher, respectively, in the TG of DED than sham animals (PTGS2 1.01 ± 0.07 vs. 6.08 ± 0.62, PTGE S3 1.01 ± 0.09 vs. 6.05 ± 0.98, $P < 0.05$, and PTGER3 1.01 ± 0.08 vs. 4.47 ± 0.94, $P < 0.01$; Fig. 5f).

Capsazepine treatment resulted in 45% and 57% lower levels of PTGS2 (COX2) and PTGES3 mRNA, respectively, than in the vehicle group (PTGS2 6.39 ± 2.30 vs. 3.51 ± 0.98, $P > 0.05$, and PTGES3 3.98 ± 0.85 vs. 1.68 ± 0.47, $P < 0.05$; Fig. 5f). However, topical capsazepine treatment did not significantly alter IL1β, CCR2, CX3CR1, TLR4, CSF1, or PTGER3 mRNA levels relative to those of the vehicle group (IL1β 1.89 ± 0.07 vs. 1.82 ± 0.06, CCR2 2.13 ± 0.50 vs. 1.62 ± 0.30, CX3CR1 1.67 ± 0.65 vs. 1.01 ± 0.60, TLR4 1.28 ± 0.17 vs. 1.10 ± 0.08, CSF1 1.51 ± 0.61 vs. 0.89 ± 0.30, PTGER3 2.60 ± 1.43 vs. 1.51 ± 0.43, $P > 0.05$; Fig. 5e). Only CSF1 mRNA expression was lower in DED animals treated with the vehicle than in untreated DED animals (CSF1 4.19 ± 0.87 vs. 1.51 ± 0.61 vs. 0.89, $P < 0.05$, Fig. 5e). However, capsazepine treatment of DED mice resulted in lower PTGE S3 and PTGER3 mRNA levels than in untreated DED mice (PTGES3 6.05 ± 0.98 vs. 1.68 ± 0.47, $P < 0.01$; PTGER3 4.47 ± 0.94 vs. 1.51 ± 0.43, $P < 0.05$, Fig. 5e).

The levels of tachykinin precursor 1 (TAC1), colony-stimulating factor 1 (CSF1), and toll-like receptor 4 (TLR4) mRNA were also higher in the TG of DED than sham animals, 421%, 315%, and 166%, respectively (TAC1 1.02 ± 0.10 vs. 5.31 ± 1.15, $P < 0.01$; CSF1 1.01 ± 0.06 vs. 4.19 ± 0.87, $P < 0.05$; and TLR4 1.00 ± 0.04 vs. 2.66 ± 0.65, $P < 0.05$; Fig. 5f), as were the levels of interleukin (IL)-1β, IL-18, and IL-6 mRNA, which were 113%, 398%, and 267% higher, respectively, in the DED animals (IL1β 1.08 ± 0.23 vs. 2.30 ± 0.36, $P < 0.05$; IL18 1.01 ± 0.07 vs. 5.03 ± 0.89, $P < 0.01$; and IL6 1.00 ± 0.05 vs. 3.67 ± 0.35, $P < 0.0001$; Fig. 5f). Furthermore, the levels of chemokine (C-C motif) ligand 2 (CCL2), C-C chemokine receptor type 2 (CCR2), and CX3C chemokine receptor 1 (CX3CR1) mRNA were 450%, 207%, and 134% higher, respectively, in the TG of DED animals (CCL2 1.05 ± 0.19 vs. 5.78 ± 1.39, $P < 0.01$; CCR2 1.01 ± 0.07 vs. 3.10 ± 0.71, $P < 0.05$; CX3CR1 1.00 ± 0.05 vs. 2.34 ± 0.64, $P < 0.05$; Fig. 5f).

Moreover, the levels of TAC1 mRNA were 54% lower in DED mice treated with 10 μM capsazepine than those treated with vehicle (3.56 ± 0.85 vs. 1.63 ± 0.46, $P < 0.05$, Fig. 5f), and IL18 and IL6 mRNA levels were also lower by 63% and 74%, respectively (IL18 3.67 ± 0.92 vs. 1.39 ± 0.27, $P < 0.05$ and IL6 5.60 ± 3.20 vs. 1.42 ± 0.43, $P > 0.05$; Fig. 5f). Treatment of DED mice with 10 μM capsazepine also resulted in chemokine CCL2 mRNA levels that were 59% lower than in mice treated with vehicle (4.28 ± 0.96 vs. 1.73 ± 0.39, $P < 0.05$; Fig. 5f). In addition, topical capsazepine administration to DED animals resulted in lower TAC1, IL18, IL6, CCL2, TLR4, and CSF1 mRNA levels than in untreated DED animals (TAC1 5.31 ± 1.15 vs. 1.63 ± 0.46, $P < 0.05$; IL18 5.03 ± 0.89 vs. 1.39 ± 0.27, $P < 0.05$; IL6 3.67 ± 0.35 vs. 1.42 ± 0.43, $P < 0.01$; CCL2 5.78 ± 1.39 vs. 1.73 ± 0.39, $P < 0.05$; TLR4 2.66 ± 0.65 vs. 1.10 ± 0.21, $P < 0.05$; and CFS1 4.19 ± 0.87 vs. 1.00 ± 0.20, $P < 0.01$; Fig. 5f).

## Pharmacological blockage of TRPV1 reduces corneal nociception and anxiety of DED mice

We next investigated the impact of topical treatment of capsazepine on corneal mechanical allodynia associated with DED. The mechanical threshold was 120% higher

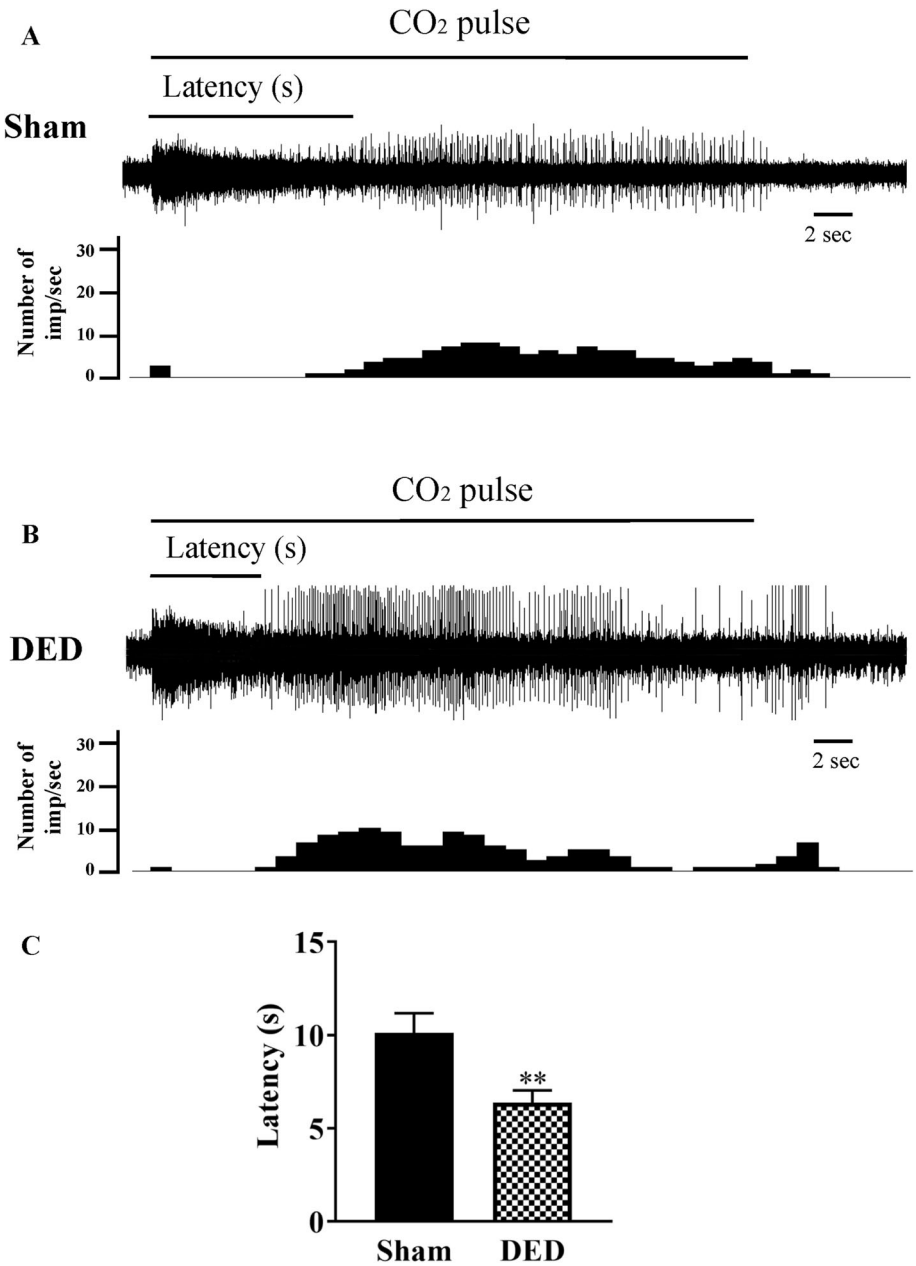


**Fig. 4** Responsiveness of corneal polymodal nociceptive fibers to $CO_2$ stimulation for sham and DED animals. **a**, **b** Electrophysiological traces and histograms illustrating corneal responsiveness to a 30-s $CO_2$ pulse. **c** Histogram showing the latency of impulse discharge evoked by $CO_2$ for sham and DED animals. Total number of mice = 16. Number of mice included in the analysis =16. Sham and DED animals: $n = 8$ per group. All experiments were conducted on d21. $^{**}P < 0.01$ relative to sham group. Results are expressed as the mean ± SEM. For statistical analysis, the Kolmogorov–Smirnov test was performed followed by a parametric *t*-test using GraphPad Prism version 7.00 (GraphPad Software, La Jolla, CA, USA)

in DED animals treated with 10 μM capsazepine than those receiving vehicle (vehicle 0.010 ± 0.002 vs. 10 μM capsazepine 0.022 ± 0.003, $P < 0.01$; Fig. 6a). The eye-closing ratio was also 9.86% higher for DED animals treated with 10 μM capsazepine than those treated with vehicle (vehicle 0.71 ± 0.02 vs. 10 μM capsazepine 0.78 ± 0.02, $P < 0.05$; Fig. 6b). Next, we investigated the effect of topical capsazepine on anxiety-like behavior associated with DED. Animals treated with capsazepine spent 94% more time in the open arms than those treated with vehicle (control animals 59.01 ± 3.31 s vs vehicle 30.91 ± 3.54 s vs. 10 μM capsazepine 59.83 ± 9.27 s, $P < 0.05$; Fig. 6c). The time spent in the open arms by control animals (WT) was significantly different from that of DED

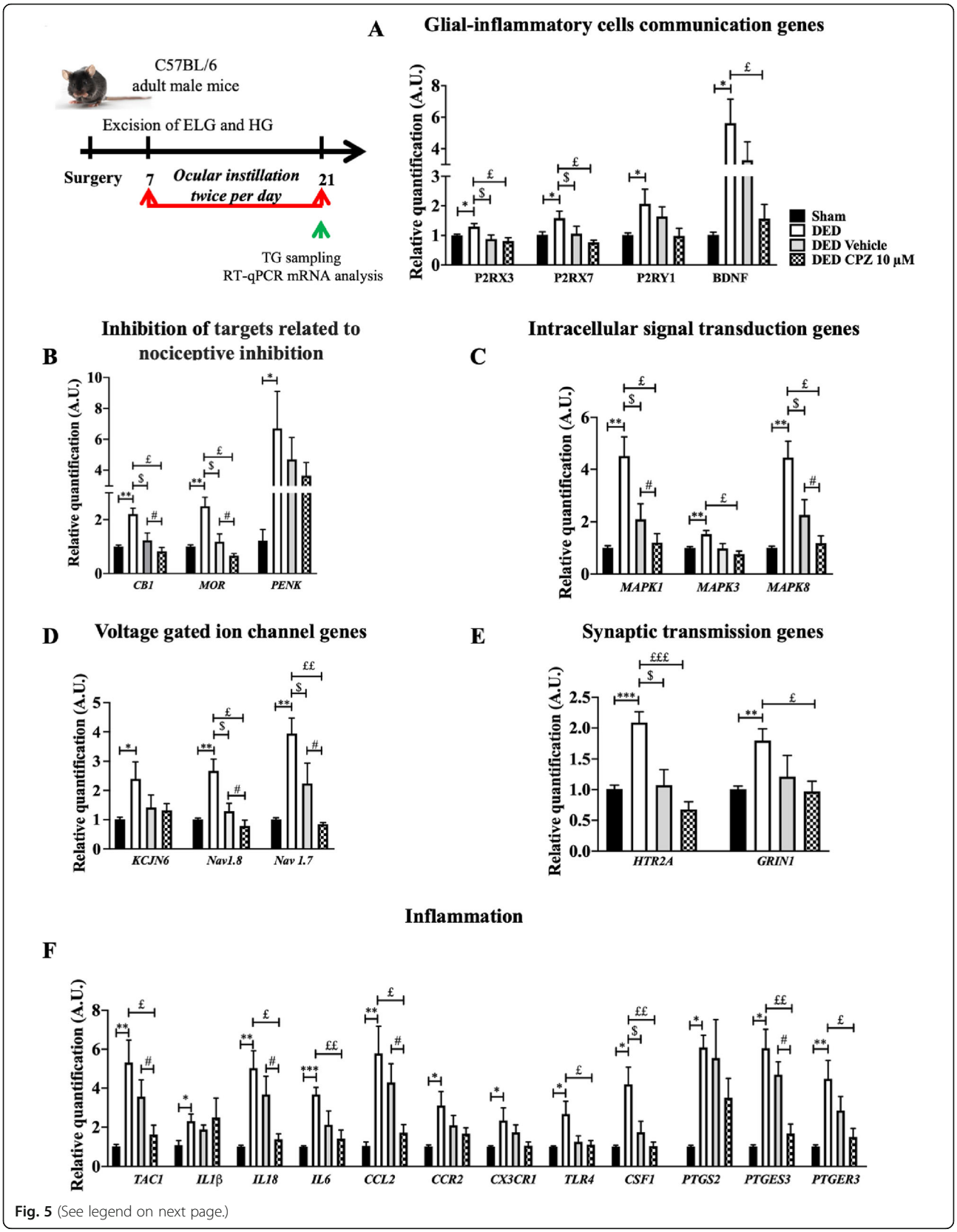


**Fig. 5** (See legend on next page.)

(See figure on previous page.)
**Fig. 5** Evaluation of the expression of genes involved in pain conduction and the modulation of pain responses in the TG of untreated sham and DED animals and DED animals treated with 10 μM capsazepine or vehicle on d21. RT-qPCR analysis of ipsilateral TG of sham mice, DED mice, and DED mice treated with 10μM capsazepine or vehicle: glial-inflammatory cell communication genes (**a**), inhibition of targets related to nociceptive inhibition (**b**), intracellular signal transduction genes (**c**), voltage-gated ion channel genes (**d**), synaptic transmission genes (**e**), inflammation genes (**f**). Total number of mice = 19. Number of mice included in the analysis = 19. Sham mice, DED mice, and DED ice-treated with 10μM capsazepine or vehicle: $n$ =4–5. *$P$ < 0.05, **$P$ < 0.01, ***$P$ < 0.001, ****$P$ < 0.0001 relative to sham animals. $ < 0.05: DED treated with vehicle relative to DED. £ < 0.05, ££ < 0.01, £££ < 0.001: DED treated with capsazepine relative to DED, # $P$<0.05: DED treated with capsazepine relative to DED treated with vehicle. Results are expressed as the mean ± SEM. For statistical analysis, the Kolmogorov–Smirnov test was performed followed by a nonparametric Mann-Whitney test or a parametric $t$-test using GraphPad Prism version 7.00 (GraphPad Software, La Jolla, CA, USA)

animals treated with vehicle but not from that of the capsazepine group. Moreover, the black and white box test showed capsazepine treatment to increase the time spent in the white zone by DED animals by 54% relative to those receiving vehicle (control animals 39.83 ± 5.47 s vs vehicle 21.80 ± 2.37 s vs. 10 μM capsazepine 33.50 ± 2.97 s, $P$ < 0.05; Fig. 6d). The time spent in the white zone by control animals was significantly different from that of DED animals treated with vehicle but not from those receiving topical 10 μM capsazepine.

### Topical treatment with capsazepine reduces corneal nociceptor sensitization in DED animals

DED animals were treated twice per day from d7 through d21 with 10 μM capsazepine and compared to DED animals treated with vehicle to determine the involvement of the TRPV1 channel in corneal nerve hyperexcitability. Spontaneous activity was 57% lower at 32°C for DED mice treated with 10 μM capsazepine than those treated with vehicle (vehicle 86.78 ± 5.57 imp/s vs. 10 μM capsazepine 37.10 ± 6.83, $P$ < 0.01; Fig. 7a). Next, we evaluated the effect of 10 μM capsazepine on corneal nerve activity triggered by heat and cold. Evoked activity was 35% and 44% lower at 20°C and 40°C, respectively for DED mice treated with 10 μM capsazepine than those treated with vehicle (20°C: vehicle 127.71 ± 13.52 vs. 10 μM capsazepine 71.41 ± 12.85, $P$ < 0.01, Fig. 7b and 40°C: vehicle 104.57 ± 12.74 vs. 10 μM capsazepine 67.20 ± 8.59, $P$ < 0.05, Fig. 7c). We also evaluated the effect of 10 μM capsazepine on corneal nerve activity in response to acid stimulation. Evoked activity was 38% and 40% lower at pH 6 and 5, respectively for DED mice treated with 10 μM capsazepine than those treated with vehicle (pH 6: vehicle 105.01 ± 14.33 vs. 10 μM capsazepine 64.60 ± 8.29, $P$ > 0.05, Fig. 7d and pH 5 99.71 ± 8.16 vs. 10 μM capsazepine 59.61 ± 7.56, $P$ < 0.05, Fig. 7e).

## Discussion

Despite the high prevalence of DED, the underlying mechanisms of this ocular surface disease are not fully understood. Here, we hypothesized that repeated instillations of a TRPV1 antagonist (capsazepine) could alleviate ocular pain syndrome in severe DED mice. Capsazepine is a synthetic analog of capsaicin that acts as a TRPV1antagonist, leading to suppression of $Ca^{2+}$influx [43]. In addition, it can target other TRP channels, such as TRPV-4 and TRPM-8. Docherty et al. reported that capsazepine non-specifically blocks voltage-activated calcium channels [44]. Kistner et al. found that capsazepine can also exhibit inhibitory effects on colitis via the modulation of TRPA1 [45]. This molecule has been extensively used in spinal and trigeminal pain studies to specifically block the TRPV1 channel [14, 43, 46–48]. A major finding of our work is that repeated instillation of capsazepine has beneficial effects on DED mice: it decreases (1) corneal polymodal responsiveness, (2) the upregulation of genes related to inflammation and pain in the TG, and (3) corneal hypersensitivity and anxiety-like behavior associated with persistent DED.

Here, we used our recently published model of severe DED obtained by excision of the ELG and HG from adult male mice [22]. We first carried out a comparative study of the behavior and electrophysiological responses related to the present study between male and female DED and sham-operated adult mice, which showed no sex-based differences (data not shown).

All animal procedures were performed in strict accordance with institutional guidelines for the care and use of experimental animals, respecting the 3Rs for the use of animals. The removal of two different functional glands (aqueous and lipid) reduces tear production by 97% [22] and closely mimics both aqueous-deficient DED by excision of the ELG and evaporative DED by excision of the HG, which produces an oily, lipid-enriched secretion. The severe DED induced by this model may be considered to be a limitation. However, our DED model, along with being associated with increased ocular nociception, is chronic and does not require repeated injections of chemical solutions with neurotropic activity (such as scopolamine) or the placing of mice in a desiccative environment, which could be stressful for them.

During inflammation, it has been demonstrated that reducing the extracellular pH enhances pain [49]. Indeed, the corneal peripheral free terminals of Aδ and C-fibers are able to detect acidosis through two polymodal channels, TRPV1 and ASICs [50, 51]. After TRPV1 and ASIC depolarization, cationic currents generate action potentials, leading to pain [52, 53]. We demonstrate that

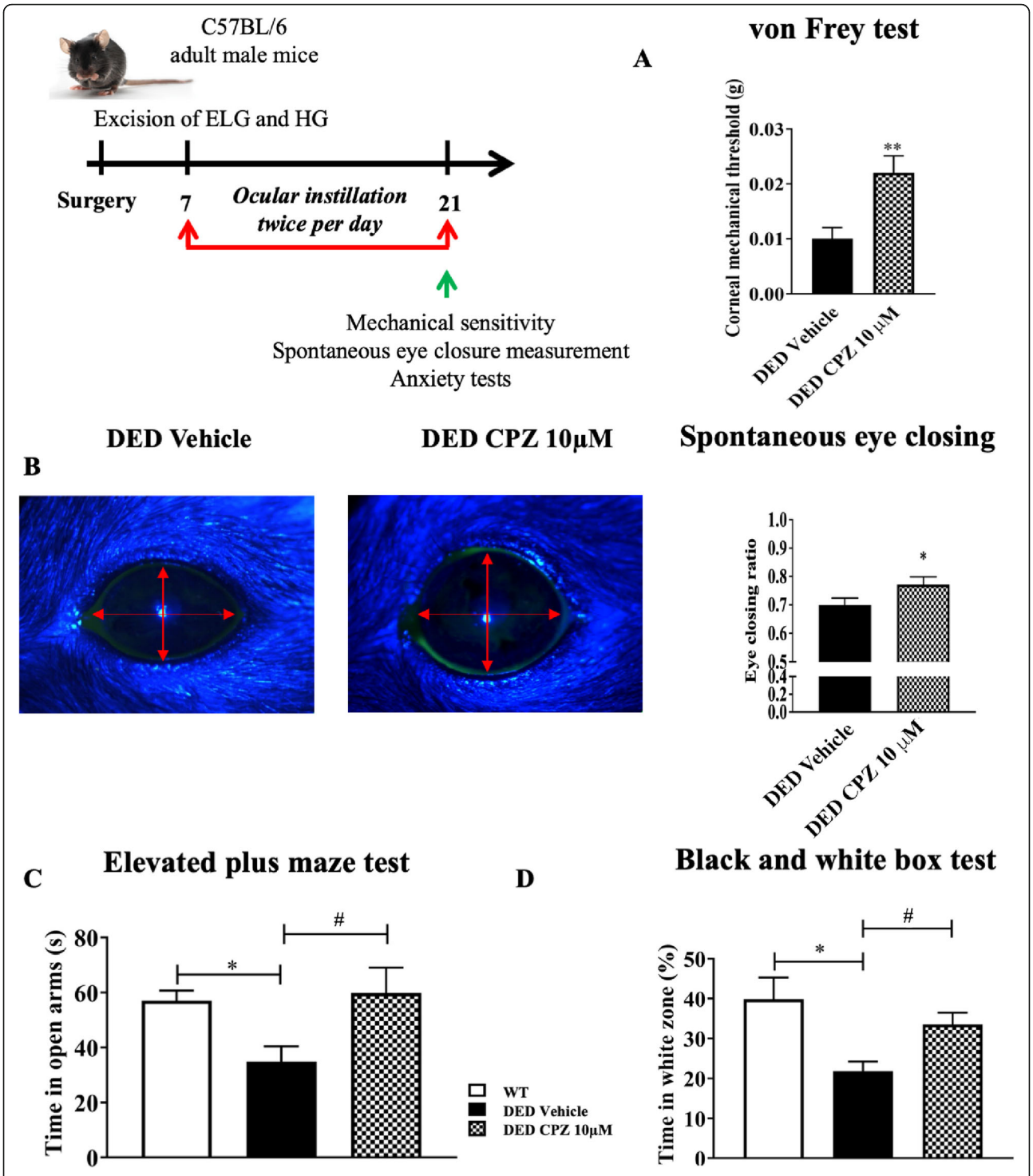


**Fig. 6** Mechanical allodynia, eye closing ratio, and anxiety of DED animals treated with 10 μM capsazepine or vehicle. **a** Corneal mechanical sensitivity measured with von Frey filaments. **b** Images and quantification of the spontaneous eye closing ratio calculated by measuring the width/height ratio. **c** Time spent in the open arms (s) in the elevated plus maze test. **d** Time spent in the white zone (%) in the black and white box test by DED animals treated with 10 μM capsazepine or vehicle. Total number of mice = 20. Number of mice included in the analysis = 20. DED animals treated with vehicle and 10 μM capsazepine: $n = 10$. All tests were conducted on d21. $^{*}P < 0.05$, $^{**}P < 0.01$ relative to DED treated with vehicle. Results are expressed as the mean ± SEM. For statistical analysis, the Kolmogorov–Smirnov test was performed followed by a parametric *t*-test (von Frey and spontaneous eye closure ratio) or the nonparametric Kruskal-Wallis test (elevated plus maze test and black and white test) using GraphPad Prism version 7.00 (GraphPad Software, La Jolla, CA, USA)

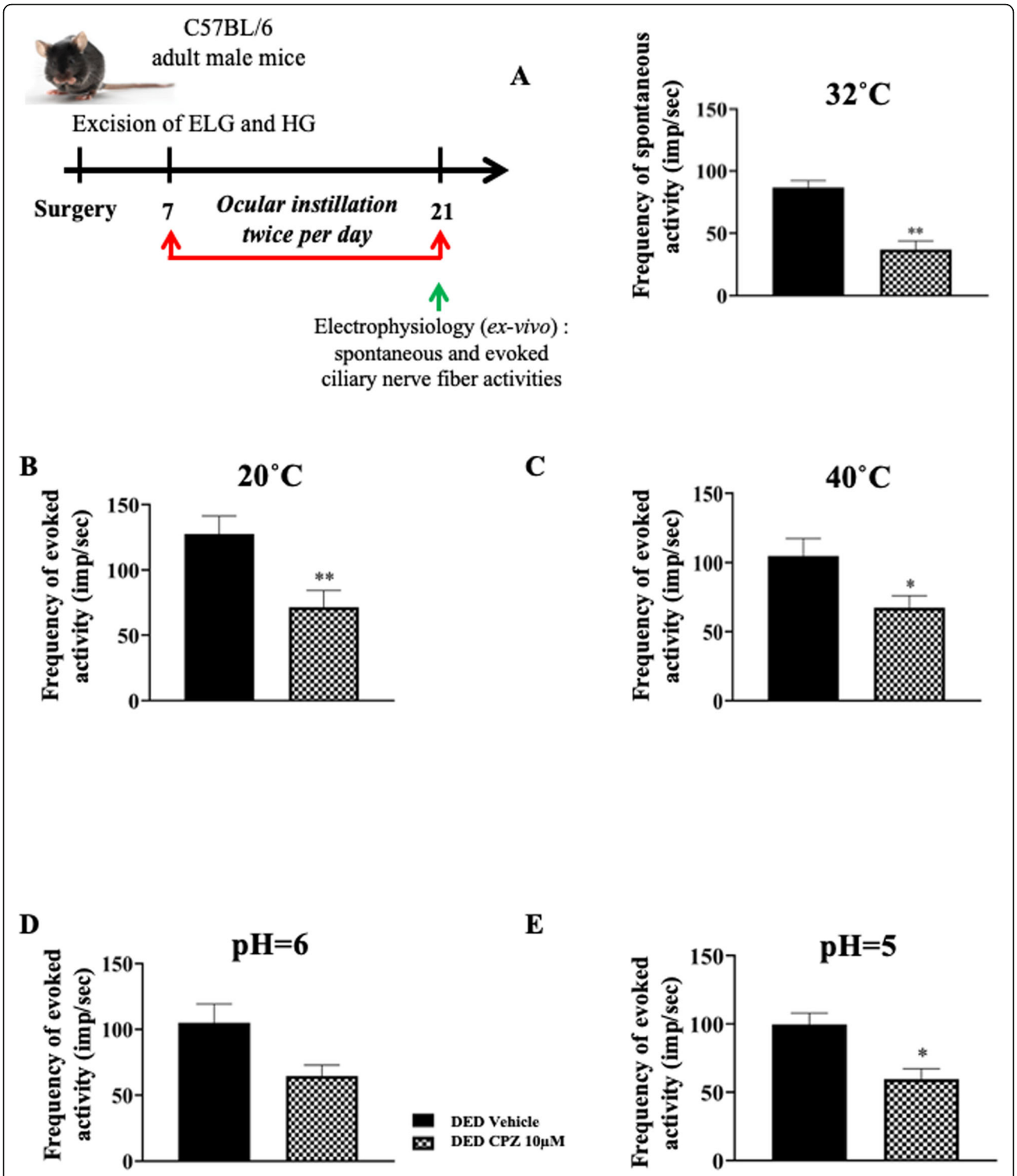


**Fig. 7** Ex vivo evaluation of spontaneous and evoked activity of the ciliary nerve in DED animals treated with 10μM capsazepine or vehicle. Histograms show the mean value of the frequency activity of the ciliary nerve at (**a**) 32°C and pH 7.4, (**b**) 20°C, (**c**) 40°C, (**d**) pH 6, and (**e**) pH 5 for DED animals treated with 10 μM capsazepine or vehicle. Total number of mice = 20. Number of mice included in the analysis = 20. DED animals treated with vehicle and 10 μM capsazepine: $n = 10$. All experiments were conducted on d21. *$P < 0.05$, **$P < 0.01$ relative to DED animals treated with vehicle. Results are expressed as the mean ± SEM. For statistical analysis, the Kolmogorov–Smirnov test was performed followed by a parametric *t*-test using GraphPad Prism version 7.00 (GraphPad Software, La Jolla, CA, USA)

chronic DED induces sensitization of corneal polymodal nerves in response to a $CO_2$ gas jet and acid stimulation (pH 5 and 6) using an electrophysiological ex vivo recording of ciliary nerve fiber activity. Such corneal nerve sensitization can be explained by higher TRPVI and ASIC mRNA expression in the ophthalmic branch of the TG of DED animals. It has been established that only 50% of all $CO_2$-activated fibers respond to stimulation by capsaicin (a TRPV1 agonist) in the cat cornea [54, 55]. Thus, we suggest that both TRPV1 and ASIC channels are involved in the response to acid stimulation in DED.

Thermal hypersensitivity is common in inflammation and nervous system damage [56]. Both TRPV1 and TRPA1 polymodal channels are known to be activated by acute heat [57]. Interestingly, the firing of ciliary nerves in DED mice increased with heat stimulation, demonstrating an intensification of polymodal responsiveness to heat. This finding is in accordance with higher mRNA levels of both TRPA1 and TRPV1 channels in the TGs of DED animals. Thus, we provide further evidence of polymodal nociceptor sensitization at the level of the cornea and peripheral nervous system in DED animals. Moreover, it is known that activation of polymodal nociceptors evokes a burning pain [10]. This is in accordance with the increased nocifensive behaviors observed after topical application of capsaicin in DED animals. We suggest that DED-induced polymodal sensitization may be a mechanism responsible for the enhanced pain and burning sensations classically observed in DED patients [58].

On the other hand, our data show that a TRPV1 antagonist (capsazepine) decreases polymodal responsiveness to acid and heat stimulation, in accordance with capsazepine-induced reduction of polymodal nociceptor responses to acid stimulation in an allergic eye model [19]. TRPV1 has high $Ca^{2+}$ permeability, and it has been reported that heat stimulation increases calcium concentrations via TRPV1; such an increase was blocked with capsazepine [59]. This finding explains the effectiveness of specific TRPV1 antagonism to heat and acid stimulation in DED animals.

Belmonte et al. showed that ongoing ciliary nerve fiber activity results mostly from cold nerve fiber activation, which represents half of corneal sensory neurons [11, 31]. Thus, the increase in spontaneous ciliary nerve fiber activity observed in DED animals may result from the triggering of corneal cold nociceptors, as already reported for DED guinea pigs [13]. Interestingly, despite the insensitivity of TRPV1 to cold stimulation, capsazepine blunted the DED-induced increase of ciliary nerve firing to cold stimulation. It was recently demonstrated that overexpression of TRPV1 in TRPM-$8^{+}$ cold-sensing fibers causes cold allodynia in DED mice obtained by extra orbital gland excision [20]. Thus, we suggest that capsazepine decreases ongoing and stimulated ciliary activity by acting on cold nociceptor responsiveness.

Mice in our DED model, characterized by a decrease in corneal intraepithelial nerve endings, develop increased mechanical sensitivity, as previously reported [22]. Such mechanical hypersensitivity has also been found in an aqueous tear deficiency model of DED in the rat [60] and in mouse models of corneal injury [27].

A reduction in the density of corneal intraepithelial nerves has been reported in several DED models [61–64] and is associated with decreased mechanical sensitivity. In the clinic, studies on patients with DED or neuropathic pain symptoms have shown reduced corneal nerve density associated with decreased sensitivity to mechanical, thermal, and chemical stimuli relative to controls [65], whereas others have shown increased mechanical sensitivity [66]. These contrasting observations from preclinical and clinical studies may be related to varying severity and differing etiology (inflammatory vs neuropathic) of patients, as well as to different models and methods used to measure corneal mechanical sensitivity in preclinical and clinical studies.

Mechano- and polymodal nociceptors respond to mechanical stimulation [8]. Moreover, capsaicin-induced mechanical allodynia in skin is mediated via Piezo-2 [67]. We found that Piezo-2 mRNA levels were not upregulated, unlike those of TRPV1, in the TG of DED mice relative to sham animals. In addition, topical capsazepine administration decreased corneal mechanical allodynia in DED animals, suggesting key involvement of polymodal nociceptors in the mechanical allodynia associated with DED. In a recent study, Fernández-Trillo et al. demonstrated that Piezo2 channels are present in the cell body and nerve endings of corneal neurons [68]. They used several modalities and multimodal approaches to show that Piezo2 channels contribute to mechanical sensitivity in sensory nerve endings of pure corneal mechanoreceptors and polymodal nociceptors. Of note, this study did not evaluate the expression of Piezo2 in the cornea or TG of DED mice. Here, we quantified the expression of Piezo2 mRNA by the RNA scope in situ hybridization technique throughout the ophthalmic branch of the TG and found Piezo2 expression to remain unchanged in the state of DED. However, polymodal nociceptors (known to express TRPV1 and to a lesser extent Piezo 2) are also activated by mechanical stimuli. Based on the results of Fernández-Trillo et al., demonstrating that Piezo2 contributes to the mechanical sensitivity in sensory nerve endings of polymodal nociceptors, and the higher expression of TRPV1 in TG in our preclinical DED model, our data suggest that topical treatment with capsazepine reduces (without completely blunting) the mechanical hypersensitivity associated with chronic DED. Such an effect may be mediated primarily

by TRPV1 expressed by corneal nociceptors, but the participation of Piezo2 in such mechanical hypersensitivity cannot be excluded.

Numerous studies have demonstrated that pain is modulated by endogenous (enkephalins, endorphins, and dynorphins) opioids and the cannabinoid system [37–39]. Here, we observed that DED induced a significant increase in CB1, MOR, and Penk expression in ipsilateral TG (relative to the sham group); such an increase may be related to sensitization of the corneal nociceptors in DED animals. We previously found higher expression of MOR in corneal nerve fibers and trigeminal sensory neurons in a mouse model of inflammatory corneal pain [69]. In addition, repeated topical ocular administration of DAMGO (a MOR-selective ligand) strongly reduced both mechanical (von Frey) and chemical (capsaicin challenge) corneal hypersensitivity. Topical DAMGO administration also reversed the elevated spontaneous activity of the ciliary nerve and responsiveness of corneal polymodal nociceptors associated with inflammatory ocular pain [69].

Nociceptor sensitization to inflammatory stimuli is a signal to protect the tissue from their harmful consequences. Much data demonstrate that nociceptive neurons express receptors for immune cell-derived inflammatory mediators [70, 71]. Thus, during inflammation, these mediators modify nociceptor responsiveness, notably by inducing phosphorylation of ligand-gated channels, i.e., TRPV1 and TRPA1, leading to increased neuronal firing [72, 73]. Inflammation is the core mechanism of DED, and we recently reported inflammatory responses in the TG from DED mice [22]. Here, we extend our knowledge by providing a molecular signature of TG during persistent DED. Our data show significant upregulation of the mRNA levels of the immune receptors and inflammatory mediators IL1β, IL18, IL6, CCL2, cyclooxygenase enzymes, prostaglandins, CX3CR1, CCR2, and TLR4 in the TG of DED animals. These receptors and inflammatory mediators are known to be linked to the pathophysiology of pain [74–76]. Thus, we suggest that these upregulated inflammatory markers may activate peptidergic polymodal nociceptor terminals and stimulate their intracellular signaling pathways. This hypothesis is corroborated by the upregulation of MAPK mRNA levels in the TG of DED animals. Overall, this cascade of events may lead to the excitation of peripheral terminals and the spread of nociceptive messages, which are controlled by potassium and sodium ion channels [41, 42]. The overexpression of mRNA for these channels in the TG could also explain the increase of ciliary nerve firing observed in DED animals.

Additionally, glutamatergic synapses modulate excitatory neurotransmission in nociceptive pathways [77]. The upregulation of glutamate receptor mRNA expression suggests higher nociceptive transduction in the TG of DED animals. Moreover, it has been demonstrated that neuronal–glial communication through purinergic signaling is involved in chronic pain [32]. P2RX3 and P2RX7 also increase pain, whereas P2RY1 decreases its intensity [32, 78]. The upregulation of P2RX3, P2RX7, and P2RY1 mRNA levels observed in the TG of DED animals highlights enhanced neuronal–glial communication in chronic DED, as we previously reported [22].

Capsazepine has been reported to reduce macrophage, eosinophil, and proinflammatory cytokine levels in a chronic asthma model [79]. These anti-inflammatory properties can explain the decrease of inflammatory markers observed in the TG of DED animals chronically treated with topical capsazepine. Moreover, substance P (SP) is encoded by the Tac1 gene and synthesized by C and Aδ nociceptive primary sensory neurons. Once depolarized, corneal polymodal nociceptor neurons release pro-inflammatory neuropeptides, leading to neurogenic inflammation [31, 80]. Ang et al. demonstrated the anti-inflammatory effects of capsazepine, showing it to reduce SP production and proinflammatory molecule levels in a model of polymicrobial sepsis [81]. Thus, the decrease in DED-induced TAC1 mRNA levels in the TG of DED animals by capsazepine highlights a reduction in neurogenic inflammation and the excitation of peripheral free terminals in DED animals. This hypothesis is supported by the decrease of sodium ion channel and MAPK mRNA levels in the TG of DED animals treated with capsazepine.

Preclinical and clinical studies have reported comorbidity between DED and anxiety [82–84]. Thus, we used two behavioral tests (elevated plus maze and black and white tests) and show that DED mice develop anxiety-like behaviors that correlate with the neuronal activation observed in the amygdala, thus linking nociceptive responses with the emotional aspects of pain [85]. These findings highlight the neuropsychiatric impact of chronic DED on these animals, which caused pain and anxiety. Moreover, through this original approach, we showed that DED animals treated with capsazepine spent more time in the anxious zones of both behavioral tests than untreated DED mice, correlating with the lower level of anxiety-related behavior observed in TRPV1 knockout mice [86] and highlighting an anxiolytic effect of capsazepine in DED animals.

## Conclusion

In conclusion, our results provide new arguments on the pharmacological effectiveness of TRPV1 antagonist instillation against DED-induced sensory abnormalities and anxiety, opening a new avenue for the repositioning of this class of molecule as a potential analgesic treatment of patients suffering from chronic DED.

### Abbreviations

AP: Action potential; ASICs: Acid-sensing ion channels; ATP: Adenosine triphosphate; BDNF: Brain-derived neurotrophic factor; CPZ: Capsazepine; CB1: Cannabinoid receptor 1; CCL2: Chemokine (C-C motif) ligand 2; CCR2: C-C chemokine receptor type 2; COX-2: Cyclooxygenase-2; CSF1: Colony-stimulating factor 1; CX3CR1: CX3C chemokine receptor 1; DED: Dry eye disease; ELG: Extraorbital lacrimal gland; GAPDH: Glyceraldehyde 3-phosphate dehydrogenase; GRIN1: Glutamate [NMDA] receptor subunit zeta-1; HG: Harderian gland; HTR2A: 5-Hydroxytryptamine receptor 2A; imp: Impulse; i.p.: Intraperitoneal; KCJN6: Potassium channel 2; IL1β: Interleukin-1β; IL6: Interleukin-6; MAPK: Mitogen-activated protein kinase; MOR: Mu opioid receptor; mRNA: Messenger RNA; Nav1.7: Sodium channel 1.7; Nav1.8: Sodium channel 1.8; PENK: Proenkephalin; Piezo-2: Piezo-type mechanosensitive ion channel component 2; P2RX: Purinergic receptor X; P2RY: Purinergic receptor Y; PTGS2: Prostaglandin-endoperoxide synthase 2; PTGES3: Prostaglandin E synthase 3; PTGER3: Prostaglandin E receptor 3; RT: Room temperature; RT-PCR: Real-time polymerase chain reaction; SEM: Standard error of the mean; TAC1: Tachykinin precursor 1; TBSC: Trigeminal brainstem sensory complex; TBP: TATA-binding protein; TG: Trigeminal ganglion; TLR-4: Toll-like receptor 4; TRPV1: Transient receptor potential vanilloid-1; TRPA1: Transient receptor potential ankyrin 1; TRPM-8: Transient receptor potential melastatin 8

### Acknowledgements

The authors thank the imagery platform and the staff of the animal housing facilities at the Institut de la Vision for their help. We also thank Sarah Gallet-Wimez from UMR-S1172 development and plasticity of the Neuroendocrine brain–Lille, France, for RNAscope in situ hybridization training.

### Authors' contributions

DF performed the experiments, analyzed and interpreted the data, generated the figures, discussed the results, and wrote the manuscript. AGM performed the cFOS immunostaining experiment in the amygdala and analyzed the data. CB interpreted the data, discussed the results and their significance, and commented on the manuscript. SMP and ARLG designed and supervised all experiments, interpreted the data, discussed the results and their significance, and wrote the manuscript. All authors approved the final article.

### Funding

This work was funded by the Laboratoires Théa, within the framework of a research collaboration with the Sorbonne Université/Institut de la Vision. Darine Fakih is supported by the Association Nationale de la Recherche et de la Technologie (Conventions Industrielles de Formation par la Recherche N° 2016/1641). This work was completed with the support of the Programme Investissements d'Avenir IHU FOReSIGHT (ANR-18-IAHU-01). Adrian Guerrero Moreno is funded by a European grant: MSCA-ITN-ETN-2017 (grant agreement 765608).

### Availability of data and materials

The datasets analyzed during this study are available from the corresponding author upon reasonable request.

## Declarations

### Ethics approval and consent to participate

All animal procedures were performed in strict accordance with the institutional guidelines for the care and use of experimental animals approved by the European Communities Council Directive 2010/63/UE (APAFIS #1501 2015081815454885 v2). A well-being unit followed all the experiments in accordance with ethics guidelines.

### Consent for publication

Not applicable

### Competing interests

The authors declare that they have no competing interests.

### Author details

[1]Sorbonne Université, INSERM, CNRS, Institut de la Vision, 17 rue Moreau, F-75012 Paris, France. [2]R&D Department, Laboratoires Théa, 12 rue Louis Biérot, F-63000 Clermont-Ferrand, France. [3]CHNO des Quinze-Vingts, INSERM-DGOS CIC 1423, 17 rue Moreau, F-75012 Paris, France. [4]Department of Ophthalmology, Ambroise Paré Hospital, AP-HP, University of Versailles Saint-Quentin-en-Yvelines, 9 avenue Charles de Gaulle, F-92100 Boulogne-Billancourt, France.

Received: 8 January 2021 Accepted: 29 April 2021
Published online: 11 May 2021

### References

1. Craig JP, Nichols KK, Akpek EK, Caffery B, Dua HS, Joo C-K, et al. TFOS DEWS II definition and classification report. Ocul Surf. 2017;15(3):276–83. https://doi.org/10.1016/j.jtos.2017.05.008.
2. Messmer EM. The pathophysiology, diagnosis, and treatment of dry eye disease. Dtsch Arztebl Int. 2015;112:71–81 quiz 82.
3. Nicolle P, Liang H, Reboussin E, Rabut G, Warcoin E, Brignole-Baudouin F, et al. Proinflammatory markers, chemokines, and enkephalin in patients suffering from dry eye disease. Int J Mol Sci. 2018;19(4). https://doi.org/10.3390/ijms19041221.
4. Kitazawa M, Sakamoto C, Yoshimura M, Kawashima M, Inoue S, Mimura M, et al. The relationship of dry eye disease with depression and anxiety: a naturalistic observational study. Transl Vis Sci Technol. 2018;7(6):35. https://doi.org/10.1167/tvst.7.6.35.
5. Wan KH, Chen LJ, Young AL. Depression and anxiety in dry eye disease: a systematic review and meta-analysis. Eye (Lond). 2016;30(12):1558–67. https://doi.org/10.1038/eye.2016.186.
6. Goyal S, Hamrah P. Understanding neuropathic corneal pain-gaps and current therapeutic approaches. Semin Ophthalmol. 2016;31(1-2):59–70. https://doi.org/10.3109/08820538.2015.1114853.
7. Cruzat A, Qazi Y, Hamrah P. In vivo confocal microscopy of corneal nerves in health and disease. Ocul Surf. 2017;15(1):15–47. https://doi.org/10.1016/j.jtos.2016.09.004.
8. Belmonte C, Nichols JJ, Cox SM, Brock JA, Begley CG, Bereiter DA, et al. TFOS DEWS II pain and sensation report. Ocular Surface. 2017;15(3):404–37. https://doi.org/10.1016/j.jtos.2017.05.002.
9. Launay P-S, Godefroy D, Khabou H, Rostene W, Sahel J-A, Baudouin C, et al. Combined 3DISCO clearing method, retrograde tracer and ultramicroscopy to map corneal neurons in a whole adult mouse trigeminal ganglion. Exp Eye Res. 2015;139:136–43. https://doi.org/10.1016/j.exer.2015.06.008.
10. Belmonte C, Acosta MC, Merayo-Lloves J, Gallar J. What causes eye pain? Curr Ophthalmol Rep. 2015;3(2):111–21. https://doi.org/10.1007/s40135-015-0073-9.
11. González-González O, Bech F, Gallar J, Merayo-Lloves J, Belmonte C. Functional properties of sensory nerve terminals of the mouse cornea. Invest Ophthalmol Vis Sci. 2017;58(1):404–15. https://doi.org/10.1167/iovs.16-20033.
12. Kurose M, Meng ID. Dry eye modifies the thermal and menthol responses in rat corneal primary afferent cool cells. J Neurophysiol. 2013;110(2):495–504. https://doi.org/10.1152/jn.00222.2013.
13. Kovács I, Luna C, Quirce S, Mizerska K, Callejo G, Riestra A, et al. Abnormal activity of corneal cold thermoreceptors underlies the unpleasant sensations in dry eye disease. Pain. 2016;157(2):399–417. https://doi.org/10.1097/j.pain.0000000000000455.
14. Hatta A, Kurose M, Sullivan C, Okamoto K, Fujii N, Yamamura K, et al. Dry eye sensitizes cool cells to capsaicin-induced changes in activity via TRPV1. J Neurophysiol American Physiological Society. 2019;121(6):2191–201. https://doi.org/10.1152/jn.00126.2018.
15. Caterina MJ, Leffler A, Malmberg AB, Martin WJ, Trafton J, Petersen-Zeitz KR, et al. Impaired nociception and pain sensation in mice lacking the capsaicin receptor. Science. 2000;288(5464):306–13. https://doi.org/10.1126/science.288.5464.306.
16. Pan Z, Wang Z, Yang H, Zhang F, Reinach PS. TRPV1 activation is required for hypertonicity-stimulated inflammatory cytokine release in human corneal epithelial cells. Invest Ophthalmol Vis Sci. 2011;52(1):485–93. https://doi.org/10.1167/iovs.10-5801.
17. Martínez-García MC, Martínez T, Pañeda C, Gallego P, Jimenez AI, Merayo J. Differential expression and localization of transient receptor potential vanilloid 1 in rabbit and human eyes. Histol Histopathol. 2013;28(11):1507–16. https://doi.org/10.14670/HH-28.1507.
18. Bereiter DA, Rahman M, Thompson R, Stephenson P, Saito H. TRPV1 and TRPM8 channels and nocifensive behavior in a rat model for dry eye. Invest

Ophthalmol Vis Sci. 2018;59(8):3739–46. https://doi.org/10.1167/iovs.18-24304.
19. Acosta MC, Luna C, Quirce S, Belmonte C, Gallar J. Changes in sensory activity of ocular surface sensory nerves during allergic keratoconjunctivitis. Pain. 2013;154(11):2353–62. https://doi.org/10.1016/j.pain.2013.07.012.
20. Li F, Yang W, Jiang H, Guo C, Huang AJW, Hu H, et al. TRPV1 activity and substance P release are required for corneal cold nociception. Nat Commun. 2019;10(1):5678. https://doi.org/10.1038/s41467-019-13536-0.
21. Moreno-Montañés J, Bleau A-M, Jimenez AI. Tivanisiran, a novel siRNA for the treatment of dry eye disease. Expert Opin Investig Drugs. 2018;27(4):421–6. https://doi.org/10.1080/13543784.2018.1457647.
22. Fakih D, Zhao Z, Nicolle P, Reboussin E, Joubert F, Luzu J, et al. Chronic dry eye induced corneal hypersensitivity, neuroinflammatory responses, and synaptic plasticity in the mouse trigeminal brainstem. J Neuroinflammation. 2019;16(1):268. https://doi.org/10.1186/s12974-019-1656-4.
23. Walf AA, Frye CA. The use of the elevated plus maze as an assay of anxiety-related behavior in rodents. Nat Protoc. 2007;2(2):322–8. https://doi.org/10.1038/nprot.2007.44.
24. Bourin M, Hascoët M. The mouse light/dark box test. Eur J Pharmacol. 2003;463(1-3):55–65. https://doi.org/10.1016/S0014-2999(03)01274-3.
25. Langford DJ, Bailey AL, Chanda ML, Clarke SE, Drummond TE, Echols S, et al. Coding of facial expressions of pain in the laboratory mouse. Nat Methods. 2010;7(6):447–9. https://doi.org/10.1038/nmeth.1455.
26. Matsumiya LC, Sorge RE, Sotocinal SG, Tabaka JM, Wieskopf JS, Zaloum A, et al. Using the Mouse Grimace Scale to reevaluate the efficacy of postoperative analgesics in laboratory mice. J Am Assoc Lab Anim Sci. 2012;51(1):42–9.
27. Joubert F, Acosta MDC, Gallar J, Fakih D, Sahel J-A, Baudouin C, et al. Effects of corneal injury on ciliary nerve fibre activity and corneal nociception in mice: a behavioural and electrophysiological study. Eur J Pain. 2019;23(3):589–602. https://doi.org/10.1002/ejp.1332.
28. Franklin K, Paxinos G. The mouse Brain in Stereotaxic Coordinates. 3rd edition. San Diago: Academic Press; 2008.
29. Andreoli M, Marketkar T, Dimitrov E. Contribution of amygdala CRF neurons to chronic pain. Exp Neurol. 2017;298(Pt A):1–12. https://doi.org/10.1016/j.expneurol.2017.08.010.
30. Simons LE, Moulton EA, Linnman C, Carpino E, Becerra L, Borsook D. The human amygdala and pain: evidence from neuroimaging. Hum Brain Mapp. 2014;35(2):527–38. https://doi.org/10.1002/hbm.22199.
31. Belmonte C, Aracil A, Acosta MC, Luna C, Gallar J. Nerves and sensations from the eye surface. Ocul Surf. 2004;2(4):248–53. https://doi.org/10.1016/S1542-0124(12)70112-X.
32. del Puerto A, Wandosell F, Garrido JJ. Neuronal and glial purinergic receptors functions in neuron development and brain disease. Front Cell Neurosci [Internet]. 2013; [cited 2020 Mar 24];7. Available from: https://www.ncbi.nlm.nih.gov/pmc/articles/PMC3808753/.
33. Calovi S, Mut-Arbona P, Sperlágh B. Microglia and the purinergic signaling system. Neuroscience. 2019;405:137–47. https://doi.org/10.1016/j.neuroscience.2018.12.021.
34. Semenova IB. Role of purinergic receptors in immune response. Zh Mikrobiol Epidemiol Immunobiol. 2016:107–19.
35. Burnstock G. Purinergic mechanisms and pain. Adv Pharmacol. 2016;75:91–137. https://doi.org/10.1016/bs.apha.2015.09.001.
36. Klein K, Aeschlimann A, Jordan S, Gay R, Gay S, Sprott H. ATP induced brain-derived neurotrophic factor expression and release from osteoarthritis synovial fibroblasts is mediated by purinergic receptor P2X4. PLoS One. 2012;7(5):e36693. https://doi.org/10.1371/journal.pone.0036693.
37. Madariaga-Mazón A, Marmolejo-Valencia AF, Li Y, Toll L, Houghten RA, Martinez-Mayorga K. Mu-opioid receptor biased ligands: a safer and painless discovery of analgesics? Drug Discov Today. 2017;22(11):1719–29. https://doi.org/10.1016/j.drudis.2017.07.002.
38. Donvito G, Nass SR, Wilkerson JL, Curry ZA, Schurman LD, Kinsey SG, et al. The endogenous cannabinoid system: a budding source of targets for treating inflammatory and neuropathic pain. Neuropsychopharmacology. 2018;43(1):52–79. https://doi.org/10.1038/npp.2017.204.
39. König M, Zimmer AM, Steiner H, Holmes PV, Crawley JN, Brownstein MJ, et al. Pain responses, anxiety and aggression in mice deficient in pre-proenkephalin. Nature. 1996;383(6600):535–8. https://doi.org/10.1038/383535a0.
40. Ji R-R, Gereau RW, Malcangio M, Strichartz GR. MAP kinase and pain. Brain Res Rev. 2009;60(1):135–48. https://doi.org/10.1016/j.brainresrev.2008.12.011.
41. Cummins TR, Sheets PL, Waxman SG. The roles of sodium channels in nociception: implications for mechanisms of pain. Pain. 2007;131(3):243–57. https://doi.org/10.1016/j.pain.2007.07.026.
42. Du X, Gamper N. Potassium channels in peripheral pain pathways: expression, function and therapeutic potential. Curr Neuropharmacol. 2013;11(6):621–40. https://doi.org/10.2174/1570159X113119990042.
43. Yang MH, Jung SH, Sethi G, Ahn KS. Pleiotropic pharmacological actions of capsazepine, a synthetic analogue of capsaicin, against various cancers and inflammatory diseases. Molecules [Internet]. 2019; [cited 2020 Mar 22];24. Available from: https://www.ncbi.nlm.nih.gov/pmc/articles/PMC6429077/.
44. Docherty RJ, Yeats JC, Piper AS. Capsazepine block of voltage-activated calcium channels in adult rat dorsal root ganglion neurones in culture. Br J Pharmacol. 1997;121(7):1461–7. https://doi.org/10.1038/sj.bjp.0701272.
45. Kistner K, Siklosi N, Babes A, Khalil M, Selescu T, Zimmermann K, et al. Systemic desensitization through TRPA1 channels by capsazepine and mustard oil - a novel strategy against inflammation and pain. Sci Rep [Internet]. 2016 [cited 2020 Jul 23];6. Available from: https://www.ncbi.nlm.nih.gov/pmc/articles/PMC4928060/
46. Bevan S, Hothi S, Hughes G, James IF, Rang HP, Shah K, et al. Capsazepine: a competitive antagonist of the sensory neurone excitant capsaicin. Br J Pharmacol. 1992;107(2):544–52. https://doi.org/10.1111/j.1476-5381.1992.tb12781.x.
47. Rosen JM, Yaggie RE, Woida PJ, Miller RJ, Schaeffer AJ, Klumpp DJ. TRPV1 and the MCP-1/CCR2 axis modulate post-UTI chronic pain. Sci Rep. 2018;8(1):7188. https://doi.org/10.1038/s41598-018-24056-0.
48. Grundy L, Daly DM, Chapple C, Grundy D, Chess-Williams R. TRPV1 enhances the afferent response to P2X receptor activation in the mouse urinary bladder. Sci Rep. 2018;8(1):197. https://doi.org/10.1038/s41598-017-18136-w.
49. Caterina MJ, Schumacher MA, Tominaga M, Rosen TA, Levine JD, Julius D. The capsaicin receptor: a heat-activated ion channel in the pain pathway. Nature. 1997;389(6653):816–24. https://doi.org/10.1038/39807.
50. Gunthorpe MJ, Benham CD, Randall A, Davis JB. The diversity in the vanilloid (TRPV) receptor family of ion channels. Trends Pharmacol Sci. 2002;23(4):183–91. https://doi.org/10.1016/S0165-6147(02)01999-5.
51. Bianchi L, Driscoll M. Protons at the gate: DEG/ENaC ion channels help us feel and remember. Neuron. 2002;34(3):337–40. https://doi.org/10.1016/S0896-6273(02)00687-6.
52. Holzer P. Acid-sensitive ion channels and receptors. Handb Exp Pharmacol. 2009:283–332. https://doi.org/10.1007/978-3-540-79090-7_9.
53. Krishtal OA, Pidoplichko VI. A receptor for protons in the membrane of sensory neurons may participate in nociception. Neuroscience. 1981;6(12):2599–601. https://doi.org/10.1016/0306-4522(81)90105-6.
54. Chen X, Belmonte C, Rang HP. Capsaicin and carbon dioxide act by distinct mechanisms on sensory nerve terminals in the cat cornea. Pain. 1997;70(1):23–9. https://doi.org/10.1016/S0304-3959(96)03256-3.
55. Yang F, Zheng J. Understand spiciness: mechanism of TRPV1 channel activation by capsaicin. Protein Cell. 2017;8(3):169–77. https://doi.org/10.1007/s13238-016-0353-7.
56. Viana F, Voets T. Heat pain and cold pain. In: The Oxford Handbook of the Neurobiology of Pain [Internet]; 2018. [cited 2020 Mar 20]; Available from: https://www.oxfordhandbooks.com/view/10.1093/oxfordhb/9780190860509.001.0001/oxfordhb-9780190860509-e-13.
57. Vandewauw I, De Clercq K, Mulier M, Held K, Pinto S, Van Ranst N, et al. A TRP channel trio mediates acute noxious heat sensing. Nature Nature Publishing Group. 2018;555:662–6.
58. Kalangara JP, Galor A, Levitt RC, Felix ER, Alegret R, Sarantopoulos CD. Burning eye syndrome: do neuropathic pain mechanisms underlie chronic dry eye? Pain Med. 2016;17(4):746–55. https://doi.org/10.1093/pm/pnv070.
59. Ikegami R, Eshima H, Mashio T, Ishiguro T, Hoshino D, Poole DC, et al. Accumulation of intramyocyte TRPV1-mediated calcium during heat stress is inhibited by concomitant muscle contractions. J Appl Physiol. 2019;126(3):691–8. https://doi.org/10.1152/japplphysiol.00668.2018.
60. Meng ID, Barton ST, Mecum NE, Kurose M. Corneal sensitivity following lacrimal gland excision in the rat. Invest Ophthalmol Vis Sci. 2015;56(5):3347–54. https://doi.org/10.1167/iovs.15-16717.
61. Stepp MA, Pal-Ghosh S, Tadvalkar G, Williams A, Pflugfelder SC, de Paiva CS. Reduced intraepithelial corneal nerve density and sensitivity accompany desiccating stress and aging in C57BL/6 mice. Exp Eye Res. 2018;169:91–8. https://doi.org/10.1016/j.exer.2018.01.024.

62. Guzmán M, Miglio M, Keitelman I, Shiromizu CM, Sabbione F, Fuentes F, et al. Transient tear hyperosmolarity disrupts the neuroimmune homeostasis of the ocular surface and facilitates dry eye onset. Immunology. 2020;161(2): 148–61. https://doi.org/10.1111/imm.13243.
63. Yamazaki R, Yamazoe K, Yoshida S, Hatou S, Inagaki E, Okano H, et al. The semaphorin 3A inhibitor SM-345431 preserves corneal nerve and epithelial integrity in a murine dry eye model. Sci Rep. 2017;7(1):15584. https://doi.org/10.1038/s41598-017-15682-1.
64. Stepp MA, Pal-Ghosh S, Tadvalkar G, Williams AR, Pflugfelder SC, de Paiva CS. Reduced corneal innervation in the CD25 null model of Sjögren syndrome. Int J Mol Sci. 2018;19(12). https://doi.org/10.3390/ijms19123821.
65. Bourcier T, Acosta MC, Borderie V, Borrás F, Gallar J, Bury T, et al. Decreased corneal sensitivity in patients with dry eye. Invest Ophthalmol Vis Sci. 2005; 46(7):2341–5. https://doi.org/10.1167/iovs.04-1426.
66. Spierer O, Felix ER, McClellan AL, Parel JM, Gonzalez A, Feuer WJ, et al. Corneal mechanical thresholds negatively associate with dry eye and ocular pain symptoms. Invest Ophthalmol Vis Sci. 2016;57(2):617–25. https://doi.org/10.1167/iovs.15-18133.
67. Murthy SE, Loud MC, Daou I, Marshall KL, Schwaller F, Kühnemund J, et al. The mechanosensitive ion channel Piezo2 mediates sensitivity to mechanical pain in mice. Sci Transl Med [Internet]. 2018; [cited 2020 Jan 14]; 10. Available from: https://stm.sciencemag.org/content/10/462/eaat9897.
68. Fernández-Trillo J, Florez-Paz D, Íñigo-Portugués A, González-González O, Del Campo AG, González A, et al. Piezo2 mediates low-threshold mechanically evoked pain in the cornea. J Neurosci. 2020;40(47):8976–93. https://doi.org/10.1523/JNEUROSCI.0247-20.2020.
69. Joubert F, Guerrero-Moreno A, Fakih D, Reboussin E, Gaveriaux-Ruff C, Acosta MC, et al. Topical treatment with a mu opioid receptor agonist alleviates corneal allodynia and corneal nerve sensitization in mice. Biomed Pharmacother. 2020;132:110794. https://doi.org/10.1016/j.biopha.2020.110794.
70. Benowitz LI, Popovich PG. Inflammation and axon regeneration. Curr Opin Neurol. 2011;24(6):577–83. https://doi.org/10.1097/WCO.0b013e32834c208d.
71. Basbaum AI, Bautista DM, Scherrer G, Julius D. Cellular and molecular mechanisms of pain. Cell. 2009;139(2):267–84. https://doi.org/10.1016/j.cell.2009.09.028.
72. Cook AD, Christensen AD, Tewari D, McMahon SB, Hamilton JA. Immune cytokines and their receptors in inflammatory pain. Trends Immunol. 2018; 39(3):240–55. https://doi.org/10.1016/j.it.2017.12.003.
73. Pinho-Ribeiro FA, Verri WA, Chiu IM. Nociceptor sensory neuron-immune interactions in pain and inflammation. Trends Immunol. 2017;38(1):5–19. https://doi.org/10.1016/j.it.2016.10.001.
74. Zhang J-M, An J. Cytokines, Inflammation and pain. Int Anesthesiol Clin. 2007;45(2):27–37. https://doi.org/10.1097/AIA.0b013e318034194e.
75. Kawabata A. Prostaglandin E2 and pain--an update. Biol Pharm Bull. 2011; 34(8):1170–3. https://doi.org/10.1248/bpb.34.1170.
76. Lacagnina MJ, Watkins LR, Grace PM. Toll-like receptors and their role in persistent pain. Pharmacol Ther. 2018;184:145–58. https://doi.org/10.1016/j.pharmthera.2017.10.006.
77. Luo C, Kuner T, Kuner R. Synaptic plasticity in pathological pain. Trends Neurosci Elsevier. 2014;37(6):343–55. https://doi.org/10.1016/j.tins.2014.04.002.
78. Nakagawa T, Wakamatsu K, Zhang N, Maeda S, Minami M, Satoh M, et al. Intrathecal administration of ATP produces long-lasting allodynia in rats: differential mechanisms in the phase of the induction and maintenance. Neuroscience. 2007;147(2):445–55. https://doi.org/10.1016/j.neuroscience.2007.03.045.
79. Choi JY, Lee HY, Hur J, Kim KH, Kang JY, Rhee CK, et al. TRPV1 blocking alleviates airway inflammation and remodeling in a chronic asthma murine model. Allergy Asthma Immunol Res. 2018;10(3):216–24. https://doi.org/10.4168/aair.2018.10.3.216.
80. Chiu IM, von Hehn CA, Woolf CJ. Neurogenic inflammation and the peripheral nervous system in host defense and immunopathology. Nat Neurosci. 2012;15(8):1063–7. https://doi.org/10.1038/nn.3144.
81. Ang S-F, Moochhala SM, MacAry PA, Bhatia M. Hydrogen sulfide and neurogenic inflammation in polymicrobial sepsis: involvement of substance P and ERK-NF-κB signaling. PLoS One [Internet]. 2011; [cited 2020 Mar 28];6. Available from: https://www.ncbi.nlm.nih.gov/pmc/articles/PMC3171449/.
82. Weatherby TJM, Raman VRV, Agius M. Depression and dry eye disease: a need for an interdisciplinary approach? Psychiatr Danub. 2019;31(Suppl 3): 619–21.
83. Labbé A, Wang YX, Jie Y, Baudouin C, Jonas JB, Xu L. Dry eye disease, dry eye symptoms and depression: the Beijing Eye Study. Br J Ophthalmol. 2013;97(11):1399–403. https://doi.org/10.1136/bjophthalmol-2013-303838.
84. Mecum NE, Demers D, Sullivan CE, Denis TE, Kalliel JR, Meng ID. Lacrimal gland excision in male and female mice causes ocular pain and anxiety-like behaviors. Sci Rep Nature Publishing Group. 2020;10:17225.
85. Corder G, Ahanonu B, Grewe BF, Wang D, Schnitzer MJ, Scherrer G. An amygdalar neural ensemble that encodes the unpleasantness of pain. Science. 2019;363(6424):276–81. https://doi.org/10.1126/science.aap8586.
86. Marsch R, Foeller E, Rammes G, Bunck M, Kössl M, Holsboer F, et al. Reduced anxiety, conditioned fear, and hippocampal long-term potentiation in transient receptor potential vanilloid type 1 receptor-deficient mice. J Neurosci. 2007;27(4):832–9. https://doi.org/10.1523/JNEUROSCI.3303-06.2007.


## Publisher's Note

## VI. Evidencing phenotypical differences in neuropathic corneal pain in etiological subsets of dry eye disease: *a retrospective nested case-control study* (*Study 3 – Guerrero-Moreno et al. Biomed. 2021*)

Similarly to other painful neuropathic conditions, corneal neuropathic pain is of difficult management, possibly stemming from difficulties in diagnosis and the probable existence of phenotypic differences between cases that could explain insufficient or lack of response to classical pharmacological management of neuropathic pain as described earlier.

Indeed, phenotyping patients suffering from neuropathic pain seems a promising approach to provide tailored treatment with drugs who act specifically on the precise neuropathic alterations in the individual patient. Such an approach has not yet been proposed and evaluated in the context of corneal neuropathic pain, especially that resulting from chronic DED.

In that respect, we conducted a retrospective case-control clinical study evaluating patient clinical and IVCM imaging data from a cohort of patients suffering from ocular surface diseases seen in the clinical investigation center of the XV-XX national ophthalmological hospital in Paris. This clinical research project was conducted as part of the secondment of the PhD research project, included in the workplan of the MSCA-ITN grant financing the thesis.

The aim of the study was to investigate clinical and IVCM characteristics of patients with corneal neuropathic pain in two etiological subsets of DED: auto-immune-related DED and primary meibomian gland dysfunction-related DED.

biomedicines

MDPI

*Article*

# Corneal Nerve Abnormalities in Painful Dry Eye Disease Patients

**Adrian Guerrero-Moreno [1], Hong Liang [1,2], Nathan Moreau [1], Jade Luzu [2], Ghislaine Rabut [2], Stéphane Melik Parsadaniantz [1], Antoine Labbé [2,3], Christophe Baudouin [1,2,3,†] and Annabelle Réaux-Le Goazigo [1,*,†]**

1 Institut de la Vision, INSERM, CNRS, Sorbonne Université, 17 rue Moreau, 75012 Paris, France; adrian.guerrero@inserm.fr (A.G.-M.); hliang-bouttaz@15-20.fr (H.L.); nthmoreau@gmail.com (N.M.); stephane.melik-parsadaniantz@inserm.fr (S.M.P.); cbaudouin@15-20.fr (C.B.)
2 CHNO des Quinze-Vingts, INSERM-DGOS CIC 1423, 17 rue Moreau, 75012 Paris, France; jluzu@15-20.fr (J.L.); grabut@15-20.fr (G.R.); alabbe@15-20.fr (A.L.)
3 Department of Ophthalmology, Ambroise Paré Hospital, AP-HP, University of Versailles Saint-Quentin-en-Yvelines, 9 Avenue Charles de Gaulle, 92100 Boulogne-Billancourt, France
* Correspondence: annabelle.reaux@inserm.fr; Tel.: +33-153462572
† These authors contributed equally to this study.

**Abstract: Background**: This study aimed to compare the corneal nerve structural abnormalities detected using in vivo confocal microscopy (IVCM) in patients with neuropathic corneal pain (NCP) secondary to primary meibomian gland dysfunction (MGD) or autoimmune dry eye (AIDE). **Methods**: A two-stage retrospective nested case–control study was conducted. First, data from patients with either MGD or AIDE were assessed, selecting only cases with no corneal pain (VAS = 0) or severe pain (VAS $\geq$ 8). Ocular signs and symptoms of the 238 selected patients were compared between painful and painless cases. Next, painful patients with no corneal damage (Oxford score $\leq$ 1) were selected within each study group, defining the cases with NCP (i.e., "pain without stain"). IVCM images from all groups were compared with prospectively-recruited healthy controls, focusing on dendritiform cell density and nerve abnormalities (density, tortuosity, microneuromas). **Results**: AIDE patients had more ocular signs/symptoms than MGD patients. Compared with healthy controls, AIDE-related NCP patients showed increased nerve tortuosity and number of neuromas, whereas MGD-related NCP patients had reduced nerve density and increased number, perimeter, and area of microneuromas. Microneuromas were also observed in healthy controls. Furthermore, a higher number of microneuromas was found in MGD-related NCP compared to AIDE-related NCP or painless MGD. **Conclusions**: MGD-related NCP was associated with significantly more corneal nerve abnormalities than AIDE-related NCP or healthy controls. Although IVCM can be useful to detect NCP-related corneal nerve changes in such patients, the diagnosis of dry eye disease-related NCP will require an association of several IVCM-based criteria without relying solely on the presence of microneuromas.

**Keywords:** neuropathic pain; nerve abnormalities; cornea; dry eye; microneuroma



**Citation:** Guerrero-Moreno, A.; Liang, H.; Moreau, N.; Luzu, J.; Rabut, G.; Melik Parsadaniantz, S.; Labbé, A.; Baudouin, C.; Réaux-Le Goazigo, A. Corneal Nerve Abnormalities in Painful Dry Eye Disease Patients. *Biomedicines* **2021**, *9*, 1424. https://doi.org/10.3390/biomedicines9101424

Academic Editor: Stefania Raimondo

Received: 18 August 2021
Accepted: 7 October 2021
Published: 9 October 2021



## 1. Introduction

Dry eye symptoms are among the most frequent complaints observed in general ophthalmological practice. They include visual disturbances, discomfort, and pain. When such symptoms become chronic, they can alter the patient's quality of life, especially considering the absence of efficient treatments to date [1–4].

Dry eye disease (DED) is "a multifactorial disease of the ocular surface characterized by a loss of homeostasis of the tear film, and accompanied by ocular symptoms, in which tear film instability and hyperosmolarity, ocular surface inflammation and damage, and neurosensory abnormalities play etiological roles", as defined in 2017 by the TFOS Dry

Eye Workshop [5]. DED can be subclassified as aqueous deficient dry eye (ADDE) and/or evaporative dry eye (EDE) based on the underlying predominant pathophysiological mechanism involved, each group including multiple etiologies and risk factors of DED. The most common etiologies of DED are autoimmune-associated DED (AIDE, e.g., Sjögren syndrome) in ADDE and meibomian gland dysfunction (MGD) in EDE [6].

As encompassed in this definition, recent studies have focused on the role of neurosensory abnormalities in the pathophysiology and semiology of DED [1,7–9]. Indeed, reduced tear secretion and/or tear film instability lead to inflammation and peripheral nerve damage, triggering sensitization and abnormal activity in corneal nerves, evoking painful symptoms of dry eye associated with dryness, itching, and foreign body sensation [1].

Clinical diagnosis of DED is based on the assessment of these symptoms, but more importantly, on the observation of signs such as ocular surface damage (corneal stain), tear volume, and tear film hyperosmolarity [10]. However, there is a discordance between symptoms and signs in an important proportion of patients. Among them, some patients can present asymptomatic ocular surface alterations, and conversely, they can be highly symptomatic without obvious signs of ocular surface damage (i.e.,"pain without stain") [9,11,12]. In the second case, patients present with complaints of burning, stinging, eye-ache, photophobia, or severe eye pain without significant findings on slit-lamp examination [8,13]. The concept of "neuropathic corneal pain" (NCP), increasingly investigated in the past 20 years in clinical research [4,14], has been suggested to play a central role in those cases. NCP represents a current clinical challenge, as those patients are commonly not responding to classic dry eye treatments [15], and the ocular pathology is often associated with depressive disorders [16].

In the clinical setting, NCP has been investigated using ocular surface pain questionnaires (such as the Ocular Pain Assessment Survey [OPAS]) [17], corneal esthesiometry, proparacaine challenge test (to ascertain the peripheral and/or central origin of the NCP) [18], and finally, in vivo confocal microscopy (IVCM), allowing non-invasive imaging of the cornea at the cellular level [14,19–23].

IVCM has been used to image subbasal nerve attributes in various ocular surface diseases, including DED [24–26]. IVCM has identified subbasal nerve alterations such as reduced nerve density, increased tortuosity, reflectivity, and presence of microneuromas [27–30]. Although it has recently been suggested that the visualization of microneuromas in IVCM could represent an objective biomarker for the diagnosis of NCP [31], there are scarce data regarding the IVCM-assessed ultrastructural characteristics of corneal nerves and microneuromas in patients with DED-related NCP. In particular, no study has investigated the potential differences in structural corneal nerve characteristics within the various ADDE/EDE etiological subgroups. As with other neuropathic pain conditions, proper phenotyping within the respective patient clusters is a mandatory prerequisite for tailored pharmacological management [32].

This retrospective clinical study thus aimed to investigate the clinical profiles of painful DED patients and the corneal nerve ultrastructural abnormalities in two subsets of DED-related NCP patients (MGD and AIDE) using IVCM.

## 2. Materials and Methods

### *2.1. Study Design*

To further elucidate the various corneal nerve changes associated with dry eye diseases, a retrospective nested case–control study was performed to assess the clinical features of patients suffering from primary MGD and AIDE and severe corneal pain, compared with their respective painless counterparts. Ultrastructural corneal characteristics were studied among patients presenting NCP characteristics (high pain score and absence of clinical signs) and compared with their painless counterparts and healthy volunteers. The study flowchart is summarized in Figure 1.

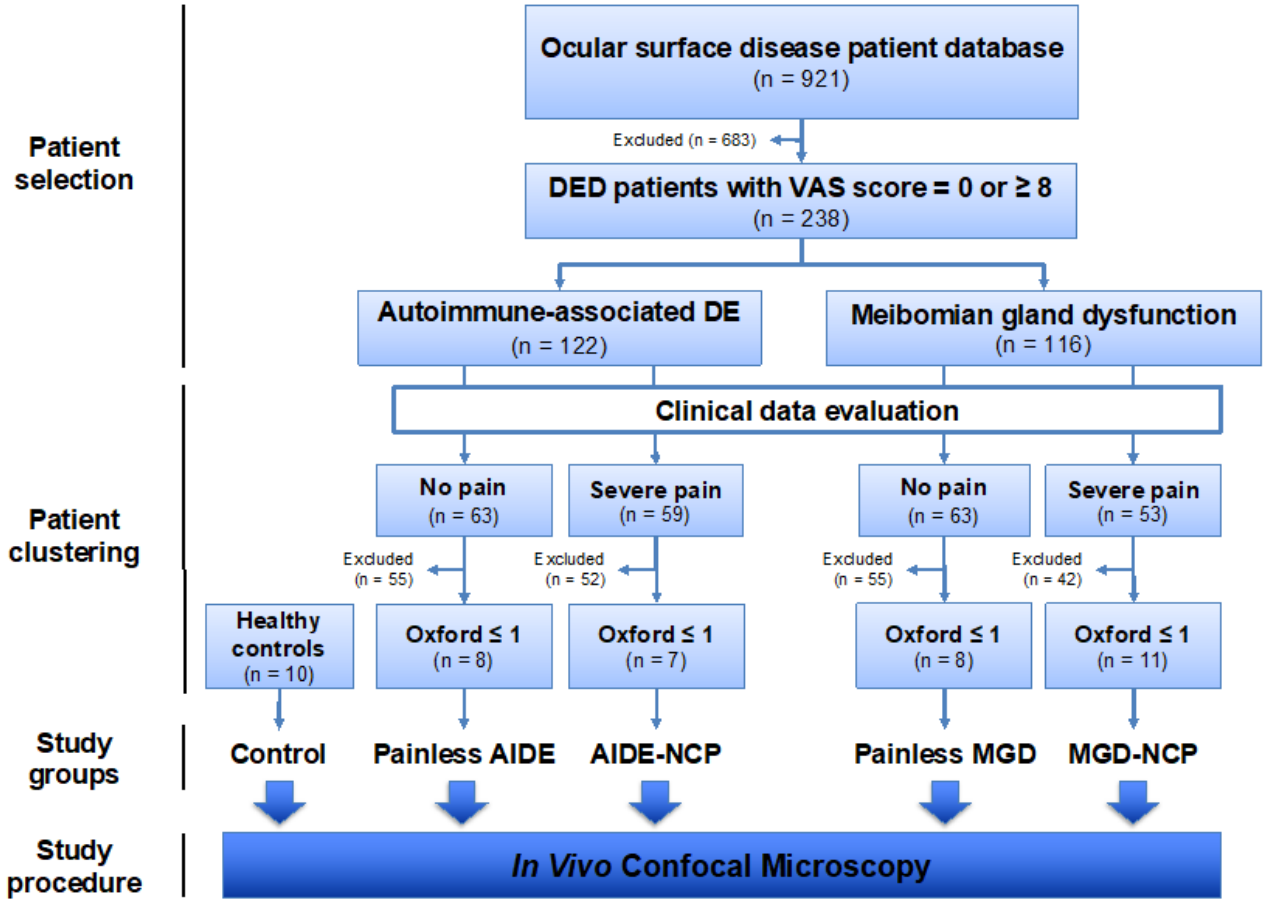


**Figure 1.** Retrospective nested case–control study flowchart.

### *2.2. Patient Cohorts*

#### 2.2.1. Patient Selection for Clinical Features Study

This retrospective single-center study was conducted at the Center for Clinical Investigation (CIC INSERM 1423) of the Quinze-Vingts National Ophthalmology Hospital, Paris, France, between March 2012 and January 2020. The study was conducted in accordance with the tenets of the Declaration of Helsinki and approved by the Ethics Committee CPP-Ile de France (Number 10793). All patients gave written consent to use their data for research purposes.

This study included 921 patients with various ocular surface diseases. All patients had systematic pain history and ocular examination as part of their routine workup, and the clinical data were systematically collected in a secure spreadsheet (in adherence with national guidelines on data collection and protection). Patients were included in the study based on the following criteria: (1) a diagnosis of primary MGD or of an AIDE was made; (2) the patient reported no ocular pain (visual analog scale [VAS] score = 0) or severe ocular pain (VAS score $\geq$ 8) during history.

#### 2.2.2. Patient Clustering for Ultrastructural IVCM Study of the Cornea

Previously selected patients were clustered into one of two study groups (MGD- or AIDE-related NCP) or two control groups (painless MGD or painless AIDE) based on the following diagnostic criteria.

Dry-Eye Disease-Related Neuropathic Corneal Pain Diagnostic Criteria

In the absence of validated diagnostic criteria, NCP was diagnosed in patients with DED who presented severe pain in the absence or with minimal corneal damage, in

adherence with the relevant literature [2,3,14,31]. Patients were thus diagnosed with DED-related NCP if they presented the following criteria: (1) a diagnosis of primary MGD or AIDE was made, accordingly to relevant diagnostic criteria; (2) the patient reported severe ocular pain (VAS score $\geq$ 8); (3) clinical examination revealed low corneal damage (Oxford score $\leq$ 1).

Painless Dry-Eye Disease Diagnostic Criteria

Patients with painless primary MGD or painless AIDE served as control conditions to their painful neuropathic counterparts (MGD-related NCP and AIDE-related NCP, respectively). Patients were thus diagnosed with painless DED if they presented the following criteria: (1) a diagnosis of primary MGD or AIDE was made, accordingly to relevant diagnostic criteria; (2) the patient reported no ocular pain (VAS score = 0); (3) clinical examination revealed low corneal damage (Oxford score $\leq$ 1).

Study Conditions for IVCM Study

Meibomian Gland Dysfunction-Related Neuropathic Corneal Pain

Of the previously included 116 MGD patients, 53 reported severe pain. Patients without corneal injury (Oxford score $\leq$ 1) and a minimum of 30 IVCM images from the subbasal plexus were selected for the IVCM study, excluding 42 of those 53 patients. The final MGD-NCP group thus comprised 11 patients (with severe pain and low corneal damage) (Figure 1).

Autoimmune-Associated Dry Eye-Related Neuropathic Corneal Pain

Of the previously included 122 AIDE patients, 59 reported severe pain. Patients without corneal damage (Oxford score $\leq$ 1) and a minimum of 30 IVCM images from the subbasal plexus were selected, excluding 52 of those 59 patients. The final AIDE-NCP group thus comprised 7 patients (Figure 1).

Study Controls

Painless Meibomian Gland Dysfunction

Of the previously included 116 MGD patients, 63 reported no pain. To provide a comparable control condition to the neuropathic pain condition (MGD-related NCP), patients without corneal damage (Oxford score $\leq$ 1) and a minimum of 30 IVCM images from the subbasal plexus were selected (as in the relevant study group). The final painless MGD group thus comprised 8 patients (no pain and no corneal damage).

Painless Autoimmune-Associated Dry Eye

Of the previously included 122 AIDE patients, 63 reported no pain. To provide a comparable control condition to the neuropathic pain condition (AIDE-related NCP), patients without corneal damage (Oxford score $\leq$ 1) and a minimum of 30 IVCM images from the subbasal plexus were selected (as in the relevant study group). The final painless AIDE group thus comprised 8 patients (with no pain and no corneal damage).

Healthy Controls

Healthy volunteers ($n$ = 10) were prospectively recruited and paired in age and sex with the various study groups to provide healthy controls for ultrastructural corneal analysis.

### *2.3. Clinical Data Evaluation*

#### 2.3.1. General Data

Patient age, gender, and dry eye diagnosis were recorded systematically in all patients.

#### 2.3.2. Patient History

We investigated the VAS (scored from 0 to 10) for quantifying ocular pain score, the ocular surface disease index (OSDI, scored from 0 to 100), and frequency of self-reported adverse ocular surface symptoms such as itching, burning, foreign body sensation or dryness sensation (scored as never, rarely, sometimes, always).

#### 2.3.3. Ocular Examination

Dry eye signs were assessed with fluorescein corneal staining (Oxford score, 0 to 5), tear break-up time (BUT, seconds), non-invasive keratograph tear break-up time (NIKBUT, seconds), Shirmer test (millimeters of wetting after 5 min), tear meniscus length (millimeters), and tear osmolarity (mOsmol/L).

### *2.4. In Vivo Confocal Microscopy: Image Selection and Analysis*

Corneal IVCM images were obtained using the Rostock Cornea Module (RCM) of the Heidelberg Retina Tomograph II (Heidelberg Engineering GmbH, Heidelberg, Germany) as previously described [28,29]. All images were obtained by experienced ophthalmologists, following the prior administration of one drop of topical anesthetic (oxybuprocaine 0.4%, MSD-Chibret, Paris, France). The x-y position and depth (z) of the optical section were controlled manually, with the focus position (in µm) automatically calculated by the HRT II/RCM, allowing the selection of high-quality representative images. Each IVCM-generated image comprised an area of 384 × 384 pixels (400 µm × 400 µm), focused on the central cornea.

#### Image Selection and Analysis

Representative, high-quality images were chosen for patients of each study group, selecting only images with the subbasal plexus clearly in focus. To limit interoperator variability, a single investigator (A.G.M.) analyzed all the images using ImageJ (National Institutes of Health, Bethesda, MD) and assessed the following corneal ultrastructural parameters. Dendritiform cell density was calculated at the level of the Bowman layer to assess corneal inflammation, as previously described [29,33], using cell counter plugging from ImageJ (median (range): 15 (11–18) representative images/patient). The morphological study of the corneal nerves was analyzed by the following parameters: (1) nerve tortuosity classified in four grades according to an *ad hoc* tortuosity scale (Figure 2) (median (range): 77 (31–193) images/patient); (2) density of nerves (µm/mm$^2$) was calculated using only images with clear uninterrupted visualization of the corneal nerves and less than 20% overlap between slices, to avoid any miscounts (median (range):11 (5–31) representative images/patient). These images were analyzed using the NeuronJ plugin in ImageJ; (3) number, area, and perimeter of microneuromas (Figure 3); microneuromas were defined as nerve abnormalities that present as irregularly shaped, hyperreflective, terminal enlargements of subbasal nerve endings, according to the relevant literature [27,31] (median (range): 77 (31–193) images/patient).

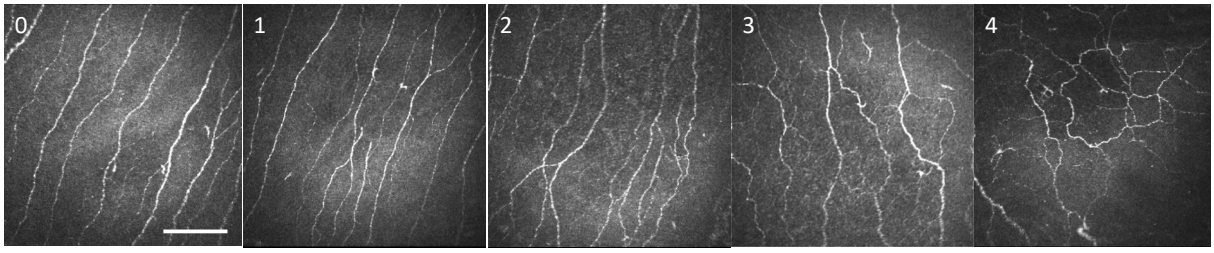


**Figure 2.** Corneal nerve fiber tortuosity scale graded from (**0**) to (**4**) based on in vivo confocal microscopy image. Scale bar = 100 µm.

### *2.5. Statistical Analyses*

Statistical analyses were performed using SPSS v.23 (SPSS Inc., Chicago, IL, USA). The normal distribution of the variables was tested independently in each study group using the Kolmogorov–Smirnov test. Parametric variables were compared with a *t*-test, non-parametric variables with Mann–Whitney U test, and nominal variables with $\chi^2$. Graphical representations were made using GraphPad Prism v.9 (GraphPad Software Inc., La Jolla, CA, USA). Data were expressed as mean ± SD.

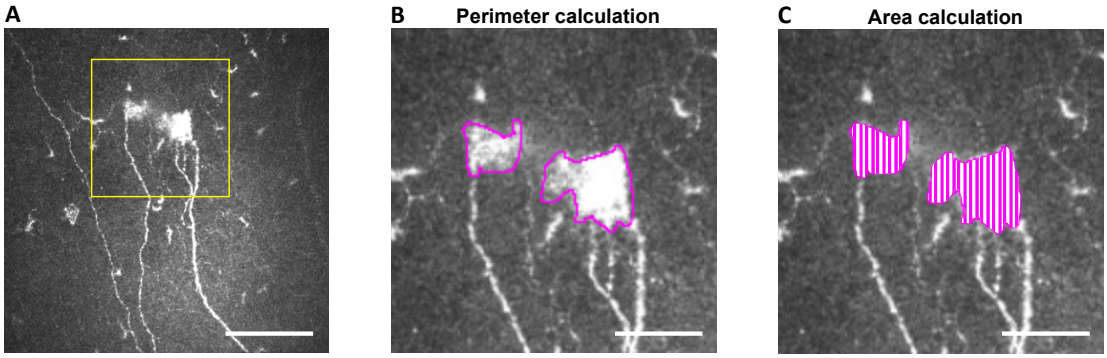


**Figure 3.** Microneuroma perimeter and area calculation methodology using IVCM images. Illustration of microneuroma analysis (yellow square): (**A**) The perimeter of microneuroma is delimited using ImageJ, (**B**) and the area is subsequently calculated (**C**) based on previous perimeter delimitation. Scale bar = 100 µm for (**A**) and 40 µm for (**B**,**C**).

## 3. Results

### *3.1. Clinical Variable Comparisons between Painful and Painless DED Patients*

In the first part of the study, we investigated possible differences in signs and symptoms between patients suffering from MGD and AIDE both in painless patients (VAS = 0) and in patients with severe pain (VAS $\geq$ 8). Out of the 921 patients, 238 fit the initial inclusion criteria, with 122 cases of AIDE and 116 cases of primary MGD selected for patient clustering (Figure 1, Table 1). The mean age of patients was 56.8 $\pm$ 15.4 years, and 83% were female. A female predominance was observed in the AIDE group, compared with MGD both in the painless (VAS = 0; $p < 0.05$) and painful (VAS $\geq$ 8; $p < 0.01$) conditions. Demographic parameters are summarized in Table 1.

**Table 1.** Demographic parameters. Intergroup comparisons were made with *t*-test (age) and $\chi^2$ test (gender).

| | | | Autoimmune Dry Eye (AIDE) | | Meibomian Gland Dysfunction (MGD) | |
|---|---|---|---|---|---|---|
| | | All Patients in the Study | Painless | Painful | Painless | Painful |
| VAS | | - | 0 | 8–10 | 0 | 8–10 |
| Number of patients (%) | | 238 (100%) | 63 (27%) | 59 (25%) | 63 (27%) | 53 (22%) |
| Age (mean $\pm$ SD) | | 56.8 $\pm$ 15.4 | 58.1 $\pm$ 13.8 | 57.0 $\pm$ 15.0 | 55.4 $\pm$ 16.0 | 56.8 $\pm$ 16.9 |
| Gender (n, %) | Male | 40 (17%) | 6 (10%) | 4 (7%) | 16 (25%) | 14 (26%) |
| | Female | 198 (83%) | 57 (91%) † | 55 (93%) ‡‡ | 47 (75%) | 39 (74%) |

† Significant difference between painless AIDE vs. painless MGD, ‡ Significant difference between painful AIDE vs. painful MGD. Statistical significance is illustrated based on number of signs as follows: one sign = $p < 0.05$, two signs = $p < 0.01$.

### *3.2. Higher Symptoms and Signs in Painful DED Patients Compared with Their Respective Painless Counterparts*

Compared with their painless counterparts, painful DED (both MGD and AIDE) patients had significantly higher OSDI scores ($p < 0.0001$) and reported significantly more itching ($p < 0.001$), burning ($p < 0.01$ for MGD and $p < 0.001$ for AIDE) and foreign body sensations ($p < 0.0001$) (Table 2). Dryness sensation was significantly more often reported in painful AIDE, compared with painless AIDE ($p < 0.0001$) but not in painful MGD, compared with painless MGD (Table 2). In the MGD group, corneal damage (assessed by Oxford score) was significantly higher in painful MGD, compared with painless MGD ($p < 0.01$) (Table 3).

**Table 2.** Ocular surface symptomatology. Intergroup and intragroup comparisons were made with Mann–Whitney U test.

| | | | Autoimmune Dry Eye (AIDE) | | Meibomian Gland Dysfunction (MGD) | |
|---|---|---|---|---|---|---|
| | | **All Patients in the Study** | **Painless** | **Painful** | **Painless** | **Painful** |
| OSDI score (mean ± SD) | | 62.5 ± 24.8 | 57.5 ± 25.7 † | 76.8 ± 15.1 #### | 46.6 ± 24.1 | 70.8 ± 21.0 •••• |
| Itching (n, %) | Never | 115 (49%) | 38 (62%) | 20 (34%) | 35 (56%) | 22 (42%) |
| | Rarely | 44 (19%) | 10 (16%) | 8 (14%) | 17 (27%) | 9 (17%) |
| | Sometimes | 51 (22%) | 10 (16%) | 21 (36%) | 8 (13%) | 12 (23%) |
| | Always | 26 (11%) | 3 (5%) | 10 (17%) ### | 3 (5%) | 10 (19%) ••• |
| Burning (n, %) | Never | 66 (28%) | 22 (35%) | 4 (7%) | 35 (57%) | 5 (9%) |
| | Rarely | 39 (16%) | 18 (29%) | 6 (10%) | 9 (14%) | 6 (11%) |
| | Sometimes | 86 (36%) | 18 (29%) | 31 (52%) | 15 (24%) | 22 (41%) |
| | Always | 46 (19%) | 5 (8%) † | 18(30%) #### | 3(5%) | 20 (38%) •• |
| Foreign body sensation (n, %) | Never | 73 (31%) | 21 (33%) | 5 (8%) | 32 (52%) | 15 (28%) |
| | Rarely | 38 (16%) | 15 (24%) | 5 (8%) | 11 (18%) | 7 (13%) |
| | Sometimes | 84 (35%) | 17 (27%) | 33 (56%) | 13 (21%) | 21 (40%) |
| | Always | 42 (18%) | 10 (16%) † | 16 (27%) ####, ‡ | 6 (10%) | 10 (19%) •••• |
| Dryness sensation (n, %) | Never | 94 (39%) | 28 (44%) | 11 (19%) | 33 (52%) | 22 (42%) |
| | Rarely | 32 (13%) | 14 (22%) | 6 (10%) | 6 (10%) | 6 (11%) |
| | Sometimes | 71 (30%) | 15 (24%) | 23 (39%) | 19 (30%) | 14 (26%) |
| | Always | 41 (17%) | 6 (10%) | 19 (32%) ####, ‡ | 5 (8%) | 11 (21%) |

# significant difference between painless AIDE vs. painful AIDE; • significant difference between painless MGD vs. painful MGD; † significant difference between painless AIDE vs. painless MGD; ‡ significant difference between painful AIDE vs. painful MGD. Statistical significance is illustrated based on number of signs as follows: one sign = $p < 0.05$, two signs = $p < 0.01$, three signs = $p < 0.001$, four signs = $p < 0.0001$.

**Table 3.** Ocular surface semiology. Intergroup comparisons were made with Mann–Whitney U test (Oxford score, BUT, NIKBUT (first), Schirmer, tear meniscus, osmolarity) and *t*-test (NIKBUT (average)).

| | | Autoimmune Dry Eye (AIDE) | | Meibomian Gland Dysfunction (MGD) | |
|---|---|---|---|---|---|
| | **All Patients in the Study** | **Painless** | **Painful** | **Painless** | **Painful** |
| Oxford score<br>0<br>1<br>2<br>3<br>4<br>5 | | ††††<br> 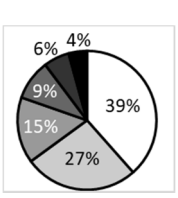 | ‡‡<br> 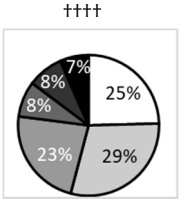 | 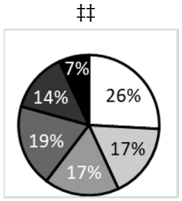 | ••<br> 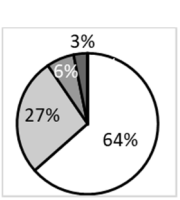 | 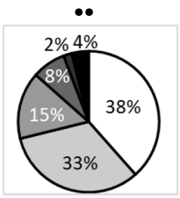 |
| BUT (s, mean ± SD) | 4.94 ± 0.18 | 4.82 ± 0.35 | 4.19 ± 0.31 | 5.70 ± 0.36 | 5.00 ± 0.39 ‡ |
| NIKBUT (first, mean ± SD) | 5.06 ± 5.35 | 4.08 ± 4.77 | 3.55 ± 3.65 | 5.83 ± 5.14 | 6.66 ± 7.45 |
| NIKBUT (average, mean ± SD) | 7.78 ± 6.90 | 6.8 ± 6.52 | 5.10 ± 5.41 | 9.24 ± 6.87 | 9.27 ± 8.18 ‡ |
| Schirmer (mm/5 min, mean ± SD) | 10.9 ± 10.0 | 10.1 ± 10.1 | 8.8 ± 9.1 | 12.8 ± 10.6 | 12.0 ± 9.8 |
| Tear meniscus (mm, mean ± SD) | 0.209 ± 0.188 | 0.172 ± 0.198 | 0.224 ± 0.193 | 0.235 ± 0.200 | 0.196 ± 0.141 |
| Osmolarity (mOsmol/L, mean ± SD) | 309 ± 17 | 307 ± 15 | 311 ± 19 | 306 ± 16 | 310 ± 19 |

• significant difference between painless MGD vs. painful MGD; † significant difference between painless AIDE vs. painless MGD; ‡ significant difference between painful AIDE vs. painful MGD. Statistical significance is illustrated based on number of signs as follows: one sign = $p < 0.05$, two signs = $p < 0.01$, four signs = $p < 0.0001$.

### *3.3. Higher Symptoms and Signs in Painful AIDE Patients Compared with Painful MGD*

Patients suffering from painful AIDE presented significantly more foreign body sensations and dryness sensations, compared with painful MGD ($p < 0.05$) (Table 2). This was associated with significantly more corneal damage (higher Oxford scores; darker colors in Table 3) in painful AIDE patients, compared with painful MGD ($p < 0.01$). An important finding was that 71 % of the patients with painful MGD had low (0–1) Oxford score, while in patients with painful AIDE, the percentage was 42 % (Table 3). Regarding tear quality, painful MGD patients had significantly longer BUT and average NIKBUT, compared with painful AIDE patients ($p < 0.01$) (Table 3).

### *3.4. Higher Symptoms and Signs in Painless AIDE Compared with Painless MGD*

Similarly, patients with painless AIDE had significantly higher OSDI scores ($p < 0.05$) and more foreign body or burning sensations than patients with painless MGD ($p < 0.05$) (Table 2). This was associated with significantly more corneal staining in painless AIDE patients, compared with painless MGD patients ($p < 0.0001$) (Table 3).

### *3.5. IVCM Image Analysis*

In the second part of the study, DED patients were clustered into different groups (see Section 2.2.2. and Figure 1 for details)—namely, AIDE-related NCP (7 patients) and MGD-related NCP (11 patients), compared with painless AIDE (8 patients) and painless MGD (8 patients), respectively, and paired healthy controls (10 subjects). Dendritiform cell density and corneal nerve alterations (density, tortuosity, and microneuromas), detected using IVCM, were compared between the study groups.

### *3.6. DED-Related NCP Patients Have Significant IVCM-Identified Corneal Nerve Alterations Compared with Healthy Controls*

No significant differences could be observed between the various study groups regarding dendritiform cell density (Figure 4), suggesting limited corneal inflammation in the present experimental setting. MGD-related NCP patients had significantly lower nerve density ($p < 0.01$) (Figure 5A), a higher number of microneuromas per patient ($p < 0.0001$) (Figure 6A,B), higher microneuroma perimeter ($p < 0.05$) (Figure 6C) and area ($p < 0.05$) (Figure 6D), compared to healthy controls. Similarly, AIDE-related NCP patients had significantly higher corneal nerve tortuosity ($p < 0.05$) (Figure 5B) and number of microneuromas per patient, compared to healthy controls ($p < 0.01$) (Figure 6B). Collectively, these results suggest that the patients defined in this study as having DED-related NCP ("pain with no stain") did indeed show neuropathic corneal nerve alterations. This conclusion is further supported by the limited inflammation indicated by the low dendritiform cell density in all experimental conditions (Figure 4), suggesting limited (if any) involvement of nociceptive inflammatory mechanisms in the corneal nerve alterations identified in IVCM.

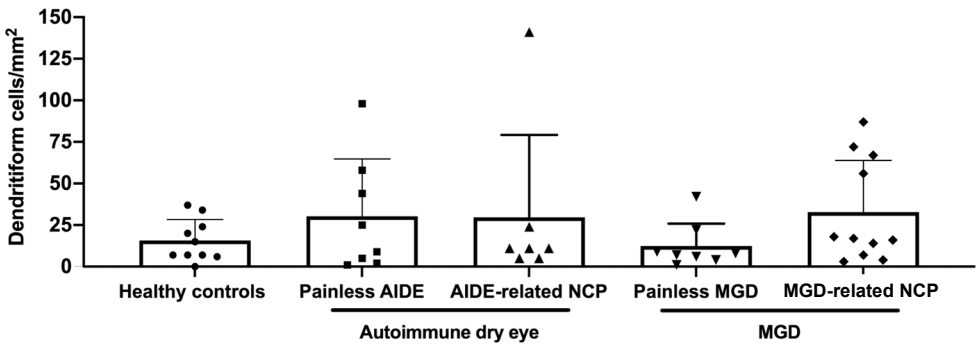


**Figure 4.** Dendritiform cell density (expressed as the number of cells per $mm^2$) in the various study groups. Intergroup comparisons were made using Mann–Whitney U test, without any statistically significant differences between any of the study groups.

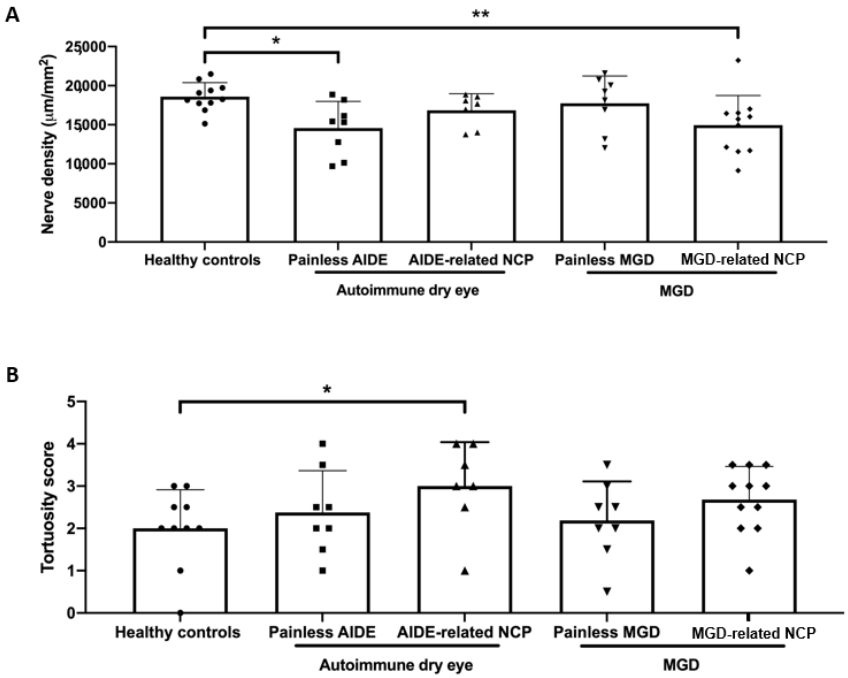


**Figure 5.** (**A**) Corneal nerve density (expressed as total nerve length in µm per mm$^2$) in the various study groups. Intergroup comparisons were made using an unpaired *t*-test; (**B**) corneal nerve tortuosity (expressed as mean tortuosity score, as defined in Figure 2). Intergroup comparisons were made using Mann–Whitney U test. Statistical significance was illustrated as follows: * $p < 0.05$, ** $p < 0.01$.

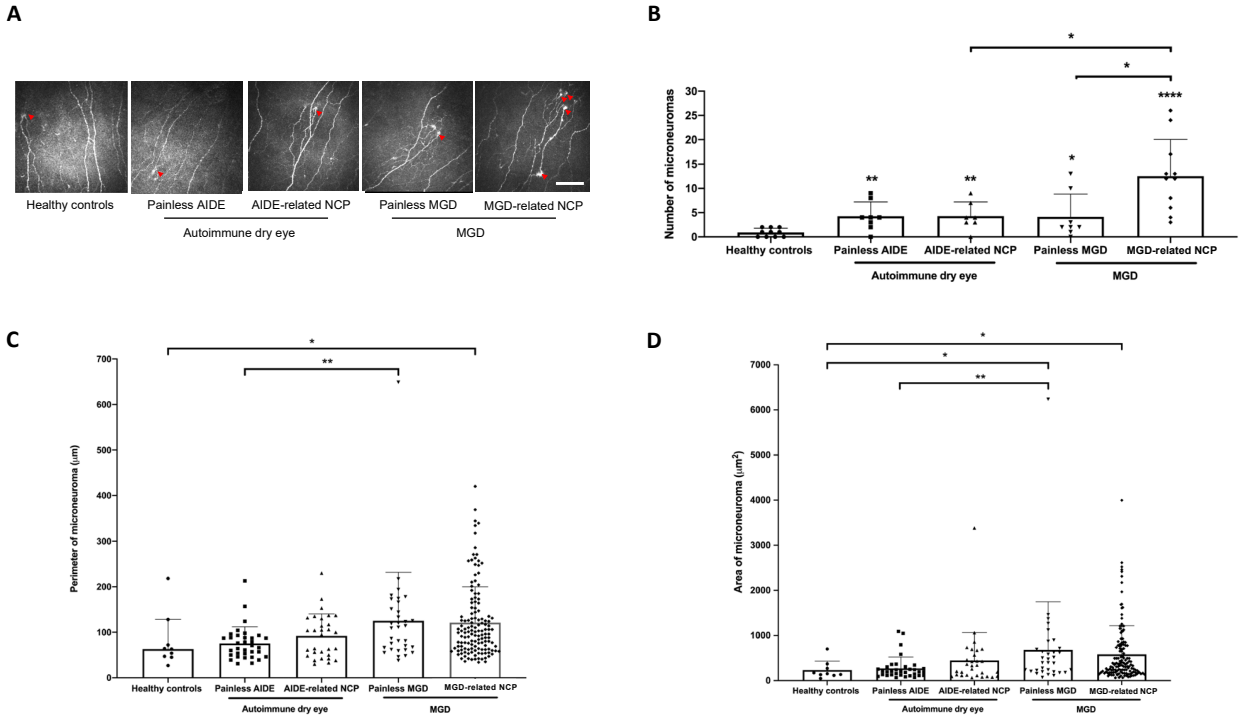


**Figure 6.** (**A**) In vivo confocal microscopy images evidencing microneuromas (red arrowheads) in both painful neuropathic conditions (MGD-related NCP and AIDE-related NCP), both painless DED control conditions (painless MGD and painless AIDE), and healthy volunteers. Scale bar = 100 µm; (**B**) microneuroma quantification (expressed as the number of microneuromas per patient in each study group); (**C**) microneuroma perimeter (expressed as the perimeter in µm for each microneuroma of each patient); (**D**) microneuroma area (expressed as the area in µm$^2$ for each microneuroma of each patient). Intergroup comparisons were made using Mann–Whitney U test. Statistical significance was illustrated as follows: * $p < 0.05$, ** $p < 0.01$, **** $p < 0.0001$ versus control group; except when a bar line is used.

### *3.7. MGD-Related NCP Patients Had Higher Microneuromas Compared with Painless MGD and AIDE-Related NCP Patients*

Interestingly, MGD-related NCP patients had a significantly higher number of microneuromas per patient compared to painless MGD patients ($p < 0.05$) and AIDE-related NCP patients ($p < 0.05$) (Figure 6B), suggesting that MGD could induce substantial corneal nerve alterations and possibly neuropathic pain development, more so than AIDE diseases.

### *3.8. Higher Microneuroma Found in Painless DED Patients Compared with Healthy Controls*

Even in the absence of a neuropathic pain phenotype, microneuromas were observed in painless DED patients. Indeed, painless MGD patients had a significantly higher number of microneuromas per patient ($p < 0.05$) (Figure 6B) and higher microneuroma area ($p < 0.05$) (Figure 6D), compared with healthy patients, and similarly, painless AIDE patients had significantly lower nerve density ($p < 0.05$) (Figure 5A) and a significantly higher number of microneuromas per patient ($p < 0.01$) (Figure 6B), compared to healthy controls.

### *3.9. Structural Differences in Microneuromas between Painless MGD Patients and AIDE Patients*

Finally, microneuroma perimeter (Figure 6C) and area (Figure 6D) were both significantly higher in painless MGD patients than painless AIDE ($p < 0.01$), suggesting that such IVCM parameters (area and perimeter) could help differentiate corneal nerve alterations in these two subsets of DED patients.

## 4. Discussion

DED, frequently observed in ophthalmological practice, affects between 5 and 50% of the adult population and is gaining recognition as a public health issue, given its prevalence, morbidity, and associated financial burden [1–4].

DED is a heterogeneous clinical condition with growing evidence of underlying neurosensory abnormalities [1]. Furthermore, increasing preclinical and clinical lines of evidence suggest that DED could lead to NCP, a still ill-defined, high burden, painful ocular condition with few efficient treatment options [14,31]. Understanding NCP is thus of paramount clinical importance.

Significant heterogeneity could exist between DED subsets, such as AIDE and primary MGD, in terms of ocular surface symptomatology, semiology, and corneal nerve alterations, as evidenced in this study. Interestingly, the most important ultrastructural corneal nerve changes were found in the MGD-related NCP group—namely, decreased nerve density, higher number of microneuromas and increased microneuroma perimeter and area, even compared with the rest of DED groups. These observations suggest, for the first time, that primary MGD could be a previously unsuspected purveyor of NCP. Therefore, patients reporting severe ocular pain with mild-to-no corneal damage (aptly referred to as "pain with no stain") in cases of primary MGD should be considered as possibly suffering from NCP and managed accordingly [2,14].

Compared with the previous literature in the field, this study is the first to analyze the clinical profiles of these painful DED patients. We found that overall, painless or painful AIDE groups were more severe than corresponding MGD groups; the painful groups (AIDE and MGD) had higher symptoms and signs scores than the painless ones. Painful neuropathic conditions are notoriously difficult to manage, and NCP is no exception. Such difficulties in management stem from both complex diagnosis (in the absence of validated diagnostic criteria) and partially effective treatments with unpredictable results [2,15,34]. Regarding the former, several authors have investigated possible biomarkers of NCP, suggesting for instance that the sole presence of IVCM-identified corneal nerve microneuromas could be indicative of neuropathic pain [31]. Results from this study tend to disprove such a claim, as microneuromas were observed in painless DED patients and even in healthy subjects (Figure 6B), as recently reported [35].

Although microneuromas do bear witness of corneal nerve abnormalities [27,36], the latter seem insufficient to produce neuropathic pain. Therefore, from a diagnostic

standpoint, the mere presence of microneuromas seems insufficient to suggest corneal neuropathic alterations. Additional IVCM parameters, such as microneuroma perimeter and area, could thus be necessary, which in this experimental setting were both significantly higher in MGD-related NCP than in healthy subjects (Figure 6C,D).

There is growing evidence in the literature suggesting high phenotypic diversity, evidenced as different sensory profiles in painful neuropathic conditions with the same underlying etiology that could account for the often-observed partial treatment response in the clinical setting [32]. Therefore, phenotyping neuropathic pain could help in providing tailored treatment options with higher effectiveness and lower untoward effects [32,37,38]. In the present context of DED-related NCP, IVCM identified significantly diverse corneal nerve alterations, different between the painful neuropathic and painless conditions but also between the two DED subsets, suggestive of such aforementioned neuropathic phenotypic diversity. Based on data from the relevant literature [2,19,31,39,40] and from the results of this study, DED-related NCP patients could be stratified based on IVCM-identified corneal nerve alterations, as illustrated in Table 4.

**Table 4.** Comparison of in vivo confocal microscopy-assessed corneal ultrastructural characteristics associated with NCP.

| | | IVCM-Assessed Corneal Ultrastructural Characteristics (vs. Healthy Controls) | | | | | |
|---|---|---|---|---|---|---|---|
| | | ↘ Nerve Density | ↗ Nerve Tortortuosity | ↗ Number of Dendritic Cells | ↗ Number of MN | ↗ Perimeter of MN | ↗ Area of MN |
| MGD | MGD-NCP | ✓ | ns | ns | ✓ | ✓ | ✓ |
| | Painless | ns | ns | ns | ✓ | ns | ✓ |
| AIDE | AIDE-NCP | ns | ✓ | ns | ✓ | ns | ns |
| | Painless | ✓ | ns | ns | ✓ | ns | ns |

↘ decrease; ↗ increase; ns: non-significant difference (vs. healthy controls); ✓ significant difference (vs. healthy controls).

Further studies will be needed to determine whether this stratification provides new insights into the management of NCP.

The precise causal relationship between DED symptomatology/semiology and IVCM-identified corneal nerve abnormalities also warrants future studies to elucidate this "chicken-or-egg" conundrum. Indeed, DED has been shown to lead to NCP (with associated corneal nerve alterations), and conversely, NCP often presents as a "dry eye" sensation [1,9].

Several limitations in the present study warrant discussion. First, the retrospective nature of the study and small sample size are obvious limitations, at least partially, mitigated by nested paired group analysis and proper patient clustering. Second, DED subsets were divided arbitrarily between primary MGD and all AIDE patients. This was voluntary to provide cohorts of comparable sizes separated by major underlying pathophysiological mechanisms (i.e., ADDE vs. EDE) even though overlap is most probable in several conditions (such as in AIDE patients who develop secondary MGD). Future multicentric studies are warranted to provide better clustering between DED subsets. Finally, there was a limited number of patients in each final study group (after appropriate clustering), which could hamper the proper interpretation of IVCM results. Nevertheless, considering the rigorous IVCM image analysis methodology and the high number of images analyzed per patient (to our knowledge, never included in earlier studies), we believe our results to be sound and thus worthy of consideration.

## 5. Conclusions

Patients suffering from primary MGD-related NCP could present a different neuropathic phenotype, compared to the one observed in AIDE-related NCP patients, as proven herein using IVCM. Specifically, primary MGD-related NCP was associated with significantly more ultrastructural corneal nerve alterations than AIDE-related NCP or healthy controls. From a diagnostic standpoint, although IVCM can be useful to evidence NCP-related corneal nerve changes in DED patients, the diagnosis of DED-related NCP

will require an association of several IVCM-based criteria without relying solely on the presence of microneuromas.

**Author Contributions:** Conceptualization, A.G.-M., H.L., C.B. and A.R.-L.G.; Data curation, A.G.-M., H.L., J.L., G.R., A.L. and C.B.; Formal analysis, A.G.-M., H.L., C.B. and A.R.-L.G.; Funding acquisition, A.R.-L.G.; Investigation, J.L., G.R., S.M.P., A.L., C.B. and A.R.-L.G.; Methodology, A.G.-M., H.L., N.M. and A.R.-L.G.; Supervision, C.B. and A.R.-L.G.; Writing—original draft, A.G.-M., H.L. and N.M.; Writing—review and editing, H.L., N.M., S.M.P., C.B. and A.R.-L.G. All authors have read and agreed to the published version of the manuscript.

**Funding:** This work was funded by Sorbonne Université and the Institut National de la Santé et de la Recherche Médicale, ANR, LabEx LIFESENSES (ANR-10-LABX-65) and IHU FOReSIGHT (ANR-18-IAHU-01). Adrian Guerrero Moreno (AGM) is funded by a H2020-MSCA-ETN program (IT-DED3) (Grant Agreement 765608).

**Institutional Review Board Statement:** The study was conducted in accordance with the guidelines of the Declaration of Helsinki and approved by the Ethics Committee CPP-Ile de France (number 10793). All patients gave written consent to use their data for research purposes.

**Informed Consent Statement:** Informed consent was obtained from all subjects involved in the study.

**Data Availability Statement:** The datasets used and/or analyzed during the current study are available from the corresponding author on reasonable request.

**Conflicts of Interest:** The authors declare no conflict of interest. The funders had no role in the design of the study; in the collection, analyses, or interpretation of data; in the writing of the manuscript, or in the decision to publish the results.

## References

1. Belmonte, C.; Nichols, J.J.; Cox, S.M.; Brock, J.; Begley, C.G.; Bereiter, D.A.; Dartt, D.A.; Galor, A.; Hamrah, P.; Ivanusic, J.; et al. TFOS DEWS II pain and sensation report. *Ocul. Surf.* **2017**, *15*, 404–437. [CrossRef] [PubMed]
2. Dieckmann, G.; Goyal, S.; Hamrah, P. Neuropathic Corneal Pain. *Ophthalmology* **2017**, *124*, S34–S47. [CrossRef]
3. Galor, A.; Levitt, R.C.; Felix, E.; Martin, E.R.; Sarantopoulos, C. Neuropathic ocular pain: An important yet underevaluated feature of dry eye. *Eye* **2015**, *29*, 301–312. [CrossRef] [PubMed]
4. Galor, A.; Moein, H.-R.; Lee, C.; Rodriguez, A.; Felix, E.; Sarantopoulos, K.D.; Levitt, R.C. Neuropathic pain and dry eye. *Ocul. Surf.* **2018**, *16*, 31–44. [CrossRef] [PubMed]
5. Craig, J.P.; Nichols, K.K.; Akpek, E.K.; Caffery, B.; Dua, H.S.; Joo, C.-K.; Liu, Z.; Nelson, J.D.; Nichols, J.J.; Tsubota, K.; et al. TFOS DEWS II Definition and Classification Report. *Ocul. Surf.* **2017**, *15*, 276–283. [CrossRef] [PubMed]
6. Bron, A.J.; de Paiva, C.; Chauhan, S.K.; Bonini, S.; Gabison, E.E.; Jain, S.; Knop, E.; Markoulli, M.; Ogawa, Y.; Perez, V.; et al. TFOS DEWS II pathophysiology report. *Ocul. Surf.* **2017**, *15*, 438–510. [CrossRef]
7. Fakih, D.; Zhao, Z.; Nicolle, P.; Reboussin, E.; Joubert, F.; Luzu, J.; Labbé, A.; Rostène, W.; Baudouin, C.; Parsadaniantz, S.M.; et al. Chronic dry eye induced corneal hypersensitivity, neuroinflammatory responses, and synaptic plasticity in the mouse trigeminal brainstem. *J. Neuroinflamm.* **2019**, *16*, 1–20. [CrossRef] [PubMed]
8. Guerrero-Moreno, A.; Baudouin, C.; Parsadaniantz, S.M.; Goazigo, A.R.-L. Morphological and Functional Changes of Corneal Nerves and Their Contribution to Peripheral and Central Sensory Abnormalities. *Front. Cell. Neurosci.* **2020**, *14*, 610342. [CrossRef]
9. Mcmonnies, C.W. The potential role of neuropathic mechanisms in dry eye syndromes. *J. Optom.* **2017**, *10*, 5–13. [CrossRef]
10. Wolffsohn, J.S.; Arita, R.; Chalmers, R.; Djalilian, A.; Dogru, M.; Dumbleton, K.; Gupta, P.K.; Karpecki, P.; Lazreg, S.; Pult, H.; et al. TFOS DEWS II Diagnostic Methodology report. *Ocul. Surf.* **2017**, *15*, 539–574. [CrossRef]
11. Baudouin, C.; Aragona, P.; Van Setten, G.; Rolando, M.; Irkeç, M.; Del Castillo, J.B.; Geerling, G.; Labetoulle, M.; Bonini, S.; ODISSEY European Consensus Group Members. Diagnosing the severity of dry eye: A clear and practical algorithm. *Br. J. Ophthalmol.* **2014**, *98*, 1168–1176. [CrossRef]
12. Rosenthal, P.; Baran, I.; Jacobs, D.S. Corneal Pain without Stain: Is it Real? *Ocul. Surf.* **2009**, *7*, 28–40. [CrossRef]
13. Levitt, E.A.; Galor, A.; Chowdhury, A.R.; Felix, E.; Sarantopoulos, C.D.; Zhuang, G.Y.; Patin, D.; Maixner, W.; Smith, S.B.; Martin, E.R.; et al. Evidence that dry eye represents a chronic overlapping pain condition. *Mol. Pain* **2017**, *13*, 1744806917729306. [CrossRef]
14. Goyal, S.; Hamrah, P. Understanding Neuropathic Corneal Pain—Gaps and Current Therapeutic Approaches. *Semin. Ophthalmol.* **2016**, *31*, 59–70. [CrossRef] [PubMed]
15. Yoon, H.-J.; Kim, J.; Yoon, K.C. Treatment Response to Gabapentin in Neuropathic Ocular Pain Associated with Dry Eye. *J. Clin. Med.* **2020**, *9*, 3765. [CrossRef] [PubMed]
16. Galor, A.; Feuer, W.; Lee, D.J.; Florez, H.; Faler, A.L.; Zann, K.L.; Perez, V.L. Depression, Post-traumatic Stress Disorder, and Dry Eye Syndrome: A Study Utilizing the National United States Veterans Affairs Administrative Database. *Am. J. Ophthalmol.* **2012**, *154*, 340–346.e2. [CrossRef] [PubMed]

17. Qazi, Y.; Hurwitz, S.; Khan, S.; Jurkunas, U.V.; Dana, R.; Hamrah, P. Validity and Reliability of a Novel Ocular Pain Assessment Survey (OPAS) in Quantifying and Monitoring Corneal and Ocular Surface Pain. *Ophthalmology* **2016**, *123*, 1458–1468. [CrossRef] [PubMed]
18. Crane, A.M.; Feuer, W.; Felix, E.; Levitt, R.C.; McClellan, A.L.; Sarantopoulos, K.D.; Galor, A. Evidence of central sensitisation in those with dry eye symptoms and neuropathic-like ocular pain complaints: Incomplete response to topical anaesthesia and generalised heightened sensitivity to evoked pain. *Br. J. Ophthalmol.* **2017**, *101*, 1238–1243. [CrossRef]
19. Bayraktutar, B.N.; Ozmen, M.C.; Muzaaya, N.; Dieckmann, G.; Koseoglu, N.D.; Müller, R.T.; Cruzat, A.; Cavalcanti, B.M.; Hamrah, P. Comparison of clinical characteristics of post-refractive surgery-related and post-herpetic neuropathic corneal pain. *Ocul. Surf.* **2020**, *18*, 641–650. [CrossRef]
20. Cruzat, A.; Qazi, Y.; Hamrah, P. In Vivo Confocal Microscopy of Corneal Nerves in Health and Disease. *Ocul. Surf.* **2017**, *15*, 15–47. [CrossRef]
21. Labbé, A.; Liang, Q.; Wang, Z.; Zhang, Y.; Xu, L.; Baudouin, C.; Sun, X. Corneal Nerve Structure and Function in Patients With Non-Sjögren Dry Eye: Clinical Correlations. *Investig. Opthalmol. Vis. Sci.* **2013**, *54*, 5144–5150. [CrossRef]
22. Liang, H.; Randon, M.; Michee, S.; Tahiri, R.; Labbe, A.; Baudouin, C. In vivo confocal microscopy evaluation of ocular and cutaneous alterations in patients with rosacea. *Br. J. Ophthalmol.* **2016**, *101*, 268–274. [CrossRef]
23. Ross, A.R.; Al-Aqaba, M.A.; Almaazmi, A.; Messina, M.; Nubile, M.; Mastropasqua, L.; Dua, H.S.; Said, D.G. Clinical and in vivo confocal microscopic features of neuropathic corneal pain. *Br. J. Ophthalmol.* **2019**, *104*, 768–775. [CrossRef] [PubMed]
24. Al-Aqaba, M.A.; Dhillon, V.K.; Mohammed, I.; Said, D.G.; Dua, H.S. Corneal nerves in health and disease. *Prog. Retin. Eye Res.* **2019**, *73*, 100762. [CrossRef] [PubMed]
25. Goazigo, A.R.-L.; Guerrero-Moreno, A.; Fakih, D.; Parsadaniantz, S.M. How does chronic dry eye shape peripheral and central nociceptive systems? *Neural Regen. Res.* **2021**, *16*, 306–307. [CrossRef] [PubMed]
26. Patel, S.; Hwang, J.; Mehra, D.; Galor, A. Corneal Nerve Abnormalities in Ocular and Systemic Diseases. *Exp. Eye Res.* **2021**, *202*, 108284. [CrossRef] [PubMed]
27. Chinnery, H.R.; Rajan, R.; Jiao, H.; Wu, M.; Zhang, A.C.; De Silva, M.E.H.; Makrai, E.; Stepp, M.A.; Di Girolamo, N.; Downie, L.E. Identification of presumed corneal neuromas and microneuromas using laser-scanning in vivo confocal microscopy: A systematic review. *Br. J. Ophthalmol.* **2021**, *10*, 1136. [CrossRef]
28. Labbé, A.; Alalwani, H.; Van Went, C.; Brasnu, E.; Georgescu, D.; Baudouin, C. The Relationship between Subbasal Nerve Morphology and Corneal Sensation in Ocular Surface Disease. *Investig. Opthalmol. Vis. Sci.* **2012**, *53*, 4926–4931. [CrossRef]
29. Nicolle, P.; Liang, H.; Reboussin, E.; Rabut, G.; Warcoin, E.; Brignole-Baudouin, F.; Melik-Parsadaniantz, S.; Baudouin, C.; Labbe, A.; Goazigo, A.R.-L. Proinflammatory Markers, Chemokines, and Enkephalin in Patients Suffering from Dry Eye Disease. *Int. J. Mol. Sci.* **2018**, *19*, 1221. [CrossRef] [PubMed]
30. Tervo, T.M.; Moilanen, J.A.O.; Rosenberg, M.E.; Tuominen, I.S.J.; Valle, T.; Vesaluoma, M.H. In Vivo Confocal Microscopy for Studying Corneal Diseases and Conditions Associated with Corneal Nerve Damage. *Adv. Exp. Med. Biol.* **2002**, *506*, 657–665. [CrossRef]
31. Moein, H.-R.; Akhlaq, A.; Dieckmann, G.; Abbouda, A.; Pondelis, N.; Salem, Z.; Müller, R.T.; Cruzat, A.; Cavalcanti, B.M.; Jamali, A.; et al. Visualization of microneuromas by using in vivo confocal microscopy: An objective biomarker for the diagnosis of neuropathic corneal pain? *Ocul. Surf.* **2020**, *18*, 651–656. [CrossRef] [PubMed]
32. Bouhassira, D.; Wilhelm, S.; Schacht, A.; Perrot, S.; Kosek, E.; Cruccu, G.; Freynhagen, R.; Tesfaye, S.; Lledó, A.; Choy, E.; et al. Neuropathic pain phenotyping as a predictor of treatment response in painful diabetic neuropathy: Data from the randomized, double-blind, COMBO-DN study. *Pain* **2014**, *155*, 2171–2179. [CrossRef] [PubMed]
33. Aggarwal, S.; Kheirkhah, A.; Cavalcanti, B.M.; Cruzat, A.; Jamali, A.; Hamrah, P. Correlation of corneal immune cell changes with clinical severity in dry eye disease: An in vivo confocal microscopy study. *Ocul. Surf.* **2021**, *19*, 183–189. [CrossRef] [PubMed]
34. Jacobs, D.S. Diagnosis and Treatment of Ocular Pain: The Ophthalmologist's Perspective. *Curr. Ophthalmol. Rep.* **2017**, *5*, 271–275. [CrossRef] [PubMed]
35. Dermer, H.; Hwang, J.; Mittal, R.; Cohen, A.K.; Galor, A. Corneal sub-basal nerve plexus microneuromas in individuals with and without dry eye. *Br. J. Ophthalmol.* **2021**, *10*, 1136. [CrossRef]
36. Stepp, M.A.; Pal-Ghosh, S.; Downie, L.E.; Zhang, A.C.; Chinnery, H.R.; Machet, J.; Di Girolamo, N. Corneal Epithelial "Neuromas": A Case of Mistaken Identity? *Cornea* **2020**, *39*, 930–934. [CrossRef]
37. van Hecke, O.; Kamerman, P.R.; Attal, N.; Baron, R.; Bjornsdottir, G.; Bennett, D.L.; Bennett, M.I.; Bouhassira, D.; Diatchenko, L.; Freeman, R.; et al. Neuropathic pain phenotyping by international consensus (NeuroPPIC) for genetic studies. *Pain* **2015**, *156*, 2337–2353. [CrossRef] [PubMed]
38. Vollert, J.; Maier, C.; Attal, N.; Bennett, D.L.; Bouhassira, D.; Enax-Krumova, E.K.; Finnerup, N.B.; Freynhagen, R.; Gierthmühlen, J.; Haanpää, M.; et al. Stratifying patients with peripheral neuropathic pain based on sensory profiles: Algorithm and sample size recommendations. *Pain* **2017**, *158*, 1446–1455. [CrossRef] [PubMed]
39. Kallinikos, P.; Berhanu, M.; O'Donnell, C.; Boulton, A.J.M.; Efron, N.; Malik, R. Corneal Nerve Tortuosity in Diabetic Patients with Neuropathy. *Investig. Opthalmol. Vis. Sci.* **2004**, *45*, 418–422. [CrossRef] [PubMed]
40. Kim, J.; Yoon, H.J.; You, I.C.; Ko, B.Y.; Yoon, K.C. Clinical characteristics of dry eye with ocular neuropathic pain features: Comparison according to the types of sensitization based on the Ocular Pain Assessment Survey. *BMC Ophthalmol.* **2020**, *20*, 1–7. [CrossRef]

# Chapter 3: Discussion

## I. DED-related ocular pain: *does sex matter?*

Chronic pain diseases are more prevalent in women than in men overall (Berkley, 1997; Mogil, 2012). Apart from obvious hormonal implications, some cellular mechanisms have been proposed to explain this prevalence, such as male-specific involvement of spinal cord microglia in painful conditions (Sorge et al. , 2011; Taves et al. , 2016; Mapplebeck et al., 2018) or genes that are sex-specifically transcribed in primary sensory neurons at the DRG level (Tavares-Ferreira et al., 2022). For example, female-predominant expression of genes related to inflammation, synaptic transmission and extracellular matrix reorganization have been found in trigeminal primary sensory neurons (Mecklenburg et al., 2020). Another study has found higher levels of $K_{ir}$ 6.2, a subunit of the inward-rectifier potassium channel responsible of maintaining resting potential and triggering hyperpolarization, in male than female rats (Niu et al., 2011), providing novel information on sex differences in ATP-sensitive $K^+$ channel expression in the TG and its contribution in an orofacial muscle pain condition. Female rats exposed to infra-orbital nerve chronic constriction injury developed significantly higher mechanical allodynia than male rats, correlating with increased levels of Csf1 and CX3CR1 in the TG (Korczeniewska et al., 2018). Furthermore, in a model of orofacial inflammatory pain induced by complete Freund's adjuvant administration, an increased expression of CGRP was found in female mice, while male mice showed increased IL-1β, IL-6, TNF and BDNF at the TG level (Kuzawinska et al., 2014). Altogether these data illustrate preliminary evidence regarding the molecular basis of sexual dimorphism in trigeminal pain processing.

As previously mentioned, DED affects women more frequently than men. This sex-related difference in DED prevalence is due to in large part to the effects of sex steroids (e.g. androgens, estrogens), hypothalamic-pituitary hormones, glucocorticoids, insulin, insulin-like growth factor 1 and thyroid hormones, as well as to the sex chromosome complement, sex-specific autosomal factors and epigenetics (e.g. microRNAs) (Sullivan et al., 2017). The magnitude of this increased risk in women varies significantly from study to study, usually ranging from 20 to 80% (Sullivan et al., 2017).

Sexual dimorphism in DED-related pain has also been found in animal models of DED. Differences between male and female C57BL/6J mice have been reported in studies inducing

DED with environmental desiccating stress + scopolamine injection. DED female mice showed more severe DED (*i.e.* increased ocular surface fluorescence staining, decreased tear production and higher goblet cell loss), increased effector T cells ($T_H1$ and $T_H17$) and decreased regulatory T cells in cervical draining lymph nodes with respect to male mice (Gao et al., 2015).

Regarding surgical models of DED, two studies explored the effects of unilateral vs. bilateral excision of the extra-orbital lacrimal gland comparing male and female C57BL/6J mice (Mecum et al., 2019, Mecum et al., 2020). When gland excision was unilateral, an increase in ocular discomfort was observed only in female mice, whereas bilateral gland excision had a similar impact on ocular discomfort in both sexes (Mecum et al., 2020). In our studies, corneal sensitivity and spontaneous ocular discomfort were found similar in male (Fakih et al., 2020, Fakih et al., 2021) and female (Fakih et al., 2019) mice submitted to unilateral extra-orbital lacrimal gland and harderian gland excision.

Chemical sensitivity also differed depending on sex and model (bilateral vs. unilateral extra-orbital gland excision). Chemical sensitivity, evaluated with the capsaicin test among the four experimental groups (male/female, bilateral/unilateral), was only increased in unilaterally operated female mice (Mecum et al., 2020). In our studies, only female animals were tested and we found a chemical hypersensitivity to capsaicin in extra-orbital lacrimal gland and harderian gland operated mice (Fakih et al., 2021). The fact that bilateral excision of the extra-orbital lacrimal gland and unilateral excision of both extra-orbital lacrimal gland and harderian gland gave rise to different results could be explained by 1) the surgery (the nature of the excised glands is different) and 2) the concentrations of the capsaicin solution used: 3.23 mM (0.1 %) for bilateral extra-orbital lacrimal gland excision (Mecum et al., 2020) and 0.1 mM for unilateral excision of extra-orbital lacrimal gland and harderian gland (Fakih et al., 2021).

Cold corneal sensitivity was also tested in those studies with different outcomes. In Mecum et al., 2020, only unilateral extra-orbital lacrimal gland excision in female mice triggered cold allodynia (but not bilaterally excision in mice of both sexes), while conversely our data showed an increased sensitivity to menthol in unilateral double gland-excised male animals (Fakih et al., 2020). This discrepancy could be explained by the menthol concentration used which was different (200 µM vs. 50 µM) and the parameters measured during the behavioral test.

Behavioral sexual dimorphism was also reported regarding anxiety-like behaviors associated to DED. Both sexes presented anxiety-like behaviors (evidenced using an elevated plus maze test) in bilaterally operated animals but only females when operated unilaterally (Mecum et al., 2020). Our study revealed that adult male mice showed an increase in anxiety-like behaviors as measured by the elevated plus maze and black & white box test as compared to sham animals (Fakih et al., 2021). Female animals were not investigated in this study.

## II. Could microneuromas serve as a diagnostic biomarker for neuropathic corneal pain?

Diagnosis and management of NCP remain challenging in both general and specialized ophthalmological practice. Similarly to other painful neuropathic conditions and as defined by 2016 NeuPSIG (Neuropathic pain special interest group of the International Association for the Study of Pain) guidelines (Finnerup et al., 2016) the diagnosis of definite neuropathic pain will require:

1. An history of relevant neurological lesion or disease and pain distribution neuroanatomically plausible;
2. Pain associated with sensory signs in the same neuroanatomically plausible distribution;
3. Diagnosis test confirming a lesion or disease of the somatosensory nervous system explaining the pain.

In some cases, the diagnosis of definite neuropathic pain will be quite straightforward as in the case of neuropathic corneal pain secondary to LASIK surgery, where the surgery is known to induce corneal nerve injury (corneal nerve transection) (criteria 1) easily evidenced using IVCM (criteria 3) and that can lead, *inter alia*, to corneal hypoesthesia (criteria 2).

Nevertheless, in other cases such as in numerous etiologies of DED, the diagnosis of NCP is clearly more difficult, especially in the absence of validated diagnostic criteria.

Among the attempts to define specific biomarkers of NCP, several authors have suggested that microneuromas evidenced using IVCM could be a hallmark of NCP (Moein et al., 2020) as they were observed exclusively in painful patients, especially in those with “pain without stain”, *i.e.* with significant corneal pain in the absence of corneal damage evidenced using slit-lamp biomicroscopy. Unfortunately, the results from our IVCM-based retrospective clinical study would contradict such statement, as we have found microneuromas in healthy patients

(Guerrero-Moreno et al., 2021b), Figure 6B). Several hypotheses can be proposed to explain such discrepancies between previous clinical studies (including Moein et al., 2020 and ours Guerrero-Moreno et al., 2021b):

- Previous clinical studies have only selected between 3 and 7 IVCM images per patient considered as "representative" images. This sampling may be insufficient considering that each IVCM image represents a small area (0.16 $mm^{2)}$ corresponding to 4% of the human cornea (380 $mm^2$). In our work, we included as many images per patient as possible. For example, between 31 and 193 images (median = 77) of non-overlapping images were used for quantification of microneuroma number, area and perimeter.
- Although the concept of "neuroma" in other medical fields is somewhat well defined (Sist and Greene, 1981; Lee et al. , 1998; Vernadakis et al. , 2003) this does not seem to be the case in ophthalmology as evidenced in our literature review (see **Table 3**) that found several hypotheses proposed regarding the nature of corneal microneuromas, namely:
    - Damaged axons producing abnormal ectopic neural activity, initiated at the site of injury;
    - Entry points of corneal nerves from the stroma through Bowman's layer and epithelial basement membrane to the level of the sub-basal plexus;
    - Corneal axons regenerating from an insult/injury or having recently crossed the stroma/epithelium interface.

  Therefore, in some cases it could be possible that corneal nerve entry points could be mistaken for actual sites of corneal nerve injury, underlying the difficulty in proper and reproducible analysis of such IVCM structures. Furthermore, analyzing large and complex image datasets to extract meaningful information can be a tedious and time-consuming process. By using machine learning algorithms, the risk of human error and incorrect interpretation of IVCM images can be diminished as well as the time required for the analysis. Recently, Setu and colleagues have reported a deep learning-based automatic meibomian gland segmentation and morphology assessment in infrared meibography (Setu et al., 2021). Other applications of artificial intelligence have been applied to the analysis of IVCM corneal images (Giannaccare et al. , 2019; Wei et al. , 2020), with specific focus on detection and quantification of sub-basal nerve plexuses and DCs (Setu et al., 2022).
- If we consider "microneuromas" observed in IVCM to be traumatic neuromas of the corneal nerves (as per its classical histological definition (Cravioto and Battista, 1981; Abreu et al., 2013,), this does not necessarily imply that they actually participate in the ectopic nerve activity that drives peripheral post-traumatic neuropathic pain development (Tal and Devor,

1992; Xie et al. , 2005; Poppler et al. , 2018) . Indeed, cases of non-painful traumatic neuromas have been described (Lee et al., 1998; Abreu et al., 2013) and thus, microneuromas evidenced in healthy patients could represent painless traumatic neuromas of the corneal nerves. This is further supported by the fact that microneuromas have been reported in non-painful ocular diseases such as keratoconus (Patel and McGhee, 2006; Niederer et al., 2008; Parissi et al., 2016).

All in all, despite the controversies surrounding the nature and diagnostic relevance of IVCM-evidenced microneuromas, it seems quite clear that the diagnosis of NCP cannot be suggested based solely on the presence of microneuromas.

Furthermore, as illustrated in our clinical study (Guerrero-Moreno et al., 2021b), additional IVCM-based parameters described microneuromas, such as microneuroma area and perimeter could actually be useful to discriminate between etiological subsets of DED, an initial step towards better patient phenotyping and thus better personalized pain management.

## III. Could peripheral activation of corneal opioid receptors be a promising strategy to treat corneal pain and corneal inflammation?

In the context of ocular pain, only a few studies have explored the analgesic properties of topically administered opioid agonists. Several studies have investigated topical morphine in a variety of species (rabbit, dog, cat, rat and human), with varying regimen (from a single instillation to as often as 4 per day) and measures of effectiveness (mechanical sensitivity, capsaicin challenge test and pain assessment by VAS) (Peyman et al., 1994; Stiles et al., 2003; Wenk et al., 2003; Faktorovich and Basbaum, 2010). In the clinical setting, we found that patients with DED-related chronic corneal pain had lower enkephalin levels in their ocular surface as compared to healthy controls (Nicolle et al., 2018), suggesting a link between endogenous opioid dysregulation and corneal pain (Reaux-Le Goazigo et al., 2019).

A previous study from our team also showed that activation of corneal opioid receptors by endogenous enkephalins could be an effective approach to reduce ocular pain in inflammatory (scraping + LPS instillation) and toxically-induced (BAK instillation) pain models (Reaux-Le Goazigo et al., 2019).

Next, in (Joubert et al., 2020), we provided the first demonstration of MOR immunoreactivity in mouse corneal nerves and anatomical data confirming a higher MOR mRNA expression in the $V_1$ region of the TG under inflammatory pain conditions, in line with previous publications (Truong et al., 2003). This indicates that MOR is triggered under inflammatory pain conditions, reinforcing the idea that inflamed tissues will be more susceptible to the action of opioid agonists, as previously evidenced in other spinal inflammatory pain models (Hassan et al. , 1993). Interestingly, repeated topical administration of DAMGO was able to reverse corneal nerve sensitization and mediated analgesic effects on mechanical and chemical corneal allodynia (Joubert et al., 2020). However, these studies were performed in an acute (5 days) inflammatory pain model. Considering that DED is a chronic painful disease, a non-reversible model would be more suitable for the study of the mechanisms involved in this chronicity.

In this line, we assessed similar experiments to evaluate the effects of topical DAMGO in our model of DED-associated chronic pain induced by the excision of the extra-orbital lacrimal gland and harderian gland. We found an increase in MOR mRNA in the $V_1$ region of the TG, 21 days after surgery confirming molecular changes of MOR under persistent DED (**Fig. 33**). More importantly, we demonstrated that repeated administration of DAMGO for 2 weeks twice daily was able to decrease ocular discomfort, mechanical allodynia and hypersensitivity to capsaicin (**Fig. 34**). Together, these results point to MOR as a good topical therapeutic target for the treatment of inflammatory and DED-associated ocular pain.

The fact that topical DAMGO mitigated capsaicin-induced corneal hypersensitivity raised interesting questions about a possible interaction between MOR and TRPV1 in the cornea. Indeed, previous studies have confirmed that capsaicin or inflammatory conditions activating peripheral TRPV1 channels could promote nuclear internalization of β-arrestin 2, a protein implicated in MOR desensitization. Therefore, activation of TRPV1 may prevent tolerance to topical opioids (Endres-Becker et al. , 2007; Bao et al. , 2015; Basso et al. , 2019). These two events (*i.e.* overexpression of MOR and MOR being expressed in $TRPV1^+$ primary sensory neurons) could contribute to explain the lack of tolerance and lack of OIH of topically- and repeatedly-applied DAMGO in such as model of chronic ocular pain.

Another interesting question to be raised pertains to the capacity of topical DAMGO to reduce DED-induced corneal inflammation.

Several mechanisms of action of opioids on inflammatory responses and on immune cells have been reported:

1) Sensitization of primary neurons triggers neurogenic inflammation (Bignami et al., 2016), a process that can be prevented by opioids.
2) Exogenous and endogenous opioids are able to reduce immune cell activation via G-protein inhibition of adenylyl cyclase and calcium channels (Stein, 2016), reducing chemotaxis and immune response (Wetzel et al. , 2000; Kulkarni-Narla et al. , 2001; Benard et al., 2008).
3) Heterologous desensitization between opioids and chemokine receptors have been reported in a variety of conditions and cell types (for review see (Melik Parsadaniantz et al., 2015), leading in certain cases to anti-inflammatory and anti-nociceptive effects.

The anti-inflammatory activity of topical opioids was first elegantly demonstrated in a rat model of inflammatory pain (Wenk et al., 2003). Repeated instillations of 5 µM morphine significantly reduced the number of neutrophils on the ocular surface. This process was completely prevented by a specific MOR inhibitor (CTAP 1 mM) but only partially by a specific DOR inhibitor (naltrindole 200 nM) (Wenk et al., 2003). In a previous study from our laboratory, topical PL265 reduced the number of corneal $CD11b^+$ cells in a mouse model of acute inflammatory pain (**Fig. 25**, (Reaux-Le Goazigo et al., 2019)). Both models represent acute injuries to the ocular surface that would tend to subside, whereas DED is a chronic inflammation of the ocular surface. Therefore, we aimed to investigate whether repeated ocular application of DAMGO is able to alleviate the inflammatory response in our DED-associated chronic ocular pain model. Thus, DED mice were treated twice daily for two weeks with DAMGO or PBS (**Fig. 29**). Corneas were then immunostained to detect macrophage and dendritic cells (Iba1 marker) and nerve fibers (beta III tubulin marker). Preliminary quantifications revealed that, in contrast to what had been found in an acute inflammatory corneal pain model, the number of $Iba1^+$ cells was not reduced at the central or peripheral cornea following topical DAMGO treatment (**Fig. 32**). Further experiments and quantification are currently under investigation to subdivide $Iba1^+$ cells according to their morphology: from a rounder phenotype and broader shape characteristic of macrophages, to a more dendritiform and elongated shape, representative of dendritic cells (Foulsham et al., 2018).

## IV. Perspectives and future research avenues

The analgesic effects obtained after the activation of corneal opioid receptors reinforce the idea of pursuing our research on this direction. Several axes, described below, could be evaluated

### IV.1 Could topical DAMGO reverse peripheral and central neuroinflammation?

In order to better understand the effects of topical DAMGO on neuroinflammatory responses in both the TG and CNS, we aim to provide the first transcriptomic analysis of gene signatures associated with DED-related ocular pain using RNA sequencing (RNA-seq). RNA-seq has been successfully applied to the mouse TG (Lopes et al. , 2017; Megat et al. , 2019); however, in the context of trigeminal pain only one study has been performed in a rat model of masseter muscle inflammation (Chung et al., 2016). In that line, we recently started performing additional experiments in which TG and brainstem from sham and DED mice treated with PBS, DAMGO and DAMGO + naloxone will be extracted and processed for RNA-seq analysis. The large dataset will serve as a resource for examining TG and brainstem transcriptional changes that are associated with DED and related signatures of nociceptive mechanisms underlying chronic DED pain. We hope this study will help determine new molecular candidates as ocular pain biomarkers and therapeutic targets.

### IV.2 Can topical activation of DOR in the ocular surface treat ocular pain?

As previously mentioned, we reported the antinociceptive properties of the dual enkephalinase inhibitor PL265 in several animal models of corneal pain (Reaux-Le Goazigo et al., 2019). Enkephalins exert their analgesic effects by acting on MOR and DOR, but the contribution of each receptor in mitigating corneal pain is still unknown. Drugs targeting peripheral DOR produce fewer side effects in animals and have a much lower abuse potential. The development of selective non-peptidergic DOR agonists (such as SNC80, deltorphin II) and novel mouse lines with DOR mutations have clarified the role of this receptor in pain control and mood disorders (Gaveriaux-Ruff and Kieffer, 2011). Indeed, pharmacological studies in rodents have found that DOR agonist deltorphin II efficiently decreased persistent inflammatory and neuropathic pain (Holdridge and Cahill, 2007). In addition, SNC80 administration triggered anxiolytic-like effects (Perrine et al., 2006). Altogether, these data

suggest that DOR may represent also a promising target for the treatment of ocular pain and anxiety.

Further studies will be required to investigate possible changes in DOR protein levels (via immunohistochemistry) and mRNA expression levels (via fluorescent *in situ* hybridization, RNA scope) in the cornea, TG and brainstem from mice suffering from corneal pain. The next step will be to evaluate whether topical DOR agonists (SNC80, deltorphin II) improve:

1) ocular discomfort (spontaneous eye closure);
2) mechanical (von Frey test) and chemical (capsaicin challenge test) corneal sensitivity;
3) responsiveness of polymodal and cold nociceptors (ciliary nerve fibers electrophysiological studies);
4) expression of inflammatory and nociceptor markers (immunostaining, flow cytometry, *in situ* hybridization, qPCR).

Finally, anxiolytic-like effects of DOR agonists will be assessed using a combination of behavioral tests, such as the elevated plus maze test (based on an innate aversion to the elevated open areas on the maze), the open-field test and light/dark tests (based on an innate aversion to mild stressors, such as a novel environment and/or a bright light).

### IV.3 Biased opioid agonists and drugs targeting opioid receptor heterodimers: *an opportunity to develop new treatments for corneal pain?*

Chronic opioid therapy can cause many side effects including respiratory depression, nausea, sedation, itch, constipation, analgesic tolerance or opioid-induced hyperalgesia. In order to design new opioid analgesics without significant side effects (such as tolerance and OIH), biased opioid receptor agonists are being investigated, that could activate a specific downstream signaling pathway (for review see (Che et al., 2021; De Neve et al., 2021)) known to produce the analgesic effect (most often the G-protein-mediated pathway), without activating the downstream signaling pathway known to produce the adverse effects (most often the β-arrestin-mediated pathway).

For example, TRV130 (oliceridine) which preferentially activates G protein-mediated but not β-arrestin-mediated signaling, was constructed and developed to reduce opioid adverse events. TRV130 was approved by the Food and Drug Administration in 2020 for the treatment

of moderate to acute pain. Another compound, PZM21, is able to reduce pain in mice whilst being devoid of both respiratory depression and constipation (Che et al., 2021).

Bifunctional-biased μ-opioid agonists have been also designed. For example, KGFF09 is a μ-opioid biased agonist that also acts as an antagonist of neuropeptide FF receptors 1 and 2. Neuropeptide FF and its receptors (NPFF1R and NPFF2R) are recognized as an important pronociceptive system involved in opioid-induced hyperalgesia and analgesic tolerance. KGFF09 was shown to promote analgesia with limited side effects (reduced respiratory depression, OIH, analgesic tolerance and physical dependence) in a model of persistent inflammatory pain (Drieu la Rochelle et al., 2018). This study demonstrated that G-protein-biased MOR agonism and NPFFR antagonism have beneficial effects on both acute and chronic adverse effects of conventional opioid analgesics.

Receptor heterodimerization represents another important layer of functional complexity of opioid receptors and provides an additional opportunity to modulate the function of opioid receptors (Machelska and Celik, 2018). Some examples of MOR heterodimers that could be potentially targeted are:

1) **MOR-CB1 heterodimers:** Cannabinoid receptor 1 (CB1) is expressed in the peripheral and central nervous system, including primary sensory neurons and some brain regions related to pain processing. The activation of MOR-CB1 heterodimers *in vitro* by DAMGO, morphine and Hu-210 (a CB1 agonist) was shown to inhibit neuronal plasticity (Rios et al., 2006). Thus, MOR-CB1 heterodimers may be a target to modulate neuronal plasticity associated with persistent corneal pain.
2) **MOR-DOR heterodimers** are the most described heterodimer and found both *in vitro* and *in vivo* (Erbs et al., 2015). Increasing data highlight that MOR heterodimers could emerge as novel therapeutic targets for pain management (for review see Zhang et al., 2020a). Indeed, co-administration of drugs that block MOR-DOR heteromerization together with an opioid agonist treatment have been shown to decrease tolerance (He et al., 2011). Furthermore, CYM51010, a drug targeting the MOR-DOR heterodimer, showed an analgesic activity comparable to morphine and chronic administration of CYM51010 resulted in less analgesic tolerance than morphine (Gomes et al., 2013).

In sum, such aforementioned data from the literature pointing to analgesic effects of biased agonists without any significant adverse effect or compounds targeting heterodimers may provide new therapeutic avenues in the field of ocular pain. It would be interesting to

evaluate some of these molecules in the various existing models of acute or chronic corneal pain.

## Conclusion

Dry eye disease is a chronic debilitating ocular condition, still insufficiently diagnosed and managed, often leading to chronic ocular pain, with limited efficient treatment options. In numerous cases it can be associated with neuropathic corneal pain, even more difficult to manage.

Similarly to other painful neuropathic conditions, neuropathic corneal pain is difficult to diagnose, especially in cases without any evident nerve damage (as is the case for dry eye disease for instance). Furthermore, it is associated with an important phenotypic variability that can account for the often disappointing results of current treatment options.

Such unmet medical needs served as the impetus for the present translational research project that aimed to improve the management of DED-related neuropathic pain by increasing our understanding of DED pathophysiology, by investigating new treatment options for DED-related pain and by trying to improve the diagnosis of DED-related neuropathic pain.

We showed using animal models developed in our laboratory that chronic DED is associated with peripheral and central neuroplastic changes that drive peripheral and central sensitization.

Furthermore, we showed in the same models that targeting the corneal opioid system using topical opioids such as DAMGO could provide a novel interesting treatment option for DED, that will need to be explored in patients.

Finally, from a clinical standpoint, although IVCM can provide an interesting non invasive assessment of the corneal nerves in patients, the presence of microneuromas alone cannot be considered sufficient for the diagnosis of DED-related neuropathic corneal pain and additional IVCM parameters will be necessary, especially to distinguish the various neuropathic phenotypes of each etiological subset of DED.

All in all, this research project explored new avenues for the management of DED with the hope of eventually helping to improve the quality of life of patients suffering from this highly burdensome ocular disease.

# Bibliography

The definition and classification of dry eye disease: report of the Definition and Classification Subcommittee of the International Dry Eye WorkShop (2007). Ocul Surf. 2007;5:75-92.

Abels C, Soeberdt M. Can we teach old drugs new tricks?-Repurposing of neuropharmacological drugs for inflammatory skin diseases. Exp Dermatol. 2019;28:1002-9.

Abreu E, Aubert S, Wavreille G, Gheno R, Canella C, Cotten A. Peripheral tumor and tumor-like neurogenic lesions. Eur J Radiol. 2013;82:38-50.

Acosta MC, Peral A, Luna C, Pintor J, Belmonte C, Gallar J. Tear secretion induced by selective stimulation of corneal and conjunctival sensory nerve fibers. Invest Ophthalmol Vis Sci. 2004;45:2333-6.

Aggarwal S, Colon C, Kheirkhah A, Hamrah P. Efficacy of autologous serum tears for treatment of neuropathic corneal pain. Ocul Surf. 2019;17:532-9.

Aggarwal S, Kheirkhah A, Cavalcanti BM, Cruzat A, Colon C, Brown E, et al. Autologous Serum Tears for Treatment of Photoallodynia in Patients with Corneal Neuropathy: Efficacy and Evaluation with In Vivo Confocal Microscopy. Ocul Surf. 2015;13:250-62.

Aggarwal S, Kheirkhah A, Cavalcanti BM, Cruzat A, Jamali A, Hamrah P. Correlation of corneal immune cell changes with clinical severity in dry eye disease: An in vivo confocal microscopy study. Ocul Surf. 2021;19:183-9.

Akpek EK, Bunya VY, Saldanha IJ. Sjogren's Syndrome: More Than Just Dry Eye. Cornea. 2019;38:658-61.

Al-Aqaba M, Alomar T, Lowe J, Dua HS. Corneal nerve aberrations in bullous keratopathy. Am J Ophthalmol. 2011;151:840-9 e1.

Al-Aqaba MA, Dhillon VK, Mohammed I, Said DG, Dua HS. Corneal nerves in health and disease. Prog Retin Eye Res. 2019;73:100762.

Alio JL, Rodriguez AE, Ferreira-Oliveira R, Wrobel-Dudzinska D, Abdelghany AA. Treatment of Dry Eye Disease with Autologous Platelet-Rich Plasma: A Prospective, Interventional, Non-Randomized Study. Ophthalmol Ther. 2017;6:285-93.

Anderson SR, Losin EAR. A sociocultural neuroscience approach to pain. Culture and Brain. 2016;5:14-35.

Appenteng Osae E, Steven P. Meibomian Gland Dysfunction in Ocular Graft vs. Host Disease: A Need for Pre-Clinical Models and Deeper Insights. Int J Mol Sci. 2021;22.

Arden JR, Segredo V, Wang Z, Lameh J, Sadee W. Phosphorylation and agonist-specific intracellular trafficking of an epitope-tagged mu-opioid receptor expressed in HEK 293 cells. J Neurochem. 1995;65:1636-45.

Baddack-Werncke U, Busch-Dienstfertig M, Gonzalez-Rodriguez S, Maddila SC, Grobe J, Lipp M, et al. Cytotoxic T cells modulate inflammation and endogenous opioid analgesia in chronic arthritis. J Neuroinflammation. 2017;14:30.

Bai X, Wang C, Zhang X, Feng Y, Zhang X. The role of testosterone in mu-opioid receptor expression in the trigeminal ganglia of opioid-tolerant rats. Neurosci Lett. 2020;723:134868.

Bang SP, Yeon CY, Adhikari N, Neupane S, Kim H, Lee DC, et al. Cyclosporine A eyedrops with self-nanoemulsifying drug delivery systems have improved physicochemical properties and efficacy against dry eye disease in a murine dry eye model. PLoS One. 2019;14:e0224805.

Bao Y, Gao Y, Yang L, Kong X, Yu J, Hou W, et al. The mechanism of mu-opioid receptor (MOR)-TRPV1 crosstalk in TRPV1 activation involves morphine anti-nociception, tolerance and dependence. Channels (Austin). 2015;9:235-43.

Barabino S, Antonelli S, Cimbolini N, Mauro V, Bouzin M. The effect of preservatives and antiglaucoma treatments on the ocular surface of mice with dry eye. Invest Ophthalmol Vis Sci. 2014;55:6499-504.

Barabino S, Dana MR. Animal models of dry eye: a critical assessment of opportunities and limitations. Invest Ophthalmol Vis Sci. 2004;45:1641-6.

Barros A, Queiruga-Pineiro J, Lozano-Sanroma J, Alcalde I, Gallar J, Fernandez-Vega Cueto L, et al. Small fiber neuropathy in the cornea of Covid-19 patients associated with the generation of ocular surface disease. Ocul Surf. 2022;23:40-8.

Basso L, Aboushousha R, Fan CY, Iftinca M, Melo H, Flynn R, et al. TRPV1 promotes opioid analgesia during inflammation. Sci Signal. 2019;12.

Baudouin C. [A new approach for better comprehension of diseases of the ocular surface]. J Fr Ophtalmol. 2007;30:239-46.

Baudouin C, Aragona P, Messmer EM, Tomlinson A, Calonge M, Boboridis KG, et al. Role of hyperosmolarity in the pathogenesis and management of dry eye disease: proceedings of the OCEAN group meeting. Ocul Surf. 2013;11:246-58.

Baudouin C, Aragona P, Van Setten G, Rolando M, Irkec M, Benitez del Castillo J, et al. Diagnosing the severity of dry eye: a clear and practical algorithm. Br J Ophthalmol. 2014;98:1168-76.

Baudouin C, Haouat N, Brignole F, Bayle J, Gastaud P. Immunopathological findings in conjunctival cells using immunofluorescence staining of impression cytology specimens. Br J Ophthalmol. 1992;76:545-9.

Baudouin C, Labbe A, Liang H, Pauly A, Brignole-Baudouin F. Preservatives in eyedrops: the good, the bad and the ugly. Prog Retin Eye Res. 2010;29:312-34.

Baudouin C, Messmer EM, Aragona P, Geerling G, Akova YA, Benitez-del-Castillo J, et al. Revisiting the vicious circle of dry eye disease: a focus on the pathophysiology of meibomian gland dysfunction. Br J Ophthalmol. 2016;100:300-6.

Beck TC, Hapstack MA, Beck KR, Dix TA. Therapeutic Potential of Kappa Opioid Agonists. Pharmaceuticals (Basel). 2019;12.

Belkouch M, Dansereau MA, Reaux-Le Goazigo A, Van Steenwinckel J, Beaudet N, Chraibi A, et al. The chemokine CCL2 increases Nav1.8 sodium channel activity in primary sensory neurons through a Gbetagamma-dependent mechanism. J Neurosci. 2011;31:18381-90.

Belmonte C, GarciaHirschfeld J, Gallar J. Neurobiology of ocular pain. Progress in Retinal and Eye Research. 1997;16:117-56.

Belmonte C, Nichols JJ, Cox SM, Brock JA, Begley CG, Bereiter DA, et al. TFOS DEWS II pain and sensation report. Ocul Surf. 2017;15:404-37.

Benard A, Boue J, Chapey E, Jaume M, Gomes B, Dietrich G. Delta opioid receptors mediate chemotaxis in bone marrow-derived dendritic cells. J Neuroimmunol. 2008;197:21-8.

Berardelli A, Cruccu G, Manfredi M, Rothwell JC, Day BL, Marsden CD. The corneal reflex and the R2 component of the blink reflex. Neurology. 1985;35:797-801.

Berkley KJ. Sex differences in pain. Behav Brain Sci. 1997;20:371-80; discussion 435-513.

Bignami F, Rama P, Ferrari G. Substance P and its Inhibition in Ocular Inflammation. Curr Drug Targets. 2016;17:1265-74.

Borsook D, DaSilva AF, Ploghaus A, Becerra L. Specific and somatotopic functional magnetic resonance imaging activation in the trigeminal ganglion by brush and noxious heat. J Neurosci. 2003;23:7897-903.

Borsook D, Rosenthal P. Chronic (neuropathic) corneal pain and blepharospasm: five case reports. Pain. 2011;152:2427-31.

Brignole-Baudouin F, Riancho L, Ismail D, Deniaud M, Amrane M, Baudouin C. Correlation Between the Inflammatory Marker HLA-DR and Signs and Symptoms in Moderate to Severe Dry Eye Disease. Invest Ophthalmol Vis Sci. 2017;58:2438-48.

Brissette-Storkus CS, Reynolds SM, Lepisto AJ, Hendricks RL. Identification of a novel macrophage population in the normal mouse corneal stroma. Invest Ophthalmol Vis Sci. 2002;43:2264-71.

Bron AJ, de Paiva CS, Chauhan SK, Bonini S, Gabison EE, Jain S, et al. TFOS DEWS II pathophysiology report. Ocul Surf. 2017;15:438-510.

Butovich IA. Meibomian glands, meibum, and meibogenesis. Exp Eye Res. 2017;163:2-16.

Buzas B, Cox BM. Quantitative analysis of mu and delta opioid receptor gene expression in rat brain and peripheral ganglia using competitive polymerase chain reaction. Neuroscience. 1997;76:479-89.

Cavalcanti BM, Cruzat A, Sahin A, Pavan-Langston D, Samayoa E, Hamrah P. In vivo confocal microscopy detects bilateral changes of corneal immune cells and nerves in unilateral herpes zoster ophthalmicus. Ocul Surf. 2018;16:101-11.

Celik MO, Labuz D, Henning K, Busch-Dienstfertig M, Gaveriaux-Ruff C, Kieffer BL, et al. Leukocyte opioid receptors mediate analgesia via Ca(2+)-regulated release of opioid peptides. Brain Behav Immun. 2016;57:227-42.

Chang YA, Wu YY, Lin CT, Kawasumi M, Wu CH, Kao SY, et al. Animal models of dry eye: Their strengths and limitations for studying human dry eye disease. Journal of the Chinese Medical Association : JCMA. 2021;84:459-64.

Che T, Dwivedi-Agnihotri H, Shukla AK, Roth BL. Biased ligands at opioid receptors: Current status and future directions. Sci Signal. 2021;14.

Chen Y, Chauhan SK, Lee HS, Saban DR, Dana R. Chronic dry eye disease is principally mediated by effector memory Th17 cells. Mucosal Immunol. 2014;7:38-45.

Chen Y, Dana R. Pathophysiology of Dry Eye Disease Using Animal Models. In: Galor A, editor. Dry Eye Disease: Elsevier; 2023. p. 41-68.

Chen Y, Wang S, Alemi H, Dohlman T, Dana R. Immune regulation of the ocular surface. Exp Eye Res. 2022;218:109007.

Cher I. Ocular surface concepts: development and citation. Ocul Surf. 2014;12:10-3.

Chinnery HR, Zhang XY, Wu CY, Downie LE. Corneal immune cell morphometry as an indicator of local and systemic pathology: A review. Clin Exp Ophthalmol. 2021;49:729-40.

Cho J, Bell N, Botzet G, Vora P, Fowler BJ, Donahue R, et al. Latent Sensitization in a Mouse Model of Ocular Neuropathic Pain. Transl Vis Sci Technol. 2019;8:6.

Chu Sin Chung P, Kieffer BL. Delta opioid receptors in brain function and diseases. Pharmacol Ther. 2013;140:112-20.

Chung MK, Park J, Asgar J, Ro JY. Transcriptome analysis of trigeminal ganglia following masseter muscle inflammation in rats. Mol Pain. 2016;12.

Corder G, Castro DC, Bruchas MR, Scherrer G. Endogenous and Exogenous Opioids in Pain. In: Roska B, Zoghbi HY, editors. Annual Review of Neuroscience, Vol 412018a. p. 453-73.

Corder G, Castro DC, Bruchas MR, Scherrer G. Endogenous and Exogenous Opioids in Pain. Annu Rev Neurosci. 2018b;41:453-73.

Corder G, Tawfik VL, Wang D, Sypek EI, Low SA, Dickinson JR, et al. Loss of mu opioid receptor signaling in nociceptors, but not microglia, abrogates morphine tolerance without disrupting analgesia. Nat Med. 2017;23:164-73.

Craig JP, Nichols KK, Akpek EK, Caffery B, Dua HS, Joo CK, et al. TFOS DEWS II Definition and Classification Report. Ocul Surf. 2017;15:276-83.

Cravioto H, Battista A. Clinical and ultrastructural study of painful neuroma. Neurosurgery. 1981;8:181-90.

Cruzat A, Qazi Y, Hamrah P. In Vivo Confocal Microscopy of Corneal Nerves in Health and Disease. Ocul Surf. 2017;15:15-47.

DaSilva AF, Becerra L, Makris N, Strassman AM, Gonzalez RG, Geatrakis N, et al. Somatotopic activation in the human trigeminal pain pathway. J Neurosci. 2002;22:8183-92.

De Neve J, Barlow TMA, Tourwe D, Bihel F, Simonin F, Ballet S. Comprehensive overview of biased pharmacology at the opioid receptors: biased ligands and bias factors. RSC Med Chem. 2021;12:828-70.

DelMonte DW, Kim T. Anatomy and physiology of the cornea. J Cataract Refract Surg. 2011;37:588-98.

Deng S, Wang M, Zhang F, Sun X, Hou W, Guo N. Corneal subbasal nerve fiber regeneration in myopic patients after laser in situ keratomileusis. Neural Regen Res. 2012;7:1556-62.

Denk F, McMahon SB. Neurobiological basis for pain vulnerability: why me? Pain. 2017;158 Suppl 1:S108-S14.

Dermer H, Hwang J, Mittal R, Cohen AK, Galor A. Corneal sub-basal nerve plexus microneuromas in individuals with and without dry eye. Br J Ophthalmol. 2022;106:616-22.

Desai BK. Slit Lamp Examination. In: Ganti L, editor. Atlas of Emergency Medicine Procedures. New York, NY: Springer New York; 2016. p. 271-7.

Dieckmann G, Goyal S, Hamrah P. Neuropathic Corneal Pain: Approaches for Management. Ophthalmology. 2017;124:S34-S47.

Dieckmann G, Ozmen MC, Cox SM, Engert RC, Hamrah P. Low-dose naltrexone is effective and well-tolerated for modulating symptoms in patients with neuropathic corneal pain. Ocul Surf. 2021;20:33-8.

Dong ZY, Ying M, Zheng J, Hu LJ, Xie JY, Ma Y. Evaluation of a rat meibomian gland dysfunction model induced by closure of meibomian gland orifices. Int J Ophthalmol. 2018;11:1077-83.

Donica CL, Awwad HO, Thakker DR, Standifer KM. Cellular mechanisms of nociceptin/orphanin FQ (N/OFQ) peptide (NOP) receptor regulation and heterologous regulation by N/OFQ. Mol Pharmacol. 2013;83:907-18.

Doughty MJ, Naase T, Button NF. Frequent spontaneous eyeblink activity associated with reduced conjunctival surface (trigeminal nerve) tactile sensitivity. Graefes Arch Clin Exp Ophthalmol. 2009;247:939-46.

Downie LE, Bandlitz S, Bergmanson JPG, Craig JP, Dutta D, Maldonado-Codina C, et al. CLEAR - Anatomy and physiology of the anterior eye. Cont Lens Anterior Eye. 2021;44:132-56.

Drieu la Rochelle A, Guillemyn K, Dumitrascuta M, Martin C, Utard V, Quillet R, et al. A bifunctional-biased mu-opioid agonist-neuropeptide FF receptor antagonist as analgesic with improved acute and chronic side effects. Pain. 2018;159:1705-18.

Dua HS, Faraj LA, Said DG, Gray T, Lowe J. Human corneal anatomy redefined: a novel pre-Descemet's layer (Dua's layer). Ophthalmology. 2013;120:1778-85.

Dursun D, Wang M, Monroy D, Li DQ, Lokeshwar BL, Stern ME, et al. A mouse model of keratoconjunctivitis sicca. Invest Ophthalmol Vis Sci. 2002;43:632-8.

Eghrari AO, Riazuddin SA, Gottsch JD. Overview of the Cornea: Structure, Function, and Development. Prog Mol Biol Transl Sci. 2015;134:7-23.

Eisenstein TK. The Role of Opioid Receptors in Immune System Function. Front Immunol. 2019;10:2904.

Elevation vision. Dry Eye Treatment. Squarespace.

Endres-Becker J, Heppenstall PA, Mousa SA, Labuz D, Oksche A, Schafer M, et al. Mu-opioid receptor activation modulates transient receptor potential vanilloid 1 (TRPV1) currents in sensory neurons in a model of inflammatory pain. Mol Pharmacol. 2007;71:12-8.

Erbs E, Faget L, Scherrer G, Matifas A, Filliol D, Vonesch JL, et al. A mu-delta opioid receptor brain atlas reveals neuronal co-occurrence in subcortical networks. Brain Struct Funct. 2015;220:677-702.

Fakih D, Baudouin C, Reaux-Le Goazigo A, Melik Parsadaniantz S. TRPM8: A Therapeutic Target for Neuroinflammatory Symptoms Induced by Severe Dry Eye Disease. Int J Mol Sci. 2020;21.

Fakih D, Guerrero-Moreno A, Baudouin C, Reaux-Le Goazigo A, Parsadaniantz SM. Capsazepine decreases corneal pain syndrome in severe dry eye disease. J Neuroinflammation. 2021;18:111.

Fakih D, Zhao Z, Nicolle P, Reboussin E, Joubert F, Luzu J, et al. Chronic dry eye induced corneal hypersensitivity, neuroinflammatory responses, and synaptic plasticity in the mouse trigeminal brainstem. J Neuroinflammation. 2019;16:268.

Faktorovich EG, Basbaum AI. Effect of topical 0.5% morphine on postoperative pain after photorefractive keratectomy. J Refract Surg. 2010;26:934-41.

Farazifard R, Safarpour F, Sheibani V, Javan M. Eye-wiping test: a sensitive animal model for acute trigeminal pain studies. Brain Res Brain Res Protoc. 2005;16:44-9.

Fillingim RB. Individual differences in pain: understanding the mosaic that makes pain personal. Pain. 2017;158 Suppl 1:S11-S8.

Finnerup NB, Haroutounian S, Kamerman P, Baron R, Bennett DLH, Bouhassira D, et al. Neuropathic pain: an updated grading system for research and clinical practice. Pain. 2016;157:1599-606.

Foulsham W, Coco G, Amouzegar A, Chauhan SK, Dana R. When Clarity Is Crucial: Regulating Ocular Surface Immunity. Trends Immunol. 2018;39:288-301.

Frutos-Rincon L, Gomez-Sanchez JA, Inigo-Portugues A, Acosta MC, Gallar J. An Experimental Model of Neuro-Immune Interactions in the Eye: Corneal Sensory Nerves and Resident Dendritic Cells. Int J Mol Sci. 2022;23.

Galor A, Moein HR, Lee C, Rodriguez A, Felix ER, Sarantopoulos KD, et al. Neuropathic pain and dry eye. Ocul Surf. 2018;16:31-44.

Gao N, Lee P, Yu FS. Intraepithelial dendritic cells and sensory nerves are structurally associated and functional interdependent in the cornea. Sci Rep. 2016;6:36414.

Gao Y, Min K, Zhang Y, Su J, Greenwood M, Gronert K. Female-Specific Downregulation of Tissue Polymorphonuclear Neutrophils Drives Impaired Regulatory T Cell and Amplified Effector T Cell Responses in Autoimmune Dry Eye Disease. J Immunol. 2015;195:3086-99.

Gaveriaux-Ruff C, Kieffer BL. Delta opioid receptor analgesia: recent contributions from pharmacology and molecular approaches. Behav Pharmacol. 2011;22:405-14.

Giannaccare G, Buzzi M, Fresina M, Velati C, Versura P. Efficacy of 2-Month Treatment With Cord Blood Serum Eye Drops in Ocular Surface Disease: An In Vivo Confocal Microscopy Study. Cornea. 2017;36:915-21.

Giannaccare G, Pellegrini M, Sebastiani S, Moscardelli F, Versura P, Campos EC. In vivo confocal microscopy morphometric analysis of corneal subbasal nerve plexus in dry eye disease using newly developed fully automated system. Graefes Arch Clin Exp Ophthalmol. 2019;257:583-9.

Gomes I, Fujita W, Gupta A, Saldanha SA, Negri A, Pinello CE, et al. Identification of a mu-delta opioid receptor heteromer-biased agonist with antinociceptive activity. Proc Natl Acad Sci U S A. 2013;110:12072-7.

Gossman MV. Systematic Evaluation of the Mouse Eye: Anatomy, Pathology, and Biomethods. Journal of Neuro-Ophthalmology. 2004;24:84-5.

Grace PM, Hutchinson MR, Maier SF, Watkins LR. Pathological pain and the neuroimmune interface. Nat Rev Immunol. 2014;14:217-31.

Guerrero-Moreno A, Baudouin C, Melik Parsadaniantz S, Reaux-Le Goazigo A. Morphological and Functional Changes of Corneal Nerves and Their Contribution to Peripheral and Central Sensory Abnormalities. Front Cell Neurosci. 2020;14:610342.

Guerrero-Moreno A, Fakih D, Parsadaniantz SM, Reaux-Le Goazigo A. How does chronic dry eye shape peripheral and central nociceptive systems? Neural Regen Res. 2021a;16:306-7.

Guerrero-Moreno A, Liang H, Moreau N, Luzu J, Rabut G, Melik Parsadaniantz S, et al. Corneal Nerve Abnormalities in Painful Dry Eye Disease Patients. Biomedicines. 2021b;9.

Guthoff RF, Baudouin C, Stave J. Atlas of Confocal Laser Scanning In-vivo Microscopy in Ophthalmology. 2006.

Guzman M, Keitelman I, Sabbione F, Trevani AS, Giordano MN, Galletti JG. Mucosal tolerance disruption favors disease progression in an extraorbital lacrimal gland excision model of murine dry eye. Exp Eye Res. 2016;151:19-22.

Hamrah P, Zhang Q, Liu Y, Dana MR. Novel characterization of MHC class II-negative population of resident corneal Langerhans cell-type dendritic cells. Invest Ophthalmol Vis Sci. 2002;43:639-46.

Hassan AH, Ableitner A, Stein C, Herz A. Inflammation of the rat paw enhances axonal transport of opioid receptors in the sciatic nerve and increases their density in the inflamed tissue. Neuroscience. 1993;55:185-95.

Hattori T, Takahashi H, Dana R. Novel Insights Into the Immunoregulatory Function and Localization of Dendritic Cells. Cornea. 2016;35 Suppl 1:S49-S54.

He SQ, Zhang ZN, Guan JS, Liu HR, Zhao B, Wang HB, et al. Facilitation of mu-opioid receptor activity by preventing delta-opioid receptor-mediated codegradation. Neuron. 2011;69:120-31.

Henriksson JT, McDermott AM, Bergmanson JP. Dimensions and morphology of the cornea in three strains of mice. Invest Ophthalmol Vis Sci. 2009;50:3648-54.

Henriquez VM, Evinger C. Modification of cornea-evoked reflex blinks in rats. Exp Brain Res. 2005;163:445-56.

Henriquez VM, Evinger C. The three-neuron corneal reflex circuit and modulation of second-order corneal responsive neurons. Exp Brain Res. 2007;179:691-702.

Hiraga SI, Itokazu T, Nishibe M, Yamashita T. Neuroplasticity related to chronic pain and its modulation by microglia. Inflamm Regen. 2022;42:15.

Hirata H, Meng ID. Cold-sensitive corneal afferents respond to a variety of ocular stimuli central to tear production: implications for dry eye disease. Invest Ophthalmol Vis Sci. 2010;51:3969-76.

Hirata H, Oshinsky ML. Ocular dryness excites two classes of corneal afferent neurons implicated in basal tearing in rats: involvement of transient receptor potential channels. J Neurophysiol. 2012;107:1199-209.

Hirschberg J. Hirschberg history of ophthalmology : [11 Vol.]. 1 1. Bonn: Wayenborgh; 1982.

Holdridge SV, Cahill CM. Spinal administration of a delta opioid receptor agonist attenuates hyperalgesia and allodynia in a rat model of neuropathic pain. Eur J Pain. 2007;11:685-93.

Hommes FA. Mechanism of the Crabtree effect in yeast grown with different glucose concentrations. Arch Biochem Biophys. 1966;113:324-30.

Hou M, Uddman R, Tajti J, Edvinsson L. Nociceptin immunoreactivity and receptor mRNA in the human trigeminal ganglion. Brain Res. 2003;964:179-86.

Hu Y, Matsumoto Y, Adan ES, Dogru M, Fukagawa K, Tsubota K, et al. Corneal in vivo confocal scanning laser microscopy in patients with atopic keratoconjunctivitis. Ophthalmology. 2008;115:2004-12.

Inyang KE, George SR, Laumet G. The micro-delta opioid heteromer masks latent pain sensitization in neuropathic and inflammatory pain in male and female mice. Brain Res. 2021;1756:147298.

Ji RR, Berta T, Nedergaard M. Glia and pain: is chronic pain a gliopathy? Pain. 2013;154 Suppl 1:S10-S28.

Ji RR, Chamessian A, Zhang YQ. Pain regulation by non-neuronal cells and inflammation. Science. 2016;354:572-7.

John T, Tighe S, Sheha H, Hamrah P, Salem ZM, Cheng AMS, et al. Corneal Nerve Regeneration after Self-Retained Cryopreserved Amniotic Membrane in Dry Eye Disease. J Ophthalmol. 2017;2017:6404918.

Jones L, Downie LE, Korb D, Benitez-Del-Castillo JM, Dana R, Deng SX, et al. TFOS DEWS II Management and Therapy Report. Ocul Surf. 2017;15:575-628.

Joubert F, Acosta MDC, Gallar J, Fakih D, Sahel JA, Baudouin C, et al. Effects of corneal injury on ciliary nerve fibre activity and corneal nociception in mice: A behavioural and electrophysiological study. Eur J Pain. 2019;23:589-602.

Joubert F, Guerrero-Moreno A, Fakih D, Reboussin E, Gaveriaux-Ruff C, Acosta MC, et al. Topical treatment with a mu opioid receptor agonist alleviates corneal allodynia and corneal nerve sensitization in mice. Biomed Pharmacother. 2020;132:110794.

Keith DE, Murray SR, Zaki PA, Chu PC, Lissin DV, Kang L, et al. Morphine activates opioid receptors without causing their rapid internalization. J Biol Chem. 1996;271:19021-4.

Khoutorsky A, Price TJ. Translational Control Mechanisms in Persistent Pain. Trends Neurosci. 2018;41:100-14.

Kim YH, Jung JC, Jung SY, Yu S, Lee KW, Park YJ. Comparison of the Efficacy of Fluorometholone With and Without Benzalkonium Chloride in Ocular Surface Disease. Cornea. 2016;35:234-42.

Kimura N, Watanabe A, Suzuki K, Toyoda H, Hakamata N, Fukuoka H, et al. Measurement of spontaneous blinks in patients with Parkinson's disease using a new high-speed blink analysis system. J Neurol Sci. 2017;380:200-4.

Klimek L, Bergmann KC, Biedermann T, Bousquet J, Hellings P, Jung K, et al. Visual analogue scales (VAS): Measuring instruments for the documentation of symptoms and therapy monitoring in cases of allergic rhinitis in everyday health care: Position Paper of the German Society of Allergology (AeDA) and the German Society of Allergy and Clinical Immunology (DGAKI), ENT Section, in collaboration with the working group on Clinical Immunology, Allergology and Environmental Medicine of the German Society of Otorhinolaryngology, Head and Neck Surgery (DGHNOKHC). Allergo J Int. 2017;26:16-24.

Knop E, Knop N, Millar T, Obata H, Sullivan DA. The international workshop on meibomian gland dysfunction: report of the subcommittee on anatomy, physiology, and pathophysiology of the meibomian gland. Invest Ophthalmol Vis Sci. 2011;52:1938-78.

Kobayashi K, Endoh F, Ohmori I, Akiyama T. Action of antiepileptic drugs on neurons. Brain Dev. 2020;42:2-5.

Korczeniewska OA, Husain S, Khan J, Eliav E, Soteropoulos P, Benoliel R. Differential gene expression in trigeminal ganglia of male and female rats following chronic constriction of the infraorbital nerve. Eur J Pain. 2018;22:875-88.

Koschmieder A, Stachs O, Kragl B, Stahnke T, Sterenczak KA, Henze L, et al. Non-invasive detection of corneal sub-basal nerve plexus changes in multiple myeloma patients by confocal laser scanning microscopy. Biosci Rep. 2020;40.

Kremer M, Megat S, Bohren Y, Wurtz X, Nexon L, Ceredig RA, et al. Delta opioid receptors are essential to the antiallodynic action of Beta2-mimetics in a model of neuropathic pain. Mol Pain. 2020;16:1744806920912931.

Kulkarni-Narla A, Walcheck B, Brown DR. Opioid receptors on bone marrow neutrophils modulate chemotaxis and CD11b/CD18 expression. Eur J Pharmacol. 2001;414:289-94.

Kuzawinska O, Lis K, Cudna A, Balkowiec-Iskra E. Gender differences in the neurochemical response of trigeminal ganglion neurons to peripheral inflammation in mice. Acta Neurobiol Exp (Wars). 2014;74:227-32.

Labbe A, Alalwani H, Van Went C, Brasnu E, Georgescu D, Baudouin C. The relationship between subbasal nerve morphology and corneal sensation in ocular surface disease. Invest Ophthalmol Vis Sci. 2012;53:4926-31.

Labbe A, Liang Q, Wang Z, Zhang Y, Xu L, Baudouin C, et al. Corneal nerve structure and function in patients with non-sjogren dry eye: clinical correlations. Invest Ophthalmol Vis Sci. 2013;54:5144-50.

Labetoulle M, Rolando M, Baudouin C, van Setten G. Patients' perception of DED and its relation with time to diagnosis and quality of life: an international and multilingual survey. Br J Ophthalmol. 2017;101:1100-5.

Lagali N, Germundsson J, Fagerholm P. The role of Bowman's layer in corneal regeneration after phototherapeutic keratectomy: a prospective study using in vivo confocal microscopy. Invest Ophthalmol Vis Sci. 2009;50:4192-8.

Langford DJ, Bailey AL, Chanda ML, Clarke SE, Drummond TE, Echols S, et al. Coding of facial expressions of pain in the laboratory mouse. Nat Methods. 2010;7:447-9.

Launay PS, Godefroy D, Khabou H, Rostene W, Sahel JA, Baudouin C, et al. Combined 3DISCO clearing method, retrograde tracer and ultramicroscopy to map corneal neurons in a whole adult mouse trigeminal ganglion. Exp Eye Res. 2015;139:136-43.

Launay PS, Reboussin E, Liang H, Kessal K, Godefroy D, Rostene W, et al. Ocular inflammation induces trigeminal pain, peripheral and central neuroinflammatory mechanisms. Neurobiol Dis. 2016;88:16-28.

Lee EJ, Calcaterra TC, Zuckerbraun L. Traumatic neuromas of the head and neck. Ear Nose Throat J. 1998;77:670-4, 6.

Lemp MA. Report of the National Eye Institute/Industry workshop on Clinical Trials in Dry Eyes. CLAO J. 1995;21:221-32.

Levy O, Labbe A, Borderie V, Hamiche T, Dupas B, Laroche L, et al. Increased corneal sub-basal nerve density in patients with Sjogren syndrome treated with topical cyclosporine A. Clin Exp Ophthalmol. 2017;45:455-63.

Lewanowitsch T, Irvine RJ. Naloxone methiodide reverses opioid-induced respiratory depression and analgesia without withdrawal. Eur J Pharmacol. 2002;445:61-7.

Liang H, Brignole-Baudouin F, Labbe A, Pauly A, Warnet JM, Baudouin C. LPS-stimulated inflammation and apoptosis in corneal injury models. Mol Vis. 2007;13:1169-80.

Liang H, Kessal K, Rabut G, Daull P, Garrigue JS, Melik Parsadaniantz S, et al. Correlation of clinical symptoms and signs with conjunctival gene expression in primary Sjogren syndrome dry eye patients. Ocul Surf. 2019;17:516-25.

Lin HC, Yen CT. Differential Expression of Phosphorylated ERK and c-Fos of Limbic Cortices Activities in Response to Tactile Allodynia of Neuropathic Rats. Chin J Physiol. 2018;61:240-51.

Lin Z, Liu X, Zhou T, Wang Y, Bai L, He H, et al. A mouse dry eye model induced by topical administration of benzalkonium chloride. Mol Vis. 2011;17:257-64.

Lin Z, Zhou Y, Wang Y, Zhou T, Li J, Luo P, et al. Serine protease inhibitor A3K suppressed the formation of ocular surface squamous metaplasia in a mouse model of experimental dry eye. Invest Ophthalmol Vis Sci. 2014;55:5813-20.

Liu J, Li Z. Resident Innate Immune Cells in the Cornea. Front Immunol. 2021;12:620284.

Loeser JD, Melzack R. Pain: an overview. Lancet. 1999;353:1607-9.

Lopes DM, Denk F, McMahon SB. The Molecular Fingerprint of Dorsal Root and Trigeminal Ganglion Neurons. Front Mol Neurosci. 2017;10:304.

Lopez-Ramos JC, Delgado-Garcia JM. Role of the motor cortex in the generation of classically conditioned eyelid and vibrissae responses. Sci Rep. 2021;11:16701.

Machelska H, Celik MO. Advances in Achieving Opioid Analgesia Without Side Effects. Front Pharmacol. 2018;9:1388.

Machelska H, Celik MO. Opioid Receptors in Immune and Glial Cells-Implications for Pain Control. Front Immunol. 2020;11:300.

MacIver MB, Tanelian DL. Free nerve ending terminal morphology is fiber type specific for A delta and C fibers innervating rabbit corneal epithelium. J Neurophysiol. 1993;69:1779-83.

Maduna T, Audouard E, Dembele D, Mouzaoui N, Reiss D, Massotte D, et al. Microglia Express Mu Opioid Receptor: Insights From Transcriptomics and Fluorescent Reporter Mice. Front Psychiatry. 2018;9:726.

Mapplebeck JCS, Dalgarno R, Tu Y, Moriarty O, Beggs S, Kwok CHT, et al. Microglial P2X4R-evoked pain hypersensitivity is sexually dimorphic in rats. Pain. 2018;159:1752-63.

Marfurt CF, Cox J, Deek S, Dvorscak L. Anatomy of the human corneal innervation. Exp Eye Res. 2010;90:478-92.

Marfurt CF, Del Toro DR. Corneal sensory pathway in the rat: a horseradish peroxidase tracing study. J Comp Neurol. 1987;261:450-9.

Masli S, Dartt DA. Mouse Models of Sjogren's Syndrome with Ocular Surface Disease. Int J Mol Sci. 2020;21.

Masterton S, Ahearne M. Mechanobiology of the corneal epithelium. Exp Eye Res. 2018;177:122-9.

Matsumiya LC, Sorge RE, Sotocinal SG, Tabaka JM, Wieskopf JS, Zaloum A, et al. Using the Mouse Grimace Scale to reevaluate the efficacy of postoperative analgesics in laboratory mice. J Am Assoc Lab Anim Sci. 2012;51:42-9.

Matynia A, Parikh S, Deot N, Wong A, Kim P, Nusinowitz S, et al. Light aversion and corneal mechanical sensitivity are altered by intrinscally photosensitive retinal ganglion cells in a mouse model of corneal surface damage. Exp Eye Res. 2015;137:57-62.

May A. Morphology of the long and short uveal nerves in the human eye. J Anat. 2004;205:113-20.

McKay TB, Seyed-Razavi Y, Ghezzi CE, Dieckmann G, Nieland TJF, Cairns DM, et al. Corneal pain and experimental model development. Prog Retin Eye Res. 2019;71:88-113.

McMahon S. Wall & Melzack's Textbook of Pain. 2013.

McMonnies CW. The potential role of neuropathic mechanisms in dry eye syndromes. J Optom. 2017;10:5-13.

Mecklenburg J, Zou Y, Wangzhou A, Garcia D, Lai Z, Tumanov AV, et al. Transcriptomic sex differences in sensory neuronal populations of mice. Sci Rep. 2020;10:15278.

Mecum NE, Cyr D, Malon J, Demers D, Cao L, Meng ID. Evaluation of Corneal Damage After Lacrimal Gland Excision in Male and Female Mice. Invest Ophthalmol Vis Sci. 2019;60:3264-74.

Mecum NE, Demers D, Sullivan CE, Denis TE, Kalliel JR, Meng ID. Lacrimal gland excision in male and female mice causes ocular pain and anxiety-like behaviors. Sci Rep. 2020;10:17225.

Megat S, Ray PR, Tavares-Ferreira D, Moy JK, Sankaranarayanan I, Wanghzou A, et al. Differences between Dorsal Root and Trigeminal Ganglion Nociceptors in Mice Revealed by Translational Profiling. J Neurosci. 2019;39:6829-47.

Melik Parsadaniantz S, Rivat C, Rostene W, Reaux-Le Goazigo A. Opioid and chemokine receptor crosstalk: a promising target for pain therapy? Nat Rev Neurosci. 2015;16:69-78.

Meng ID, Bereiter DA. Differential distribution of Fos-like immunoreactivity in the spinal trigeminal nucleus after noxious and innocuous thermal and chemical stimulation of rat cornea. Neuroscience. 1996;72:243-54.

Messmer EM, Benitez-del-Castillo J, Baudouin C. Chapter 13 - Treatment of Dry Eye Disease in Europe. In: Galor A, editor. Dry Eye Disease: Elsevier; 2023. p. 203-11.

Moein HR, Akhlaq A, Dieckmann G, Abbouda A, Pondelis N, Salem Z, et al. Visualization of microneuromas by using in vivo confocal microscopy: An objective biomarker for the diagnosis of neuropathic corneal pain? Ocul Surf. 2020;18:651-6.

Mogil JS. Sex differences in pain and pain inhibition: multiple explanations of a controversial phenomenon. Nat Rev Neurosci. 2012;13:859-66.

Montes-Mico R. Role of the tear film in the optical quality of the human eye. J Cataract Refract Surg. 2007;33:1631-5.

Morkin MI, Hamrah P. Efficacy of self-retained cryopreserved amniotic membrane for treatment of neuropathic corneal pain. Ocul Surf. 2018;16:132-8.

Moulton EA, Becerra L, Rosenthal P, Borsook D. An approach to localizing corneal pain representation in human primary somatosensory cortex. PLoS One. 2012;7:e44643.

Muhafiz E, Demir MS. Ability of non-invasive tear break-up time to determine tear instability in contact lens wearers. Int Ophthalmol. 2022;42:959-68.

Muller LJ, Marfurt CF, Kruse F, Tervo TM. Corneal nerves: structure, contents and function. Exp Eye Res. 2003;76:521-42.

Nelson JD, Shimazaki J, Benitez-del-Castillo JM, Craig JP, McCulley JP, Den S, et al. The international workshop on meibomian gland dysfunction: report of the definition and classification subcommittee. Invest Ophthalmol Vis Sci. 2011;52:1930-7.

Nichols KK, Redfern RL, Jacob JT, Nelson JD, Fonn D, Forstot SL, et al. The TFOS International Workshop on Contact Lens Discomfort: report of the definition and classification subcommittee. Invest Ophthalmol Vis Sci. 2013;54:TFOS14-9.

Nicolle P, Liang H, Reboussin E, Rabut G, Warcoin E, Brignole-Baudouin F, et al. Proinflammatory Markers, Chemokines, and Enkephalin in Patients Suffering from Dry Eye Disease. Int J Mol Sci. 2018;19.

Niederer RL, Perumal D, Sherwin T, McGhee CN. Laser scanning in vivo confocal microscopy reveals reduced innervation and reduction in cell density in all layers of the keratoconic cornea. Invest Ophthalmol Vis Sci. 2008;49:2964-70.

Niu K, Saloman JL, Zhang Y, Ro JY. Sex differences in the contribution of ATP-sensitive K+ channels in trigeminal ganglia under an acute muscle pain condition. Neuroscience. 2011;180:344-52.

Obara I, Przewlocki R, Przewlocka B. Local peripheral effects of mu-opioid receptor agonists in neuropathic pain in rats. Neurosci Lett. 2004;360:85-9.

Obata H. Anatomy and histopathology of human meibomian gland. Cornea. 2002;21:S70-4.

Obata H. Anatomy and histopathology of the human lacrimal gland. Cornea. 2006;25:S82-9.

Ogawa Y, Kim SK, Dana R, Clayton J, Jain S, Rosenblatt MI, et al. International Chronic Ocular Graft-vs-Host-Disease (GVHD) Consensus Group: proposed diagnostic criteria for chronic GVHD (Part I). Sci Rep. 2013;3:3419.

Oliveira-Soto L, Efron N. Morphology of corneal nerves using confocal microscopy. Cornea. 2001;20:374-84.

Ongun N, Ongun GT. Is gabapentin effective in dry eye disease and neuropathic ocular pain? Acta Neurol Belg. 2021;121:397-401.

Ophthalmology AAo. Ocular Neuropathic Pain. 2022.

OptometryWeb. CORNEA 550 Corneal Surface Analyzer from Essilor Instruments USA. 2020.

Ozawa A, Brunori G, Mercatelli D, Wu J, Cippitelli A, Zou B, et al. Knock-In Mice with NOP-eGFP Receptors Identify Receptor Cellular and Regional Localization. J Neurosci. 2015;35:11682-93.

Ozmen MC, Dieckmann G, Cox SM, Rashad R, Paracha R, Sanayei N, et al. Efficacy and tolerability of nortriptyline in the management of neuropathic corneal pain. Ocul Surf. 2020;18:814-20.

Pakravan M, Roshani M, Yazdani S, Faramazi A, Yaseri M. Pregabalin and gabapentin for post-photorefractive keratectomy pain: a randomized controlled trial. Eur J Ophthalmol. 2012;22 Suppl 7:S106-13.

Parissi M, Randjelovic S, Poletti E, Guimaraes P, Ruggeri A, Fragkiskou S, et al. Corneal Nerve Regeneration After Collagen Cross-Linking Treatment of Keratoconus: A 5-Year Longitudinal Study. JAMA Ophthalmol. 2016;134:70-8.

Parra A, Madrid R, Echevarria D, del Olmo S, Morenilla-Palao C, Acosta MC, et al. Ocular surface wetness is regulated by TRPM8-dependent cold thermoreceptors of the cornea. Nat Med. 2010;16:1396-9.

Patel DV, McGhee CN. Mapping of the normal human corneal sub-Basal nerve plexus by in vivo laser scanning confocal microscopy. Invest Ophthalmol Vis Sci. 2005;46:4485-8.

Patel DV, McGhee CN. Mapping the corneal sub-basal nerve plexus in keratoconus by in vivo laser scanning confocal microscopy. Invest Ophthalmol Vis Sci. 2006;47:1348-51.

Pauly A, Brignole-Baudouin F, Labbe A, Liang H, Warnet JM, Baudouin C. New tools for the evaluation of toxic ocular surface changes in the rat. Invest Ophthalmol Vis Sci. 2007;48:5473-83.

Payne AP. The harderian gland: a tercentennial review. J Anat. 1994;185 ( Pt 1):1-49.

Pellegrini JJ, Horn AK, Evinger C. The trigeminally evoked blink reflex. I. Neuronal circuits. Exp Brain Res. 1995;107:166-80.

Perrine SA, Hoshaw BA, Unterwald EM. Delta opioid receptor ligands modulate anxiety-like behaviors in the rat. Br J Pharmacol. 2006;147:864-72.

Peyman GA, Rahimy MH, Fernandes ML. Effects of morphine on corneal sensitivity and epithelial wound healing: implications for topical ophthalmic analgesia. Br J Ophthalmol. 1994;78:138-41.

Pflugfelder SC, Gumus K, Feuerman J, Alex A. Tear Volume-based Diagnostic Classification for Tear Dysfunction. Int Ophthalmol Clin. 2017;57:1-12.

Poppler LH, Parikh RP, Bichanich MJ, Rebehn K, Bettlach CR, Mackinnon SE, et al. Surgical interventions for the treatment of painful neuroma: a comparative meta-analysis. Pain. 2018;159:214-23.

Portal C, Gouyer V, Gottrand F, Desseyn JL. Preclinical mouse model to monitor live Muc5b-producing conjunctival goblet cell density under pharmacological treatments. PLoS One. 2017;12:e0174764.

Preibisch S, Saalfeld S, Tomancak P. Globally optimal stitching of tiled 3D microscopic image acquisitions. Bioinformatics. 2009;25:1463-5.

Qazi Y, Hurwitz S, Khan S, Jurkunas UV, Dana R, Hamrah P. Validity and Reliability of a Novel Ocular Pain Assessment Survey (OPAS) in Quantifying and Monitoring Corneal and Ocular Surface Pain. Ophthalmology. 2016;123:1458-68.

Qu M, Qi X, Wang Q, Wan L, Li J, Li W, et al. Therapeutic Effects of STAT3 Inhibition on Experimental Murine Dry Eye. Invest Ophthalmol Vis Sci. 2019;60:3776-85.

Quallo T, Vastani N, Horridge E, Gentry C, Parra A, Moss S, et al. TRPM8 is a neuronal osmosensor that regulates eye blinking in mice. Nat Commun. 2015;6:7150.

Rahim-Williams B, Riley JL, 3rd, Williams AK, Fillingim RB. A quantitative review of ethnic group differences in experimental pain response: do biology, psychology, and culture matter? Pain Med. 2012;13:522-40.

Rahman MM, Kim DH, Park CK, Kim YH. Experimental Models, Induction Protocols, and Measured Parameters in Dry Eye Disease: Focusing on Practical Implications for Experimental Research. Int J Mol Sci. 2021;22.

Raja SN, Carr DB, Cohen M, Finnerup NB, Flor H, Gibson S, et al. The revised International Association for the Study of Pain definition of pain: concepts, challenges, and compromises. Pain. 2020;161:1976-82.

Ramón y Cajal S. Histologie du système nerveux de l'homme et des vertébrés. Paris: Maloine; 1909.

Rao K, Leveque C, Pflugfelder SC. Corneal nerve regeneration in neurotrophic keratopathy following autologous plasma therapy. Br J Ophthalmol. 2010;94:584-91.

Reaux-Le Goazigo A, Alvear-Perez R, Zizzari P, Epelbaum J, Bluet-Pajot MT, Llorens-Cortes C. Cellular localization of apelin and its receptor in the anterior pituitary: evidence for a direct stimulatory action of apelin on ACTH release. Am J Physiol Endocrinol Metab. 2007;292:E7-15.

Reaux-Le Goazigo A, Poras H, Ben-Dhaou C, Ouimet T, Baudouin C, Wurm M, et al. Dual enkephalinase inhibitor PL265: a novel topical treatment to alleviate corneal pain and inflammation. Pain. 2019;160:307-21.

Rios C, Gomes I, Devi LA. mu opioid and CB1 cannabinoid receptor interactions: reciprocal inhibition of receptor signaling and neuritogenesis. Br J Pharmacol. 2006;148:387-95.

Robbins A, Kurose M, Winterson BJ, Meng ID. Menthol activation of corneal cool cells induces TRPM8-mediated lacrimation but not nociceptive responses in rodents. Invest Ophthalmol Vis Sci. 2012;53:7034-42.

Roeckel LA, Le Coz GM, Gaveriaux-Ruff C, Simonin F. Opioid-induced hyperalgesia: Cellular and molecular mechanisms. Neuroscience. 2016;338:160-82.

Rosenthal P, Baran I, Jacobs DS. Corneal pain without stain: is it real? Ocul Surf. 2009;7:28-40.

Rosenthal P, Borsook D. Ocular neuropathic pain. Br J Ophthalmol. 2016;100:128-34.

Ross AR, Al-Aqaba MA, Almaazmi A, Messina M, Nubile M, Mastropasqua L, et al. Clinical and in vivo confocal microscopic features of neuropathic corneal pain. Br J Ophthalmol. 2020;104:768-75.

Rozsa AJ, Guss RB, Beuerman RW. Neural remodeling following experimental surgery of the rabbit cornea. Invest Ophthalmol Vis Sci. 1983;24:1033-51.

Rubin MSJENFH. Netter's concise neuroanatomy. Philadelphia, Pa: Saunders Elsevier; 2007.

Saldanha IJ, Petris R, Han G, Dickersin K, Akpek EK. Research Questions and Outcomes Prioritized by Patients With Dry Eye. JAMA Ophthalmol. 2018;136:1170-9.

Satoh Y, Gesase AP, Habara Y, Ono K, Kanno T. Lipid secretory mechanisms in the mammalian harderian gland. Microsc Res Tech. 1996;34:104-10.

Schafer MK, Bette M, Romeo H, Schwaeble W, Weihe E. Localization of kappa-opioid receptor mRNA in neuronal subpopulations of rat sensory ganglia and spinal cord. Neurosci Lett. 1994;167:137-40.

Schechter JE, Warren DW, Mircheff AK. A lacrimal gland is a lacrimal gland, but rodent's and rabbit's are not human. Ocul Surf. 2010;8:111-34.

Schiffman RM, Christianson MD, Jacobsen G, Hirsch JD, Reis BL. Reliability and validity of the Ocular Surface Disease Index. Arch Ophthalmol. 2000;118:615-21.

Setu MAK, Horstmann J, Schmidt S, Stern ME, Steven P. Deep learning-based automatic meibomian gland segmentation and morphology assessment in infrared meibography. Sci Rep. 2021;11:7649.

Setu MAK, Schmidt S, Musial G, Stern ME, Steven P. Segmentation and Evaluation of Corneal Nerves and Dendritic Cells From In Vivo Confocal Microscopy Images Using Deep Learning. Transl Vis Sci Technol. 2022;11:24.

Sezgin M, Sankur B. Survey over image thresholding techniques and quantitative performance evaluation. Journal of Electronic Imaging. 2004;13:146-68.

Shaheen BS, Bakir M, Jain S. Corneal nerves in health and disease. Surv Ophthalmol. 2014;59:263-85.

Shen F, Dong X, Zhou X, Yan L, Wan Q. Corneal subbasal nerve plexus changes in patients with episodic migraine: an in vivo confocal microscopy study. J Pain Res. 2019;12:1489-95.

Shinomiya K, Ueta M, Kinoshita S. A new dry eye mouse model produced by exorbital and intraorbital lacrimal gland excision. Sci Rep. 2018;8:1483.

Simsek C, Kojima T, Nagata T, Dogru M, Tsubota K. Changes in Murine Subbasal Corneal Nerves After Scopolamine-Induced Dry Eye Stress Exposure. Invest Ophthalmol Vis Sci. 2019;60:615-23.

Sist TC, Jr., Greene GW. Traumatic neuroma of the oral cavity. Report of thirty-one new cases and review of the literature. Oral Surg Oral Med Oral Pathol. 1981;51:394-402.

Situ P, Simpson TL. Interaction of corneal nociceptive stimulation and lacrimal secretion. Invest Ophthalmol Vis Sci. 2010;51:5640-5.

Small LR, Galor A, Felix ER, Horn DB, Levitt RC, Sarantopoulos CD. Oral Gabapentinoids and Nerve Blocks for the Treatment of Chronic Ocular Pain. Eye Contact Lens. 2020;46:174-81.

Sorge RE, LaCroix-Fralish ML, Tuttle AH, Sotocinal SG, Austin JS, Ritchie J, et al. Spinal cord Toll-like receptor 4 mediates inflammatory and neuropathic hypersensitivity in male but not female mice. J Neurosci. 2011;31:15450-4.

Sridhar MS. Anatomy of cornea and ocular surface. Indian J Ophthalmol. 2018;66:190-4.

Stapleton F, Alves M, Bunya VY, Jalbert I, Lekhanont K, Malet F, et al. TFOS DEWS II Epidemiology Report. Ocul Surf. 2017;15:334-65.

Stapleton F, Marfurt C, Golebiowski B, Rosenblatt M, Bereiter D, Begley C, et al. The TFOS International Workshop on Contact Lens Discomfort: report of the subcommittee on neurobiology. Invest Ophthalmol Vis Sci. 2013;54:TFOS71-97.

Stein C. Opioids, sensory systems and chronic pain. Eur J Pharmacol. 2013;716:179-87.

Stein C. Opioid Receptors. Annu Rev Med. 2016;67:433-51.

Stein C. New concepts in opioid analgesia. Expert Opin Investig Drugs. 2018a;27:765-75.

Stein C, Lang LJ. Peripheral mechanisms of opioid analgesia. Curr Opin Pharmacol. 2009;9:3-8.

Stein G-R. The Oxford handbook of the neurobiology of pain: Opioids and Pain2018b.

Stepp MA, Pal-Ghosh S, Downie LE, Zhang AC, Chinnery HR, Machet J, et al. Corneal Epithelial "Neuromas": A Case of Mistaken Identity? Cornea. 2020;39:930-4.

Stepp MA, Pal-Ghosh S, Tadvalkar G, Williams A, Pflugfelder SC, de Paiva CS. Reduced intraepithelial corneal nerve density and sensitivity accompany desiccating stress and aging in C57BL/6 mice. Exp Eye Res. 2018;169:91-8.

Stern ME, Beuerman RW, Fox RI, Gao J, Mircheff AK, Pflugfelder SC. The pathology of dry eye: the interaction between the ocular surface and lacrimal glands. Cornea. 1998;17:584-9.

Stern ME, Schaumburg CS, Dana R, Calonge M, Niederkorn JY, Pflugfelder SC. Autoimmunity at the ocular surface: pathogenesis and regulation. Mucosal Immunol. 2010;3:425-42.

Stevenson W, Chen Y, Lee SM, Lee HS, Hua J, Dohlman T, et al. Extraorbital lacrimal gland excision: a reproducible model of severe aqueous tear-deficient dry eye disease. Cornea. 2014;33:1336-41.

Stiles J, Honda CN, Krohne SG, Kazacos EA. Effect of topical administration of 1% morphine sulfate solution on signs of pain and corneal wound healing in dogs. Am J Vet Res. 2003;64:813-8.

Sullivan DA, Rocha EM, Aragona P, Clayton JA, Ding J, Golebiowski B, et al. TFOS DEWS II Sex, Gender, and Hormones Report. Ocul Surf. 2017;15:284-333.

Sun M, Moreno IY, Dang M, Coulson-Thomas VJ. Meibomian Gland Dysfunction: What Have Animal Models Taught Us? Int J Mol Sci. 2020;21.

Tal M, Devor M. Ectopic discharge in injured nerves: comparison of trigeminal and somatic afferents. Brain Res. 1992;579:148-51.

Tanelian DL. Cholinergic activation of a population of corneal afferent nerves. Exp Brain Res. 1991;86:414-20.

Tavares-Ferreira D, Ray PR, Sankaranarayanan I, Mejia GL, Wangzhou A, Shiers S, et al. Sex Differences in Nociceptor Translatomes Contribute to Divergent Prostaglandin Signaling in Male and Female Mice. Biol Psychiatry. 2022;91:129-40.

Taves S, Berta T, Liu DL, Gan S, Chen G, Kim YH, et al. Spinal inhibition of p38 MAP kinase reduces inflammatory and neuropathic pain in male but not female mice: Sex-dependent microglial signaling in the spinal cord. Brain Behav Immun. 2016;55:70-81.

Tei Y, Mikami Y, Ito M, Tomida T, Ohshima D, Hori Y, et al. Pathogenic Mechanism of Dry Eye-Induced Chronic Ocular Pain and a Mechanism-Based Therapeutic Approach. Invest Ophthalmol Vis Sci. 2022;63:7.

Theophanous C, Jacobs DS, Hamrah P. Corneal Neuralgia after LASIK. Optom Vis Sci. 2015;92:e233-40.

Therithal info (Chennai). Chapter: Ophthalmology: Conjunctiva; Conjunctiva: Basic Knowledge. 2018-2023.

Truong W, Cheng C, Xu QG, Li XQ, Zochodne DW. Mu opioid receptors and analgesia at the site of a peripheral nerve injury. Ann Neurol. 2003;53:366-75.

Tsubota K, Pflugfelder SC, Liu Z, Baudouin C, Kim HM, Messmer EM, et al. Defining Dry Eye from a Clinical Perspective. Int J Mol Sci. 2020;21.

Varga EV. The molecular mechanisms of cellular tolerance to delta-opioid agonists. A minireview. Acta Biol Hung. 2003;54:203-18.

Vatani N, Enayatifar RJOALJ. Gray Level Image Edge Detection Using a Hybrid Model of Cellular Learning Automata and Stochastic Cellular Automata. 2015;2:1-8.

Vera LS, Gueudry J, Delcampe A, Roujeau JC, Brasseur G, Muraine M. In vivo confocal microscopic evaluation of corneal changes in chronic Stevens-Johnson syndrome and toxic epidermal necrolysis. Cornea. 2009;28:401-7.

Vernadakis AJ, Koch H, Mackinnon SE. Management of neuromas. Clin Plast Surg. 2003;30:247-68, vii.

Vila-Pueyo M, Hoffmann J, Romero-Reyes M, Akerman S. Brain structure and function related to headache: Brainstem structure and function in headache. Cephalalgia. 2019;39:1635-60.

Wang G, Li H, Long H, Gong X, Hu S, Gong C. Exosomes Derived from Mouse Adipose-Derived Mesenchymal Stem Cells Alleviate Benzalkonium Chloride-Induced Mouse Dry Eye Model via Inhibiting NLRP3 Inflammasome. Ophthalmic Res. 2022;65:40-51.

Watkins LR, Hutchinson MR, Johnston IN, Maier SF. Glia: novel counter-regulators of opioid analgesia. Trends Neurosci. 2005;28:661-9.

Wei S, Ren X, Wang Y, Chou Y, Li X. Therapeutic Effect of Intense Pulsed Light (IPL) Combined with Meibomian Gland Expression (MGX) on Meibomian Gland Dysfunction (MGD). J Ophthalmol. 2020;2020:3684963.

Wenk NH, Nannenga NM, Honda NC. Effect of morphine sulphate eye drops on hyperalgesia in the rat cornea. Pain. 2003;105:455-65.

Wetzel MA, Steele AD, Eisenstein TK, Adler MW, Henderson EE, Rogers TJ. Mu-opioid induction of monocyte chemoattractant protein-1, RANTES, and IFN-gamma-inducible protein-10 expression in human peripheral blood mononuclear cells. J Immunol. 2000;165:6519-24.

Winkler M, Shoa G, Tran ST, Xie Y, Thomasy S, Raghunathan VK, et al. A Comparative Study of Vertebrate Corneal Structure: The Evolution of a Refractive Lens. Invest Ophthalmol Vis Sci. 2015;56:2764-72.

Wolffsohn JS, Arita R, Chalmers R, Djalilian A, Dogru M, Dumbleton K, et al. TFOS DEWS II Diagnostic Methodology report. Ocul Surf. 2017;15:539-74.

Wu Z, Begley CG, Situ P, Simpson T, Liu H. The effects of mild ocular surface stimulation and concentration on spontaneous blink parameters. Curr Eye Res. 2014;39:9-20.

Xiang Y, Zhou W, Wang P, Yang H, Gao F, Xiang H, et al. Alkali Burn Induced Corneal Spontaneous Pain and Activated Neuropathic Pain Matrix in the Central Nervous System in Mice. Cornea. 2017;36:1408-14.

Xiao X, He H, Lin Z, Luo P, He H, Zhou T, et al. Therapeutic effects of epidermal growth factor on benzalkonium chloride-induced dry eye in a mouse model. Invest Ophthalmol Vis Sci. 2012;53:191-7.

Xiao X, Luo P, Zhao H, Chen J, He H, Xu Y, et al. Amniotic membrane extract ameliorates benzalkonium chloride-induced dry eye in a murine model. Exp Eye Res. 2013;115:31-40.

Xie W, Strong JA, Meij JTA, Zhang JM, Yu L. Neuropathic pain: early spontaneous afferent activity is the trigger. Pain. 2005;116:243-56.

Yamagami S, Usui T, Amano S, Ebihara N. Bone marrow-derived cells in mouse and human cornea. Cornea. 2005;24:S71-S4.

Yang F, Zheng J. Understand spiciness: mechanism of TRPV1 channel activation by capsaicin. Protein Cell. 2017;8:169-77.

Yang Q, Zhang Y, Liu X, Wang N, Song Z, Wu K. A Comparison of the Effects of Benzalkonium Chloride on Ocular Surfaces between C57BL/6 and BALB/c Mice. Int J Mol Sci. 2017;18.

Yavuz Saricay L, Bayraktutar BN, Kenyon BM, Hamrah P. Concurrent ocular pain in patients with neurotrophic keratopathy. Ocul Surf. 2021;22:143-51.

Zhang L, Zhang JT, Hang L, Liu T. Mu Opioid Receptor Heterodimers Emerge as Novel Therapeutic Targets: Recent Progress and Future Perspective. Front Pharmacol. 2020a;11:1078.

Zhang R, Park M, Richardson A, Tedla N, Pandzic E, de Paiva CS, et al. Dose-dependent benzalkonium chloride toxicity imparts ocular surface epithelial changes with features of dry eye disease. Ocul Surf. 2020b;18:158-69.

Zhang Z, Yang WZ, Zhu ZZ, Hu QQ, Chen YF, He H, et al. Therapeutic effects of topical doxycycline in a benzalkonium chloride-induced mouse dry eye model. Invest Ophthalmol Vis Sci. 2014;55:2963-74.

Zhao C, Lu S, Truffert A, Tajouri N, Zhao K, Mateo Montoya A, et al. Corneal nerves alterations in various types of systemic polyneuropathy, identified by in vivo confocal microscopy. Klin Monbl Augenheilkd. 2008;225:413-7.

Zheng X, Shiraishi A, Okuma S, Mizoue S, Goto T, Kawasaki S, et al. In vivo confocal microscopic evidence of keratopathy in patients with pseudoexfoliation syndrome. Invest Ophthalmol Vis Sci. 2011;52:1755-61.

Zöllner C, Mousa S, Klinger A, Förster M, Schäfer M. Topical fentanyl in a randomized, double-blind study in patients with corneal damage. Clin J Pain. 2008 Oct;24(8):690-6. doi: 10.1097/AJP.0b013e318175929e. PMID: 18806534.